ЖУРНАЛ
ПРИКЛАДНОЙ ХИМИИ

Volume 32, No. 9
September, 1959

JOURNAL OF
APPLIED CHEMISTRY
OF THE USSR

(ZHURNAL PRIKLADNOI KHIMII)

IN ENGLISH TRANSLATION

CONSULTANTS BUREAU, INC.

RESEARCH BY SOVIET EXPERTS

Translated by Western Scientists

INSTABILITY CONSTANTS OF COMPLEX COMPOUNDS

by K. B. Yatsimirskii and V. P. Vasil'ev

Instability constants quantitatively characterize the equilibrium in solutions of complex compounds and, in this connection, are very widely used by chemists in different fields (analytical chemistry, electrochemistry, technology of nonferrous and rare metals, etc.) for appropriate calculations.

The instability constants of 1381 complex compounds are given. The authors have prefaced the summary of instability constants with an introductory section which examines methods of calculating instability constants from experimental data, the effect of external conditions (temperature and ionic strength) on the stability of complexes and the main factors determining the stability of complex compounds in aqueous solutions.

Cloth **200 pages** **$6.75**

SOVIET RESEARCH ON COMPLEXES AND CO-ORDINATION CHEMISTRY

This collection consists of 372 articles by Russian scientists in the general area of the chemistry of complexes. These reports have been complied from the Consultants Bureau translations of the following Soviet journals:

Journal of General Chemistry
Journal of Analytical Chemistry
Bulletin of the Academy of Sciences
Division of Chemical Sciences
Proceedings of the Academy of Sciences
Journal of Applied Chemistry
Soviet Journal of Atomic Energy

The articles have been grouped into five volumes, each of which may be purchased separately.

I. Inorganic Complexes—103 articles **$65.00**
II. Metal-Organic Complexes—86 articles **$45.00**
III. Thermodynamic and Kinetic Studies—57 articles .. **$37.50**
IV. Complexes in Analytical Chemistry—57 articles .. **$37.50**
V. Condensed Inorganic Systems; Miscellaneous —38 articles .. —31 articles .. **$45.00**

Complete collection .. **$200.000**

Tables of contents on request

Payment in sterling may be made to Barclays Bank in London, England

CONSULTANTS BUREAU

227 West 17th Street • New York 11, N. Y.

Volume 32, No. 9
September, 1959

JOURNAL OF
APPLIED CHEMISTRY
OF THE USSR

(ZHURNAL PRIKLADNOI KHIMII)

A publication of the Academy of Sciences of the USSR

IN ENGLISH TRANSLATION

Year and issue of first translation:
Vol. 23, No. 1 January 1950

	U. S. and Canada	*Foreign*
Annual subscription	*$60.00*	*$65.00*
Annual subscription for libraries of nonprofit academic institutions	*20.00*	*25.00*
Single issue	*7.50*	*7.50*

Copyright 1960
CONSULTANTS BUREAU ENTERPRISES, INC.
227 West 17th Street, New York, N. Y.

Editorial Board
(ZHURNAL PRIKLADNOI KHIMII)

P. P. Budnikov, S. I. Vol'fkovich, A. F. Dobrianskii,
O. E. Zviagintsev, N. I. Nikitin (Editor in Chief),
G. V. Pigulevskii, M. E. Pozin, L. K. Simonova
(Secretary), V. V. Skorchelletti, N. P. Fedot'ev

Note: The sale of photostatic copies of any portion of this copyright translation is expressly prohibited by the copyright owners.

Printed in the United States of America

JOURNAL OF APPLIED CHEMISTRY OF THE USSR

Volume 32, Number 9 September, 1959

CONTENTS

	PAGE	RUSS. PAGE
Present-Day Applications of the Platinum Metals. O. E. Zvyagintsev	1937	1889
Ferrocyanide Method of Extracting Small Amounts of Thallium From Solutions of Non-ferrous Metals. L. V. Tananaev and M. A. Glushkova	1947	1899
Extraction of Tantalum and Niobium From Sulfuric Acid Solutions with Cyclohexanone. Ya. G. Goroshchenko, M. L. Andreeva and A. G. Babkin	1952	1904
Extraction and Separation of Niobium and Titanium From Oxalic Acid Solutions by An Ion-Exchange Method. L. D. Fridman and L. N. Yudina	1962	1914
On The Quality of Titanium Sponge Prepared by the Magnesiothermic Process. V. V. Sergeev, V. V. Vlasov, and R. A. Sandler	1967	1919
Acetone Solutions of Silicic Acid, Their Properties and Use. Yu. V. Morachevskii and E. N. Egorova	1973	1925
On the Partial Pressure of SO_2 Over Ammonium Sulfite-Bisulfite Solutions. R. A. Berdyanskaya, S. M. Golyand, and B. A. Chertkov	1978	1930
Use of Porous Sorbents for Extraction of Metallic Microimpurities from Tervalent Chromium Salt Solutions. L. D. Muzyka and V. A. Molodtsova	1985	1936
On the Conditions of Formation of a Continuous Series of Solid Solutions in the Pseudobinary System $CrB_2 - TiB_2$. N. G. Sevast'yanov, V. A. Epel'baum, M. A. Gurevich, B. F. Ormont, and G. S. Zhdanov	1990	1941
Utilization of Diagrams of the Reciprocal System of Ammonium Monophosphate – Sodium Nitrate – Water in the Process of Nitric Acid Decomposition of Phosphates. S. Ya. Shpunt	1994	1945
Preparation and Investigation of Phosphate Films on Zinc. L. V. Krotov, V. V. Grinina and N. A. Zapol'skaya	2001	1952
The Anomalous Aging of Solids Obtained by Chemical Precipitation. L. M. Vasserman	2008	1959
Extraction of Fine Suspensions From Solutions by the Emulsification Method. S. G. Mokrushin and V. I. Borisikhina	2012	1963
The Separation of Coals Into Fractions of Different Densities. N. S. Goloushin	2016	1967
The Employment of Normal and Differential Polarography for the Analysis of Coke – Chemical Products. A. G. Pozdeeva, N. Kh. Cherkasov and F. L. Kruglova	2022	1973
Comparative Characterization of Some Anionites. A. T. Davydov and Yu. A. Tolmacheva	2028	1979
High-Temperature Ceramic Heaters. E. K. Keler and E. N. Nikitin	2033	1984

CONTENTS (continued)

	PAGE	RUSS. PAGE
The Temperature of the Vapor of Boiling Liquids. A. G. Bol'shakov, A. V. Kortnev and G. N. Gasyuk	2037	1988
Generalized Equations for Calculation of Packed Columns Under Various Hydrodynamic Conditions. V. V. Kafarov and V. S. Murav'ev.	2042	1992
Investigation of the Process of Fractional Distillation in a Filled Column Under Reduced Pressure. H. L. Gel'perin and N. N. Zelenetskii	2050	2001
Hydraulic Resistance of the Gas–Liquid Layer in Sieve Apparatuses. L. P. Mukhlenov and E. Ya. Tarat	2055	2006
Electrochemical Deposition of Gold–Copper Alloys. N. P. Fedot'ev, E. C. Kruglova, and P. M. Vyacheslavov	2063	2014
Hydrogen Overvoltages on Lead and Some of its Alloys in Concentrated Sulfuric Acid Solution. I. A. Aguf and M. A. Dasoyan.	2071	2022
The Effect of Some Organic Compounds in the Anodic Oxidation of Aluminum. L. Donev and L. Boyadzhiev	2080	2031
Study of Effect of Composition and Concentration of Electrolyte Solutions on Electrochemical Activity of Ion-Exchange Membranes. Z. P. Koz'mina, T. P. Zharinova and G. P. Kisova.	2083	2034
Intensification of Electrolysis Processes by Introduction of Compounds with Covalent Bonds Into Solutions. P. P. Belyaev	2089	2039
Study of Corrosion Resistance of Sheet Cast Iron. A. S. Afanas'ev and B. Sh. Shteinberg	2097	2046
Study of The Electroconductivity in the Sulfonation of Naphthalene. E. I. Matrosov.	2106	2056
Residence Time of the Reactants in the Contact Zone in Heterogeneous Catalytic Synthesis of Vinyl Acetate. E. N. Rostovskii and S. N. Ushakov	2110	2060
Study of The Polymerization of Hexafluorobutadiene. A. L. Klebanskii and O. A. Timofeev	2114	2064
Simultaneous Synthesis of Butadiene and Normal Butyl Alcohol From Propylene and Formaldehyde. M. I. Farberov, A. M. Kut'in, A. F. Frolov and T. P. Vernova	2120	2070
Preparation and Investigation of Methyl Acrylate–Methacrylic Acid Polymer. A. Ya. Drinberg, B. M. Fundyler, and E. A. Volynskaya.	2126	2075
Lacquer Coatings Based on Colloidal Dispersions of Carbon Black in Cellulose Acetate Phthalate Esters. L. V. Rozental' and G. I. Burdygina.	2131	2080
Application of Chromatographic Method for Investigation of Changes in the Carbohydrate Complex of Sugar Beet During Prolonged Storage. O. V. Braun	2136	2084
On Certain Catalytic Conversions of Ethylene Glycol. B. N. Dolgov and V. I. Ivanskii	2142	2091
The Effect of Certain Physicochemical Factors on the Yield of γ-Hexachlorane From the Photochemical Chlorination of Tetrachlorocyclohexenes. L. S. Pereslegina and A. I. Finkel'shtein	2148	2096
Recovery of Organomercury Compounds from Spent Activated Carbon Saturated With Organomercury Compounds by Extraction with Organic Solvents. I. F. Zemskov and G. I. Sidel'nikova	2152	2100

CONTENTS (continued)

	PAGE	RUSS. PAGE
Dependence of the Extent of Cyclohexane Dehydrogenation on Feed Rate and Catalyst Particle Size (0.5% Pt on Al_2O_3). N. F. Kononov, Kh. M. Minachev and N. I. Shuikin.	2159	2107
Identification of Branched Octenes Obtained by Alkylation of Tertiary Butyl Chloride with 2-Butene. M. M. Ketslakh, D. M. Rudkovskii and F. A. Éppel'	2167	2115
On The Conversion of Higher Phenols to Phenol, Cresols and Xylenols. M. K. D'yakova, A. B. Vol'-Épshtein, M. N. Zharova and E. A. Zasukhina	2172	2120

PRESENT-DAY APPLICATIONS OF THE PLATINUM METALS

O. E. Zvyagintsev

The plan adopted by the XXIst Session of the Communist Party of the Soviet Union for the development of the country's national economy requires the mobilization of all available resources for its fulfilment.

Platinum and the other metals of the platinum group: palladium, rhodium, iridium, ruthenium and osmium, can and must serve this end. The lack of attention paid to the industrial application of these metals until recently has been due to their scarcity and to the difficulties encountered in their isolation. In the past ten years, following the discovery of new deposits in Canada, the USSR and South Africa the world supply of platinum metals has increased to such an extent that not only the technological industries, but also the jewellery trade and medical practice (dentistry), have begun to make wider use of these materials. In his message of June 2, 1958, to President Eisenhower, Mr. Khrushchev included platinum and palladium in the list of goods which the USSR might sell to the USA. All this shows that use may be made of the platinum metals in the national economy of the USSR. Of particular interest in this connection is the metal palladium, for which output considerably exceeds the demand.

Table 1 gives data for the world output of platinum metals in recent years (with the exception of the USSR) [1].

No statistics are available for the consumption of the platinum metals in the various branches of industry, the jewellery trade and medical practice in the capitalist countries. An exception is the USA, for which these data are published. Since the USA consumes the greater part of the total world supply of platinum metals, the figures given in Table 2 for the USA may be taken as characterizing the demand for platinum and palladium by the various consumers [2].

Table 2 shows that the consumption of platinum and palladium in the USA increased up to 1957, and was only halted by the start of the economic crisis. A particularly marked increase was shown in the consumption of palladium by the electrotechnical industries, dentistry and the chemical manufacturing industries.

It is of interest to examine in more detail the uses to which the platinum metals are put, and the forms in which they are used, in the various branches of the national economy, and also to examine the possible directions in which their applications may be developed.

Applications of the Platinum Metals in the Chemical and Oil-Refining Industries

Platinum has for long been used as a chemically resistant material for the manufacture of apparatus. Thus for example, platinum was used to prepare apparatus for the evaporation of sulfuric acid as early as the beginning of the XIXth century. Because of the high cost of platinum, however, such articles were very seldom produced. In recent years the position has changed. A start has been made in the introduction of platinum and its alloys as materials for the construction of apparatus in a number of chemical industries. These include particularly those industries producing various fluorine-containing compounds, especially when a very pure product is required. The reaction vessels or parts of such vessels are seldom made entirely of platinum, however; normally the apparatus or its parts are lined with platinum foil. The construction of even large-scale plants is thus possible at comparatively low cost. One square meter of platinum foil of thickness 0.025 mm weighs only 540 kg. In addition, practically no platinum is lost during the operation of the plant, and when the latter is replaced the platinum can be recovered as scrap. Thus the cost of the product is increased only by the cost of preparing the lining and the very slight cost of the platinum lost.

For these reasons, plant lined with platinum has found application not only for the preparation of very pure chemicals, but also for the production of comparatively heavy chemicals, and in the food industry.

In those cases where the chemical stability and refractory properties of platinum are insufficient, attention is turned to alloys of platinum with other metals which improve these properties. In the manufacture of glass fiber, for example, the vessels used for melting the glass, and the nozzles through which the thin jets of molten glass are forced to produce the fiber on solidification, are made from an alloy of platinum and rhodium (7% rhodium). The rhodium increases the melting point of the platinum and its chemical stability.

Platinum is also used in certain electrochemical industries as an inert electrode material. In plants for the electrolytic preparation of hydrogen peroxide, peroxysulfates and organic peroxides, for example, the anodes are made of platinum.

The use of platinum in chemical laboratories is well-known and there is no need to enumerate the various platinum articles used in laboratory practice. We might mention, however, that foreign firms often prepare crucibles and dishes from an alloy of platinum with 1-3% rhodium in order to increase the mechanical strength of these articles: the working life of the apparatus is considerably increased.

The chief demand for the platinum metals, however, does not arise from their use as constructional materials for chemical plant. In the chemical and oil-refining industries, these metals are used chiefly as catalysts.

The use of platinum and palladium for the acceleration of various reactions dates from the beginning of the XIXth centruy [3].

In recent years a very large number of works, chiefly American, has appeared, devoted to catalytic reactions using platinum and palladium. The vast majority of these relate to processes of organic synthesis, oxidation, hydrogenation and dehydrogenation. A particularly large number of papers and patents has appeared in recent years on the application of platinum in the oil-refining industry for the preparation of high-octane gasoline and other products.

Both platinum and palladium can be used in catalytic reactions in a variety of forms. In heterogeneous catalysis, the following types of catalyst are used.

1. The compact metals in the form of sheet, foil, wire or, most frequently, gauze. As a result of their small specific surface, these catalysts are the least active. They are used for reactions in the vapor phase at high temperatures.

2. Platinum and palladium sponge, obtained by igniting the salts of these metals until thermal decomposition and sintering is complete.

3. Platinum and palladium black, i.e., the metals as obtained by reduction of the metal salts to produce highly dispersed powders. As a result of their large specific surface, they have a high adsorptive capacity and catalytic activity.

4. The metals in colloidal form, obtained under conditions ensuring very high dispersion of the particles (in the presence of protective colloids). These catalysts are used chiefly to carry out reactions in the liquid phase.

5. Catalysts with platinum and palladium on carriers. The finely divided metal is deposited on an inert substance such as a ceramic solid, pumice, carbon, barium sulfate or alumina. These supports act as stabilizers and prevent any changes taking place in the degree of dispersion of the metal. Platinum and palladium black and the colloidal metals lose their activity rapidly at temperatures above 400°. When the metals are deposited on a solid carrier, they do not lose their catalytic properties when heated.

6. Promoted or activated mixed catalysts with platinum and palladium resemble the catalysts on carriers, but the carrier itself has an effect on the process and alters the rate or selectivity of the chemical reactions.

7. Skeletal catalysts, obtained from platinum or palladium alloys by dissolving out the base component in acid. Such catalysts are solids with a high porosity and large surface. At the same time the dissolution of the base metal atoms from the crystals produces defect crystal lattices with increased catalytic activity.

In homogeneous catalysis in the liquid phase, extensive use is made of compounds and salts of platinum and palladium which are soluble in the reacting liquids, particularly chloroplatinic and chloropalladic acids, which are readily soluble in alcohols and other organic substances.

TABLE 1

Output of Platinum Group Metals in the Capitalist Countries (kg)

Year	1937	1949	1954	1955	1956	1957
Total quantity	11300	14800	21500	25500	28500	30100
Platinum	6550	7800	12300	14500	16500	18200
Palladium	4000	6500	8500	10000	11000	11500
Including:						
Union of South Africa*	1232	2718	10518	11873	15072	15600
Platinum	800	1770	840	7700	10264	10800
Palladium	370	815	3150	3500	4500	4600
Canada	8062	10451	10690	11967	9792	12733
Platinum	4335	4783	4801	5303	4708	6099
Other platinum metals	3727	5668	5889	6664	5084	6634
Columbia	912	647	770	848	871	800
USA	640	772	918	778	746	650
Platinum	459	591	632	535	—	500
Palladium	—	—	122	183	—	130

* The figures for the Union of South Africa are conjectural. No official statistics are published. Colombia supplies raw platinum consisting chiefly of platinum with small quantities of other metals. The data for some years for the USA are not complete.

TABLE 2

Demand for Platinum and Palladium by Various Branches of Industry in the USA (kg)

	Total quantity	Industry				
		chemical and oil-refining	electro-technology	jewellery	medical	others
1937						
Platinum	2984	569	294	1550	346	225
Palladium	2164	5	649	257	1251	2
1949						
Platinum	4748	1001	893	2501	296	57
Palladium	3615	298	1688	997	619	13
1954						
Platiinum	9960	5658	1614	1174	441	73
Palladium	7295	465	4788	853	892	297
1955						
Platinum	14527	10827	1514	1639	383	164
Palladium	10938	1127	7798	892	896	225
1956						
Platinum	13395	9628	1676	1205	387	499
Palladium	12441	978	9486	492	944	241
1957						
Platinum*	10960	7650	1550	950	200	160
Palladium*	11400	900	8820	550	600	200

* Data incomplete.

We shall not dwell at this stage on the methods for preparing platinum, palladium and mixed catalysts – an extremely important question which requires special consideration. We shall mention merely the high degree of purity required of metals used for the preparation of catalysts.

A large number of studies have shown that many impurities alter the catalytic activity of platinum and palladium. In the oxidation of ammonia, for example, rhodium alloyed with platinum increases the activity, while gold, even in very small concentrations in the platinum, poisons the catalyst. The refining (purification) of the metals of the platinum group used to prepare catalysts must therefore be very thorough. The total amount of impurities in the refined metal should not exceed several hundredths of one percent.

The usual impurities in platinum are iron, iridium, palladium, nickel and copper. Palladium contains iron, platinum, rhodium, nickel and copper. Occasionally other elements are present in very small quantities. When, however, the total concentration of impurities does not exceed the limit of several hundredths of one percent mentioned above, the metals may be regarded as suitable for the preparation of catalysts. In certain cases, however, the metals must have a higher degree of purity: in the above example, i.e., the catalytic oxidation of ammonia, no trace of gold should be present.

The refining plants in the Soviet Union prepare very pure metals, and if necessary are able to supply platinum and palladium of spectroscopically pure grade. Methods have been developed for the preparation of spectroscopically pure platinum by Chernyaev and Rubinshtein [4], and of spectroscopically pure palladium by Rubinshtein and Sokol [5], in the N. S. Kurnakov Institute of General and Inorganic Chemistry.

In certain industries use in made not of pure platinum but of its alloys with rhodium, palladium, iridium, etc.

After a certain period of use, catalysts lose part of their activity and have to be replaced by new material. The used catalyst is then regenerated.

It is impossible in a short article to give a review of all the catalytic reactions which are accelerated by the platinum metals. We shall try to give examples of different chemical processes which illustrate the importance of these metals in the modern chemical and oil-refining industries.

In courses of chemical technology, descriptions are often given of the contact process for the preparation of sulfuric acid using a platinum catalyst. Examples include the contact apparatus of the Tentelen chemical plant in St. Petersburg using platinized asbestos, and the Grillo-Schroder method [6] using platinum on magnesium sulfate, etc. At the present time, however, practically no sulfuric acid plants make use of platinum catalysts, which have been replaced by the less expensive vanadium catalysts, although the latter are less active.

In the technology of inorganic substances, the process making use of the greatest quantity of platinum metals at the present time is the oxidation of ammonia to nitric acid. The theory of the catalytic oxidation of ammonia on platinum was developed by Ostwald and Brauer [7] and by Neumann and Rose [8]. The first plant for the manufacture of nitric acid by the contact process was constructed in Russia by I. I. Andreev and co-workers in 1916 [9]. At the present time the production of nitric acid by this method has reached vast proportions. Many large-scale nitric acid plants have been constructed and are operating in the USSR. The platinum-based alloys used as catalysts are now considered insurpassable with respect to activity and stability under industrial conditions.

The oxidation of ammonia can be carried out either at atmospheric pressure at a temperature of 700-750° or under a pressure of 7-8 atmospheres at a temperature of 850-900°. If the oxidation is carried out at low pressure, the gauze in the contact apparatus is arranged in 3 layers, but when high pressure is used, 15-20 layers are included. The gauze is made from a platinum alloy containing 5-7% rhodium. The addition of the rhodium makes the gauze more resistant and long-lasting, without altering its catalytic activity. Soviet scientists have proposed the replacement of part of the rhodium by the cheaper palladium. This has proved to be doubly advantageous since it not only reduces the cost of the gauze but also increases its catalytic activity. At the optimum temperature and rate of flow of gases, the yield of oxides of nitrogen amounts to 97-98%. The size of the gauzes varies between 1 and 2 metres, depending on the design of the apparatus. The gauze is prepared from wire of diameter 0.05-0.09 m.m. The number of meshes per cm^2 amounts to 1024 [9].

The gauze undergoes certain changes during use: it becomes covered with dust (chiefly oxides of iron) and becomes brittle as a result of prolonged exposure to high temperatures; the surface becomes loose and friable.

The catalytic activity of the gauze then decreases, and particles of the loose surface of the wire break off and are carried away by the gases. When the gauze has been in use for a definite length of time it is replaced and sent to the refining plant for regeneration of the platinum metals. The working life of the gauze is approximately 1-1.5 years for operation at atmospheric pressure.

The loss of platinum alloy for operating conditions under pressures of 7-8 atmospheres amounts to 0.3-0.4 g per ton of 100% nitric acid, and 0.04-0.06 g for operation at atmospheric pressure.

Attempts to replace the platinum metals by other cheaper materials have proved unsuccessful, and platinum remains the most efficient catalyst for the oxidation of ammonia.

The catalytic dehydrogenation of organic compounds is now of very great importance in chemistry and chemical technology. The first studies in this field were carried out by Berthelot, Reiset and Millon [10], Sabatier and Senderens [11], Willand [12] and others. Extremely important work in this field was carried out by Zelinskii and his school, from 1911 onwards [13].

Zelinskii and co-workers [13-14] established that not all cyclic hydrocarbons are dehydrogenated on platinum and palladium: those which are dehydrogenated consist of six-membered rings or contain six-membered hydroaromatic rings. Other hydrocarbons are unable to split off hydrogen. On the basis of these catalytic reactions, studies have been carried out on hydrocarbon mixtures, which have made it possible to separate the components of the mixtures. The detailed study of the catalytic dehydrogenation of hydrocarbons, carried out by N. D. Zelinskii and his school, have led to the development of important and reliable methods for the study of oil [15, 16].

In addition, a method was found for increasing the quantity of aromatic hydrocarbons in oil fractions by hydrogenation of the hexahydroaromatic compounds present in certain oil deposits of the USSR [17].

The Zelinskii method has played an important part in the analysis of gasolines, and has become one of the principal technological methods for improving gasolines (increasing the aromatic hydrocarbon content). The method or variations of the method are used particularly widely in the American oil refining industry. This partly explains the considerable increase in the consumption of platinum in this branch of industry in the past ten years. •

All the dehydrogenation reactions are carried out in the vapor phase using platinum, palladium or other catalysts on a solid carrier such as charcoal, ceramics, alumina or silica gel.

Mention must be made of a recently published work by Shuikin and co-workers [19] on the improvement of straight gasolines by a low-temperature dehydrogenation on platinized carbon. The reaction is carried out at a temperature of 300° in the vapor phase over carbon containing 2-4% platinum. Another paper by the same authors [19] describes experiments on the preparation of toluene concentrates by low-temperature dehydrogenation on platinized carbon. The experiments were carried out with the 98-112° gasoline fractions from refined and nonrefined oil (from Iiskiy and Khadyzhensk). The catalyst consisted of wood charcoal containing 4% platinum. The temperature of the reaction was approximately 300°. The concentrates obtained contained 30-40 vol. % toluene, which was separated by azeotropic distillation with methanol. The purified toluene satisfied the requirements of GOST (All Union State Standard).

Unlike the above reactions, the process of hydrogenation (the addition of hydrogen) can be carried out either in the vapor phase or in the liquid phase. In the case of liquid-phase hydrogenation, the catalyst is used in the colloidal form.

In 1902, S. A. Fokin carried out the hydrogenation of fats in the liquid phase. In 1904, V. N. Ipat'ev began an extensive series of experiments on hydrogenation using hydrogen at increased pressure.

Platinum, palladium, osmium and ruthenium can be used as catalysts for the hydrogenation of a variety of substances: olefins and poly-olefins, acetylene and its derivatives, cyclic and aromatic hydrocarbons, aldehydes and ketones, organic acids and their derivatives, nitro-compounds and a number of others.

As an example, mention may be made of the reaction discovered in 1933 by N. D. Zelinskii, B. A. Kazanskii and A. F. Plate. The reaction involves the opening of cyclopentane by the action of hydrogen over platinum. The five-membered ring is very stable. This reaction served as the starting point for an extensive series of studies. Its

---

• The terms "reforming process" or "hydroforming process" are used in various capitalist countries, particularly the USA, to describe the industrial catalytic processes for treating oil products to obtain high-octane aviation and automobile fuels. The output from the USA plants in 1957 amounted to approximately 1,300,000 barrels per day. This amounts to 14% of the total production of all oil refinery products in the USA [18].

practical importance as far as motor fuel is concerned lies in the fact that this hydrogenation increases the octane number of the fuel [20].

As early as 1872, Zaitsev [21] carried out the vapor-phase reduction of nitrobenzene to aniline using a palladium catalyst. This reaction, which was subsequently studied by many workers, forms the basis of a large branch of dye chemistry and is of considerable importance in other fields of organic synthesis.

The hydrogenation of fats plays an important part in the preparation of solid fats from liquid vegetable oils. Normally a nickel catalyst is used for this purpose. The reaction is carried out in the liquid phase and the catalyst remains in the reaction product. The nickel catalyst is therefore unsuitable for the preparation of high-quality solid fats for food production, and it is replaced by palladium, which is separated after the reaction.

An example of the use of ruthenium as catalyst is the synthesis of high-melting paraffins, studied by Kolbel and Bhattacharyya in 1958 [22]. The reaction is carried out in the liquid phase, using a ruthenium suspension (1 g in 150 ml water).

Of still greater importance for practical purposes is the catalytic reaction by which glycerol and other polyhydric alcohols may be obtained from cellulose or polysaccharides using ruthenium.

Polyhydric alcohols – glycols, glycerol, pentaerythritol, pentitols and hexitols – have a high reactivity which makes it possible to use them for the preparation of a large number of varied organic compounds. This explains the continuous increase in the production of polyhydric alcohols, which are steadily becoming more important in the development of many branches of the chemical industry, and in the increased output of consumer goods.

One important approach to the practical solution of the problem of preparing polyhydric alcohols, particularly glycerol and sorbitol, from inedible raw materials, is the catalytic preparation of these alcohols from polysaccharides found in vegetable materials. For this purpose use may be made of the waste products from the timber-cutting and wood industries, various agricultural vegetable wastes (maize stalks, cotton husks, sunflower seed shells, straw, etc.), and reeds.

The organization of the industrial production of polyhydric alcohols from inedible vegetable raw materials makes it possible to find new sources for the production of a variety of chemical products which at present use up considerable quantities of cereals, potatoes and edible fats. At the same time the production of polyhydric alcohols in this way extends the range of raw materials on which the development of the industrial synthesis of heavy organic chemicals may be based.

As a result of its particular chemical and physical properties and consequent variety of applications, glycerol has attracted greater interest, and is of greater practical importance, than any other polyhydric alcohol [23].

The hydrogenation of cellulose to polyhydric alcohols has until now been restricted by the lack of a suitable catalyst. The nickel catalyst, as a result of its solubility, is unsuitable for hydrogenation in acid medium.

The discovery of an acid-insoluble catalyst provides a solution to the problem of hydrogenating cellulose and producing glycerol economically from an inedible raw material.

Such a catalyst is ruthenium. A. A. Balandin, N. A. Vasyunina, G. S. Barysheva and S. V. Chepigo (N. D. Zelinskii Institute of Organic Chemistry, USSR Academy of Sciences, and the All-Union Scentific Research Institute for the Hydrolysis Industry) [24] have found that by using ruthenium in acid medium (sulfuric or phosphoric acid) it is possible to convert cellulose, hemicelluloses and starch to the corresponding monohydric alcohols or monosaccharides in 78-95% yield, the reaction products containing no free reducing substances. Thus in the presence of 2% H_2SO_4 and 0.1% ruthenium on carbon or silica gel at a temperature of 156-160° and a pressure of 70 atmospheres for 2 hours, sulfite cellulose is converted to a transparent colorless solution, which yields sorbitol monoanhydride in 82% yield, relative to the orginal cellulose, taking account of the added water.

In the presence of 1% H_2SO_4 and 0.1% ruthenium at a temperature of 155-160° and 70 atmospheres pressure for 1 hour, unpurified hemicellulose (waste from the viscose industry) gives 78% yields of monohydric alcohols.

The same authors have found that similar results are obtained using palladium, but it is to be assumed that a certain fraction is lost as a result of dissolution.

The Application of the Platinum Metals in Electrotechnology, The Radio Industry, Machine Construction and Instrument Manufacture

These branches of technology make use chiefly of alloys, since the chemical and physical properties of the pure metals are not suitable for the required purposes. The variety of applications to which the alloys are put results from the detailed study of the binary and ternary alloys-systems formed by the platinum metals. These studies have been carried out by the USA Bureau of Standards and by industrial laboratories in the USA, Germany, and England. The most significant results, however, have been obtained in the USSR. This work was started in 1922 in the Institute of Platinum of the USSR Academy of Sciences under the direction of N. S. Kurnakov, and in 1934 was transferred to the Institute of General and Inorganic Chemistry of the USSR Academy of Sciences, where a special laboratory was organized under the direction of V. A. Nemilov [25]. In 1953 the work was transferred to the Institute of Metallurgy of the USSR Academy of Sciences and brought to the M. V. Lomonosov State University, Moscow.

N. S. Kurnakov and his students and successors studied approximately forty binary systems and more than 15 ternary systems formed by the noble metals. Many of the alloys studied have found application in various branches of technology [26].

The refractory platinum alloys resistant to high-temperature oxidation are widely used to prepare heating elements for resistance furnaces. Whereas furnaces with platinum windings can operate for prolonged periods at a temperature of 1200-1300°, furnaces with heating elements made from an alloy of platinum with 15% rhodium can operate at 1500° and above. In high-temperature furnaces, use is also made of alloys of platinum with higher iridium and rhodium contents, which are capable of operating at prolonged periods at temperatures of 1500-1700°.

Alloys of the platinum metals are used extensively in the electrical industry for the preparation of different types of contact. Contacts made from other metals become corroded or lose their shape during passage of the spark or the short voltaic arc produced when the circuit is closed or opened. Contacts made from alloys of platinum containing 25% iridium have a high mechanical stability and are little affected by the passage of current. For this reason, platinum-iridium contacts are used in aircraft motors and other important machines using powerful currents.

In low-current apparatus, extensive use is made of contacts and shoes made of platinum-silver, or more often, palladium-silver alloys of different composition. Palladium-silver alloys are also used to prepare wires, tubes, rings and other parts for electrical apparatus, aircraft instruments, heavy transport machinery and in ship-building (20, 40, and 80% silver).

In the radio and electronics industries, the platinum metals are again being more widely used. They are very suitable for use as anti-emission coating in electrical vacuum apparatus. These coatings can be deposited electrolytically or by drawing out the metal inside a tube of the platinum metal.

The platinum metals are useful materials for cathode supports, being inert toward the active coating, and may also be used in the form of alloys with active metals, for example barium, as the active core in oxide-based cathodes.

Of particular interest is the electronic emission of osmium, as the nearest neighbor of ruthenium, which gives a more stable emission than tungsten. Iridium is used as inactive core in the sodium oxide cathode, which operates in an atmosphere of oxygen at pressures of 0.1-0.01 mm mercury.

Alloys of palladium with silver and copper are used to prepare electrical resistances for industrial purposes (30% silver and 4% copper, 50% silver and 20% copper).

Another extremely interesting alloy is that formed by palladium with 18% iridium, which has a high elasticity. This alloy has been used in the manufacture of electrical spring contacts for aircraft instruments.

Le Chatelier's platinum-platinorhodium thermocouple is well known, and has been widely used for the measurement of high temperatures (up to 1500°). These thermocouples consist of a platinum wire and a wire of an alloy containing platinum with 10% rhodium. The materials used should be of very high quality and the composition of the alloy controlled very accurately. The thermocouples are very stable under definite conditions.

Certain overseas firms supply iridium-ruthenium thermocouples for the measurement of even high temperatures (up to 1800°).

In some cases pure palladium is used in vacuum technology to absorb hydrogen and other gases, and also as a filter permitting the passage of hydrogen while retaining all other gases.

Finally, mention must be made of anti-corrosion and strengthening coatings of platinum, palladium and rhodium, which are applied to the parts of watches and other instruments. Rhodium-plating not only increases the strength of the coated article, but also gives it a nontarnishable polish. The reflective power of a rhodium surface is very high (85%) and is exceeded only by that of silver. Silver, however, tarnishes rapidly. For this reason, rhodium is used to cover the surface of optical reflectors and projectors. Electrolytic methods for plating with platinum, palladium and rhodium are fairly well developed [27].

The Application of the Platinum Metals in Medical Practice

Alloys of platinum with iridium (10%) are used to prepare corrosion resistant needles for the syringes used for injections and infusions. Platinum is used to prepare the tips of the instruments used for cauterization.

In other countries, large quantities of platinum and palladium are used as alloys in dentistry. In the USSR, the platinum metals are comparatively seldom used for these purposes, since platinum discs were only recently available commercially, and palladium and its alloys are not yet available, so that Soviet dentists are not familiar with their use. At the same time, the external appearance (a soft matt white luster), resistance to oxidation, and low cost of palladium alloys should enable them to replace gold for crowns and artificial teeth.

Platinum with 5% copper or silver is used for the preparations of crampons (locking pins) for artificial porcelain teeth. Crowns and cast teeth can be prepared using various binary, ternary or more complex alloys based on platinum or palladium. These metals are alloyed with gold, silver, copper or other metals (for example nickel) to give them hardness and resistance to wear.

Alloys with higher concentrations of low-melting components (gold, palladium and silver) are used as cements in dentistry.

The Application of the Platinum Metals in Jewellery

During the First World War, when the price of platinum rose steeply, platinum jewellery became very fashionable in the USA and later in the capitalist countries of Europe. It was considered obligatory for a prosperous person to possess watches, pendants, chains and other articles. Later, in the middle of the twenties, the fashion passed. Lovers of adornment were convinced, however, that many pieces of platinum jewelery were intrinsically beautiful and elegant. Jewels set in platinum, for example, have a very pleasing soft luster, which is more beautiful than that from stones set in gold or silver. A combination of gold and platinum links in bracelet chains and fine chains for pendants is very pleasing. Platinum watches, properly made, have a very beautiful appearance.

Palladium and palladium-platinum alloys were at first used to imitate platinum, and were sold at a lower price. It was subsequently realized, however, that palladium articles have a beautiful appearance, so may therefore be considered as an excellent material for jewellery. Its density is half that of platinum, so that only half the weight is required for a given volume, and palladium is slightly cheaper than platinum. The warm matt luster from palladium gives articles a particular charm which silver articles do not have. At the same time palladium does not tarnish in use as silver does. Palladium may be plated with gold by electrolytic methods, and the gold covering adheres very firmly.

In England a medal made of palladium has been struck to honour Wallaston, the discoverer of the metal, and the medal is awarded for scientific merit.

After the discovery of platinum in S. America, the Spanish Government in 1735 was afraid that the new metal might be used to adulterate gold, and a law was passed which required the destruction of all reserves of platinum raw materials. Government officials in the mints in Santa Fe and Papayani were required to retain all the platinum produced as a by-product in the purification of gold dust, and, as the metal accumulated, they had to dump it, in the presence of witnesses, into the neighboring rivers of Bogota and Cauca [28].

No uses for platinum were known for a long time, since its noble properties were not realized.

At the present time, scientific studies have shown that all the platinum metals have many valuable properties, and they have found many applications in the most varied branches of technology. In many cases the platinum metals, particularly platinum itself, cannot be replaced by other metals. If the consumption of platinum is measured in tons, the quantity is slight compared with that of other metals such as copper, lead and tin. Its value, however, is very great. It can be compared with the importance of salt in the preparation of food: little is used, but a meal cannot be prepared without it.

The Soviet Union possesses vast natural reserves of platinum metals. These reserves must be fully exploited for the development of industry and the production of consumer goods.

LITERATURE CITED

[1] Statistical Summary of Mineral Industry 1938, 1957; Minerals, Oct.-Dec., 1956; Eng. Min. J., Feb.-Jul. 1958.

[2] Metal Statistics 1957; Mineral Industry Service, 2693 (1958).

[3] A. M. Rubinshtein, Izv. Sektora Platiny, Akad. Nauk SSSR 19, 61 (1943).

[4] L. L. Chernyaev and A. M. Rubinshtein, Dokl. Akad. Nauk SSSR 48, 5, 353 (1945).

[5] A. M. Rubinshtein and S. K. Sokol, Zhur. Prikl. Khim. XXXII, 4, 930 (1959).•

[6] F. Meyer, J. Soc. Chem. Ind. 22, 348 (1903).

[7] W. Ostwald, Brit. Pat. 698 (1902); 8300 (1902).

[8] B. Neumann and H. Rose, Z. Ang. Ch. 33, 45 (1920).

[9] S. L. Vol'fkovich, A. P. Egorov, and D. A. Ėpshtein, "Obshchaya Khimicheskaya Tekhnologiya" (General Chemical Technology), 1. Goskhimizdat, M., 243 (1952); A. K. Kolosov, "Materialy po Istorii Otechestvennoi Khimii Sb. Dokladov na 2-m Vsesoyuznom Soveshchanii po Istorii Khimii v 1951 g" (History of Russian Chemistry. Reports presented at the 2nd All-Union Conference on the History of Chemistry, 1951), Izd. Akad. Nauk SSSR, M., 196 (1933).

[10] I. Reiset and E. Millon, Ann. Chem. 3, 8, 280 (1843).

[11] P. Sabatier and J. B. Senderens, Ann. Chem. 8, 4, 473 (1905).

[12] H. Willand, Ber., 45, 1606 (1912).

[13] N. D. Selynskiy, Ber., 44, 3122 (1911).

[14] N. D. Selynskiy, et al., Ber., 63, 1485 (1930).

[15] N. D. Selynskiy, Ber., 45, 3678 (1912).

[16] N. D. Zelinskii and Yu. K. Yur'ev, Izv. Akad. Nauk SSSR, 851 (1930).

[17] A. F. Plate, "Kataliticheskaya Aromatizatsiya Parafinovykh Uglevodorodov" (Catalytic Aromatization of Paraffinic Hydrocarbons), M.-L., 1948.

[18] M. F. Fouwl, Platinum Metals Review 1, 4 (1957); 2, 2, 3, 4 (1958).

[19] N. I. Shuikin, Kh. M. Minachev, S. S. Novikov, N. F. Kononov, and I. L. Gagarin, Zhur. Prikl. Khim., XXXI, 1732 (1958).•

[20] N. D. Zelinskii and A. A. Balandin, "Sovetskaya Khimiya za 25 Let" (Soviet Chemistry After 25 Years), Izd. Akad. Nauk SSSR, M.-L., 188 (1944).

[21] M. Saytzeff, J. Pr. Chem. 6, 128 (1872).

[22] H. Kōlbelu and K. K. Bhattacharyya, Lieb. Ann. 618, 67 (1958).

[23] S. V. Chepigo, A. A. Balandin, N. A. Vasyunina, and A. P. Sergeev, Khim Nauka i Prom. 2, 4, 416 (1957).

• Original Russian pagination. See C. B. Translation.

[24] A. A. Balandin et al., Izv. Akad. Nauk SSSR, Otd. Khim. Nauk 3, 392 (1957).

[25] O. E. Zvyagintsev, "Materialy po Istorii Otechestvennoi Khimii. Sb. Dokladov na 2-m Vsesoyuznom Soveshchanii po Istorii Khimii v 1951 g" (The History of Russian Chemistry. Reports presented at the All-Union Conference on the History of Chemistry, 1951), M., 146 (1953).

[26] V. A. Nemilov, Izv. Sektora Platiny 19, 21 (1943).

[27] M. A. Klochko and Z. S. Medvedeva, Izv. Sektora Platiny 19, 103 (1943).

[28] L. A. Chugaev, Izv. Inst. po Izucheniyu Platiny i Drugikh Blagorodnykh Metallov 1, 1, 2 (1920).

Received May 22, 1959

FERROCYANIDE METHOD OF EXTRACTING SMALL AMOUNTS OF THALLIUM FROM SOLUTIONS OF NONFERROUS METALS

I. V. Tananaev and M. A. Glushkova

Thallium is a disperse element and so its extraction from raw materials and industrial intermediates in a pure state is time-consuming and involves considerable difficulties. The main sources of thallium are dusts from sulfuric acid factories and copper-cadmium precipitates obtained in the purification of zinc electrolyte.

Due to the small thallium content of the processed raw material, the extraction consists of two main stages: 1) preparation of a thallium concentrate (by hydrometallurgical or pyrometallurgical methods) and 2) processing of the concentrate to obtain thallium salts [1].

In the starting material, the thallium is accompanied by a whole series of metals: nickel, cobalt, copper, cadmium, zinc, lead, and sometimes germanium, arsenic and silver so that the technology of thallium is a side process accompanying the production of these nonferrous metals in a pure state.

In the present article we present a new method of extracting small amounts of thallium (of the order of 0.01 g/liter) from solutions of nonferrous metals by means of suspensions of simple ferrocyanides of these metals. Due to the difficulties of working with thallium at low concentrations, we used Tl^{204} as a radioactive tracer in the experiments.

Alkali metals, especially rubidium and cesium, are known to interact with ferrocyanide ions in the presence of ions of nonferrous metals to mixed ferrocyanides of low solubility. As was shown previously [2], as regards its capacity to form mixed ferrocyanides thallium behaves like alkali metals and is most similar to rubidium and cesium.

EXPERIMENTAL

For experiments on the isolation of small amounts of thallium from mixtures of nonferrous metals, we prepared solutions of $Fe(NO_3)_3$, $NiSO_4$, $CoSO_4$, $CuSO_4$, $CdSO_4$, $ZnSO_4$ and $Na_4[Fe(CN)_6]$. The concentrations of the $TlNO_3$ solution was determined by precipitation of the thallium as Tl_2CrO_4. The titers of the other solutions were determined by the usual methods: $NiSO_4$ by means of dimethylglyoxime, and $CoSO_4$, $CdSO_4$ and $ZnSO_4$ by the phosphate method. The determination of the concentration of an $Na_4[Fe(CN)_6]$ solution was described previously [3].

By investigating systems of the type $Tl^+ - Me_2[Fe(CN)_6 - H_2O$ (Me – Ni, Co, Cu, Cd, Zn) by the action of Tl^+ ions on aqueous suspensions of $Me_2[Fe(CN)_6]$ it was established that in all cases the thallium ions displaced ions of the nonferrous metals from the simple ferrocyanide precipitates to a certain extent. It was shown that the following compounds were formed during the displacement process: $Tl_4Ni_4[Fe(CN)_6]_3$, $Tl_2Cu_3[Fe(CN)_6]_2$, $Tl_2Co_3[Fe(CN)_6]_2$, $Tl_2Zn[Fe(CN)_6]$ and $Tl_2Cd[Fe(CN)_6]$, and the solubility of these was so low that at extremely low concentrations, thallium could be isolated from solution in the form of these compounds.

Before beginning the isolation of thallium from a solution containing a mixture of nonferrous metals, it was necessary to determine the capacity of individual simple ferrocyanides of nonferrous metals to trap thallium in the precipitate at different degrees of precipitation by them by sodium ferrocyanide. For this purpose we prepared mixtures containing 0.1 mole/liter of nonferrous metal salts and 0.01 g/liter of thallium nitrate. The mixture was precipitated with $Na_4[Fe(CN)_6]$ solution in amounts such that 100, 20, 15, 5 and 1% of the nonferrous metal was precipitated. The total volume was 100 ml.

TABLE 1

Isolation of Thallium From a Solution of a Mixture of $NiSO_4$, $CoSO_4$, $CuSO_4$, $ZnSO_4$ and $CdSO_4$ at a Total Concentration in the Starting Mixture of 0.5 mole/liter

Taken				Precipitated (in % of total metals)	Filtrate analysis		Tl found (in % of amount taken)	
blank sample		$Tl^{\bullet}NO_3$						
$Tl^{\bullet}NO_3$ solution (br)	counts/min	solution (br)	counts/min		counts per min in 2 ml	counts per min in 100 ml	in filtrate	in precipitate
0.0818	11290	0.2957	40812	5	Background	—	—	100
0.0818	11290	0.2615	36092	5				
0.0818	11290	0.2898	39998	2				
0.0818	11290	0.2985	41198	2				
0.0818	11290	0.2744	37872	1.0				
0.0818	11290	0.1760	24291	1.0				
0.0818	11290	0.2657	36671	0.8				
0.0818	11290	0.2763	37256	0.6	71	3550	9.5	90.5
0.0818	11290	0.2684	36191	0.2	208	10400	28.6	71.4
0.0597	11726	0.1960	37319	0.2	56	2800	7.4	92.6

To be able to follow the distribution of thallium between the precipitate and the solution more easily, we introduced a negligible weight of radioactive thallium (Tl^{204}) as the nitrate into the solution before the addition of $Na_4[Fe(CN)_6]$.

The mixtures prepared in this way were shaken on a mechanical shaker for 30 minutes. After this the solutions with the precipitates were left to stand for 3-4 hours (for the solid phase to settle completely) and then a definite amount of the clear solution above the precipitate was deposited on a filter and its activity determined. Knowing the activity of the amount of $Tl^{\bullet}NO_3$ introduced before precipitation of the metal and the activity of the solution obtained after precipitation, it was possible to assess the amount of thallium in the precipitate.

The investigation showed that the simple ferrocyanides of nickel, cobalt, copper, zinc, and cadmium were to a greater or lesser extent capable of abstracting thallium from solution when the concentration of the latter was 0.01 g/liter. The simple ferrocyanides of the metals investigated did not show this capacity to the same extent: the thallium was isolated in the precipitate most completely when the simple ferrocyanides of Ni, Co and Cu were used. In this case, when 1/100 of the metal taken was precipitated, the thallium was isolated practically completely from solution as indicated by the absence of radioactivity from the filtrate analyzed. The capacity of the simple ferrocyanides of cadmium and zinc to extract thallium was considerably weaker, but this was not reflected in the completeness of thallium isolation if the starting mixture contained the nonferrous metals mentioned above. Experiments on the isolation of thallium from a solution containing zinc, cadmium and nickel ions showed that the complete isolation of thallium required the presence of copper as otherwise 30% of the thallium remained in the filtrate when 1.5% of the total nonferrous metals was precipitated.

Table 1 gives the results of the isolation of thallium from a mixture of solutions of $NiSO_4$, $CoSO_4$, $CuSO_4$, $CdSO_4$ and $ZnSO_4$ with a constant content of each metal in the starting mixture of 0.1 mole/liter or a total concentration of them of 0.5 mole/liter.

The data in Table 1 indicate that 1% precipitation of the metals present is quite sufficient for complete isolation of the thallium from the mixture of solutions of nonferrous metals when the total concentration of the latter in the starting mixture is 0.5 mole/liter; a small amount of thallium remains in solution with a lower percent precipitation.

Preparation of Thallium in a Pure Form From a Precipitate of Mixed Ferrocyanides

To prepare thallium in a pure form from a precipitate of mixed ferrocyanides we attempted to decompose the ferrocyanide precipitate with alkali. It was found that up to 30% of the thallium was held by the nonferrous metal hydroxides in the decomposition process. More satisfactory results were obtained after firing the precipitate and extracting it with water. For this purpose the precipitate was collected by filtration, transferred together

TABLE 2

Extraction of Thallium From a Mixed Ferrocyanide Precipitate

Amt. of Tl introduced into mixture (g)	Obtained (in g)		Amt. of thallium extracted (in %)
	Tl_2CrO_4	Tl	
0.0997	0.0944	0.0736	74.0
0.0997	0.0810	0.0707	70.8
0.0997	0.1003	0.0781	78.3
0.0498	0.0564	0.0439	88.1
0.0498	0.0648	0.0495	99.3
0.0249	0.0320	0.0247	99.1
0.0100	0.0110	0.0086	86.0
0.0025	0.0028	0.0020	71.4
0.0025	0.0033	0.0025	100
0.0025	0.0030	0.0022	88.0

with the filter to a porcelain dish and fired in a half open muffle furnace at 700-800°.* The fired precipitate was extracted with boiling water. The solid part of the precipitate was removed by filtration and then a few drops of ammonia added to the filtrate and the thallium determined by the chromate method.

Table 2 gives data showing the qualitative aspects of the extraction of thallium from a ferrocyanide precipitate by extraction of the fired precipitate with water.

The amount of thallium introduced into the starting solution was from 0.01 g/liter to 0.40 g/liter. The total volume of the starting mixture was 250 ml with a total concentration of nonferrous metals of 0.5 mole/liter; sufficient $Na_4[Fe(CN)_6]$ was added to precipitate 1% of the total amount of nonferrous metals present in the solution.

From the data presented it follows that small amounts of thallium may be extracted from solutions containing nonferrous metals in a yield of from 80 to 100%. The ferrocyanide method proposed is convenient in that the precipitation of industrial solutions with sodium ferrocyanide does not contaminate them as the $[Fe(CN)_6]^{4-}$ ion passes quantitatively into the precipitate and not even traces remain in the solution. As regards the nonferrous metal ferrocyanides precipitated (1/100 of those contained in the solution), after extraction of the thallium they may be regenerated quantitatively.

The only complication here is the presence of ferric iron in the precipitate. However, after solution of the extracted precipitate in acid and precipitation with excess ammonia, the iron was practically completely separated from the nonferrous metals (Cu, Ni, Co, Zn, and Cd), which could be returned to the industrial cycle. Precipitation of the thallium as chromate is convenient for quantitative control of the process but is not obligatory and the thallium may be isolated as the chloride, for example, or other sparingly soluble compounds.

In the experiments the solution of extracted thallium was diluted somewhat but these solutions may be evaporated preliminarily in industry. It should be noted that it is possible to obtain comparatively concentrated solutions directly by working with large amounts of fired precipitate. In this case countercurrent principles may be used and this makes it possible to obtain practically saturated solutions of thallium salts. The thallium precipitate isolated cannot be considered a preparation of reagent purity, but its further purification and processing to a degree of purity corresponding to a reagent grade preparation present no difficulty.

The following scheme is proposed on the basis of the above account of the extraction of thallium from nonferrous metals. To the starting solution, containing a total of about 0.5 g-ion/liter (~30-40 g/liter) or less of nonferrous metals and 1-10 g/liter of H_2SO_4, is added sufficient $Na_4[Fe(CN)_6]$ solution to precipitate 1/100 of the nonferrous metal. This amount may be calculated from the mean equivalent of the nonferrous metals according to the equation

$$2E^{2+} + Na_4[Fe(CN)_6] \rightarrow E_2[Fe(CN)_6]\downarrow + 4Na^+.$$

The starting solution must contain copper equivalent to 1/5 of the total concentration of nonferrous metals. After the mixture has been stirred for 30 minutes, the precipitate is separated by filtration (or decantation), washed with water and fired at a temperature of not less than 700-900°. The residue from the firing is extracted with hot water, the solution filtered and the thallium precipitated as the chromate (or as TlCl after evaporation

*Firing at a lower temperature had disadvantages as the ferrocyanide precipitate adsorbed SO_4^{2-} ions during precipitation. During firing the latter could lead to the formation of soluble sulfates of the nonferrous metals. As a result the firing temperature of the precipitate had to be high enough (not less than 700°) to convert the soluble sulfates into insoluble oxides.

of the solution).* When countercurrent is used, the precipitation of thallium as TlCl does not require preliminary evaporation of the solution.

The residue from the thallium extraction is dissolved in H_2SO_4 and treated with excess NH_4OH. The $Fe(OH)_3$ precipitate is removed by filtration and the solution may be returned to one of the stages of the industrial process.

The isolation of thallium from solutions of nonferrous metals by the ferrocyanide method is illustrated by the following scheme.

SCHEME

Extraction of Small Amounts of Thallium From Solutions of Nonferrous Metals By the Ferrocyanide Method

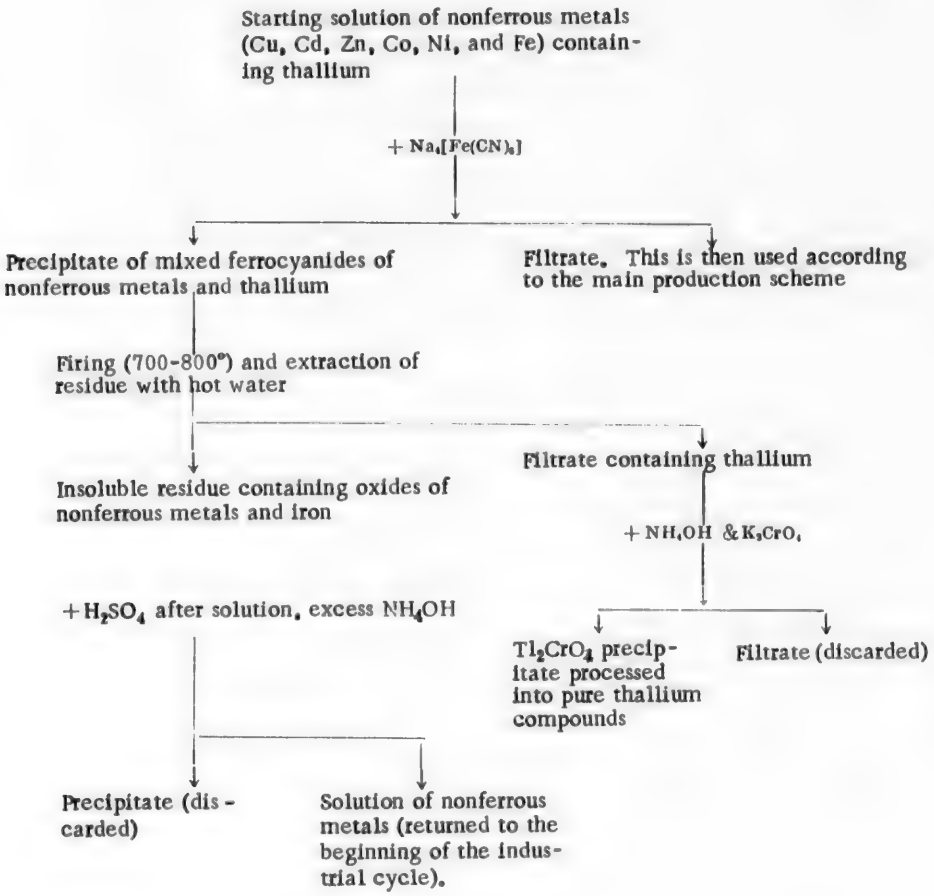
Starting solution of nonferrous metals (Cu, Cd, Zn, Co, Ni, and Fe) containing thallium
+ $Na_4[Fe(CN)_6]$
Precipitate of mixed ferrocyanides of nonferrous metals and thallium
Filtrate. This is then used according to the main production scheme
Firing (700-800°) and extraction of residue with hot water
Insoluble residue containing oxides of nonferrous metals and iron
Filtrate containing thallium
+ NH_4OH & K_2CrO_4
+ H_2SO_4 after solution, excess NH_4OH
Tl_2CrO_4 precipitate processed into pure thallium compounds
Filtrate (discarded)
Precipitate (discarded)
Solution of nonferrous metals (returned to the beginning of the industrial cycle).

SUMMARY

A method is proposed for isolating small amounts (~0.01 g/liter) of thallium from solutions of nonferrous metals (Cu, Ni, Co, Cd, and Zn), containing ~0.5 g-ion/liter (total) of the latter. The method consists of precipitating the starting solution with sufficient $Na_4[Fe(CN)_6]$ solution to precipitate 1% of the total amount of metals present. The precipitate obtained is fired at 700-800°, the thallium extracted with water and the insoluble residue of nonferrous metals returned to the process.

* It is also possible to precipitate the thallium as $Tl(OH)_3$ with alkali in the presence of an oxidant.

LITERATURE CITED

[1] G. A. Meerson and A. N. Zelikman, Metallurgy of Rare Elements [In Russian], Moscow, 1955, p. 528.

[2] I. V. Tananaev and M. A. Glushkova, Zhur. Neorg. Khim. II, 3, 586 (1957).

[3] I. V. Tananaev, M. A. Glushkova and G. B. Seifer, Chemistry of Rare Elements [In Russian], 1, 60 (1954).

Received September 5, 1958

EXTRACTION OF TANTALUM AND NIOBIUM FROM SULFURIC ACID SOLUTIONS WITH CYCLOHEXANONE*

Ya. G. Goroshchenko, M. I. Andreeva and A. G. Babkin

Extraction with organic liquids together with chromatography is one of the contemporary methods of fine chemical technology. A positive aspect of extraction methods of separation is high specificity and selectivity. Successful experiments on the separation of niobium and tantalum by liquid extraction were carried out by Stevenson and Hicks [1] for developing chemical analysis methods and by Werning and his co-workers [2] for developing an industrial method of separating these elements.

Tantalum is extracted from hydrofluoric acid solutions and from solutions of hydrofluoric and mineral acids by methyl isobutyl ketone, cyclohexanone and other ketones. Niobium is extracted into the organic phase only at high concentrations of mineral and hydrofluoric acids. Extraction of niobium and tantalum with these ketones is specific and convenient for freeing them from traces of iron, aluminum, titanium, tin, etc. Tantalum is selectively extracted into the aqueous phase by treatment of a solution of anhydrous niobium and tantalum chlorides in methyl isobutyl ketone and diisobutyl ketone with concentrated hydrochloric acid [3]. Dilute hydrochloric acid extracts niobium from the organic phase.

We carried out experiments on the extraction of tantalum and niobium with cyclohexanone, applicable to the sulfuric acid treatment of loparite and perovskite concentrates.**

Niobium and tantalum were not extracted from sulfuric acid solutions by cyclohexanone without the addition of complex-forming ions. Extractions of tantalum by cyclohexanone were promoted by the addition of fluoride ion to the solution; niobium was extracted from sulfuric acid solution in the presence of fluoride and thiocyanate ions (Table 1). Our investigations showed that tantalum was practically irreversibly extracted by cyclohexanone from solutions of sulfuric acid and ammonium sulfate with fluoride ion added. Niobium, which was partially extracted together with the tantalum, was completely re-extracted from the organic phase and separated from the tantalum. This characteristic of the extraction of tantalum by cyclohexanone may be used as the basis of a method of separating it from niobium.

Characteristics of the Extraction of Tantalum and Niobium by Cyclohexanone From Solutions of Sulfuric Acid and Ammonium Sulfate

Procedure. Sulfuric acid solutions of niobium and tantalum were prepared from technical niobium pentoxide, obtained from loparite, and metallic tantalum powder containing 0.32% Nb. In individual cases, niobium pentoxide, freed from tantalum by cyclohexanone extraction, was used. To the starting niobium- and tantalum-containing materials was added about 20% of titanium dioxide and then they were fused with ammonium sulfate and sulfuric acid at 300°. The melt was extracted with water. The solutions obtained contained 400-500 g/liter of H_2SO_4, about 200 g/liter of $(NH_4)_2SO_4$ and varying concentrations of niobium and tantalum. The titanium was introduced as a complex-former to stabilize the niobium and tantalum solutions. The concentration of sulfuric acid and ammonium sulfate in the starting solutions corresponded to the conditions of the separation of titanium and earth acids by the sulfuric acid method [4].

*Communication II of a series of papers on the problem of separating niobium and tantalum.

**Cyclohexanone was chosen as it is obtained from a cheap organic synthesis product, namely phenol.

TABLE 1

Effect of Complex-Formers on the Extraction of Tantalum and Niobium From Sulfuric Acid Solutions With Cyclohexanone

Complex-formers	Amt. of complex former (in g/ liter)	Amt. extracted into organic phase (in %)	
		Nb_2O_5	Ta_2O_5
NH_4F	100	60.0	100.0
NH_4Cl	200	0.3	0.0
KBr	200	0.0	1.4
KI	200	0.0	0.0
NH_4CNS	200	39.4	0.0
NH_4NO_3	200	0.0	0.0
CH_3COONH_4	200	0.0	1.9
NH_4NaHPO_4	50	0.0	0.0
$KClO_3$	200	0.0	1.0
Na_2SiF_6	10	1.5	2.5
H_3BO_3	Saturated solution	1.5	1.8
$(NH_4)_2C_2O_4$	30	2.3	0.0
$C_4H_6O_6$ (tartaric acid)	140	1.5	0.0
$C_6H_8O_7$ (citric acid)	160	1.4	0.0

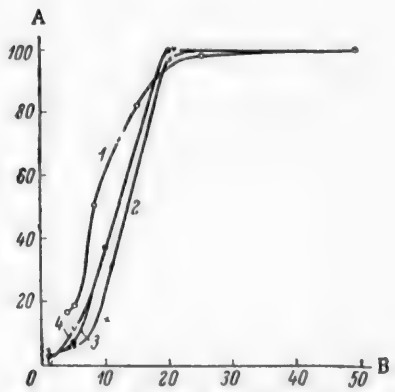

Fig. 1. Extraction of tantalum with cyclohexanone from solutions of sulfuric acid and ammonium sulfate. A) Amount of Ta_2O_5 extracted into organic phase (in %); B) NH_4F content (in g/liter). Amounts of H_2SO_4, $(NH_4)_2SO_4$, Ta_2O_5, Nb_2O_5, TiO_2 in solutions, respectively (in g/liter): 1) 470, 215, 7.65, 1.95, 0.28; 2) 314, 143, 5.10, 1.28, 0.19; 3) 235, 108, 3.83, 0.96, 0.14; 4) 157, 72, 2.55, 0.64, 0.93.

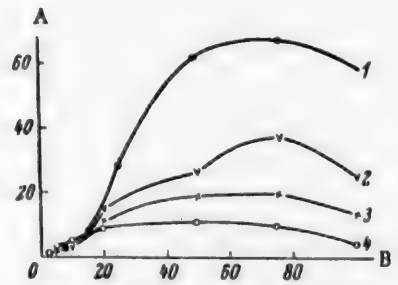

Fig. 2. Extraction of niobium with cyclohexanone from solutions of sulfuric acid and ammonium sulfate. A) Amount of Nb_2O_5 extracted into cyclohexanone phase (in %); B) NH_4F content (in g/liter). Amount of H_2SO_4, $(NH_4)_2SO_4$, Ta_2O_5, Nb_2O_5, TiO_2 in solution, respectively (in g/liter): 1) 470, 215, 1.86, 7.11, 0.50; 2) 314, 143, 1.23, 4.74, 0.33; 3) 235, 108, 0.93, 3.55, 0.25; 4) 157, 72, 0.62, 2.37, 0.17.

The cyclohexanone used was "pure" grade.

The fluoride ion was introduced into the solution as ammonium fluoride of "analytically pure" grade.

The extraction and re-extraction were carried out by shaking the sulfuric acid solution and cyclohexanone in a glass separating funnel for 5 minutes. The layers were separated after 10 minutes. The distribution of niobium and tantalum between the aqueous and cyclohexanone phases was determined with the aid of the radioactive isotopes Ta^{182} and Nb^{95}.

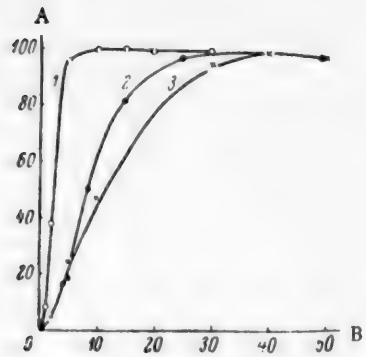

Fig. 3. Effect of tantalum concentration and NH_4F added on the extraction by cyclohexanone from a solution containing 470 g/liter of H_2SO_4 and 215 g/liter of $(NH_4)_2SO_4$. A) Amount of Ta extracted into cyclohexanone phase (in %); B) NH_4F content (in g/liter). Amounts of Ta_2O_5, Nb_2O_5 and TiO_2 in solution, respectively (in g/liter): 1) 3.11, 0.31, 0.13; 2) 7.65, 1.92, 0.28; 3) 32.3, 0, 0, 1.3.

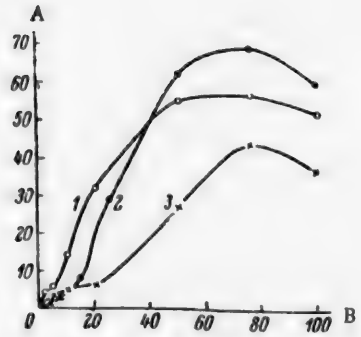

Fig. 4. Effect of niobium concentration and NH_4F added on extraction by cyclohexanone. A) Amount of Nb extracted into cyclohexanone phase (in %); B) NH_4F content (in g/liter). Amounts of Ta_2O_5, Nb_2O_5 and TiO_2 in solution, respectively (in g/liter): 1) 3.0, 3.0, 0.33; 2) 1.86, 7.11, 0.50; 3) 5.2, 20.0, 1.4.

The radioactive isotopes were introduced into the starting solutions as ammonium sulfate solutions. Where necessary radioactive isotopes of high activity were used for measuring the distribution of niobium and tantalum with high accuracy.

Effect of Dilution of the Solution With Water and the NH_4F Concentration on the Extraction of Niobium and Tantalum. The starting solutions contained 470 g/liter of H_2SO_4 and 215 g/liter of $(NH_4)_2SO_4$. They were extracted with equal volumes of cyclohexanone.

Extraction of tantalum from the sulfuric acid solution into the cyclohexanone layer was increased by the addition of a large amount of ammonium fluoride. The extraction of tantalum by cyclohexanone reached 100% over a wide range of sulfuric acid concentrations (Fig. 1).

The niobium was extracted by cyclohexanone best from solutions with a high sulfuric acid concentration (Fig. 2). An increase in the ammonium fluoride concentration of the solution promoted niobium extraction.

Effect of the Niobium and Tantalum Concentrations in the Starting Solution and the Addition of NH_4F on Extraction by Cyclohexanone. The extraction was carried out on a solution containing 470 g/liter of H_2SO_4 and 215 g/liter of $(NH_4)_2SO_4$ with an equal volume of cyclohexanone.

When a small amount of ammonium fluoride was added, 98-99% of the tantalum was extracted with cyclohexanone (Fig. 3). Practically complete extraction of tantalum was observed when the amount of ammonium fluoride added was 8-20 g/liter in excess of the amount theoretically required for formation of the complexes TaF_7'', $NbOF_5''$ and TiF_6''.

The curves of niobium extraction by cyclohexanone have maxima (Fig. 4). The extraction of 40-50% (to the left of the maximum on the curve) of the niobium in solution required the addition of 40-50 g/liter excess of NH_4F. The niobium concentration in the cyclohexanone phase was 2-8 g/liter, depending on the niobium content of the original solution.

The appearance of the maximum on the niobium extraction curves may be explained by a fall in the concentration of free sulfuric acid on addition of ammonium fluoride due to the formation of ammonium bisulfate.

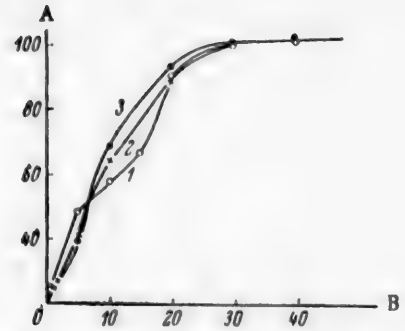

Fig. 5. Extraction of tantalum by cyclohexanone in the presence of niobium from sulfuric acid solutions containing 400 g/liter of H_2SO_4 and 200 g/liter of $(NH_4)_2SO_4$. A) Amount of Ta_2O_5 extracted into cyclohexanone phase (in %); B) NH_4F content (in g/liter). Amounts of Ta_2O_5 and Nb_2O_5 in solution, respectively (in g/liter): 1) 0.87, 12.68; 2) 1.79, 12.02; 3) 2.84, 11.31.

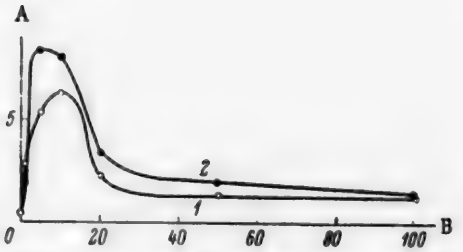

Fig. 6. Extraction of titanium by cyclohexanone from sulfuric acid solution containing 400 g/liter of H_2SO_4 and 200 g/liter of $(NH_4)_2SO_4$. A) Amount of TiO_2 extracted into cyclohexanone phase (in %); B) NH_4F content (in g/liter). TiO_2 content of starting solution (in g/liter): 1) 1.04, 2) 0.50.

TABLE 2

Extraction of Tantalum by Cyclohexanone From Solutions Containing 400 g/liter of H_2SO_4 and 200 g/liter of $(NH_4)_2SO_4$ in the Presence of Niobium

Amount of NH_4F (in g/liter)	$K = \frac{C_{Ta\ org.}}{C_{Ta\ aq.}}$	Amt. of tantalum extracted into cyclohexanone phase (in %)
Contents of starting solution (in g/liter): Ta_2O_5 0.87, Nb_2O_5 12.68, TiO_2 3.25		
5	0.92	47.9
10	1.33	57.1
15	2.01	66.8
20	8.77	89.8
30	295.60	99.662 ± 0.007
40	3910.00	99.974 ± 0.003
Contents of starting solution (in g/liter): Ta_2O_5 1.79, Nb_2O_5 12.02, TiO_2 3.17		
5	0.68	40.3
10	1.80	64.3
20	8.69	89.7
30	394.70	99.747 ± 0.006
40	2480.0	99.960 ± 0.002
Contents of starting solution (in g/liter): Ta_2O_5 2.84, Nb_2O_5 11.31, TiO_2 3.13		
5	0.65	39.3
10	2.17	68.4
20	13.27	93.0
30	354.7	99.719 ± 0.006
40	3668.7	99.973 ± 0.003
50	3533.7	99.972 ± 0.003
100	833.8	99.887 ± 0.002

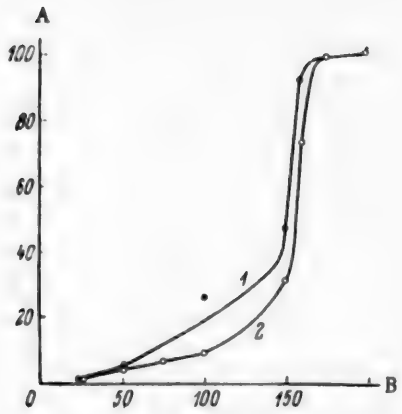

Fig. 7. Extraction of tantalum with cyclohexanone from sulfuric acid solutions obtained by dissolving loparite and perovskite in sulfuric acid. A) Amount of Ta_2O_5 extracted into organic phase (in %); B) NH_4F content (in g/ liter). Amount of Ta_2O_5, Ng_2O_5, TiO_2, TR_2O_3, H_2SO_{4act} in solution, respectively (in g/ liter): 1) 0.14, 1.5, 68, 4.5, 408; 2) 1.0, 16.5. 66, 4.5, 414. Solutions from concentrates (1) perovskite (2) loparite.

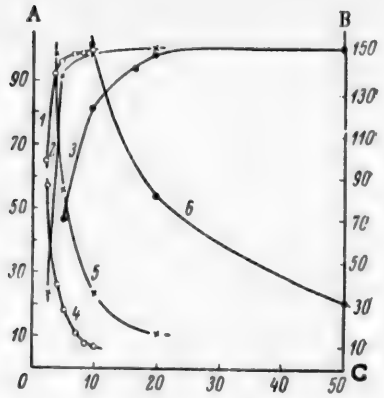

Fig. 8. Effect of amount of cyclohexanone used on the extraction of tantalum from sulfuric acid solution containing 400 g/liter of H_2SO_4 and 200 g/liter of $(NH_4)_2SO_4$. A) Amount of Ta_2O_5 extracted into organic phase (in %); B) concentration of Ta_2O_5 in organic phase (in %); C) cyclohexanone used per 100 ml of solution (in ml). Amounts of Ta_2O_5 and Nb_2O_5, respectively, contained in starting solution (in g/liter); 1) 4-0.83 and 11.3; 2) 5-2.84 and 11.31; 3) 6-15.1 and 17.1. Curves: 1, 2 and 3) extraction of Ta_2O_5; 4, 5 and 6) Ta_2O_5 concentration in cyclohexanone phase.

Extraction of Tantalum With Cyclohexanone in the Presence of Niobium. The tantalum was extracted from a solution containing 400 g/liter of H_2SO_4, 200 g/liter of $(NH_4)_2SO_4$ and 11-13 g/liter of Nb_2O_5.

Tantalum was extracted by cyclohexanone in the presence of niobium just as well as in its absence (Fig. 5). However, the extraction of practically 100% of the tantalum required the addition of more NH_4F as part of the fluoride ion was bound by niobium.

A high degree of extraction of tantalum by cyclohexanone was achieved with the corresponding addition of ammonium fluoride. The residual concentration of tantalum in the aqueous phase after extraction fell to 0.03-0.04% of its initial value (Table 2). The extraction of tantalum with cyclohexanone from solutions of sulfuric acid and ammonium sulfate made it possible to obtain niobium in the aqueous phase with very small traces of tantalum. In our experiments the tantalum pentoxide impurity in niobium pentoxide in aqueous solution was reduced from 7-25% to 0.003-0.013% by one extraction with an ammonium fluoride content of 40 g/liter.

The data presented in Table 2 for close to 100% extraction of tantalum were obtained by measurements of high accuracy. They showed that the maximum extraction of tantalum occurred at an NH_4F concentration of about 50 g/liter. A further increase in the NH_4F concentration produced a reduction in tantalum extraction, probably due to decrease in the concentration of sulfuric acid in the solution.

Extraction of Titanium By Cyclohexanone. A solution containing 400 g/liter of H_2SO_4 and 200 g/liter of $(NH_4)_2SO_4$ was used for the experiments. An equal volume of cyclohexanone was used for extraction.

Titanium was extracted by cyclohexanone to a very small extent (less than 10%) (Fig. 6). The titanium extraction curves had a maximum at an NH_4F concentration of 5-10 g/liter. The presence of titanium did not affect the extraction of tantalum.

TABLE 3

Distribution of H_2F_2 Between Aqueous and Cyclohexanone Phases at Room Temperature

H_2F_2 concentration (in %)		H_2F_2 in cyclohexanone phase
in cyclohexanone phase	in aqueous phase	H_2F_2 in aqueous phase
Cyclohexanone + H_2O + H_2F_2		
0.28	0.29	0.97
1.65	1.66	0.99
2.38	2.33	1.02
5.42	6.25	0.87
10.10	12.90	0.78
Cyclohexanone + [400 g/liter of H_2SO_4 and 200 g/liter of $(NH_4)_2SO_4$] + H_2F_2		
0.3	0.07	4.3
0.6	0.21	2.9
2.52	1.21	1.88
4.68	3.15	1.49
8.55	7.89	1.08

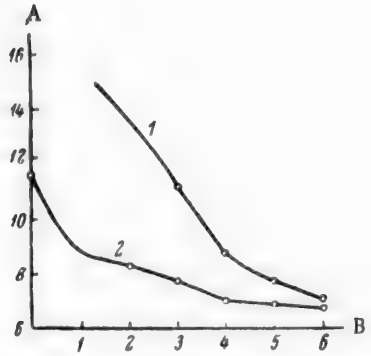

Fig. 9. Change in F:Ta ratio (atomic) during a water wash of cyclohexanone saturated with the fluoride complex of tantalum from hydrofluoric acid solution. A) Ratio F:Ta (atomic), B) re-extraction number. Phase: 1) aqueous, 2) cyclohexanone.

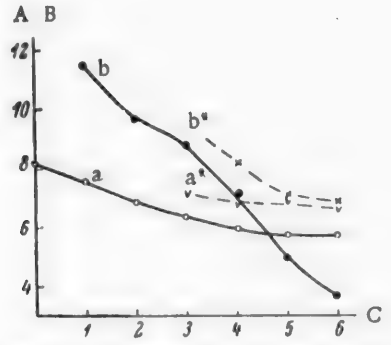

Fig. 10. Change in the F:Ta and $(F + {}^1/_2SO_4)$:Ta ratios (atomic) during a water wash of cyclohexanone saturated with the fluoride complex of tantalum from an ammonium sulfate solution with hydrofluoric acid added. A) $(F + {}^1/_2SO_4)$:Ta ratio (atomic), B) F:Ta ratio (atomic), C) re-extraction number. F:Ta ratio in the cyclohexanone (a) and aqueous (b) phases and $(F + {}^1/_2SO_4)$:Ta ratio in the cyclohexanone (a') and aqueous (b') phases.

Tantalum was completely extracted from solutions containing a high concentration of titanium but in this case the NH_4F requirement was increased. As Fig. 7 shows, with the addition of an appropriate amount of NH_4F, tantalum may be extracted completely from solutions obtained by dissolving perovskite and loparite in sulfuric acid without a preliminary separation of the titanium.

Effect of the Amount of Cyclohexanone Used on the Extraction of Tantalum From Sulfuric Acid Solution. A decrease in the amount of cyclohexanone used reduced the extraction of tantalum only after a certain limit which depended on the tantalum concentration in the starting aqueous solution (Fig. 8).

TABLE 4

Re-Extraction of Tantalum and Niobium From Cyclohexanone With a Solution of Sulfuric Acid and Ammonium Sulfate Containing 400 g/liter of H_2SO_4 and 200 g/liter of $(NH_4)_2SO_4$. Diluted With Water

Re-extraction No.	$K = \frac{C_{Ta\ org.}}{C_{Ta\ aq.}}$ $(K \cdot 10^3)$	Total extraction of tantalum into aqueous phase	Niobium pentoxide impurity in tantalum pentoxide in organic phase (in %)	$K = \frac{C_{Nb\ org.}}{C_{Nb\ aq.}}$	Total extraction of niobium into aqueous phase (in %)	Tantalum pentoxide impurity in niobium pentoxide in aqueous phase (in %)
			Dilution	1 : 0		
1	10.8	0.009	64.3	0.458	68.6	0.0023
2	4.4	0.032	22.6	0.194	94.9	0.0059
3	4.3	0.055	1.46	0.0546	99.74	0.0096
4	1.82	0.11	0.11	0.086	99.98 ± 0.01	0.019
5	1.98	0.16	0.05	0.7	99.991 ± ± 0.003	0.028
			Dilution	2 : 1		
1	18.9	0.005	60.6	0.370	73.0	0.0012
2	4.0	0.031	14.7	0.126	97.0	0.0054
3	3.8	0.057	0.29	0.02	99.95 ± 0.1	0.010
4	1.91	0.11	—	—	100.00 ± 0.1	0.019
5	0.72	0.25				0.044
6	0.20	0.73				0.128
7	0.055	2.51				0.44
			Dilution	1 : 1		
1	1.17	0.086	55.1	0.274	78.5	0.019
2	2.86	0.12	9.47	0.093	98.2	0.021
3	1.44	0.19	0.34	0.04	99.94	0.034
4	0.58	0.36	—	—	100.00	0.063
5	0.184	0.90	—	—		0.158
			Dilution	1 : 2		
1	1.12	0.089	39.1	0.127	88.8	0.018
2	2.44	0.13	2.24	0.04	99.60	0.023
3	1.31	0.21	—	—	100.00	0.037
4	1.23	0.29				0.051
5	1.05	1.23				0.22
			Dilution	1 : 4		
1	0.82	0.122	34.3	0.100	90.86	0.024
2	1.31	0.20	1.80	0.04	99.68	0.035
3	0.47	0.41	—	—	100.00	0.072
4	0.169	1.00				0.175
5	0.041	3.37				0.59

Distribution of H_2F_2 Between Aqueous and Cyclohexanone Phases at Room Temperature. The extraction of H_2F_2 by cyclohexanone from hydrofluoric acid and from mixtures of hydrofluoric and sulfuric acids in the presence of ammonium sulfate was investigated.

In the extraction of H_2F_2 from an aqueous solution of hydrofluoric acid with cyclohexanone, the H_2F_2 was approximately equally distributed between the aqueous and organic phases (Table 3). Hydrofluoric acid was extracted mainly into the organic phase from a solution of sulfuric acid and ammonium sulfate by cyclohexanone and the extraction was greater the lower the hydrofluoric acid concentration in the aqueous phase.

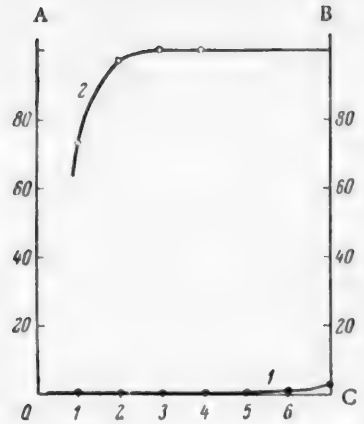

Fig. 11. Re-extraction of tantalum and niobium from cyclohexanone with a solution of sulfuric acid and ammonium sulfate containing 400 g/liter of H_2SO_4 and 200 g/liter of $(NH_4)_2SO_4$, diluted with water in a ratio of 2 : 1. A) Amount of Ta_2O_5 extracted (in %), B) amount of Nb_2O_5 extracted (in %), C) wash number. Extraction of tantalum (1) and niobium (2).

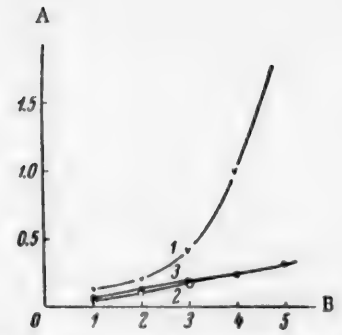

Fig. 12. Effect of the addition of NH_4F on the re-extraction of tantalum from cyclohexanone with a solution of sulfuric acid and ammonium sulfate containing 400 g/liter of H_2SO_4 and 200 g/liter of $(NH_4)_2SO_4$, diluted with water in a ratio of 1 : 4. A) Amount of Ta_2O_5 extracted into aqueous phase (in %); B) number of wash. Re-extraction of tantalum with the addition of NH_4F (in g/liter): 1) without additive, 2) 5, 3) 10.

Investigation of the Composition of the Tantalum Complex Extracted By Cyclohexanone. To establish the composition of the tantalum complex extracted by cyclohexanone we studied the change in the ratio F : Ta and $(F + {}^1/_2SO_4)$: Ta during the re-extraction of tantalum from the organic phase with water. The cyclohexanone for the experiments was saturated with tantalum from a solution in hydrofluoric acid and in a mixture of sulfuric acid and ammonium sulfate with hydrofluoric acid added. After each re-extraction, the tantalum, fluorine and sulfate ion contents of the aqueous and organic phases were determined. In experiments with hydrofluoric acid solutions, the fluorine was determined by titration with KOH in the presence of $CaCl_2$ with methyl red as indicator [5] and in experiments with sulfate fluoride solutions, by distillation as H_2SiF_6 [6]. The sulfate ion was determined by titration with KOH with the introduction of a correction for H_2F_2 from data on the determination of fluorine as H_2SiF_6.

The ratio of F : Ta and $(F + {}^1/_2SO_4)$: Ta (atomic) in the re-extraction of tantalum with water from cyclohexanone was approximately 7 (Figs. 9 and 10). This indicates that tantalum was extracted from hydrofluoric acid by cyclohexanone in the form of H_2TaF_7 and from sulfuric and hydrofluoric acids as $H_2TaF_x(SO_4)^{1}/_2(7-x)$. When judged by chemical analysis data, from 1 to 3 fluorine atoms in the tantalum fluoride – sulfate complex were replaced by sulfate groups.

Re-Extraction of Tantalum and Niobium From Cyclohexanone. For the experiments we used a solution of tantalum and niobium in cyclohexanone, obtained by extraction from an equal volume of an aqueous solution containing the following (in g/liter): H_2SO_4 400, $(NH_4)_2SO_4$ 200, Ta_2O_5 1.50, Nb_2O_5 12.5 and TiO_2 2.97. Before the extraction, 60 g/liter of ammonium fluoride was added to the aqueous solution. Under these conditions the tantalum passed into the organic phase completely and 30-40% of the niobium was extracted.

To determine the conditions for washing out tantalum from niobium impurity and extracting it from the organic phase, experiments were carried out on re-extraction with water, ammonium sulfate solution, sulfuric acid and a mixture of sulfuric acid and ammonium sulfate.

The re-extraction was carried out by shaking equal volumes of the cyclohexanone phase and the wash liquid in a glass separating funnel.

Water, sulfuric acid and ammonium sulfate solution showed no great selectivity in the re-extraction of tantalum and niobium from cyclohexanone. Although tantalum was re-extracted to a lesser estent than niobium

by these liquids, the tantalum removed by one re-extraction exceeded 2-3%. Due to this the niobium in the aqueous phase contained appreciable tantalum impurity.

A mixture of sulfuric acid and ammonium sulfate only re-extracted niobium from cyclohexanone at first (Table 4, Fig. 11). Tantalum was re-extracted by solutions of sulfuric acid and ammonium sulfate after many washes with the liquid or with considerable dilution of the wash liquid with water.

The re-extraction of tantalum with a mixture of sulfuric acid and ammonium sulfate was reduced by the addition of a small amount of NH_4F to the wash liquid (Fig. 12).

By using a wash liquid with an appropriate composition it is possible to achieve an extremely good separation of niobium and tantalum, extracted by cyclohexanone, and obtain them as pure products. The niobium pentoxide impurity in tantalum in cyclohexanone may be reduced to 0.05%. Niobium may be obtained with a tantalum pentoxide impurity of less than 0.01%.

DISCUSSION OF RESULTS

Cyclohexanone has a high specificity with respect to only tantalum in extraction from solutions of sulfuric acid and ammonium sulfate in the presence of fluoride ion. The extraction of tantalum is a chemical process which may be represented by the following equation:

$$C_5H_{10}CO + H_2TaF_x(SO_4)_{1/2(7-x)} = C_5H_{10}C\begin{matrix}OH\\ [TaF_x(SO_4)_{1/2(7-x)}]H.\end{matrix}$$

The compound of tantalum with cyclohexanone is only stable when there is excess fluoride ion in the organic phase, as follows from the extraction experiments. The extraction of tantalum by cyclohexanone and its re-extraction by aqueous solutions is therefore controlled by the distribution of hydrofluoric acid between the aqueous and organic phases.

A mixture of sulfuric acid and ammonium sulfate favors the extraction of tantalum because the equilibrium distribution of H_2F_2 between this mixture and cyclohexanone is displaced towards the latter (Table 3).

The very small re-extraction of tantalum by this mixture is also the results of the predominant concentration of H_2F_2 in the organic phase. The re-extraction of tantalum from cyclohexanone occurs to an appreciable extent only after the hydrofluoric acid has been washed out of the latter; as a mixture of sulfuric acid and ammonium sulfate extracts little H_2F_2 from the organic phase, the re-extraction of tantalum increases slowly with an increase in the number of washes.

With the addition of NH_4F, niobium is partially extracted by cyclohexanone but not more than 60-70%. The fact that niobium shows acidic properties more than tantalum is of importance here. The formation of the fluoride complex of niobium, which is extracted by cyclohexanone, requires a higher concentration of hydrofluoric acid than in the case of tantalum. For this reason niobium is re-extracted from cyclohexanone before tantalum.

SUMMARY

1. By studying the extraction of tantalum and niobium with cyclohexanone from solutions of sulfuric acid and ammonium sulfate with the addition of ammonium fluoride it was confirmed that cyclohexanone is specific for the extraction of tantalum and niobium from sulfate – fluoride solutions. Cyclohexanone extracts predominantly tantalum and, to a lesser extent, niobium. The extraction of tantalum by cyclohexanone made it possible to reduce the tantalum concentration in the aqueous phase to 0.03-0.04% and less of the initial value. Not more than 60-70% of the niobium was extracted by cyclohexanone.

2. Tantalum was extracted by cyclohexanone from solutions of sulfuric acid and ammonium sulfate in the presence of fluoride ion in the form of a fluoride – sulfate complex with the composition $H_2TaF_X(SO_4)^1/_2(_{7-X})$. The fluoride – sulfate complex of tantalum was very poorly extracted from cyclohexanone by solutions of sulfuric acid and ammonium sulfate, while niobium was readily extracted by the latter. This property may be used as the basis of a method of separating niobium and tantalum and obtaining highly pure pentoxides of these elements.

3. The extraction by cyclohexanone may find application in the preparation of tantalum and niobium pentoxides from intermediates in the processing of loparite, perovskite and other titanium – niobium – tantalum concentrates, including products of high purity.

LITERATURE CITED

[1] P. C. Stevenson and P. C. Hicks, Anal. Chem. 25 (10), 1519 (1953).

[2] I. R. Werning, K.B.Higbie, I. T. Grace, B. F. Speece and H. L. Gilbert, Ind. Eng. Ch. 46, 644 (1954).

[3] I. R. Werning and K. B. Higbie, Ind. Eng. Ch. 46, (12), 2491 (1954).

[4] Ya. G. Goroshchenko, Candidate's Dissertation (1951).

[5] I. V. Tananaev and G. S. Savchenko, Zhur. Priklad. Khim. 7, 1071 (1934).

[6] I. V. Tananaev, Zhur. Priklad. Khim. 5, 6-7 (1932).

Received May 30, 1958

EXTRACTION AND SEPARATION OF NIOBIUM AND TITANIUM FROM OXALIC ACID SOLUTIONS BY AN ION-EXCHANGE METHOD

I. D. Fridman and I. N. Yudina

Central Scientific Research Institute of Geological Prospecting

One of the known methods of processing niobium – titanium concentrates is a combined treatment of them with sulfuric and oxalic acids: the concentrate is broken down with sulfuric acid of sp. g. 1.84 and then the break-down product is leached with dilute oxalic acid. Niobium, titanium, iron and other components pass into solution.

The extraction of titanium-free niobium from the solution is one of the complex problems in the processing of titanium – niobium raw materials. The hydrolytic methods used in this case for separating titanium from niobium, which are based on the difference in the pH at which the hydroxides of these metals separate, do not give niobium free from titanium. The degree of contamination of the niobium hydroxide by titanium depends on the titanium content of the raw material processed.

Ion-exchange methods of separating rare elements have become widespread in recent years. This method is effective in the separation of niobium and tantalum from hydrofluoric acid solutions [1], zirconium and titanium from nitric acid solutions [2], zirconium and hafnium from hydrochloric acid solutions [3] and especially in the separation of rare earths [4].

Work has been reported on the use of ion exchange for freeing niobium from titanium. To prepare a pure niobium preparation, the Ural Polytechnic Institute developed a method of freeing niobium from titanium by means of cationites in the H-form. The separation method was based on the capacity of freshly precipitated niobic acid to form a colloidal solution after treatment with concentrated hydrochloric acid and subsequent dilution with water, when the niobium was not adsorbed from this solution by a cationite while titanium and other impurities, which were present as cations, were removed from the solution by an ion-exchange process [5]. The Hydronickel [Gidronikel'] Institute and the Metallurgy Institute of the Academy of Sciences of the USSR used an ion-exchange method for freeing niobium chlorides (hydroxides) from titanium. The niobium was introduced into hydrofluoric [6] or hydrochloric acid [7] solution for this purpose. The niobium and titanium were extracted and separated from these solutions on the anionites ÉDÉ10P and ÉDÉ10, respectively, in the Cl-form. Niobium was selectively extracted from the resins with hydrochloric acid and a mixture of it with hydrofluoric acid.

We investigated the possibility of using an ion-exchange process for the extraction and separation of niobium and titanium from oxalic acid solutions, obtained during the combined break down of zirconium – titanium – niobium gravitation concentrate with sulfuric and oxalic acids. The composition of the gravitation concentrate was as follows (in %): ZrO_2 18.0, Nb_2O_5 8.1, TiO_2 7.4, SiO_2 27.5, Fe_2O_3 8.51, CaO 4.40, MgO 0.78, Al_2O_3 13. In this case the concentrate was sintered with sulfuric acid (sp. g. 1.84) in a ratio of 1 : 1 (by weight) at 300° for an hour and then the sulfate cake was leached with 10% oxalic acid solution. At this, 95% of the niobium and 84% of the titanium passed into solution and the zirconium remained completely in the solid residue.

Experiments on the absorption of niobium and titanium by the cation-exchange resin KU-2 in the H-form and the anion-exchange resin ÉDÉ10P in the Cl-form from 8-10% oxalic acid solutions showed that in such solutions niobium and titanium were present in the form of complex anions with similar sorption properties.

Cation absorption of niobium in oxalic acid solutions was not observed at all and titanium was absorbed very weakly.

TABLE 1

Absorption of Anions of Niobium, Titanium, Iron and Oxalic Acid by ÉDÉ10P Resin in the Chloride Form During 4-Stage Ion Exchange, Amount of Solution Used, 100 ml, containing 720 mg of Nb_2O_5, 560 mg of TiO_2, 710 mg of Fe_2O_3 and 10 g of $H_2C_2O_4$

Name of product	Wt. of ash (in mg)	Content in resin ash (in %)			Content in resin (in mg)				Extracted into resin (in %)			
		Nb_2O_5	TiO_2	Fe_2O_3	Nb_2O_5	TiO_2	Fe_2O_3	$H_2C_2O_4$	Nb_2O_5	TiO_2	Fe_2O_3	$H_2C_2O_4$
Resin ash from 1st stage of absorption	690	41.25	12.0	41.56	284	82.8	286.3	4400	42.96	13.49	40.26	44
Resin ash from 2nd stage of absorption	624	27.5	34	32.2	171.5	212.6	199.68	2460	25.94	34.6	28.12	24.6
Resin ash from 3rd stage of absorption	500	30	36.25	30.18	150	181.25	150.9	1640	22.68	29.58	21.28	16.4
Resin ash from 4th stage of absorption	304	18.3	45.0	24.61	55.7	136.8	73.8	500	8.42	22.33	10.34	5
Final solution from 4th stage of absorption	300	Traces						—	—	—	—	5
		Total . . .			661	613.5	710.68	9000	100	100	100	90

It is known that metals with similar sorption properties can only be separated when the ion exchange is in two stages: the initial mixture of ions is sorbed by means of an ionite and then the ions are selectively eluted from the resin.

Sorption of Anions On ÉDÉ10P Type Anion-Exchange Resin

The oxalic acid solutions for the experiments contained 7.2 g/liter Nb_2O_5, 5.6 g/liter TiO_2, 7.1 g/liter Fe_2O_3 and 90 g/liter oxalic acid. The complex anions of niobium and titanium were sorbed on the resin under static conditions by stirring a sample of anionite with the oxalic acid solution in porcelain beakers with the stirrer operating at 140 rev/min. The anionite used was ÉDÉ10P type resin in the chloride form with a grain size of 0.4-0.1 mm.

Before use the anionite was subjected to a special process, which consisted of standing in water for a day (for swelling) and then the swollen anionite was soaked for 2-3 hours with a 5% solution of NaOH; after being washed with water, the resin was kept in 5% HCl solution for 2-3 hours. The amount of metals absorbed by the anionite was determined by combustion of a sample of the charged resin in a muffle furnace and chemical analysis of the ash.

We established that under static conditions when 100 ml of solution was stirred successively with 4 samples of resin weighing 10 g each, the niobium and tantalum passed almost completely into the resin. The contact time of the solution with each portion of resin was 60 minutes. Simultaneously with the niobium and titanium, all the iron in the solution and 90% of the oxalic acid were extracted into the resin. The results of one of these experiments are given in Table 1.

TABLE 2

Extraction of Niobium and Tantalum From Saturated Resin Sample 10 g, Containing 536 mg of Nb_2O_5 and 195 mg of TiO_2

Fraction	Volume of fraction (in ml)	Contents of fractions in g/liter			in mg			Distribution in fractions (in %)		
		Nb_2O_5	TiO_2	$H_2C_2O_4$	Nb_2O_5	TiO_2	$H_2C_2O_4$	Nb_2O_5	TiO_2	$H_2C_2O_4$
Extraction of niobium with 2 M NaCl solution										
1	450	0.90	0.05	8.82	405	22.5	3969	75.80	11.4	55.7
2	550	0.19	0.017	3.28	104.9	9.35	1802	19.65	4.76	25.2
3	500	0.02	0.008	1.51	10.0	4.00	756	1.88	2.04	10.60
Extraction of titanium with 1 M HCl solution										
4	500	0.016	0.26	0.88	8.0	130.0	441.0	1.49	66.4	6.25
5	500	0.0072	0.06	0.315	3.6	30.0	157.5	0.69	15.30	2.25
In resin after extraction	Wt. of ash and resin 53.3 mg	4.8%	0.1%	—	2.55	0.05	—	0.49	0.03	—
Total					534.05	195.9	7125.5	100	100	100.00

To establish the maximum capacity of the anionite, we carried out experiments on the sorption of anions with periodic renewal of the solution so that the anion-exchange resin was periodically put in contact with a solution with the initial niobium concentration. In this case the capacity of the anionite with respect to Nb_2O_5 was 5.5% of the weight of the air-dried anionite. From this it follows that for raising the efficiency of use of the anionite, the extraction of niobium and titanium anions from oxalic acid solution is best carried out by a counter current ion-exchange process where the first anionite must work to saturation and the last to break through.

Selective Extraction of Niobium and Titanium Anions

Absorbed niobium and titanium anions were selectively eluted from the resin under dynamic conditions. For this purpose the resin with the absorbed anions was separated from the solution, washed with water and loaded into a column. Separating funnels 28 mm in diameter were used as columns. The height of the resin bed in the column was 70 mm (with a 10 g sample of resin). The wash solutions (eluates) were passed through the column from top to bottom at a rate of 2 ml/min. The solution obtained by elution of the metals was collected in fractions, which were analyzed chemically for the niobium and titanium concentrations.

Solutions of neutral salts $(NH_4)_2SO_4$, NH_4Cl, NaCl) of various concentrations, 6 M hydrochloric acid solution and a mixture of hydrochloric and hydrofluoric acids were tested as eluates.

The best results as regards selective extraction of niobium from the resin were obtained when 2 M (10%) sodium chloride solution was used.

In this case the filtrates contained 93-97% of the niobium and not more than 9-18% of the titanium out of the amounts of them contained in the resin. The remaining 91-92% of titanium was extracted by washing the resin with 1 M HCl solution. Simultaneously with the elution of the niobium and titanium from the resin, the filtrates removed almost the whole of the iron and more than 90% of the oxalic acid with more than 90% of the latter eluted by the sodium chloride solution into the niobium fractions, which made it possible to regenerate it. The results of one of the experiments are given in Table 2.

From the data in Table 2 it follows that in the niobium filtrate and, consequently, in the niobium product precipitated from it the ratio $Nb_2O_5 : TiO_2$ was 16 : 1. For a further reduction in the titanium dioxide content of the niobium product, experiments were carried out with additional charging during the desorption process of an anionite not charged with metals. In this case the niobium filtrate issuing from a column with a charged anionite was run into a column with an uncharged anionite and then collected in a receiver.

TABLE 3

Regeneration of Initial Capacity of Resin

Absorption and elution cycles	Contents of filtrate in g/liter			
	niobium filtrate		titanium filtrate	
	Nb_2O_5	TiO_2	TiO_2	Nb_2O_5
1	0.46	0.01	0.130	0.01
4	0.47	0.03	0.131	0.012
5	0.42	0.02	0.134	0.016
7	0.42	0.02	0.130	0.01
9	0.45	0.04	Not determined	

It was found that the inclusion in the desorption process of an amount of uncharged anionite equal to 50% of the weight of that charged with metals made it possible to obtain niobium filtrates containing traces of TiO_2 and in the niobium pentoxide precipitated from the filtrate and fired, the ratio of $Nb_2O_5 : TiO_2$ was 49 : 1 or, in other words, the TiO_2 content of the Nb_2O_5 did not exceed 2% (when the ratio $Nb_2O_5 : TiO_2$ in the starting oxalic acid solution was 1 : 0.8).

Under the given conditions the extraction of niobium into the niobium filtrate was 85%, while about 8% of the niobium was held by the anionite and 7% was lost with the titanium fraction.

The investigations also showed that to obtain niobium pentoxide with a high Nb_2O_5 content, the niobium had to be desorbed with a sodium chloride solution which did not contain calcium or other ions which give insoluble oxalates in neutral or weakly alkaline media. Thus, in experiments where the niobium was desorbed from the anionite with sodium chloride solution prepared with water from the mains, the Nb_2O_5 content of the niobium pentoxide precipitated from the niobium filtrate and fired did not exceed 60-65% and the residue was calcium oxide; when distilled water was used the niobium pentoxide obtained had not less than 98% of Nb_2O_5.

The sodium chloride solution could be freed from calcium and other cations with the aid of KU-2 cationite in the Na-form.

The results of the experiments given in Table 2 show that during the elution the second and subsequent fractions of filtrate contained small amounts of niobium and titanium. In this connection we investigated the possibility of raising the niobium and titanium concentrations in the filtrates by a second passage of the filtrate through a resin containing niobium and titanium.

For this purpose we took two portions of resin, charged with the same amounts of niobium and titanium (266 mg of Nb_2O_5 and 84 mg of TiO_2), weighing 10 g each.

One portion of resin was washed with a niobium fraction containing 0.45 g/liter of Nb_2O_5 and 0.032 g/liter of TiO_2 and the second, with a niobium fraction containing 0.07 g/liter of Nb_2O_5 and 0.013 g/liter of TiO_2. Here the niobium concentration in the first fraction rose to 0.72 g/liter with a TiO_2 content of 0.042 g/liter and in the second fraction, to 0.64 g/liter with a TiO_2 content of 0.027 g/liter.

Experiments showed that it was possible to use more concentrated filtrates at the beginning of regeneration of the resin containing niobium anions. At the end of the cycle it was necessary to regenerate the resin with the weakest filtrates as otherwise the resin, free from niobium anions, could partially absorb niobium and thus reduce the concentration of it in the filtrate.

As regards the titanium filtrates, they could not be reused in the elution process as after the extraction of titanium, the resin, which had been freed from niobium, iron and the bulk of the oxalic acid during regeneration with sodium chloride, was again capable of absorbing anions very actively.

To check how completely the resin recovered its initial capacity during the regeneration process, we carried out experiments in which the alternate absorption and elution of anions was repeated 9 times on the same resin over a period of 27 days. The recovery of the capacity of the resin was checked by periodic analysis of the first, most concentrated niobium and titanium filtrates, of which 500 ml portions were collected.

The results of the experiments, which are given in Table 3, show that the initial capacity of the resin was completely recovered during regneration.

Recovery of Niobium, Titanium and Oxalic Acid From Filtrates

Recovery of Niobium. About 97-98% of pure niobium pentoxide was isolated from the slightly acidified niobium filtrate with ammonia at pH 7 and the other 2-3% of niobium pentoxide was recovered from the filtrates at pH > 7 together with iron.

Recovery of Titanium. The titanium could be precipitated from the filtrate very simply and completely with ammonia.

Recovery of Oxalic Acid. The oxalic acid was regenerated from the niobium filtrates after separation of the niobium and iron from them with ammonia. A saturated solution of calcium chloride was used for the regeneration. Regeneration of the oxalic acid from the niobium filtrates, obtained with maximum loading of the resin, made it possible to return about 70% of the acid to the leaching process.

SUMMARY

1. Niobium and titanium may be extracted and separated from oxalic acid solutions with the anionite ÉDÉ10P in the chloride form by selective elution of the niobium with 2 M (10%) sodium chloride solution and the titanium with 1 M hydrochloric acid solution.

2. The exchange capacity of the resin for niobium is 5.5% of the weight of the air-dried resin.

3. The resin is completely regenerated in the original form during the extraction of the niobium and titanium from the resin.

4. The ion-exchange method makes it possible to obtain niobium pentoxide containing 98.0% of Nb_2O_5 and 1.8-2% of TiO_2 when the Nb_2O_5: TiO_2 ratio in the starting concentrate and solution equals 1 : 0.8.

LITERATURE CITED

[1] K. A. Kraus and G. E. Moore, J. Am. Chem. Soc. 71, 5855 (1949).

[2] J. A. Ayres, J. Am. Chem. Soc. 69, 2879 (1947).

[3] G. A. Meerson and A. N. Zelikman, Metallurgy of Rare Metals [In Russian], Metallurgy Press (1955).

[4] D. I. Ryabchikov, Khim. Nauka i Prom. 1, 5 (1956).

[5] S. I. Solov'ev, E. I. Krylov and L. P. Kononova, Zhur. Neorg. Khim. 1, 4 (1956).

[6] Theory and Practice of the Application of Ion-Exchange Materials [In Russian], Coll. of Articles, Acad. Sci. USSR Press, Moscow (1955).

[7] Ion Exchange, [In Russian] Coll. of Articles, Foreign Lit. Press (1951).

Received July 5, 1958

ON THE QUALITY OF TITANIUM SPONGE PREPARED BY THE MAGNESIOTHERMIC PROCESS

V. V. Sergeev, V. V. Vlasov, and R. A. Sandler

The quality of titanium sponge is determined by its content of impurities and its homogeneity. An increased impurity content renders titanium more brittle, which makes it difficult to prepare articles with the required mechanical properties; inhomogeneity of the sponge makes it difficult to prepare articles with definite mechanical properties.

Oxygen, nitrogen, iron, chlorine, magnesium, silicon, nickel, hydrogen, and carbon are present in titanium sponge as impurities. The content of these elements in the sponge will vary within certain limits both from one batch of metal to another and between samples taken from a single batch.

The principal parameters for determination of the quality of titanium are its mechanical properties, particularly hardness and tensile strength. The effects of different impurities on the mechanical properties of titanium are not all the same, but when different impurities are simultaneously present, their effect may be considered practically additive [1]. Average values of the content of impurities in the sponge and their role in increasing the hardness of titanium are given in the table. Several batches, whose average hardness was about 140 units, were analyzed here. The values indicated in Graphs 3 and 4 were calculated on the basis of McKinley's data [1].

As is evident from the table, oxygen, iron, nitrogen, and carbon have the greatest effect on the hardness of commerical titanium sponge. The effect of silicon amounts to less than 5% of the total increase of hardness. The share of the rest of the above-mentioned impurities in the increase of hardness of the sponge amounts in sum to about 10 units.

TABLE 1

Average Content of Impurities in Titanium Sponge and Their Role in Raising the Hardness of the Metal

Element	Average content in sponge (in %)	Increase in hardness of sponge (in Brinell units), corresponding to the average content of the element	Rise in the total hardness (in %)
Nitrogen. . . .	0.0195	11.5	15.85
Oxygen.	0.053	26.5	36.5
Iron.	0.125	22.5	31.0
Carbon.	0.02	8.5	11.85
Silicon.	0.05	3.5	4.80

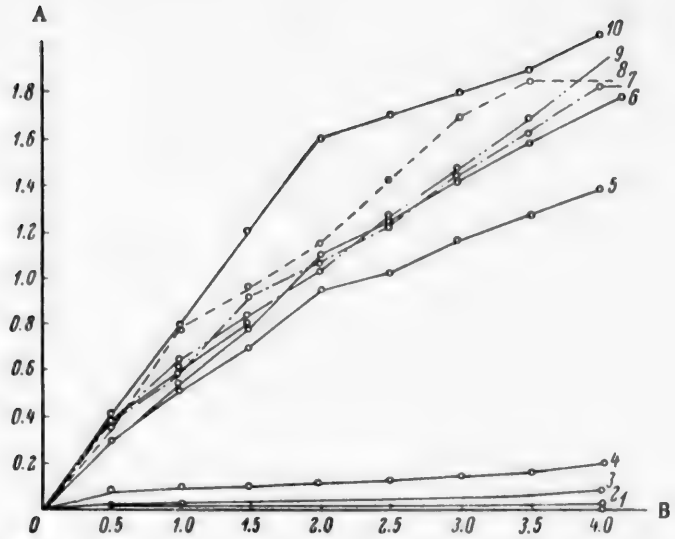

Fig. 1. Effect of the chlorine content of the sponge on the rate of its gain in weight when the humidity of the air is 6-8 g/m^3. A) Increase in weight of sponge (in %); B) time (in hours). Chlorine content (in %): 1) 0.05, 2) 0.07, 3) 0.12, 4) 0.3, 5) 1.9, 6) 6.9, 7) 13.47, 8) 10.2, 9) 18.3, 10) 6.9.

TABLE

Magnesium content (in %)	Average chlorine content (in %)
0.05	0.0819
0.06	0.0707
0.07	0.0605
0.08	0.0775
0.09	0.0640
0.10	0.0700
0.11–0.12	0.0885

Impurities enter the sponge from very diverse sources. Nickel is absorbed from the material of the reaction vessel by magnesium. Iron comes from many sources, but the main source is the apparatus used in the process of production of the sponge at high temperatutes. Analysis of a specific production period, carried out by the authors, showed that about 40-45% of the nitrogen enters the sponge from argon in the reduction process. A considerable part of the nitrogen enters during the process of reduction and air removal. About 40% of the oxygen is derived from the tetrachloride, and the rest enters the sponge in the form of oxide films on the magnesium, in the process of air removal, and in the process of dampening of the sponge.

Commercial sponge contains considerable amounts of magnesium and chlorine. The magnesium may be present in the sponge not only as $MgCl_2$, but also as Mg and MgO. This is confirmed by the data • given below, from which it is evident that there is no interrelation between the chlorine content and that of magnesium in the sponge.

In magnesium oxide only the oxygen is significant; it passes completely into the titanium when the sponge is remelted, and metallic magnesium escapes. Only the presence of $MgCl_2$ (chlorine content) can affect the quality of the titanium; however, the magnesium content cannot be used to characterize the quality of the sponge. The effect of chlorine on the quality of the sponge is due to the fact that the chlorine is present mainly in the form of $MgCl_2$ which hydrates in air, combining with one to six molecules of water per molecule of $MgCl_2$.

Depending on the conditions of treatment, storage, and melting of the sponge, three variants of the mechanism, by which the oxygen of water passes into the titanium sponge with the aid of magnesium chloride, can be considered.

• Data are given for 135 successive batches of titanium sponge, values of the Mg and Cl content in each case relating to the same batch.

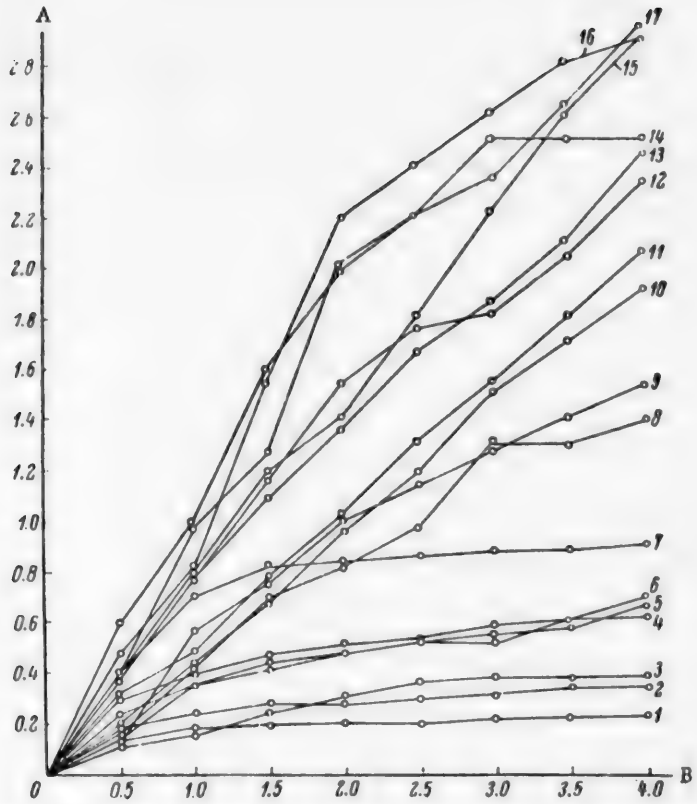

Fig. 2. Effect of the chlorine content of the sponge on the rate of its gain in weight when the humidity of the air is 12-14 g/m^3. A) Increase in weight of sponge (in %): 1) 0.05, 2) 0.05, 3) 0.09, 4) 0.16, 5) 0.23, 6) 0.41, 7) 0.45, 8) 0.86, 9) 1.1, 10) 1.8, 11) 2.19, 12) 2.95, 13) 3.35, 14) 4.1, 15) 10.78, 16) 8.8, 17) 8.0.

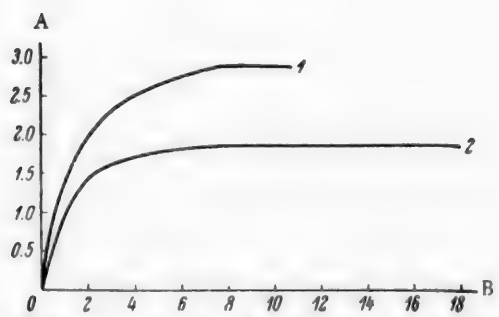

Fig. 3. Effect of the chlorine content on the rate of dampening of the sponge. A) Gain in weight after 4 hours (in %); B) chlorine content of titanium sponge (in %). Humidity: 1) 60.70% (12-14 g/m^3), 2) 30-40% (6-8 g/m^3).

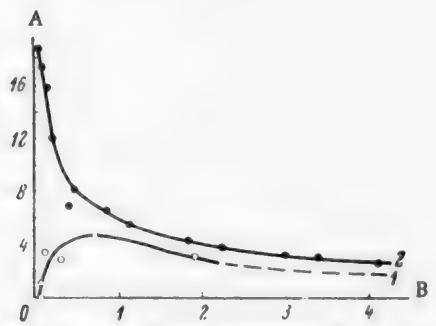

Fig. 4. Character of dampening of the sponge for different degrees of humidity of the air. A) Quantity of H_2O after standing in air for 4 hours (in moles per mole of $MgCl_2$); B) Cl content (in %). Humidity (in g/m^3): 1) 6-8, 2) 12-14 g/m^3.

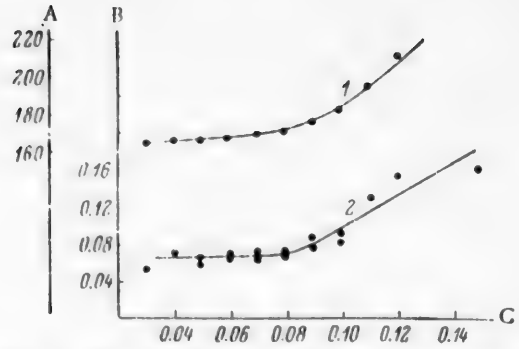

Fig. 5. Effect of chlorine on the oxygen content and hardness of titanium sponge. A) Brinell hardness; B) oxygen content (in %); C) chlorine content (in %). 1) Hardness; 2) oxygen content.

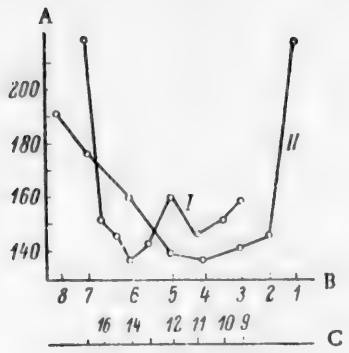

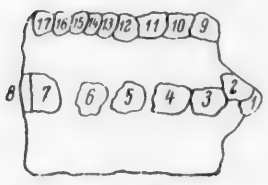

Fig. 6. Variation of quality of sponge with respect to the location in which it is formed. A) Brinell hardness; B) samples taken in the center of the mass; C) samples taken at the side of the mass. I) Side of mass; II) center of mass. 1-17) Sampling locations.

Variant of severe dampening of the sponge. The following reactions occur in magnesium chloride solution:

$$MgCl_2 + 2H_2O \rightleftarrows Mg(OH)_2 + 2HCl \quad (1)$$

$$Mg + 2HCl \rightleftarrows MgCl_2 + H_2 \quad (2)$$

$$Mg + 2H_2O \rightleftarrows Mg(OH)_2 + H_2 \quad (3)$$

Here it is suggested that metallic magnesium, a certain amount of which is always present along with magnesium chloride in the sponge, participates.

When the sponge is remelted, water evolved as a result of decomposition of $Mg(OH)_2$ will react with the titanium, yielding oxygen to it; magnesium oxide also is reduced by the titanium.

Variant of hydration of magnesium chloride beyond the monohydrate. Water is removed when the sponge is remelted and, just as in the first case, will oxidize the titanium. Dehydration of magnesium chloride monohydrate is considered below.

Variant of hydration of magnesium chloride to the monohydrate. On remelting of the sponge in the temperature interval 150-200° the following reaction wil occur:

$$MgCl_2 \cdot H_2O \rightleftarrows MgOHCl + HCl. \quad (4)$$

When the temperature is further increased to 500°, decomposition takes place:

$$MgOHCl \rightleftarrows MgO + HCl. \quad (5)$$

At its melting point in vacuo magnesium oxide is easily reduced by titanium. Simultaneously with reaction (4) there occurs the following reaction:

$$MgCl_2 \cdot H_2O \rightleftarrows MgCl_2 + H_2O, \quad (6)$$

which will take place to a great degree on rapid heating, which is probable on remelting. But then the water evolved as a result of reaction (6) will oxidize the titanium, just as in the preceding cases.

Thus in all cases where the magnesium chloride is hydrated, part of the oxygen of the water passes to the titanium in the end. Therefore the effect of chlorine on the quality of the sponge is determined mainly by the ability of the chlorides to absorb water.

The rate of dampening of titanium sponge with respect to its chlorine content was investigated by the authors in the laboratory. A reaction mass containing approximately 60% Ti, 15% Mg, and 25% $MgCl_2$ was ground to 1-2 mm particle size and separated under different conditions in order to obtain sponges with varying chlorine content. Two 5 g samples of each resulting sponge were taken. The weighed samples, forming a 4-6 mm layer in a tube, were placed in an atmosphere with a humidity of 6-8 or 12-14 g/m^3. They were weighed every 30 minutes for 4 hours. At the end of each experiment the sample was analyzed for chlorine. Experimental results are given in Figures 1 and 2.

The character of dampening of the sponge varies with respect to its chlorine content and the humidity of the air. The rate of dampening of the sponge decreases as the degree of dampening increases. Naturally the decrease in the dampening rate with time is the more appreciable, the lower the chlorine content of the sponge and the higher the humidity of the air. It is evident from Figure 2 that with a chlorine content of 0.05-0.07% and a humidity of 12-14 g/m^3 the sample becomes saturated within 1.5-2 hours. With a humidity of 6-8 g/m^3 the saturation period is more prolonged.

In Figure 3 are shown curves of the rate of dampening of the sponge with respect to its chlorine content. The dampening rate rises sharply as the chlorine content increases to 1.5-2%, but remains practically constant on further increase of the latter. This is due to the fact that when the chlorine content is 1.5-2%, a film of magnesium chloride covers the entire surface of the sponge. On further increase of the chlorine content, the chloride surface in contact with air does not increase; it may even decrease owing to the fact that the pores of the sponge are filled with magnesium chloride.

In Figure 4 are given curves showing the character of dampening of the sponge for different degrees of humidity, with respect to the chlorine content. When the humidity is far from the dew point (6-8 g/m^3, or 30-40%) and the chlorine content is low, one mole of $MgCl_2$ combines with a much smaller number of moles of water than when the humidity is near the dew point (12-14 g/m^3, or 60-70%). This is due to the fact that at high humidity not only the magnesium chloride, but also the titanium itself takes part in the dampening of the sponge. With a high chlorine content, near that at which the entire surface of the sponge is covered with chloride, the humidity of the air has no effect on the character of dampening of the sponge.

From the data given here, which were obtained as a result of laboratory investigations, it is evident that in order to avoid dampening of the sponge, chlorides must be carefully removed from it. To judge according to the data given in Figures 1 and 2, the chlorine content of the sponge must not exceed about 0.1%.

In order to determine the effect of the chlorine content on the quality of commerical sponge, the authors analyzed plant data. Several hundred batches of sponge, having nearly identical contents of all impurities except oxygen and chlorine, were taken, and the curves shown in Figure 5 were constructed. From these curves it is evident that the presence of chlorides begins to affect the quality of the sponge appreciably when the chlorine content reaches about 0.08%. This may be explained by the fact that a quantity of chlorides, corresponding to about 0.08% chlorine content, occurs in closed pores or very fine capillaries. The curves shown in Figure 5 are in accord with the hypothesis that certain batches of the metal, having a chlorine content of 0.1% or more, correspond in their mechanical properties to high grades of titanium. As a result of the influence of chlorine, only part of the oxygen in the sponge combines with the titanium. If a batch contains less of other impurities, and also less oxygen from other sources, a high chlorine content need not cause deterioration of the metal to a low grade. It should be noted, however, that oxygen that has entered the metal with the aid of magnesium chloride is a greater hazard than, for instance, oxygen introduced with the titanium tetrachloride, which is more uniformly distributed through the metal.

As was stated above, the second important parameter characterizing the quality of the metal is its homogeneity. A nonuniform content of impurities and hence a nonuniform hardness of the sponge obtained are the result of the technology of titanium production.

In Figure 6 is shown the hardness of titanium formed in different zones of the reaction vessel. The preparation of homogeneous metal is furthered to a considerable degree by assembling batches of sponge taken from certain zones of the reaction vessel, crushing, dispersal, and sorting. However, heterogeneity of the metal remains one of the shortcomings inherent in the technology of the periodic process involving separation of a monolith.

SUMMARY

1. The principal impurities which cause a lowering of the quality of titanium sponge are iron, oxygen, carbon, nitrogen, and chlorine. The role of each of these impurities in lowering the quality of commercial sponge has been quantitatively shown.

2. The role of magnesium chloride in lowering the quality of titanium sponge has been shown; as the chlorine content rises above 0.08-0.09%, an aggravation of the effect of chlorine is noted.

3. The rate and character of dampening of the sponge on contact with air depend on the humidity of the air and the chlorine content of the sponge. When the humidity of the air is high, dampening of the sponge, corresponding to technical conditions, takes place to a great degree thru sorption of moisture by the sponge itself, rather than thru hydration of chlorides.

LITERATURE CITED

[1] McKinley, J. Electroch. Soc. 103, 10 (1956).

Received November 24, 1958

ACETONE SOLUTIONS OF SILICIC ACID, THEIR PROPERTIES AND USE•

Yu. V. Morachevskii and E. N. Egorova

Colloidal silicic acid can be used in a number of cases as a good cementing material. Thus in the production of shell forms for precision casting by the melted-out model method, the binder for the grains of refractory material in the forms is colloidal silicic acid. Hitherto, in the production of shell forms for casting by the melted-out model method, ethyl silicate, which forms colloidal silicic acid on hydrolysis, has been used. The scarcity of ethyl silicate, which is due to the complexity of the process of its production, and its relatively high cost made it necessary to seek substitutes for it.

As is generally known, silicic acid can form complexes with polar organic compounds containing electron-donor atoms. Such organic compounds include ethers, ketones, and amides, in which the donor atoms are nitrogen and oxygen [1]. The organosilicon complexes are formed in an aqueous solution containing silicic acid, and therefore the organic compounds must be soluble in water. The resulting organosilicon complex may be isolated by salting out [2]. However, organosilicon compounds of this type are relatively little-studied; only general ideas of their structure exist [1]. They are of particular practical interest because, being relatively unstable, they form colloidal silicic acid as the solvent is removed; this is easily accomplished by evaporation.

We decided to use the above-described organosilicon compounds to replace ethyl silicate. Acetone, being very inexpensive and readily available, was chosen as solvent [3].

The method of preparing acetone solutions of silicic acid, developed by us [4], consists in three main operations: 1) preparation of aqueous silicic acid solution, 2) extraction of silicic acid with acetone, and 3) separation of the aqueous and acetone solutions.

A very inexpensive and readily available technical product—water glass—was taken as the starting material for preparation of aqueous silicic acid solution. After neutralization of the water glass with acid the silicic acid so formed in the aqueous solution may be polymerized to a varying degree depending on the conditions of neutralization. On addition of acetone to the aqueous solution, compounds of acetone and polysilicic acids are formed. As experiment showed, these compounds may be quite stable, but nevertheless gel formation is observed in the separated acetone solution on standing, which indicates continuing polymerization of the silicic acid in the solution. The fact that acetone solutions with nearly the same silicic acid content, prepared under different conditions, were not equally stable, indicated that their stability is determined by the degree of polymerization of the silicic acid extracted by the acetone; the less polymerized and silicic acid extracted by the acetone is, the more stable the acetone solution will be (and vice versa).

In connection with this it was necessary to determine more precisely the conditions of neutralization, under which sufficiently concentrated silicic acid solutions could be obtained with the smallest degree of polymerization. It is generally known that the rate of polymerization of silicic acid in aqueous solutions is determined by the solu-

• The present work was done at the direction of the All-Union Planning-Technological Institute of Lensovnarkhoz and with its participation; the Institute of Silicate Chemistry of the USSR Academy of Sciences, the Electrotechnical Institute (High-Frequency Metallurgy Laboratory), and the Ship Construction Institute (Chemistry Department) took part in the work.

tion pH and increases on increase of the temperature and the concentration of silicic acid therein. The region of the most stable state of silicic acid corresponds to a pH equal to 2.

Proceeding from these data, the most favorable conditions for obtaining relatively slightly polymerized silicic acid by neutralizing water glass with acid should be considered to be the lowest possible solution temperature on neutralization, a final acidity of the neutralized solution, corresponding to a pH of 2, and very rapid carrying-out of neutralization.

In order to show the effect of the temperature of the solution being neutralized on the degree of polymerization of the silicic acid formed in it, a solution of water glass was neutralized with sulfuric acid while being cooled to various temperatures; this was achieved thru the choice of cooling medium and by varying the rate of addition of the water glass solution to the dilute sulfuric acid. The degree of polymerization of silicic acid in the solutions obtained after neutralization was characterized by the content of the simplest silicic acids, which was determined by a colorimetric method thru the molybdenum reaction.

The neutralization was carried out by pouring the water glass solution into an equal volume of dilute sulfuric acid; the quantities of reagents—water glass and sulfuric acid—were calculated to give a solution acidity after neutralization, corresponding to a pH of 2.

As a result of these investigations it was found that aqueous solutions of silicic acid, polymerized to practically the same degree and containing 130-140 g of SiO_2 per liter, may be obtained by using external cooling such as to provide a final solution temperature between 2 and 22°, the appropriate rate of addition of the water glass, and sufficiently vigorous stirring of the solution during the neutralization process. However, such a wide temperature range cannot be optimum for extracting the silicic acid with acetone; this will be discussed further.

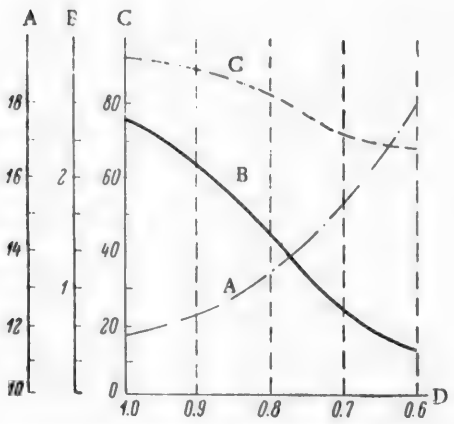

Correlation between the content of SiO_2 in acetone solution and the yield and stability thereof on extraction with different volumes of acetone. Concentration of SiO_2 in the aqueous solution, 130 g/liter; acidity 0.2 N. A) SiO_2 content (in %); B) stability of the acetone solution (in months); C) yield of acetone solution with respect to volume of acetone (in %); D) quantity of acetone (in liters/liter of aqueous solution).

In the study of the conditions for extracting silicic acid from aqueous solutions with acetone, the effect of the volume ratio of aqueous solution and acetone in the extraction, temperature and acidity of the aqueous solution, and time of interaction of the silicic acid and acetone on the properties of the acetone solutions was investigated.

By reducing the volume of acetone taken for extraction one can, of course, increase the concentration of silicic acid in the acetone solution; it was found, however, that extraction with a volume ratio of aqueous solution and acetone, less than 1:0.8 leads to a considerable decrease in the stability and yield of the acetone solution. The correlation between the content of silicic acid in the acetone solution and the stability and yield thereof for extraction with different volumes of acetone is shown in the figure.

In order to show the effect of temperature on the extraction of silicic acid by acetone, experiments were performed with and without external cooling; in the latter case solutions cooled to various temperatures between 2 and 22° were subjected to extraction. The results of the experiments in extraction with external cooling showed that after saturation of the cooled aqueous-acetone solutions with salt, stratification of the aqueous and acetone solutions was considerably retarded. On cooling of the aqueous-acetone solution to a temperature of 8° stratification of the aqueous and acetone solutions began only within 3.5-4 hours after saturation with salt, at which time the solution temperature reached 12°, and continued for 21 hours. The yield of acetone solution was only 80% with respect to the volume of acetone taken for extraction. With milder cooling (down to 13°) the time of separation of the bulk of the acetone solution from the salt-water layer was reduced to 5-6 hours, but the yield for this time was only 70%. In this case, also, complete stratification was observed only after 21-22 hours and the yield was 80%. When acetone was added to an aqueous solution cooled to 2°, the temperature of the aqueous-

acetone solution (in the absence of external cooling) rose to 18°, and the bulk of the acetone solution, which amounted to 70% with respect to the volume of acetone, separated within 45 minutes. Stratification was complete after several hours and the yield also was 80%. With regard to their silicic acid concentration, acetone solutions obtained by extraction with external cooling differed little from those obtained without cooling. However, their specific gravity was much higher. The increase in specific gravity could be due partly to the fact that the acetone solutions contained a small amount of salt-water solution, which slowly separated out on standing. The presence of salt-water solution in the acetone solutions was confirmed by chemical analysis; their sodium-salt content was increased. But even after complete separation of the salt-water solution the specific gravity of the acetone solutions was high; this was possibly due to a greater degree of hydration of silicic acid extracted under these conditions.

The results of extraction without external cooling showed that when the aqueous solution is mixed with an equal volume of acetone, the temperature of the aqueous-acetone solution rises 10-15°; in this case the stratification time is considerably shortened and the yield of acetone solution increased. Thus, when the temperature of the aqueous solution was raised (before adding acetone) from 2 to 18°, the stratification time was reduced from 45 minutes to 3-4 minutes and the yield increased from 72 to 92%. Extraction from aqueous solutions at temperatures above 18° did not lead to increased yields and is undesirable, since the temperature rises 10-12° on extraction, and the operation would be accompanied by the loss of acetone thru evaporation.

It should be noted that in aqueous solutions at a temperature below 10-12° the separation of finely-dispersed sodium sulfate crystals was observed toward the end of neutralization. This salt suspension could easily be mistaken for separated silicic acid gel, and therefore complicated observation of the course of the process. Furthermore, after mixing with acetone and saturation by salt, stratification in these solutions was retarded. In aqueous solutions at a temperature of 12-13° formation of a salt suspension was not observed, and the stratification time was reduced to a few minutes.

Thus the optimum temperature conditions of extraction, providing maximum yield and more rapid stratification, are the absence of external cooling and an aqueous solution temperature between 13 and 18°.

As stated above, silicic acid is most stable in aqueous solutions at a pH of 2; at higher or lower pH values the rate of polymerization increases, but not to the same degree. On increase of the solution pH the rate of polymerization rises considerably, while increase of the acidity to a certain limit, which depends on the concentration of silicic acid in the solution, has relatively little effect on the rate of this process. In accordance with this the extraction of silicic acid from aqueous solutions having acidity varying from 0.01 N to 0.5 N was investigated.

The results of the investigations showed that extraction from more acid solutions (0.1-0.2 N) leads to an increase in the yield of acetone solutions, and also in their silicic acid content. Furthermore, the acetone solutions were no less stable than those obtained by extraction from less acid (0.01 N) solutions with a pH of about 2. Further increase in the acidity of the aqueous solution (above 0.2 N) does not increase the yield and, although it leads to a certain increase in the silicic acid content of the acetone solution, it decreases the stability of the latter.

Thus the extraction of silicic acid from 0.1 N or 0.2 N acid solutions not only makes it possible to dispense with very precise measurements of reagents (water glass and sulfuric acid) in neutralization, but also promotes more complete extraction of silicic acid from the aqueous solution by acetone.

The effect of the time of interaction of silicic acid with acetone on the properties of the resulting acetone solutions was further investigated. It was found that by increasing the time of mixing, up to a certain limit, acetone solutions with a practically constant silicic acid concentration were obtained. The quantity of silicic acid extracted by acetone depends not only on the time of mixing, but also on the acidity of the aqueous solution. As the acidity of the aqueous solution increases, the time, required to obtain acetone solutions with practically constant silicic acid concentration, decreases. Mechanical stirring for 3-5 minutes gives acetone solutions with practically the maximum silicic acid concentration on extraction from aqueous solutions with an acidity of 0.2 N.

With manual mixing by shaking of the aqueous solution with acetone, used in the first stage of the investigation, conditions were less than ideal and could not be fully reproduced; in the acetone solutions obtained under these conditions the silicic acid content was diminished, and in their technical properties they were inferior to solutions obtained with mechanical stirring. Their silicic acid content varied in a wider range. As experiment

showed, the difference in the properties of solutions obtained with mechanical and manual mixing was more pronounced on extraction from aqueous solutions with 0.01 N acidity than on extraction from more acid solutions (0.2 N).

Detailed study of the conditions of extraction of silicic acid by acetone made it possible to determine the optimum extraction conditions for preparing that acetone solution of silicic acid, which is most suitable as a binder in the production of castings by the melted-out model method. These conditions may be formulated as follows: 1) the silicic acid concentration in the neutralized aqueous solution must correspond to 130 g of SiO_2 per liter, 2) the acidity of the neutralized aqueous solution must lie between 0.1 and 0.2 N, 3) the optimum temperature after neutralization is 13-18°, 4) equal volumes of the aqueous solution and acetone must be mechanically stirred for 3-5 minutes, 5) the mixture must be salted out by mixing the aqueous-acetone solution with 125 g per liter of sodium chloride during 8-10 minutes.

Proceeding from the optimum extraction conditions, the water glass should be neutralized with sulfuric acid in such a manner that the final solution temperature will be brought within the 13-18° range by external cooling. This is accomplished by adding the water glass solution to an equal volume of dilute sulfuric acid cooled to 8-10°, and then cooling the solution being neutralized, with vigorous stirring. The indicated silicic acid content of the solution and the acidity of the latter are calculated on the basis of the composition of the water glass and sulfuric acid.

The binder (ARK-1) prepared in the experimental production unit had the same characteristics as that obtained under laboratory conditions. Its specific gravity was 0.93-0.94. The content of silica varied from 11 to 12%, and that of sodium salts (calculated as NaCl), from 1.2 to 1.5%. The acidity of ARK-1 varied between 0.02 and 0.04 N, depending on the acidity of the aqueous solution from which the silicic acid was extracted; on extraction from 0.1 N aqueous solutions the acidity of ARK-1 was 0.02 N, while on extraction from more acid solutions (0.2 N) it was 0.04 N. The stability of ARK-1 — the time elapsed before gel formation begins — was from 2.5 to 3 months on storage in a room having a temperature of 14-18°. During this time ARK-1 can be used for the preparation of coating solutions.

In order to determine the quality of the new binder, the laboratory investigations and tests were followed by extensive production tests in a number of Leningrad plants. In this case over 12,000 castings of carbon and alloy steels and colored alloys, weighing from a few grams to 18 kg and having a maximum dimension up to 400 mm, were prepared. To prepare these castings box and shell forms with a refractory coating of ARK-1, and also shell molds, the first layers of whose refractory coatings consisted of ARK-1 and the last 1-2 (reinforcing) layers, of water glass, were used. The models were melted out with hot water and in thermostats.

The advantages of the new binder in comparison with hydrolyzed ethyl silicate and earlier-known substitutes for the latter are: use of common and inexpensive starting materials; simplicity of the method of preparation, which permits it to be made in any laboratory and any consuming plant; adequate stability (over two and one-half months), which makes it possible to organize centralized production of it within the limits of an economic region; good covering power of the coating solutions and the absence of interaction with the model materials, which insures high quality of the mold surface; low shrinkage and high fire- and heat-resistance of the refractory coating [5], which insures castings with a high-quality surface and accurate dimensions; rapidity of the setting process, which accelerates air-drying 2-2.5-fold and eliminates the use of ammonia; relatively low cost, 0.4-0.5 times the cost of hydrolyzed ethyl silicate.

In view of the positive results of testing, the technology of the preparation and use of ARK-1 was developed, and a number of units for ARK-1 production in laboratories and enterprises with variable production volume were designed.

The Council of National Economy of the Leningrad Economic Region organized the industrial production of the new binder, tentatively using a unit with an output of 90 liters per shift for this purpose.

LITERATURE CITED

[1] R. K. Iler, J. Phys. Chem. 56, 6, 673 (1952).

[2] J. S. Kirk, U. S. Pat. 2408654-2408656 (1946).

[3] Yu. V. Morachevskii and E. N. Egorova, Proc. Acad. Sci. USSR 122, 4 (1958).*

[4] E. N. Egorova, I. E. Shub, E. I. Ginzburg, and E. K. Alekseevskaya. The New Binding Material ARK-1, A Substitute For Ethyl Silicate. NTO, Mashprom, L. (1958).

[5] O. V. Stupishina, Foundry Production, No. 2 and 9 (1958).

Received January 13, 1959

* Original Russian pagination. See C. B. Translation.

ON THE PARTIAL PRESSURE OF SO_2 OVER AMMONIUM SULFITE-BISULFITE SOLUTIONS

R. A. Berdyanskaya, S. M. Golyand, and B. A. Chertkov

Ammonium sulfite-bisulfite solutions (NH_3–SO_2–H_2O system) find practical application in the extraction of sulfurous anhydride from the waste gases of various industrial enterprises [1-3].

The cyclic process of absorption of SO_2 from a dilute gas mixture by means of aqueous ammonium salt solutions, followed by its evolution in concentrated form on heating of the absorbent solution is based on the properties of the above-mentioned system and, in particular, on the form of the curves of equilibrium vapor pressure of the components for a variable ratio of the latter in the solution and variable temperature.

Equilibrium conditions in the NH_3–SO_2–H_2O system were studied by Terres and Hahn [4], Johnstone [5], and Shokin et al., [6]. The most detailed data on the equilibrium partial pressures of SO_2, NH_3, and water vapor over ammonium sulfite-bisulfite solutions for a wide range of concentrations and temperatures were obtained by Johnstone [5]. On the basis of these data he proposed the following calculation formulas:

$$P_{SO_2} = \frac{M \cdot (2S - C)^2}{C - S}, \quad (1)$$

$$P_{NH_3} = \frac{N \cdot C \cdot (C - S)}{2S - C}, \quad (2)$$

where P_{SO_2} is the equilibrium partial pressure of SO_2 over the solution (in mm); P_{NH_3} is the same for NH_3; S is the total concentration of dissolved SO_2 (in moles per 100 moles H_2O); C is the total concentration of dissolved NH_3 (in moles per 100 moles H_2O); M and N are equilibrium coefficients for SO_2 and NH_3, respectively, into which enter Henry's Law constants, the first and second dissociation constants of sulfurous acid, and the dissociation constants of ammonia and water.

The equilibrium pressure of water vapor over ammonium sulfite-bisulfite solutions, P_{H_2O}, may, within the limits of Johnstone's determinations of concentrations and temperatures, be calculated with sufficient accuracy by Raoult's Law.

The coefficients M and N in Equations (1) and (2) must undoubtedly change as the total concentration of dissolved SO_2 and NH_3 varies; however, as Johnstone found, M and N did not vary more than 10% in the wide range of solution concentrations studied by him, and they may, to a first approximation, be considered independent of the concentration. The temperature dependence of M and N, according to Johnstone's experimental data, is determined by the following equations:

$$\lg M = 5.865 - \frac{2369}{T}, \quad (3)$$

$$\lg N = 13.680 - \frac{4987}{T}, \quad (4)$$

where T is the absolute temperature.

The expression (2S - C) is the molar concentration of the ions of ammonium bisulfite, and (C - S) is that of the ions of ammonium sulfite simultaneously present in the solution. Thus P_{SO_2} proves to be directly proportional to the square of the bisulfite ion concentration in the solution and inversely proportional to the sulfite ion concentration.

Equations (1) and (2) are derived from consideration of the two equilibrium reactions:

$$SO_2\,gas + H_2O + SO_3'' \rightleftarrows 2HSO_3' \quad (a)$$

$$NH_4OH + HSO_3' \rightleftarrows NH_4^+ + SO_3'' + H_2O. \quad (b)$$

Equations (1) and (2) may be transformed and given in the following form, convenient for calculations:

$$P_{SO_2} = \frac{M \cdot C \cdot (2S/C - 1)^2}{1 - S/C}, \quad (5)$$

$$P_{NH_3} = \frac{N \cdot C \cdot (1 - S/C)}{2S/C - 1}. \quad (6)$$

The ratio S/C, entering into Equations (5) and (6), is very convenient for characterizing the variation of the ratio of bisulfite to sulfite in the solution. In the limiting case where the solution consists only of sulfite, S/C = 0.5; in that where the solution consists only of bisulfite, S/C = 1.

Johnstone's data were obtained in the interval in which C varied from 6 to 22 moles/100 moles water, S/C varied from 0.705 to 0.913, and the temperature, from 35 to 90°.

On comparison of Johnstone's experimental values of P_{SO_2}, P_{NH_3}, and P_{H_2O} with those calculated by the equations recommended by him, good agreement is found for ammonia and water vapor at all concentrations and temperatures. For P_{SO_2} (Table 1) the agreement is satisfactory only when S/C is not over 0.85 and the temperature is below 80°. When S/C $\geq$ 0.913 and the temperature is 90°, the discrepancies are very substantial, the calculated values being 0.55-0.77 times the experimental. However, the possible degree of extraction of SO_2 from a gas and the maximum capacity or saturation level of the solutions is estimated from P_{SO_2}. The P_{SO_2}: P_{NH_3} ratios are the basis of calculations of the maximum possible degree of regeneration of the solutions (when P_{SO_2}:P_{NH_3} in the gas phase becomes equal to S/C for the solution), and the P_{SO_2}:P_{H_2O} ratio is the basis for computing the amount of steam used in driving the sulfurous anhydride out of the solution.

In the extraction of SO_2 from dilute gases the value of S/C for a saturated sulfite-bisulfite solution approaches 0.97-0.98. In this region, especially at temperatures over 90°, the use of the equation given above for calculating P_{SO_2} may lead to even greater errors.

At NIIOGAZ the equilibrium pressures of SO_2 and water vapor over ammonium sulfite-bisulfite solutions, having higher S/C ratios than in Johnstone's experiments (Table 2), were measured.

Solutions with an effective ammonia* content C = 20-22 moles/100 moles H_2O and up to about 4.5 moles per 100 moles H_2O of added ammonium sulfate were prepared for the experiments.

P_{SO_2} was determined by a dynamic method similar to that described by Terres and Hahn [4] and Johnstone [5].

As is evident from Table 2, the discrepancy between measured values of P_{SO_2} and those calculated by Formula (1) for solutions with an S/C ratio over 0.9 becomes intolerably great at temperatures of 80 and 90°. This is due to the fact that as S/C increases, i.e., as the relative bisulfite content rises, the presence of H^+ ions and undissociated sulfurous acid molecules in the solution begins to play an ever-increasing role, which is not taken into account by the formulas given above.**

* In the form of the sulfite and bisulfite.

** On the basis of theoretical considerations Johnstone, Read, and Blankmeyer [7] also derived more complete equations for calculating the equilibrium pressure of SO_2 over sulfite-bisulfite solutions; however, they could not be reproduced in practice, since the values of a number of thermodynamic quantities entering into the equation have not yet been accurately determined.

TABLE 1

Equilibrium Pressure of the Anhydride Over Ammonium Sulfite-Bisulfite Solutions According to Johnstone's Experimental Data [5].

Composition of solutions				50°			70°			90°		
				P_{SO_2} (mm Hg)			P_{SO_2} (mm Hg)			P_{SO_2} (mm Hg)		
				measured	calculated by equations		measured	calculated by equations		measured	calculated by equations	
$s\left(\frac{\text{mole } SO_2}{100 \text{ mole } H_2O}\right)$	$c\left(\frac{\text{mole } NH_3}{100 \text{ mole } H_2O}\right)$	S/C	pH		(3) & (5)	(7), (8) & (9)		(3) & (5)	(7), (8) & (9)		(3) & (5)	(7), (8) & (9)
15.71	22.36	0.705	5.96	0.20	0.19	0.2	0.43	0.42	0.47	1.21	1.17	1.29	2.9	2.7	3.2
17.61	22.14	0.795	5.55	0.60	0.57	0.6	1.39	1.29	1.40	3.6	3.5	3.8	9.7	8.3	9.5
18.92	22.21	0.853	5.27	1.14	1.11	1.1	2.4	2.5	2.6	6.8	6.8	7.3	18.4	16.3	17.9
20.35	22.28	0.913	4.92	2.80	2.60	2.8	7.1	6.0	7.0	19.7	16.0	21.5	51.4	38.6	58.0
7.616	10.566	0.721	5.84	—	0.11	0.10	0.27	0.25	0.25	0.66	0.67	0.68	1.58	1.62	1.65
8.615	10.621	0.811	5.43	0.33	0.33	0.32	0.73	0.74	0.72	2.0	2.0	1.98	4.5	4.8	4.9
10.000	10.680	0.936	7.74	1.94	1.91	—	4.3	4.3	—	10.1	11.6	—	25.0	28.0	—
4.274	5.869	0.728	5.85	0.07	0.07	0.06	0.14	0.15	0.14	0.39	0.41	0.39	1.1	1.0	1.0
4.863	5.866	0.829	5.43	0.20	0.22	0.19	0.47	0.51	0.46	1.2	1.3	1.26	2.7	3.2	3.05
5.230	5.809	0.900	5.13	1.05	0.56	—	2.4	1.3	—	5.9	3.4	—	14.6	8.2	—
5.575	5.826	0.957	4.71	4.3	1.7	—	9.0	3.8	—	21.2	10.3	—	44.3	24.7	—

TABLE 2

Equilibrium Pressure of Sulfurous Anhydride Over Ammonium Sulfite-Bisulfite Solutions According to the Experimental Data of NIIOGAZ.*

Temperature (in °C)	Composition of solutions				P_{SO_2} (mm Hg)		
	S	C	S/C	pH	measured	calc. by equations (3), (5)	calc. by equations (7), (8)
40	16.2	19.0	0.855	5.29	1.52	1.25	1.52
	17.4	19.2	0.907	5.15	3.27	2.81	3.27
	18.8	20.5	0.915	4.98	3.33	3.33	3.70
	18.7	19.6	0.955	4.60	9.32	7.28	9.28
80	20.3	22.5	0.902	5.03	29.7	21.0	27.3
	20.4	22.2	0.920	4.8	40.5	28.0	40.9
	18.3	19.0	0.957	—	101	52.0	93.1
	20.8	21.7	0.960	4.23	105	66.0	98.4
	22.1	22.5	0.983	—	161	200	160
	21.3	21.5	0.990		184	294	185
90	20.2	22.5	0.900	—	49.1	31.5	42.8
	20.2	22.0	0.919	—	66.0	42.0	65.0
	21.2	22.0	0.963	—	174.0	108.0	170.0
	21.6	22.0	0.978	—	214	195	233

It should be noted also that Formula (5) cannot be used for solutions with very high ratios, since when $\underline{S/C} = 1$, $\underline{P}_{SO_2}$ is infinite. For instance, it is evident from Table 2 that $\underline{P}_{SO_2}$, calculated by Formula (5), remains less than the actual pressure for $\underline{S/C}$ values up to 0.96, and on slight further increase of $\underline{S/C}$, it suddenly rises so sharply that it begins to exceed the actually measured pressure.

A graphical comparison of the data obtained by NIIOGAZ with Johnstone's experimental data for solutions of the same concentration, i.e., $\underline{C}$ = 22 moles/100 moles H_2O, is given in logarithmic form in the figure.

As is evident from the figure, the whole investigated region may be divided into two parts: that for $\underline{S/C}$ = = 0.7-0.87 and that for $\underline{S/C}$ = 0.87-1.0.

In the first part the relation between $\underline{P}_{SO_2}$ and $\underline{S/C}$ is best expressed by the equation

$$\lg P_{SO_2} = 9.096 \lg S/C - \frac{2443}{T} + 8.616, \qquad (7)$$

and in the second part, by the equation

$$\lg P_{SO_2} = 20.541 \lg S/C - \frac{2697}{T} + 9.997. \qquad (8)$$

Values of $\underline{P}_{SO_2}$, calculated by these empirical equations, give much better agreement with actual determinations than those calculated by Equation (5) (Tables 1 and 2).

Equations (7) and (8), therefore, can be recommended as calculation formulas for determining $\underline{P}_{SO_2}$, instead of the Johnstone equation. One need only take into account the fact that with the coefficients given above, these equations are valid for solutions with an effective ammonia concentration $\underline{C}$ = 20.22 moles/100 moles H_2O. With lower values of $\underline{C}$ the calculation may be performed by means of the same equations, but the result obtained must be decreased in proportion to the decrease of $\underline{C}$, if one agrees with Johnstone's conclusion [5] that $\underline{P}_{SO_2}$ is directly proportional to $\underline{C}$.

* State Scientific Research Institute of Gas Purification for Industry and Sanitation.

TABLE 3

Equilibrium Pressure of Sulfurous Anhydride Over Ammonium Sulfite-Bisulfite Solutions According to Newall's Experimental Data [8] and Values Calculated by Equation (9).

(t = 50°)

Conc. (in moles/liter)		Conc. (moles/100 moles H_2O)		S/C	Value of pH at 20°	P_{SO_2}		
$(NH_4)_2SO_3$	NH_4HSO_3	S	C			measured (in %)	calc. (in %)	(mm Hg)
0.165	0.17	0.60	0.90	0.67	6.55	0.001	0.001	0.008
0.135	0.23	0.66	0.90	0.73	6.35	0.003	0.002	0.017
0.12	0.26	0.68	0.90	0.76	6.20	0.005	0.003	0.024
0.085	0.33	0.75	0.90	0.83	5.95	0.009	0.007	0.053
0.067	0.115	0.33	0.45	0.728	6.50	0.001	0.001	0.008
0.29	0.42	1.28	1.80	0.710	6.30	0.004	0.003	0.026
0.26	0.48	1.34	1.80	0.740	6.10	0.006	0.005	0.038
0.21	0.58	1.42	1.80	0.79	5.90	0.010	0.009	0.070
0.6	0.8	2.5	3.60	0.700	6.15	0.008	0.006	0.046
0.52	0.96	2.7	3.60	0.74	5.95	0.012	0.010	0.076
0.4	1.2	2.9	3.60	0.800	5.70	0.019	0.020	0.155
0.045	0.06	0.19	0.27	0.70	—	Trace		
0.15	0.20	0.63	0.90	0.70	—	0.002	0.0015	0.011
0.30	0.40	1.26	1.80	0.70	—	0.004	0.003	0.026
0.60	0.80	2.5	3.60	0.70	—	0.008	0.008	0.058

TABLE 4

Equilibrium Pressure of Sulfurous Anhydride Over Ammonium Sulfite-Bisulfite Solutions According to the Experimental Data of Jackson and Solbett [9] and Values Calculated by Equation (9).

d (in g/cm³)	SO_2 (in wt.%)	$(NH_4)_2SO_3$ (in wt.%)	S/C	$C\left(\frac{\text{moles}NH_3}{100\text{moles}H_2O}\right)$	P_{SO_2} (mm Hg)													
					16°		20°		25°		30°		35°		40°		50°	
					measured	calc.	measured	calc.	measured	calc.	measured	calc.	measured	calc.	measured	calc.	measured	calc.
1.202	21.1	6.2	0.877	10.25	—	—	0.24	0.24	0.31	0.33	0.45	0.46	0.55	0.60	0.85	0.82	—	—
1.214	20.8	9.3	0.775	12.1	0.06	0.07	—	—	0.12	0.13	0.15	0.18	—	—	0.26	0.32	0.42	0.55

Actually the effect of solution concentration on the variation of $\underline{P}_{SO_2}$ proves to be somewhat more important. Thus on treatment of the corresponding experimental data from Johnstone (Table 1) it is found that when the effect of solution concentration is taken into account, the empirical equation for the first part ($\underline{S/C}$ from 0.7 to 0.87) has the following form:

$$\lg P_{SO_2} = 9.096 \lg S/C - \frac{2443}{T} + 1.139 \lg C + 7.079, \qquad (9)$$

i.e., $\underline{P}_{SO_2}$ varies in proportion to $\underline{C}^{1.139}$

Recently, experimental data on the equilibrium pressure of SO_2 over ammonium sulfite-bisulfite solutions were published [8-10].

TABLE 5

Equilibrium Pressure of Sulfurous Anhydride Over Ammonium Sulfite-Bisulfite Solutions Prepared According to Sedov's Experimental Data and Values Calculated by Equations (5), (7), and (9). •

C	S/C	Equilibrium pressure (in mm Hg)								
		30°			40°			50°		
		measured	(5)	(7), (9)	measured	(5)	(7), (9)	measured	(5)	(7), (9)
22.08	0.992	18.1	125	11.1	31.2	222	21.2	42.81	382	38.5
22.32	0.987	15.1	58	10.2	24.69	103	19.5	38.75	177	35.3
22.46	0.982	12.3	23.8	9.0	22.26	42.2	17.2	33.09	73	31.3
22.85	0.976	9.5	13.4	8.0	18.43	23.8	15.2	28.60	41	27.6
23.25	0.964	6.67	8.0	6.2	14.11	14.9	11.8	20.53	25.6	21.5
23.57	0.948	4.41	4.89	4.4	9.20	8.69	8.33	14.2	14.9	15.2
25.33	0.898	1.75	1.87	1.6	3.0	3.32	2.9	5.81	5.7	5.0
26.52	0.864	0.93	1.74	1.17	2.13	2.20	2.13	4.48	3.78	3.69

• Figures in parentheses are the numbers of the equations.

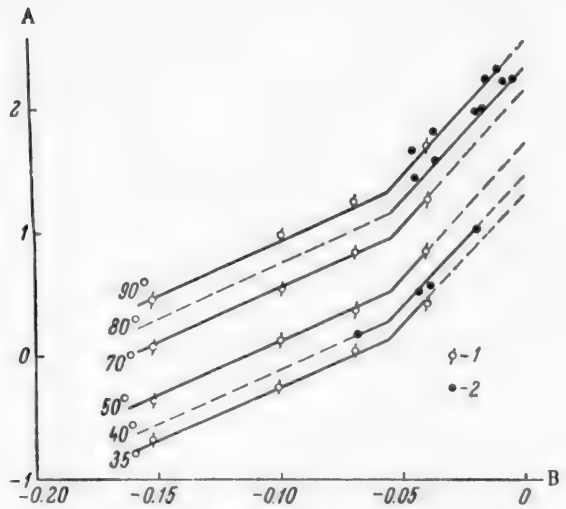

Relation between log $\underline{P}_{SO_2}$ and log $\underline{S/C}$ for an ammonium sulfite-bisulfite solution with a total concentration of dissolved ammonia $\underline{C}$ = 2.2 moles/100 moles H_2O at various temperatures. A) Value of log $\underline{P}_{SO_2}$ (mm); B) value of log $\underline{S/C}$. Experimental points: 1) Johnstone, 2) NIIOGAZ.

Data on the equilibrium pressure of SO_2 over solutions of low concentration ($\underline{C}$ = 0.33-2.5 at a temperature of 50° [8] and intermediate ($\underline{C} \simeq 10$) and existing in the temperature interval 16-50° [9] confirm the validity of Equation (9), as follows from Tables 3 and 4, in which experimental values are compared with calculated ones.

Values of the equilibrium pressure of SO_2, given by Sedov [10] for solutions with $\underline{S/C}$ between 0.864 and 0.992 and $\underline{C}$ = 22 (Table 5), at temperatures of 30 and 40°, particularly in the region of high $\underline{S/C}$, differ from values calculated by Equation (9), but far less than they do from values calculated by Equation (5).

At a temperature of 50° experimental data agree quite satisfactorily with values calculated by Equation (9) (Table 5).

Unfortunately the effect of solution concentration on the second part ($\underline{S/C} \geq 0.87$) could not be determined owing to the lack of experimental data. It should be noted that when $\underline{C}$ = 10 and 5, Johnstone's data do not correspond among themselves (Table 1) or with the data given by Jackson and Solbett [9] (experimental values of $\underline{P}_{SO_2}$ are higher for $\underline{C}$ = 5 than for $\underline{C}$ = 10, the $\underline{S/C}$ ratios being the same).

In this part, therefore, for values of $\underline{C}$ other than 22, $\underline{P}_{SO_2}$ may be calculated by Equation (7), it being arbitrarily assumed that the influence of the effective ammonia concentration in the solution is approximately linear here.

The practical value of Equations (7), (8), and (9) consists in the fact that with their aid it is possible to determine more accurately the motive force of the process of SO_2 absorption by ammonium sulfite-bisulfite

solution, and especially the process of evolution of the absorbed SO_2 from the saturated solution on heating; this makes it possible to choose the surface of contact between phases more correctly. Greater accuracy in the calculation of the equilibrium pressure of sulfurous anhydride over the solution will be correspondingly reflected in the calculation of the theoretical amount of steam used in distilling off the SO_2 (minimum consumption, determined in the ideal case of perfect equilibrium in the distillation column), which depends on the ratio $P_{SO_2}:P_{H_2O}$.

SUMMARY

1. It has been shown that the simplified equation for calculating the equilibrium partial pressure of SO_2 over ammonium sulfite-bisulfite solutions, proposed by Johnstone, gives large errors when applied to solutions in which more than 85% of the dissolved SO_2 is bound in the form of bisulfite ($S/C > 0.87$), especially at temperatures over 80°.

2. Empirical equations are proposed, which cover all the practically important region of bisulfite:sulfite ratios in the solutions up to the point of pure bisulfite ($S/C = 1$) and permit determination of the equilibrium partial pressure of SO_2 over these solutions with sufficient accuracy for practical purposes.

LITERATURE CITED

[1] Z. P. Rozenknop. Extraction of Sulfur Dioxide from Gases. Goskhimizdat (1952).

[2] N. G. Zalogin and S. M. Shukher. Elimination of Ashes and Oxides of Sulfur from Flue Gases. Gosenergoizdat (1954).

[3] A. P. Andrianov and B. A. Chertkov, J. Chem. Ind. 7, 10 (1954).

[4] E. Terres and E. Hahn, G. W. F., 70, 14, 15, 16, 17 (1927).

[5] H. F. Johnstone, Ind. Eng. Ch. 27, 5, 587 (1935).

[6] L N. Shokin, L M. Egorkin, and M. L Khaitovich, J. Chem. Ind. 15, 7 (1938).

[7] H. F. Johnstone, H. L Read, and H. C. Blankmeyer, Ind. Eng. Ch. 30, 1 (1938).

[8] H. E. Newall. Problems and Control of Air Pollution, Reinhold Publ. Corp. N.Y. (1955).

[9] A. Jackson and J. M. Solbett, Chem. Ind. 42, 1304 (1955).

[10] N. V. Sedov, Sci.-Techn. Inform. Bull. of the NITsIF, 5-6, 94 (1957).

Received August 6, 1958

USE OF POROUS SORBENTS FOR EXTRACTION OF METALLIC MICROIMPURITIES FROM TERVALENT CHROMIUM SALT SOLUTIONS

I. D. Muzyka and V. A. Molodtsova

Questions of the development of methods for the thorough separation of elements have recently received considerable attention in connection with the demand for metals (and their compounds) of a high degree of purity.

We shall not dwell on achievements in this field; however, we shall point out the possibility and prospects of using porous sorbents for the purposes of thorough separation of elements and extraction of valuable constituents in the complex treatment of polymetallic ores and alloys.

Among the porous sorbents which can be used for these purposes, activated charcoal should be mentioned first of all; it is a widely available and highly adsorbent substance. The use of this property of charcoal in combination with the difference in the adsorption of simple and complex ions of elements is the basis of the employment of porous sorbents for purposes of thorough separation of metals.

Methods of preparing chromium compounds of high purity are described in the present paper.

At this time methods of preparing chromium of high purity (ductile) are being developed in the following directions: 1) electrolysis from aqueous solutions of 6- and 3-valent chromium and electrolysis of fused salt mixtures containing chromic chloride and alkali metal chlorides, 2) reduction of chromic oxide with carbon in vacuo [1], 3) thermal decomposition of chromium iodide [2], and certain other methods.

Regardless of the method of preparing metallic chromium, the purity of the latter will be determined in most cases by the purity of the starting materials – the chromium compounds.

In most cases the chromium compounds manufactured by industry do not fulfill the requirements (with regard to impurity content) for the stated purposes. In view of this, we conducted an investigation in the development of methods for the extraction of metallic microimpurities from chromium compounds, chromic salts in particular.

It is quite obvious that in selecting reagents for thorough separation of microimpurities from the macrocomponent it will be most expedient (from the technological point of view) to use a group reagent for the microimpurities, which at the same time is inert to the macrocomponent. In this case the latter (reagent) must be widely available and inexpensive.

On the basis of an analysis of literature material and our preliminary data on chromic salts and heavy-metal microimpurities, we selected alkali-metal ferrocyanides (II), especially $K_4Fe(CN)_6$, for possible use as reagents for microimpurities (Fe, Ni, Cu, Co, etc.), fulfilling the above-mentioned requirements. Further experimental data fully confirmed the correctness of this choice.

Our problem in using the ferrocyanide reaction for purposes of separating microimpurities in the presence of a background of chromium salts was greatly facilitated as a result of the works of Tananaev and co-workers [3-5], and also others [6, 7], in the field of interaction processes between heavy-metal and ferrocyanide ions.

EXPERIMENTAL

The work was divided as follows: 1) study of the degree of separation in the case of an impurity taken by itself and in the case of a multicomponent (with regard to the number of impurities) system; 2) study of the

TABLE 1

Extraction of the Impurities: Fe, Cu, Ni, and Co from Chromic Salts

Salt being purified	Cr content (in g/ liter)	Content of metal impurities (in g/ liter) before purification				after purification				Added K_4R reckoned on
		Fe	Cu	Ni	Co	Fe	Cu	Ni	Co	
$Cr_2(SO_4)_3$	20	111.2	—	—	—	< 0.01	—	—	—	$Fe_4R_3 \cdot K_4R$
		111.2	—	—	—	0.005	—	—	—	$Fe_4R_3 \cdot K_4R$
		—	60.0	—	—	—	0.7	—	—	$5Cu_2R \cdot K_4R$
		—	—	67.0	—	—	—	18.0	—	Ni_2R
		—	—	67.0	—	—	—	Not found	—	$Ni_4K_4R_3$
		—	—	—	68.0	—	—	—	0.7	$5Co_2R \cdot K_4R$
		—	—	—	68.0	—	—	—	0.18	$4Co_2R \cdot 3K_4R$
		111.2	60.0	—	—	0.1	0.12	—	—	Fe_4R_3; $5Cu_2R \cdot K_4R$
		—	60.0	—	68.0	—	0.12	—	0.17	$5Cu_2R \cdot K_4R$; $4Co_2R \cdot 3K_4R$
		111.2	—	—	68.0	0.06	—	—	0.05	Fe_4R_3; $4Co_2R \cdot 3K_4R_3$
$Cr(NO_3)_3$	20	111.2	60.0	67.0	—	Not found	0.12	Not found	—	Fe_4R_3; $5Cu_2R \cdot K_4R$; $Ni_4K_4R_3$
$Cr_2(SO_4)_3$	20	116	60.0	67.0	68.0	0.064	0.20	Not found		Fe_4R_3; $5Cu_2R \cdot K_4R$; $Ni_4K_4R_3$; $4CO_2R \cdot 3K_4R_3$
	20	111.2	60.0	67.0	68.0	< 0.064	< 0.12	< 0.3	< 0.05	
	52	111.2	60.0	67.0	68.0	0.060	< 0.12	< 0.3	< 0.05	
$(NH_4)_2SO_4 \cdot Cr_2(SO_4)_3$	20	111.2	—	—	—	0.005	—	—	—	$Fe_4R_3 \cdot K_4R$
$K_2SO_4 \cdot Cr_2(SO_4)_3$	20	111.2	—	—	—	0.005	—	—	—	
$Cr(NO_3)_3$	20	111.2	—	—	—	Not found	—	—	—	

TABLE 2

Separation of the Elements $Cr^{3+} - Fe^{3+}$ with Respect to the Content of $K_4Fe(CN)_6$ in the Solution

Salt being purified	Cr conc. (in g/ liter)	Quantity of iron impurity (in mg/ liter)		Added K_4R reckoned on the compound
		before purification	after purification*	
$Cr_2(SO_4)_3$	20.0	111.25	26.4	K_4R 95% of theoretical, reckoned on Fe_4R_3
$Cr_2(SO_4)_3$	20.0	116.0	0.15	Fe_4R_3
$CrCl_3$	13.0	104.0	0.17	Fe_4R_3
$Cr_2(SO_4)_3$	20.0	111.25	0.01	$Fe_4R \cdot K_4R$
	20.0	111.25	0.01	
	20.0	111.25	0.005	
	20.0	111.25	Not found	
	20.0	111.25	0.013	$Fe_4R_3 \cdot 2K_4R$
	20.0	111.25	0.019	$Fe_4R_3 \cdot 3K_4R$
	20.0	111.25	0.026	$Fe_4R \cdot 4K_4R$
	20.0	111.25	0.026	$Fe_4R \cdot 5K_4R$

quality of reagent with respect to composition and proportions of microimpurities; 3) study of factors which may affect the degree of separation: the concentrations of macrocomponent and impurities, the effects of temperature, rate of precipitation, and keeping of precipitates, the amount of sorbent, the possibility of regenerating the reagent and sorbent, and the kinetics and composition of the precipitates formed.

The experiments were done in synthetic solutions of chromium salts: $Cr(NO_3)_3$, $CR_2(SO_4)_3$, $CrCl_3$, and potassium-chrome and ammonium-chrome alums, to which suitable amounts of heavy-metal impurities were added.

The separation process was carried out under static conditions.

The separation method was based on the principles of precipitation-adsorption chromatography [8, 9], where potassium ferrocyanide was used as reagent for the metal impurities, as mentioned above, and activated wood charcoal was used as sorbent (carrier).

The experimental technique was as follows:

To a solution of a chromium salt (20-60 g/liter Cr) with a definite content of metal impurity (60-200mg/liter) consisting of one or several cations, was gradually added a solution of the precipitant, K_4R (where R = [Fe $(CN)_6$]). In this case the solution in the vessel was stirred with a mechanical stirrer at a rate up to 100 rpm.

The amount of reagent (K_4R) used was based on a calculation of the extent of formation of the stable reaction products: $Fe_4R \cdot K_4R$, K_4Ni_4R3 (or $2Ni_2R \cdot K_4R$), $4Co_2R \cdot 3K_4R$ [3-5], and $5Cu_2R \cdot K_4R$ [6]* for iron, nickel, cobalt, and copper, respectively.

After addition of the required quantity of reagent, "OU"-type activated charcoal (treated beforehand with dilute HCl and water in order to remove soluble mineral constituents) was added in about 10 times the quantity calculated on the basis of the amount of metal impurity present, and the solution was left to stand for about an hour. After this the solid phases were separated from the liquid by filtration thru a dense filter bearing a layer of sorbent, or else the first portions of the filtrate were refiltered.

The experiments showed that in the temperature range 18-40°C there are no substantial differences in the completeness of separation. A further rise in temperature leads to an increase in the content of impurities (especially iron) in the filtrate, apparently owing to the increased solubility of the precipitates.

* Later, however, we found that for copper, the quantity of reagent, calculated on the basis of the assumption that $4Cu_2R \cdot K_4R$ is formed, gave more complete precipitation.

Time (up to 1 day) has no appreciable effect. However, prolonged keeping of precipitates is undesirable, since a tendency toward increase of impurities on the filtrate is observed after the precipitates have been kept for a day.

The concentration of impurities in the solution has no appreciable effect on the degree of purification. An increase in the concentration of the macrocomponent (the salt being purified) increases (in percentage) the degree of purification. In practice, however, it is better to carry out purification with solutions containing 20-60 g/liter chromium, since the viscosity of the solutions increases at higher concentrations, which hinders the filtration process.

The experiments showed also that the reagent and sorbent could be regenerated (for instance, in the case of iron precipitates: $Fe_4R_3 + 12KOH \rightarrow 4Fe(OH)_3\downarrow + 3K_4R$). However, use of the method for separating microimpurities involves very insignificant expenditures, and it may be more practicable to use fresh materials.

In Tables 1 and 2 are given part of the data on separation of heavy-metal microimpurities (Fe, Cu, Ni, and Co) from a number of chromic salts, by the method described above, in cases where the stated metal impurities are separately and jointly present in the chromium salt solution.

On analysis of the data of our investigation and especially Tables 1 and 2, the following conclusion may be drawn.

By the method described above, the following binary systems can be throughly separated: $Cr^{3+} - Fe^{3+}$, $Cr^{3+} - Ni^{2+}$, $Cr^{3+} - Cu^{2+}$, $Cr^{3+} - Co^{2+}$.

In the case where the stated impurities are jointly present in the solution, the degree of extraction of each of them also is quite high, so that simultaneous (single operation) removal of a number of metallic impurities from chromium salt solutions is possible.

Table 2 characterizes the degree of extraction of iron with respect to the quantity of precipitant, where the optimum quantity of the latter (K_4R) corresponds to the compound $Fe_4R_3 \cdot K_4R$.

In conclusion a certain (although insignificant) effect of the anionic composition of the macrocomponent on the degree of separation must be pointed out. Chromium nitrate behaves best in this respect, chromium sulfate being next best. In the case of chromic chloride, the degree of extraction of impurities (especially iron) is somewhat lower. In a hydrochloric acid medium the solubility of the precipitates apparently is higher than in other media [7]. The structural properties of the precipitates, which depend to a certain degree on the nature of the anion of the original salt, possibly play a part [10].

The method developed by us can be used in the conversion of chromium ores and alloys to salts by the acid method. Preliminary experiments showed that chromium ore may be successfully converted by the acid method--particularly the sulfuric acid method – to a soluble state (with 94-98% extraction of chromium) with simultaneous macroseparation of its Cr–Fe and other components.

SUMMARY

In an investigation of the extraction of metallic microimpurities (iron, copper, nickel, and cobalt) from solutions of chromic salts, using potassium ferrocyanide as reagent and activated wood charcoal as porous sorbent (carrier), it was shown that 3-valent chromium compounds can, by the given method, be freed to a high degree from microimpurities of other metals whether the latter are separately or jointly present in the solution.

The developed method of purifying chromium compounds is distinguished by its simplicity from the point of view of technology and apparatus, and also is inexpensive from the economic point of view.

The method can be used in the conversion of chromium ores and alloys to chromium salts of high purity.

LITERATURE CITED

[1] G. V. Karsanov, Inform. Bull. TsII MChM SSSR 11-12, 38 (1957).

[2] Coll., "Problems of Modern Metallurgy," IL 1 (37), 83 (1958).

[3] I. V. Tananaev and M. I. Levina, J. Anal. Chem. 1, 236 (1946); 1, 224 (1946); 3, 31 (1948).

[4] I. V. Tananaev and M. I. Levina, Factory Labs 8, 887 (1949).

[5] I. V. Tananaev, G. B. Seifer, and M. A. Glushkova, J. Inorg. Chem. 2, 268 (1957).

[6] N. G. Chovnyk and G. A. Kleibs, J. Anal. Chem. 3, 302 (1948).

[7] M. Kyrsh and O. E. Zvyagintsev, J. Inorg. Chem. 3, 11, 2582 (1958).

[8] T. B. Gapon and E. N. Gapon, Proc. Acad. Sci. USSR 10, 3, 401 (1948).

[9] A. M. Gurvich and T. B. Gapon, Factory Labs 9, 1037 (1957).

[10] I. F. Karpova and T. P. Spasibenko, Leningrad State Univ. Herald 16, 126 (1958); 16, 117 (1957).

Received May 23, 1958

ON THE CONDITIONS OF FORMATION OF A CONTINUOUS SERIES OF SOLID SOLUTIONS IN THE PSEUDOBINARY SYSTEM $CrB_2 - TiB_2$

N. G. Sevast'yanov, V. A. Épel'baum, M. A. Gurevich, B. F. Ormont, and G. S. Zhdanov

Karpov Physicochemical Institute

In the preceding works [1, 2] the presence of a series of boride phases in the Cr – B system, of great theoretical and practical interest, was established. In this system the most stable phase with respect to oxygen and other aggressive media, to judge from the data of Campbell and co-workers [3], for instance, is the CrB_2 phase. Furthermore, it is known from our data, as well as the cited works [4, 5], that the transition-metal diboride most chemically stable to oxygen is titanium diboride TiB_2. The conditions of preparation, structures, and properties of complex transition-metal diborides were investigated in a number of works. In certain of these [6-8] an attempt at systematizing this class of compounds and establishing certain regularities of formation of reciprocal solid solutions of diborides was made.

Double diborides of chromium and titanium were studied in the work of Post, Glasser, and Moskowitz [6]. They were prepared thru coalescence of the individual diborides CrB_2 and TiB_2, synthesized beforehand from the elements, on hot pressing in a helium atmosphere. Meerson and co-workers [9] synthesized complex chromium and titanium diborides by sintering (followed by homogenization at a temperature of 2000-2100° for 3-4 hours) of the initial, individual diborides, prepared from the corresponding mixtures of Cr_2O_3 and TiO_2 with boron carbide and soot.

In our preliminary experiments it was found that double diborides of chromium and titanium in certain ratios have greater chemical stability than the original diborides taken separately. In this case compounds synthesized from initial CrB_2 and TiB_2 were investigated, the initial diborides being prepared by the reduction of boron trioxide and the corresponding metal oxides in mixtures with carbon. The diboride mixtures were sintered: 1) by the method of hot pressing at 1900-2000°, 2) by the same method, but with subsequent homogenization in vacuo (10^{-2} mm) at 2000° for 2 hours; 3) by sintering the initial mixtures in a TVV-2 furnace in vacuo at 2000°. By the methods indicated above, however, despite the great number of experiments that have been carried out, complete homogenization of the products has not been achieved.

Taking into account the great practical importance which these materials may have in new technical fields, we considered it necessary to investigate them in detail, using other methods of synthesis.

EXPERIMENTAL

The region of compositions from $(Cr_{0.1}\ Ti_{0.9})B_2$ to $(Cr_{0.9}\ Ti_{0.1})B_2$ was investigated by x-ray and chemical methods, the subscripts of Cr and Ti being varied 0.1 unit at a time.

Method of synthesis and starting materials. The compounds were synthesized from the initial elements Cr, Ti, and B in a TVV-2 furnace in vacuo (10^{-3} mm) at a temperature of 2000° during 2 hours with subsequent heating at 2200° for 30 minutes.

Electrolytic chromium (99.9% Cr), titanium (98.7% Ti), and boron (99.6% B), obtained by the thermal decomposition of boranes, were mixed in definite proportions, moistened with alcohol, and pressed in steel pressforms into cylinders 6-8 mm in diameter and 8-10 mm high, under 150 kg/cm^2 pressure.

Variation of Identity Periods (Error of Determination not over ± 0.001 kX) of the Hexagonal Lattice of a Continuous Series of Solid Solutions (Cr, Ti)B_2 with Respect to Chemical Composition.

No. of sample	Assigned composition	Composition obtained (in wt. %)				Formula*	Identity periods (in kX)		Density	
		Cr	Ti	B	sum		a	c	σ_x, x-ray	σ_p, pycnometer
234	$CrB_{2.2}$	71.0	—	29.4	100.4	$Cr_{1.01}B_2$	2.962	3.060	5.23	5.6
237	$Cr_{0.9}Ti_{0.1}B_2$	59.4	11.0**	29.6	100.0	$Cr_{0.84}Ti_{0.16}B_2$	2.974	3.074	5.13	5.1
238	$Cr_{0.8}Ti_{0.2}B_2$	51.1	19.1	30.5	100.7	$Cr_{0.70}Ti_{0.28}B_2$	2.978	3.087	5.07	4.8
239	$Cr_{0.7}Ti_{0.3}B_2$	47.2	23.6	30.2	101.0	$Cr_{0.65}Ti_{0.35}B_2$	2.983	3.114	4.98	5.0
243	$Cr_{0.6}Ti_{0.4}B_2$	30.7	35.6	33.1	99.4	$Cr_{0.39}Ti_{0.49}B_2$	2.988	3.122	4.95	4.5
236	$Cr_{0.5}Ti_{0.5}B_2$	33.6	36.1	30.9	100.6	$Cr_{0.46}Ti_{0.54}B_2$	2.993	3.141	4.85	4.7
242	$Cr_{0.4}Ti_{0.6}B_2$	26.7	42.6**	30.7	100.0	$Cr_{0.36}Ti_{0.63}B_2$	3.001	3.158	4.77	4.7
244	$Cr_{0.3}Ti_{0.7}B_2$	18.5	51.1	30.6	100.2	$Cr_{0.25}Ti_{0.75}B_2$	3.012	3.179	4.68	4.7
240	$Cr_{0.2}Ti_{0.8}B_2$	13.4	57.0	31.4	101.8	$Cr_{0.18}Ti_{0.81}B_2$	3.016	3.190	4.62	4.5
241	$Cr_{0.1}Ti_{0.9}B_2$	6.2	63.1	32.0	101.3	$Cr_{0.08}Ti_{0.89}B_2$	3.021	3.215	4.54	4.3
229	TiB_2	—	68.9	30.8	99.7	$Ti_{1.01}B_2$	3.023	3.220	4.50	4.5

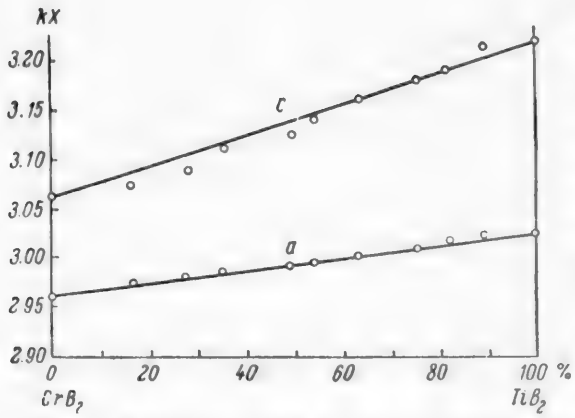

Variation of identity periods of the hexagonal lattice of a continuous series of solid solutions in the pseudo-binary system CrB_2—TiB_2. a and c) Identity periods (in kX).

The cylinders were put into specially-prepared crucibles of technical boron, with covers. The crucibles containing the cylinders were suspended vertically in the furnace by tungsten wires. For comparison, moreover, identical compositions were synthesized under the same conditions, but in one case the starting materials were the previously prepared, individual chromium and titanium diborides (CrB_2 and TiB_2), whereas in the other case they were the oxides in the corresponding proportions (Cr_2O_3, TiO_2, B_2O_3); the latter were reduced in a mixture with carbon under the same conditions.

Method of x-ray and chemical analyses and density determination. X-ray phase analysis of the starting materials and the products of synthesis was carried out by the powder method using filtered Cu radiation ($\lambda CuK\alpha_1$ = = 1.53740 kX, $\lambda CuK\alpha$ = 1.5387 kX) in RKD-type cameras about 57.3 mm in diameter and RKU-type cameras about 114.6 mm in diameter, the film being loaded asymmetrically. The error of determination of identity periods in the lattice was not over ± 0.001 kX in this case.

Owing to the chemical stability of transition-metal diborides, complex diborides in particular, it was necessary to develop a special procedure in order to determine their metallic constituents by chemical methods.

A separate weighed sample was taken for determining each constituent. To determine titanium, a weighed sample (about 0.05 g) was fused with potassium bisulfate in a platinum crucible at 500-600° during 1.5-2 hours, the temperature being raised slowly in order to avoid loss of material. The melt was then leached out with dilute sulfuric acid and filtered. The filtrate was treated with cupferron, the resulting titanium dioxide precipitate ignited and brought to constant weight, and titanium determined therefrom.

* Error of determining the subscripts in the formula, not over ± 0.02.

** The titanium content was determined by difference.

To determine chromium, weighed samples of the product under investigation were fused with a sodium carbonate-potassium nitrate mixture in a platinum crucible at 1000-1100° during 2-3 hours. The melt was then leached out with water and filtered into a 500-ml volumetric flask. An aliquot was pipetted from the solution being investigated, and its chromium content was determined by generally-known methods, either reduction (Mohr's salt) and titration with permanganate solution or by reduction with potassium iodide and titration with thiosulfate in the presence of starch.

Boron was determined, as usual, by fusing a weighed sample, leaching the melt in acidified water, and titrating the boric acid in the presence of mannitol, using phenolphthalein as indicator.

The densities of the powders were determined at 25° in a pycnometer of about 3 ml volume; the pycnometric liquid was "ethylenebenzene" of specific gravity 0.8644. The "ethylenebenzene" was dried at 0.3-0.5 mm pressure; its vapor pressure at room temperature was less than 0.1 mm.

More accurate measurements were unnecessary for our case, in view of the accuracy of the x-ray phase and chemical analyses.

Results of the investigation. X-ray analysis of the products of synthesis from the initial elements chromium, titanium, and boron showed that in all composition regions from $(Cr_{0.9}\ Ti_{0.1})B_2$ to $(Cr_{0.1}\ Ti_{0.9})B_2$ a continuous series of solid solutions is formed, the variation in the identity periods of the hexagonal lattice (space group D^1_{6h}) of which is practically in accord with Vegard's Law (figure, table). The slight fluctuations of periods $\underline{a}$ and $\underline{c}$ about the straight Vegard line are apparently due to errors in the x-ray and chemical analyses.

X-ray analysis of the products of sintering of initial chromium and titanium diborides, CrB_2 and TiB_2, showed that compounds having initial compositions from $0.9CrB_2 + 0.1TiB_2$ to $0.5CrB_2 + 0.5TiB_2$ are single-phase, and the lattice is hexagonal, but lines, for which the angle θ is large, are appreciably attenuated. Compounds with a high TiB_2 content give not only the lines of the main solid-solution phase, but also weak lines of a second phase; i.e., a continuous series of solid solutions was not formed over the entire range on synthesis from individual diborides.

The question of starting materials is often decisive in industrial production. Therefore we attempted to prepare double chromium-titanium diborides by the method of reducing chromic oxide, titanium dioxide, and boron trioxide in a mixture with carbon according to the procedure worked out by V. A. Épel'baum [10].

The initial oxides and carbon were thoroughly mixed in the corresponding proportions and the mixture pressed into cylinders, which were heated in a TVV-2 vacuum furnace (10^{-3} mm) at 2000° for 1.5 hours.

X-ray analysis showed that the preparation of double chromium and titanium diborides by this method also leads to the formation of a continuous series of solid solutions.

It should be noted, however, that with the stated method of synthesis the composition obtained in some samples differs appreciably from the assigned, calculated composition. Apparently the technology of production (preliminary synthesis at lower temperatures) must be made more precise in each individual case.

The results obtained show that under identical conditions of heating, $(Cr, Ti)B_2$ solid solutions are formed much more rapidly and completely on synthesis from initial elements than on sintering of chromium and titanium diborides.

SUMMARY

In an investigation of the conditions of formation and the structure of double chromium and titanium diborides in the composition region from $(Cr_{0.9}\ Ti_{0.1})B_2$ to $(Cr_{0.1}\ Ti_{0.9})B_2$ it was shown, by x-ray and chemical methods, and also by density determinations, that synthesis from the elements at 2100-2200° in vacuo leads, in the entire composition region, to the formation of a continuous series of solid solutions in which the period of the hexagonal lattice varies from $\underline{a}$ = 2.962 kX, $\underline{c}$ = 3.060 kX (for the composition CrB_2) to $\underline{a}$ = 3.023 kX, $\underline{c}$ = 3.220 kX (for the composition TiB_2).

In the synthesis of complex borides from the initial diborides CrB_2 and TiB_2, the formation of a continuous series of solid solutions is hindered.

Synthesis of chromium and titanium diboride by the method of reducing chromic oxide, titanium dioxide, and boron trioxide in a mixture with carbon gives a positive result.

LITERATURE CITED

[1] V. A. Épel'baum, N. G. Sevast'yanov, M. A. Gurevich, B. F. Ormont, and G. S. Zhdanov, J. Inorg. Chem. 2, 8, 1848 (1957).

[2] V. A. Épel'baum, N. G. Sevast'yanov, M. A. Gurevich, B. F. Ormont, and G. S. Zhdanov, J. Inorg. Chem. 3, 11, 2545 (1958).

[3] I. Campbell, C. Powell, D. Nowicki, and B. Gonser, J. Electroch. Soc. 96, 313 (1949).

[4] G. Weiss, Ann. Chim. 1, 446 (1946).

[5] G. V. Samsonov and N. K. Golubev, J. Phys. Chem. 30, 1258 (1956).

[6] B. Post, F. Glasser, and D. Moskowitz, Acta Metallurgica 1, 20 (1954).

[7] G. V. Samsonov, Bull. Sector Phys.-Chem. Anal. 27, 97 (1956).

[8] R. B. Kotel'nikov, J. Inorg. Chem. 3, 4, 841 (1958).

[9] G. A. Meerson, G. V. Samsonov, R. B. Kotel'nikov, M. S. Volkova, L. P. Evteeva, and S. D. Krasnenkova, J. Inorg. Chem. 3, 4, 898 (1958).

[10] V. A. Épel'baum. Auth. Cert. No. 17969 (1952).

Received July 21, 1958

UTILIZATION OF DIAGRAMS OF THE RECIPROCAL SYSTEM OF AMMONIUM MONOPHOSPHATE – SODIUM NITRATE – WATER IN THE PROCESS OF NITRIC ACID DECOMPOSITION OF PHOSPHATES

S. Ya. Shpunt

Scientific Research Institute of Fertilizers and Insectofungicides

In one variant of the nitric acid processing of phosphate developed at the Research Institute for Fertilizers and Insectofungicides (NIUIF) [1], the calcium ion is precipitated from the resulting extract with sodium sulfate to give calcium sulfate. Subsequent neutralization with ammonia gives a solution containing ammonium monophosphate, sodium nitrate and ammonium nitrate.

Methods of separation of these salts are considered in this paper. Starting from the phase diagrams of the ternary systems and the diagonal and internal sections of the quaternary systems [2-5] which were studied by the visual-polythermal method, the isotherms of the quaternary systems were constructed and tested by the isothermal method: +30, +20 and 0° [6] and -10, -15 and -20° [7]. These diagrams are used for production schedule calculations.

We shall first consider the routes to separation of the salts. The starting solution, resulting from decomposition of a phosphate rock with nitric acid followed by treatment of the slurry with sodium sulfate and neutralization with ammonia, has approximately the following composition (in %): $NaNO_3$ 27.8, $NH_4H_2PO_4$ 11.1, NH_4NO_3 1.3, H_2O 59.8. We considered two variants of the production cycles.

Since the quantity of ammonium nitrate in the original solution is very small, we ignored it in the first variant and regarded the system as the three-component one: $NaNO_3 - NH_4H_2PO_4 - H_2O$. This stable salt pair corresponds to the diagonal of Jänecke's square. We previously established the stability of this diagonal in the +110 to +1.4° temperature range [5].

In the second variant a more accurate picture is obtained by taking into consideration the ammonium nitrate present in the starting solution. The system is then regarded as a quaternary one and the production cycle calculations are based on Jänecke's square.

Since operations are nearly identical in the two variants, we shall describe the first in detail and then discuss the second one with reference to the first.

The path followed by the figurative point F of the "initial" solution*, resulting from crystallization (at 0°) of monoammonium phosphate and subjected to evaporation, is schematically represented in Fig. 1.

The production cycle is represented by the rectangle BCEF which determines the technological process schedule and the quantitative ratios of substances formed during the process.

The technological scheme delineated by the rectangle (Fig. 1) comprises three consecutive operations:

1) Evaporation of the "starting" solution; 2) mixing of the eutonic solution with a fresh batch of original solution; 3) crystallization of mixed solution with formation of "starting" solution.

* The "initial" solution is obtained on crystallization of mixture E obtained by addition of the original solution M to the eutonic C.

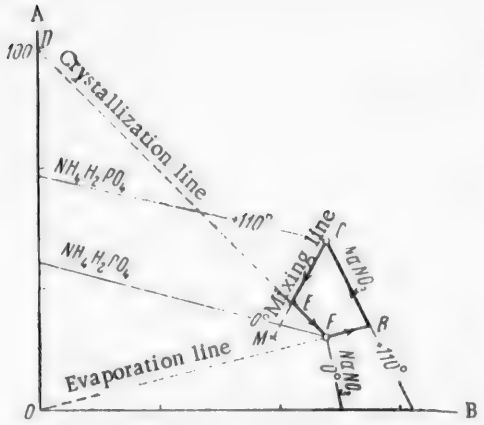

Fig. 1. Cyclic process scheme. A) % $NH_4H_2PO_4$; B) % $NaNO_3$.

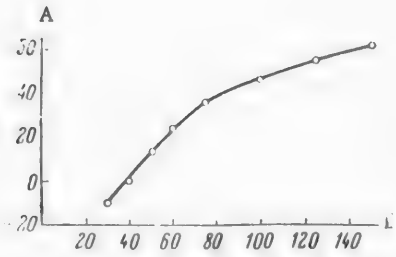

Fig. 3. Cooling temperature in dependence on quantity of +110° eutonic solution. A) cooling temperature (°C); B) quantity of +110° eutonic solution per 100 parts by weight of original solution (parts by wt.).

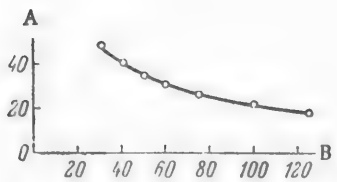

Fig. 4. Degree of precipitation of $NH_4H_2PO_4$ as a function of the quantity of +110° eutonic solution. A) % precipitation of $NH_4H_2PO_4$; B) quantity of +110° eutonic solution per 100 parts by weight of original solution (in parts by weight).

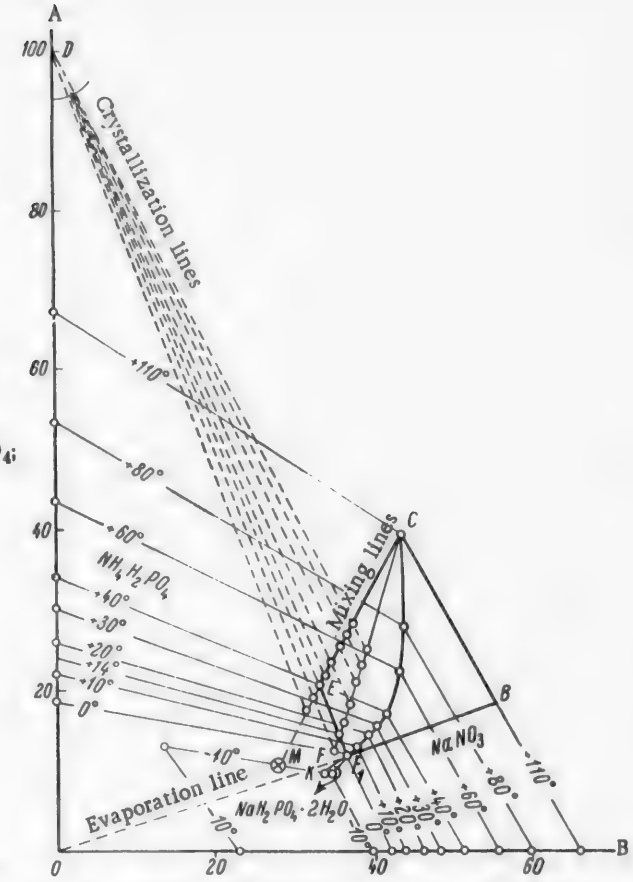

Fig. 2. Polytherm of the diagonal section of $NaNO_3$ – $NH_4H_2PO_4$ – H_2O [5]. A) $NH_4H_2PO_4$ content (%); B) $NaNO_3$ content (%).

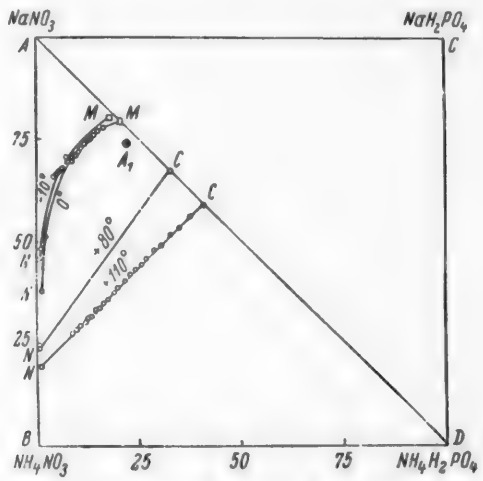

Fig. 5. Portions of the -10, 0, +80, and 110° isotherms of the system $NaNO_3$ – $NH_4H_2PO_4$ – H_2O.

TABLE 1

Composition of Mixed and Cooled Solutions Obtained by Mixing of Various Quantities of Eutonic with 100 Parts by Weight of Original Solution (the NH_4NO_3 content of the original solution is ignored).

Parts of +110° eutonic solution per 100 parts by weight of original solution (in parts by weight)				Mixed solutions (in parts by weight)				Cooled solution						Cooling temp. (°C)	Degree of precipitation of $NH_4H_2PO_4$ (%)
								in parts by weight				weight, %			
total quantity of eutonic	$NaNO_3$	$NH_4H_2PO_4$	H_2O	total quantity of mixed solution	$NaNO_3$	$NH_4H_2PO_4$	H_2O	total quantity of cooled solution	$NaNO_3$	$NH_4H_2PO_4$	H_2O	$NaNO_3$	$NH_4H_2PO_4$		
150	65.00	59.60	25.40	250	92.80	70.70	86.50	238.9	92.80	59.60	86.50	38.84	24.95	62	15.7
125	54.16	49.67	21.17	225	81.96	60.78	82.26	213.9	81.96	49.68	82.26	38.32	23.22	56	18.3
100	43.33	39.74	16.93	200	71.13	50.81	78.06	188.9	71.13	39.71	78.06	37.65	21.02	47	21.9
75	32.50	29.80	12.70	175	60.30	40.90	73.80	163.9	60.30	29.80	73.80	36.79	18.18	36	27.1
60	25.99	23.84	10.17	160	53.79	34.94	71.27	148.9	53.79	23.84	71.27	36.12	16.01	24	31.8
50	21.66	19.89	8.47	150	49.46	30.98	69.56	138.9	49.46	19.88	69.56	35.56	14.29	14	35.8
40	17.33	16.90	6.77	140	45.13	27.00	67.87	128.9	45.13	15.90	67.87	35.01	12.33	0	41.1
30	13.00	11.92	4.08	130	40.80	23.02	66.18	118.9	40.80	11.92	66.18	34.29	10.02	−10	48.3

TABLE 2

Composition of Mixed and Cooled Solutions Obtained by Mixing Various Quantities of Eutonic with 100 g of Original Solution (presence of ammonium nitrate taken into consideration).

Quantity of salt mass in eutonic solution per 100 g of salt mass in original solution (in g)					Quantity of salt mass in mixed solution (in g)					Quantity of salt mass in cooled solution (in g)									Cooling temperature (°C)
															recalculated per 100 parts by weight of salt mass				
total quantity	$NaNO_3$	$NH_4H_2PO_4$	NH_4NO_3	H_2O	total quantity	$NaNO_3$	$NH_4H_2PO_4$	NH_4NO_3	H_2O	total quantity	$NaNO_3$	$NH_4H_2PO_4$	NH_4NO_3	H_2O	$NaNO_3$	$NH_4H_2PO_4$	NH_4NO_3	H_2O	
90	50.7	33.7	5.6	94	190	125.0	55.7	9.3	850	168.1	125.0	33.7	9.3	850	74.5	20.0	5.6	506	+15
82	46.3	30.6	5.1	86	182	120.6	52.6	8.8	842	160.1	120.6	30.7	8.8	842	75.4	19.1	5.5	525	−12
75	42.4	28.0	4.6	79	175	116.8	49.9	8.3	835	153.1	116.8	28.0	8.3	835	76.3	18.3	5.4	545	+ 3
68	38.3	25.5	4.2	71	168	112.8	47.3	7.9	827	146.1	112.8	25.4	7.9	827	77.2	17.4	5.4	566	0
60	33.9	22.4	3.7	63	160	108.3	44.3	7.4	819	138.1	108.3	22.4	7.4	819	78.3	16.3	5.4	593	0

TABLE 3

Composition of Cooled Solutions Obtained on Mixing 100 Moles of Original Solution with 60 Moles of Eutonic Solution for 16 Consecutive Cycles (account taken of ammonium nitrate); Solutions Cooled to 0°.

Quantity of salt mass in the eutonic solution of the +110° isotherm per 100 g of salt mass in original solution (in g)				Quantity of salt mass in mixed solution (in g) totalling 160 g				Cooled solution							
								quantity of salt mass (in g) with an over-all salt content of 138.1				recalculated for 100 parts by weight of salt mass			
$NaNO_3$	$NH_4H_2PO_4$	NH_4NO_3	H_2O	$NaNO_3$	$NH_4H_2PO_4$	NH_4NO_3	H_2O	$NaNO_3$	$NH_4H_2PO_4$	NH_4NO_3	H_2O	$NaNO_3$	$NH_4H_2PO_4$	NH_4NO_3	H_2O
33.9	22.4	3.7	63	108.3	44.3	7.4	819	108.3	22.4	7.4	819	78.3	16.3	5.4	593
32.4	21.0	6.6	62	106.8	42.9	10.3	818	106.8	21.0	10.3	818	77.3	15.2	7.5	592
30.9	19.5	9.6	60	105.3	41.4	13.3	816	105.5	19.5	13.3	816	76.3	14.1	9.6	591
29.7	18.2	12.1	59	104.1	40.1	15.8	815	104.1	18.2	15.8	815	75.4	13.2	11.4	590
28.6	17.3	14.1	58	103.0	39.2	17.8	814	103.0	17.3	17.8	814	74.6	12.5	12.9	589
27.5	16.2	16.3	56	101.9	38.1	20.0	812	101.9	16.2	20.0	812	73.8	11.7	14.8	588
26.6	15.3	18.1	56	101.0	37.2	21.8	812	101.0	15.3	21.8	812	73.1	11.1	15.8	588
25.8	14.6	19.6	55	100.2	36.5	23.3	811	100.2	14.6	23.3	811	72.5	10.6	16.9	587
25.2	13.8	21.0	54	99.6	35.7	24.7	810	99.6	13.8	24.7	810	72.1	10.0	17.9	586
24.2	12.9	22.9	53	98.6	34.8	26.6	809	98.6	12.9	26.6	809	71.4	9.3	19.3	586
23.2	12.0	24.8	52	97.6	33.9	28.5	808	97.6	12.0	28.5	808	70.7	8.7	20.6	585
22.5	11.4	26.1	52	96.9	33.3	29.8	808	96.9	11.4	29.8	808	70.2	8.2	21.6	585
21.7	10.6	27.7	51	96.1	32.5	31.4	807	96.1	10.6	31.4	807	69.6	7.7	22.7	584
21.0	9.9	29.1	50	95.4	31.8	32.8	806	95.4	9.9	32.8	806	69.1	7.2	23.7	583
20.3	9.2	30.4	49	94.7	31.1	34.1	805	94.7	9.2	34.1	805	68.6	6.7	24.7	583
19.8	8.7	31.5	49	94.2	30.6	35.2	805	94.2	8.7	35.2	805	68.2	6.3	25.5	582

These operations are bound to lead to a specific and constant quantity of "starting" solution, say 100 parts by weight, but the cycle is not always completed.

In order to effect completion of the cycle, we must take into account the crystallization temperature; the corresponding composition of the "starting" solution is governed by quantity of eutonic (+110° isotherm) mixed with 100 wt.-% of original solution and not with an arbitrary proportion thereof. The cyclic scheme for separation of the salts is shown below.

The compositions of the mixed and frozen solutions for various eutonic quantities are presented in Table 1 and plotted in Fig. 2. Points E, corresponding to mixed solution compositions, are distributed over the mixing line CM, while points F, corresponding to the compositions of frozen solutions, are distributed along curve CF. It should be noted that the latter in most cases are located not at the eutonic points of the isotherms [5] but on the crystallilization line of monoammonium phosphate.

Reciprocal Aqueous System of Ammonium Monophosphate-Sodium Nitrate-Water

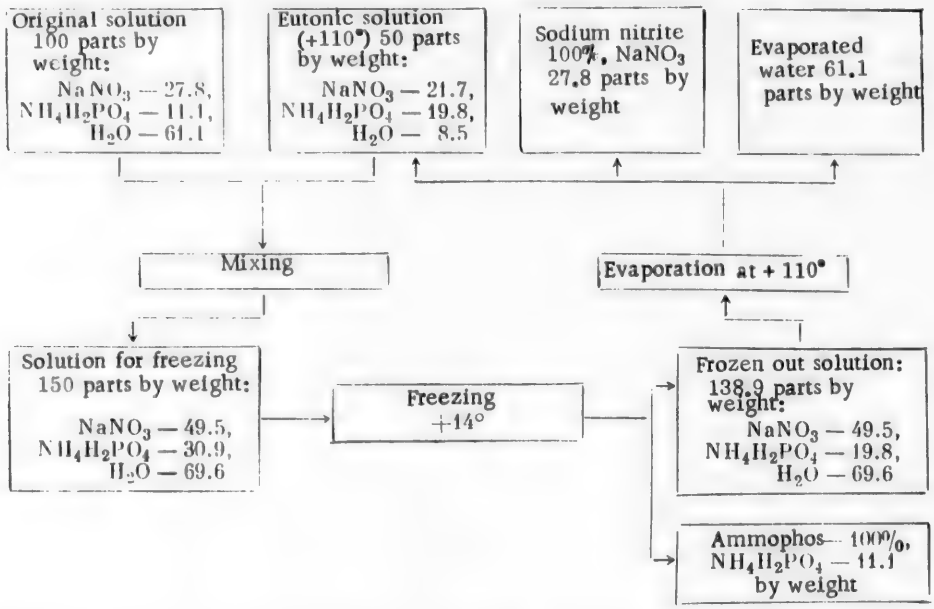
Original solution 100 parts by weight: $NaNO_3$ — 27.8, $NH_4H_2PO_4$ — 11.1, H_2O — 61.1
Eutonic solution (+110°) 50 parts by weight: $NaNO_3$ — 21.7, $NH_4H_2PO_4$ — 19.8, H_2O — 8.5
Sodium nitrite 100%, $NaNO_3$ 27.8 parts by weight
Evaporated water 61.1 parts by weight
Mixing
Evaporation at + 110°
Solution for freezing 150 parts by weight: $NaNO_3$ — 49.5, $NH_4H_2PO_4$ — 30.9, H_2O — 69.6
Freezing +14°
Frozen out solution: 138.9 parts by weight: $NaNO_3$ — 49.5, $NH_4H_2PO_4$ — 19.8, H_2O — 69.6
Ammophos — 100%, $NH_4H_2PO_4$ — 11.1 by weight

The results of Table 1 have the following implications: For given compositions of the original and eutonic solutions the cooling temperature must be the lower (and in turn the degree of precipitation of monoammonium phosphate must be the higher) the smaller is the amount of eutonic solution mixed with 100 parts by weight of the original solution. This relationship is expressed graphically in Figs. 3 and 4.

Production Cycle in Presence of Ammonium Nitrate

Two methods were employed for the four-component system (including ammonium nitrate).

The first method of separation of the salts is illustrated by Fig. 5 which is a projection plot of part of the isotherms of the quaternary system by Jänecke's procedure [6, 7].

Of the curves bounding the fields of crystallization of sodium nitrate and monoammonium phosphate, the greatest interest from the salt separation aspect is attached to curve MN. The latter divides the fields of crystallization of sodium nitrate and monoammonium phosphate. It is plotted in Fig. 5 for the 0 and -10° isotherms. We only give a portion of curve MN for the +100 and +80° isotherms.

The original solution has the following composition in grams per 100 grams of salt mass: $NaNO_3$ 74.4, $NH_4H_2PO_4$ 21.9, NH_4NO_3 3.7, H_2O 75.6. It is represented in Fig. 5 by point A.

The production cycle comprises the same three operations that were given in detail for the three-component system. These operations, like the preceding ones, do not always result in a closed cycle. Here again the composition and cooling temperature of the solution are governed by the quantity of eutonic solution mixed with 100 moles of original solution.

For this case we likewise calculated the compositions of the cooled solutions obtained on mixing 100 moles of original solution with different quantities of eutonic solution (Table 2). The corresponding crystallization temperatures are found with the help of the isotherms of the quaternary systems [6, 7]. Ammonium nitrate gradually accumulates in solution because it is not deposited either at the evaporation stage or at the cooling stage. Table 3 contains the compositions of cooled solutions obtained on mixing 100 moles of original solution with 60 moles of eutonic solution for 16 consecutive cycles. Each composition in the series differs from the preceding one by the incremental amount of ammonium nitrate. The cooled solutions and the corresponding eutonics for all of the calculated cycles are plotted in Fig. 5.

The schedule of separation of sodium nitrate and monoammonium phosphate in the four-component reciprocal aqueous system $NaNO_3 - NH_4H_2PO_4 - H_2O$ is set forth below.

The crystallization temperature of the cooled solutions is 0°. In practice it is permissible to allow ammonium nitrate to build up to 25 g per 100 g of salt mass, i.e., to perform approximately 16 cycles at a crystallization temperature of about 0°. The crystallization temperature begins to fall rapidly if more ammonium nitrate accumulates. If a temperature in the vicinity of 0° is assumed as the maximum crystallization temperature, then 16 cycles result in a cooled solution with the composition (mole fractions): $NaNO_3$ 0.682, $NH_4H_2PO_4$ 0.063, NH_4NO_3 0.255, H_2O 5.82; this solution can be evaporated to dryness to give a mixture of salts which constitutes a fertilizer.

Reciprocal Aqueous System of Ammonium Monophosphate-Sodium Nitrate-Water

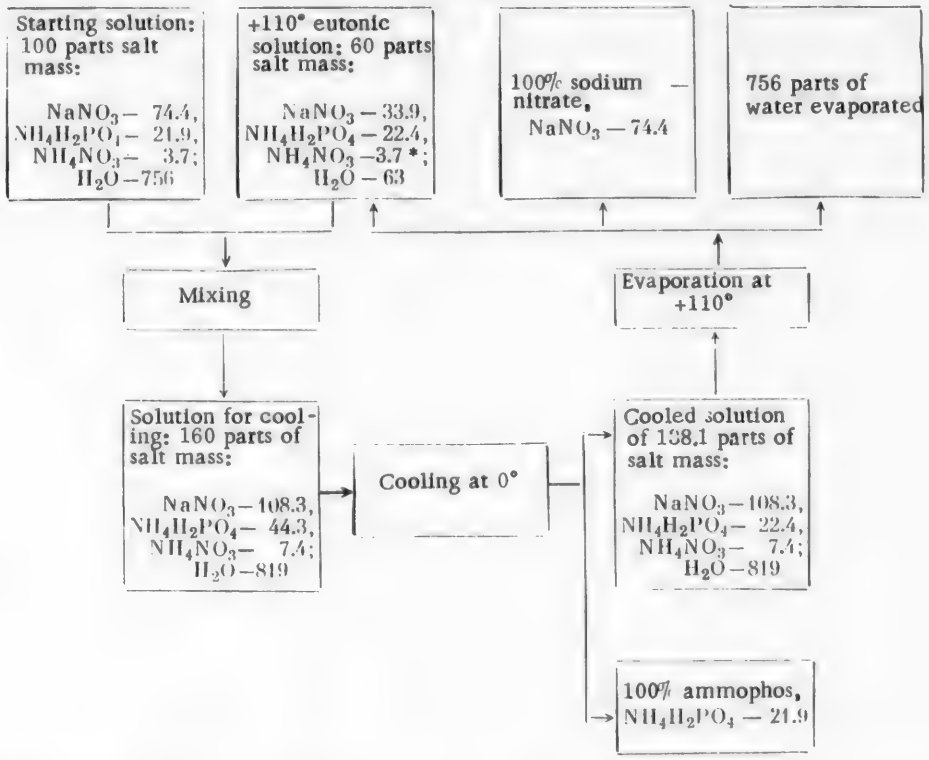
Starting solution: 100 parts salt mass: NaNO3 – 74.4, NH4H2PO4 – 21.9, NH4NO3 – 3.7; H2O – 756
+110° eutonic solution: 60 parts salt mass: NaNO3 – 33.9, NH4H2PO4 – 22.4, NH4NO3 – 3.7 *; H2O – 63
100% sodium nitrate, NaNO3 – 74.4
756 parts of water evaporated
Mixing
Evaporation at +110°
Solution for cooling: 160 parts of salt mass: NaNO3 – 108.3, NH4H2PO4 – 44.3, NH4NO3 – 7.4; H2O – 819
Cooling at 0°
Cooled solution of 138.1 parts of salt mass: NaNO3 – 108.3, NH4H2PO4 – 22.4, NH4NO3 – 7.4; H2O – 819
100% ammophos, NH4H2PO4 – 21.9

The scheme put forward is an illustrative one. We have already noted that the same principle can be applied to the planning of cycles for other temperatures of cooling and evaporation, the choice of which will depend on the basis of the technocommercial considerations.

In all of the above schemes we did not allow for the quantity of mother liquor occluded by crystals or for other losses incurred under production conditions. The changes brought about by them in the theoretically calculated values are insignificant and we therefore ignore them.

In the second method the original solution is concentrated to the eutonic point with the objective of obtaining sodium nitrate, and the residue is further evaporated to give a mixture of sodium nitrate, monoammonium phosphate and ammonium nitrate which can be utilized as fertilizers. If evaporation is conducted at 110°, then 1 mole of original solution can yield 0.413 mole of $NaNO_3$ or 55.5% of the total quantity of $NaNO_3$. The remaining 0.331 mole of $NaNO_3$, in admixture with 0.219 mole $NH_4H_2PO_4$ and 0.037 mole NH_4NO_3, is brought down in the second evaporation stage. The total N/P_2O_5 ratio in the final mixture is 1 : 2.

SUMMARY

1. Utilizing isothermal and polythermal data, calculations are made of the optimum parameters of the individual production stages that enable complete separation of monoammonium phosphate from sodium nitrate.

2. It is shown that a closed cycle is realized if the crystallization temperature and the corresponding composition of the "starting" solution are determined with the quantity of eutonic mixed with 100 parts by weight of the original solution and not with a fortuitously selected quantity.

3. It is established that, for identical compositions of original and eutonic solutions, the cooling temperature will be the lower and the degree of precipitation of monoammonium phosphate will be the higher, the smaller is the quantity of eutonic solution diluted with 100 parts by weight of original solution.

LITERATURE CITED

[1] S. I. Vol'fkovich, A. P. Belopol'skii, and A. I. Loginova, Bull. Acad. Sci. USSR, Chem. Series 5 (1940).

[2] S. Ya. Shpunt, J. App. Chem. XIII, 1, 9 (1940).

[3] S. Ya. Shpunt, J. App. Chem. XIII, 1, 19 (1940).

[4] S. Ya. Shpunt, J. App. Chem. XIX, 3, 293 (1946).

[5] S. Ya. Shpunt, J. App. Chem. XX, 7, 685 (1947).

[6] S. Ya. Shpunt, J. App. Chem. XXX, 985 (1957).*

[7] S. Ya. Shpunt, J. App. Chem. XXX, 8, 1148 (1957).*

Received March 20, 1958

* Original Russian pagination. See C. B. Translation.

PREPARATION AND INVESTIGATION OF PHOSPHATE FILMS ON ZINC

I. V. Krotov, V. V. Grinina, and N. A. Zapol'skaya

Institute of Physical Chemistry of the Academy of Sciences USSR

Application of a zinc film to steel components affords good protection against corrosion in water and in the air. Zinc plating is not recommended for steel parts and equipment subjected to the more drastic conditions of a tropical climate [1]. Use is then made of a 12μ zinc film followed by a nitrocellulose lacquer [1]. It has been reported [2] that good protection of steel against atmospheric corrosion is afforded by zinc plating followed by lacquering.

We know that chromium-plating [3] is often used to enhance the corrosion resistance of a zinc coating. Even more effective is phosphating, which can also be used for improving adhesion to the coating of a subsequently applied lacquer film [4]. The main component of solutions for phosphating of zinc in the majority of cases is soluble zinc phosphate [5].

About 40 patents deal with various means of passivating zinc with the aid of solutions containing phosphates. We tested some which in our opinion were the most promising.

Some interest is attached to a patent [6] which specifies a bath of the following composition for phosphating: $Zn(H_2PO_4)_2 \cdot 2H_2O$ 3%, $Zn(NO_3)_2 \cdot 6H_2O$ 1.5%, $FeCl_2$ 0.1%, NaF 0.22%, H_2O 95.18%. The free acidity of the solution is 3 points, the total acidity is 30-33 points. * The best results were obtained by treating zinc in a bath of the above composition at 55° for 5 min. The resulting silver-grey phosphate film is fairly resistant to the drop test [7] (up to 10 min for complete blackening of a drop), but adhesion to the metal is poor. The solution for the drop tests comprises $CuSO_4 \cdot 5H_2O$ 8 g, NaCl 3 g, HCl (0.1 N) 1 ml, water to make 100 ml. Observations are made of the periods from the instant of application of the drop up to appearance of the first specks of separated copper or up to complete blackening of the drop. We tested a bath specified in a Japanese patent [8] containing $Zn(H_2PO_4)_2 \cdot 2H_2O$ 2 g, H_3PO_4 0.45 g, $Zn(NO_3)_2 \cdot 6H_2O$ 3 g, ZnF_2 (quantity not specified – we took 0.02 g), water 100 ml. With this we obtained fairly strong phosphate films on zinc (5-6 min for complete blackening of a drop).

Another patent [9] describes the phosphating of zinc in a solution containing $Zn(H_2PO_4)_2$, $NiSO_4$, $NaBF_4$ and nitrates. We made up a mixture containing ZnO, H_3PO_4, $Zn(NO_3)_2 \cdot 6H_2O$, $Ni(NO_3)_2$, $NaNO_3$ and $NaBF_4$. The optimum composition of the solution was established on the basis of drop tests on efficient grades of phosphate films obtained in baths containing various concentrations of components. The most suitable for phosphating was found to be a solution containing ZnO and H_3PO_4 in quantities corresponding to a ratio of 1 : 2. The presence of $NaBF_4$ is useful; $NaNO_3$ should be replaced by $Zn(NO_3)_2$.

The best results are obtained by phosphating with a bath of the following composition: $Zn(NO_3)_2 \cdot 6H_2O$ 5 g/l., ZnO 4.8 g/l., H_3PO_4 (s.g., 1.259) 23 ml/l., $NaBF_4$ 2 g/l., $Ni(NO_3)_2$ 6 g/l. Free acidity of solution 2.2-2.5 points, total acidity of solution 25-26 points. Duration of phosphating 15 min, bath temperature 65°. Films obtained with the help of this formula combine satisfactory corrosion resistance with extremely good adhesion to zinc.

---

* The free acidity in points of a phosphating solution is defined as the number of milliliters of 0.1 N alkali solution consumed for titration of 10 ml of phosphating solution in presence of methyl orange. The total acidity is similarly determined but the titration is effected in presence of phenolphthalein.

TABLE

Experimental Data Serving as a Basis for Establishment of Optimum Conditions for Phosphating of Zinc; Solution Composition; Conditions of Supplementary Treatment of Phosphate Films.

		Components from which the phosphating solution was prepared •				Period of phosphating (min)	Temperature of phosphating solution (°C)	Concentration of $K_2Cr_2O_7$ solution for later treatment (%)	Period of immersion in $K_2Cr_2O_7$ solution	Remarks
		ZnO (in g/l.)	H_3PO_4 s.g., 1.259 (in ml/l.)	$Zn(NO_3)_2 \cdot 6H_2O$ (in g/l.)	20% Na_2CO_3 solution					
1	A	9.41	60	100	Not added. Added until appearance of slight turbidity	5–60	60	Not immersed	Not immersed	The zinc plates before phosphating were rubbed with dichloroethane and alcohol. There was minimum scatter of results when the test period was 40 min and soda was added to the passivating solution; at the same time the average resistance of the film was at its maximum. Prior to phosphating the zinc specimens should be treated with Na_3PO_4 solution (45 g/l.) for 20 sec.
2	B									
2		18.82	107	50, 100, 150 200, 250	Until appearance of slight turbidity	60	60	Not immersed	Not immersed	Optimum concentration of $Zn(NO_3)_2 \cdot 6H_2O$ in passivating solution 200 g/l.
3						80	20–60	Not immersed	Not immersed	Optimum temperature of passivating solution 40°.
4						40	40	0.05, 0.1, 0.2 0.4, 0.8	10 sec at 60°	Optimum concentration of $K_2Cr_2O_7$ solution 0.4%.
5		9.41	53.5	200	Until appearance of slight turbidity	10, 20, 30, 40, 50, 60, 120	40	0.4	10 sec at 60°	Optimum phosphating period 20 to 40 min.
6						40	40	0.4	from 10 sec to 10 min at 60°	Optimum immersion period 10 sec. Special experiments showed that at a $K_2Cr_2O_7$ solution temperature of 20° the results are roughly the same as at 60°.

• Zinc oxide was usually dissolved in phosphoric acid in the following way: Phosphoric acid (s.g., 1.259) was added to zinc oxide and the mixture was triturated for about 2 hr in a porcelain mortar. The mixture was then dissolved in water to which were then added the other components of the bath. Making-up of the solution was completed by addition of water to the required volume. In expts. 2-6 the zinc specimens, prior to being phosphated, were rubbed with dichloroethane and alcohol and treated with Na_3PO_4 solution. After the phosphating, the specimens were washed with water and then left to dry in the air for 24 hr either at once or after immersion in potassium dichromate solution.

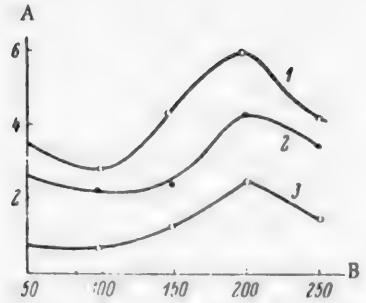

Fig. 1. Resistance of the film as a function of the concentration of the $Zn(NO_3)_2 \cdot 6H_2O$ in the passivating solution. A) Resistance of film (in min); B) quantity of $Zn(NO_3)_2 \cdot 6H_2O$ (g/l.). Resistance: 1) maximum; 2) medium; 3) minimum.

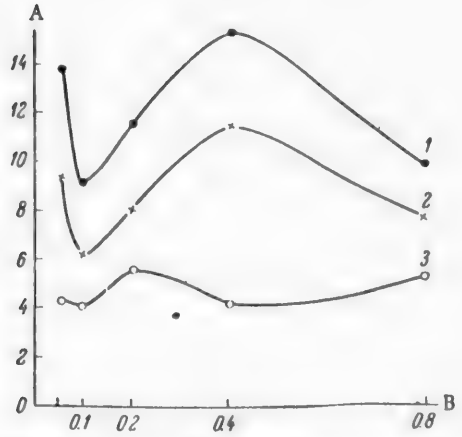

Fig. 3. Strength of film as a function of the concentration of the $K_2Cr_2O_7$ solution. A) Strength of film (in min); B) $K_2Cr_2O_7$ concentration (in %). Curve numbers have same significance as in Fig. 1.

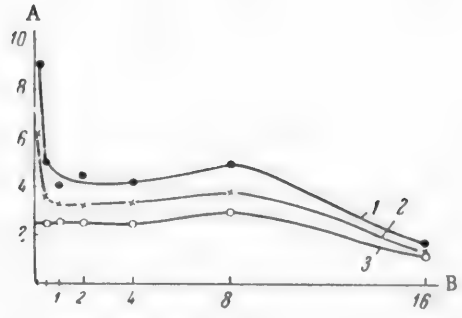

Fig. 5. Strength of film as a function of the period of immersion in 0.4 mole-% solution of $K_2Cr_2O_7$ at 60°. A) Strength of film (in min); B) time of immersion (min). The number of the curves have the same significance as in Fig. 1.

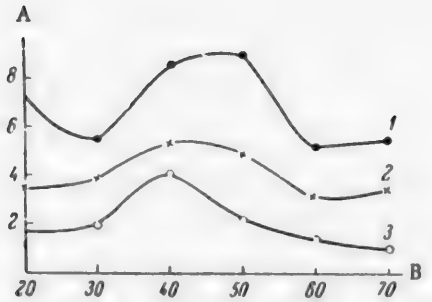

Fig. 2. Resistance of film as a function of bath temperature. A) Strength of film (in min); B) temperature (°C). Curve numbers have same significance as in Fig. 1.

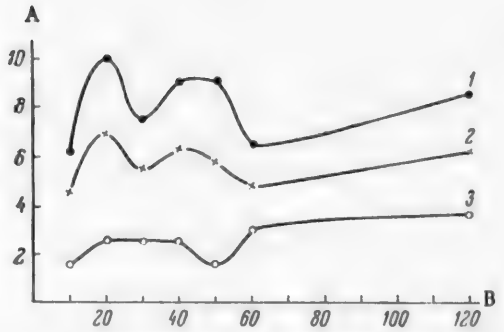

Fig. 4. Resistance of film as a function of the duration of the phosphatizing period. A) Strength of film (in min); B) time in min. The numbers on the curves have the same significance as in Fig. 1.

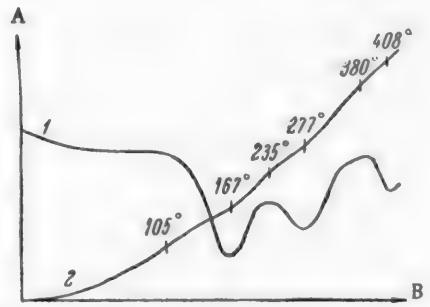

Fig. 6. Thermogram of phosphate powder of imported zinc previously brought to constant weight. A) Temperature (°C), B) time (in min). 1) differential; 2) direct recording.

For preparation of phosphate coatings on zinc, Novitskaya and Severov recommend a solution of zinc monophosphate with additions of sodium nitrate and a surface-active agent – 2-napthalenesulfonic acid [10]. The authors themselves admit that this film lacks protective value.

Fortunatov, Gopienko and Pchelkina [11] proposed to phosphate zinc at 20-25° for 5-6 min with a solution containing $Zn(NO_3)_2 \cdot$ 190 g/l., H_3PO_4 (s.g. 1.75) 36 g/l., NaF 12 g/l. Simakovskii and Vul'fson [12] recommend passivation of zinc in a solution of the preparation "Mazhef".

Gevorkyan [13] and Lopatukhin [14] proposed to passivate zinc in a solution of "Mazhef" doped with zinc nitrate.

A book by Lainer and Kudryavtsev [14] describes a solution for the phosphating of zinc consisting mainly of zinc dihydrophosphate and zinc nitrate with added sodium nitrate. The free acidity of the solution should be 1-3 points and the total acidity 55-60 points. Phosphating is carried out at 30° for 20-30 min. After washing in water, the phosphated components are kept in 0.3-molar $K_2Cr_2O_7$ solution at a temperature of 70-80°, blown with air without washing, and dried at 100-110° for 5-10 min.

A noteworthy feature of Lopatukhin's monograph on phosphating of metals is a valuable survey of the literature on problems of zinc phosphating [15].

Our preliminary experiments showed that satisfactory results are obtained by treating massive specimens of pure zinc, previously degreased with dichloroethane and rubbed with alcohol, in an aqueous solution containing 3% $Zn(H_2PO_4)_2 \cdot 2H_2O$ and 10% $Zn(NO_3)_2 \cdot 6H_2O$ at 60° for 60 min.

Determination of the Optimum Conditions of Phosphating of Zinc in an Aqueous Solution of Zinc Dihydrophosphate and Nitrate

On the basis of the experimental results detailed in the table and plotted in Figs. 1 to 5, the optimum conditions of phosphating and of further treatment of zinc were established.

Preliminary experiments led to the following conclusions: Addition of sodium carbonate to a passivating solution is favorable in the sense that, during a passivation period of 40 min and without lowering the average resistance values, it very considerably reduces the scatter in the results (i.e., the difference between lowest and highest resistance values). A preliminary 20-sec rinse (degrease) of the zinc specimens in Na_3PO_4 solution (45 g/l. at the boil) also lowers the degree of scatter in the resistance values without lowering the mean value. Later experiments showed that the optimum concentrations of components of the phosphating solution are ZnO 9.41 g/l., H_3PO_4 (s.g., 1.259) 53.5 ml/l., $Zn(NO_3)_2 \cdot 6H_2O$ 200 g/l. A 20% solution of Na_2CO_3 is added to the phosphating bath until slightly turbid. The degreased specimens are kept in the phosphating bath for 20-40 min at 40°. After being washed, the phosphated specimens of zinc are kept for 10 sec in a 0.4 mole-% $K_2Cr_2O_7$ solution and, without washing, dried in the air.

More drastic degreasing solutions [16] are advisable for dirty surfaces of zinc specimens in order to obtain a more "standard" surface quality.

We performed experiments on the phosphating of specimens of Armco iron, zinc-coated on both sides, with the aim of ascertaining the resistance of phosphated films on zinc-coated iron. Plating was effected at a current density of 1-2 amp./dm^2 in a bath [17] containing $ZnSO_4 \cdot 7H_2O$ 215 g/l., $Al_2(SO_4)_3 \cdot 18H_2O$ 30 g/l., $Na_2SO_4 \cdot 10H_2O$ 100 g/l., (in some cases 10 g/l. of dextrin was added); pH of solution 3.8-4.4; solution temperature 18-22°.

Three batches of zinc-plated specimens of Armco iron, zinc thickness 5, 10 and 20 μ, were phosphated under the above-noted optimum conditions. It was found that the resistance of phosphate films on zinc-coated iron changes little with change in thickness of the zinc. The presence or absence of dextrin during plating also made little difference in the resistance. The resistance of a film on zinc-plated and phosphated Armco iron differed little from the resistance on massive zinc specimens.

Special experiments showed that when degreased strips of zinc foil were phosphated in contact with strips of copper or aluminum, the phosphate films varied in resistance at different points on the phosphated zinc surface.

Phosphating of zinc specimens for 30 min with cathodic or anodic polarization (current density 1 amp./dm^2, in a phosphating bath of optimum composition at 17°) showed that a brittle deposit of zinc with admixture of white substance [probably $Zn_3(PO_4)_2$] appears at the cathode, and an off-white, crumbly, downward-settling deposit at the anode.

Result of drop tests of the resistance of phosphate films obtained in a bath made up from ZnO, H_3PO_4 (s.g., 1.259) and HNO_3 (s.g., 1.153) were similar to the results obtained with a solution to which $Zn(NO_3)_2 \cdot 6H_2O$ was added.

It was shown by special experiments that addition to the phosphatizing solution of sodium fluoride (0.12 to 0.45 g/l.) or zinc fluoride (0.38, 0.66, 1.32, 1.98 and 2.64 g/l.) does not improve the quality of the phosphated film on the zinc. Treatment of phosphated zinc specimens in CrO_3 solution (0.05 and 0.1% at temperatures of 40, 60, 80 and 100°) does not increase their resistance. The same is true of the addition to the passivating bath of the surface-active substance "Universol" (3.34, 6.68 and 13.36 g/l.).

Investigation of the Composition of Films on Zinc Formed During Phosphatization; Characterization of the Physical Properties of the Film

We determined the composition of the phosphate film on zinc on the basis of chemical and thermographic [18] analyses of the phosphated powder derived from the imported strip zinc with which the specimens of this investigation were prepared.

The zinc powder was not degreased before the phosphatizing. After phosphatizing and washing with water, the powder was treated in potassium dichromate solution, then dried with filter paper, and finally dried in the air.

Judging by the thermogram (Fig. 6) the substance of the phosphated film on zinc undergoes the following changes on heating: part of the water escapes from the film at 105-167°; the residual water leaves the film at 235-277°; the zinc itself melts at 380-408°.

Judging by the differential curve of the temperature recording on reheating, the substance of the film does not undergo any further changes, i.e., the water had been completely eliminated from the film during the first heating.

Chemical analysis of the original phosphated zinc powder, after bringing to constant weight in a desiccator, gave the following results: P 6.85%, Zn (free) 44.4%, Zn (total) 69.9%, Cr absent.

On the basis of the above analytical and thermographic data the composition of the film on phosphated zinc powder can be represented with fair accuracy by the formula $Zn_3(PO_4)_2 \cdot 4H_2O$. It was also shown that heating to the first endothermal minimum at about 167° result in removal of 2.5 moles of water from one mole of zinc phosphate; further heating to the second endothermal point at about 277° leads to removal of the residual 1.5 moles of water.

We also artificially prepared [19] $Zn_3(PO_4)_2 \cdot 4H_2O$. Analysis of this product, dried to constant weight in a desiccator, showed that its phosphorous (14.3%) and water (14.38%) contents were fairly close to the theoretical (13.52 and 15.73% respectively). The thermogram of the artificial preparation (not given here) is extremely similar to that of the thermogram in Fig. 6. Slight differences in the temperatures of the minima are easily explained by the different thermal conductivities of the starting materials used in the comparative thermographic work.

X-ray analysis* of phosphated zinc powder and of the artificial zinc phosphate revealed completely identical structures.

Consequently, the composition of our phosphated film on zinc corresponds to the formula $Zn_3(PO_4)_2 \cdot 4H_2O$.

The phosphate film that we obtained on zinc was about 8μ thick; its specific gravity was approximately 2 g/cm^3.

* We have to thank V. P. Moiseev and Z. V. Semenov for carrying out the x-ray analysis.

On the Mechanism of the Phosphatization of Zinc

Observations were made under the microscope of degreased specimens of zinc under a layer of phosphatizing solution of optimum composition at temperatures of -5 and +20°. They led to the conclusion that the protective phosphate film is formed very quickly and that it is difficult to detect the transition from the lustrous metal surface to the characteristic surface of the phosphate film. A sort of smoothing of the surface is at first detected at -5°, and this is followed by the formation of a white, opalescent film, then by the appearance of bright yellow particles surrounded by darker zones, and finally by the formation of the dense film of phosphates.

The odor of oxides of nitrogen is detected when zinc interacts with the phosphatizing solution.

Motoelectric measurements for zinc electrodes in phosphatizing solution of optimum composition at 40-60° showed that the motoeffect [20, 21] at first has a negative value (the moving electrode is more active) and later has a very small positive value. This demonstrates that the phosphatizing solution at first acts by activating the surface of the zinc, i.e., by destroying the original film of oxides. Subsequently the activity of the zinc surface decreases due to formation on the active particles of a film of water-insoluble phosphates.

Deposition of a film of phosphates on the surface of a zinc specimen undoubtedly proceeds with participation of colloidal zinc phosphate; it is probably responsible for the opalescent film on the zinc surface at the start of the phosphatization process to which we drew attention above.

We determined the sign of the charge of artificially prepared colloidal particles of zinc phosphate in an aqueous solution of this substance weakly acidified with phosphoric acid. It is positive.

The above observations and facts indicate with high probability that under our conditions a phosphate film is formed on zinc by an electrochemical process between cathodes (particles of original oxide film on the zinc surface) and anodes (particles of metals free of film). Processes taking place at the cathodes (which are particles of n-type conducting film) involve the binding of hydrogen ions on discharge into water due to the depolarizing action of nitrate ions. Solution of zinc occurs at the anodic particles:

$$Zn + 2H_2PO_4^- - 2e = Zn(H_2PO_4)_2.$$

The resulting increase in concentration of zinc dihydrophosphate close to the anodic particles causes the hydrolysis reaction

$$3Zn(H_2PO_4)_2 \rightleftarrows Zn_3(PO_4)_2 + 4H_3PO_4$$

to be displaced to the right, and the colloidal particles of $Zn_3(PO_4)_2$ in the immediate vicinity of the metal surface are deposited on anodic particles. These processes can be repeated in the remaining pores and lead to further reduction in the pores.

Treatment with potassium dichromate solution evidently converts the hydrated forms of zinc oxide present in the pores of the phosphate film into zinc dichromate which is poorly soluble in water.

SUMMARY

Thermographic, x-ray, and chemical investigation of phosphated zinc powder established that the phosphate film is $Zn_3(PO_4)_2 \cdot 4H_2O$.

LITERATURE CITED

[1] Anticorrosive Protection of Equipment Erected in Countries with Tropical and Subtropical Climates. Gosplan SSR, Central Scientific Research Institute of Machine-Building Technology (Moscow), 1957, 4, 45.

[2] Metalloberfläche 5, SB 85 (1957).

[3] Vestnik Inzh. i Tekhn. 2, 67 (1948).

[4] R. M. Burns and W. W. Bradley. Protective Coatings for Metals (Reinhold Publishing Corporation, N.Y., 1955) 430.

[5] A. Douty, Plating 38, 1031 (1951).

[6] G. R. Hoover and N. Cox, U. S. Pat. 2487139 (1949).

[7] Bull. Polish Acad. Sci. III, 1, 5, 191 (1953).

[8] I. Nagai, Jap. Pat., 4862 (1952).

[9] H. K. Ward, U. S. Pat. 2591479, 1 IV (1952).

[10] M. A. Novitskaya and A. A. Severov, Accelerated Phosphatizing with Zinc Salts; Atmospheric Corrosion of Metals [in Russian] (Metallurgical Press, 1951), p. 184.

[11] Scientific Yearbook of the Saratov Chernyshevskii State University, 1954, 544.

[12] A. P. Simakovskii and V. I. Vul'fson, Proc. Acad. Sci. USSR 46, 6, 251 (1945).

[13] Highly Resistant Protective Coatings, Inst. Techno-Econom. Inf. 23, 56 (1956).

[14] V. I. Lainer and N. T. Kudryavtsev, Principles of Zinc-Plating [in Russian], 1957, II, 216, 265.

[15] V. S. Lopatukhin, Phosphatizing of Metals [in Russian] (Machinery Press, 1958). p. 64.

[16] Electroplating Engineering Handbook. N.Y., 372 (1955).

[17] V. I. Lainer and N. T. Kudryavtsev, Principles of Zinc-Plating [in Russian], 1953, I, 293.

[18] I. V. Krotov, V. V. Grinina and N. A. Zapol'skaya, J. App. Chem. 31, 1, 33 (1958).*

[19] Y. W. Mellor. A Comprehensive Treatise of Inorg. and Theoretic. Chem., IV. 658 (1943).

[20] N. A. Zapol'skaya, J. Phys. Chem. 32, 2, 318 (1958).

[21] N. A. Zapol'skaya, J. Phys. Chem. 32, 3, 569 (1958).

Received June 23, 1958

* Original Russian pagination. See C. B. Translation.

THE ANOMALOUS AGING OF SOLIDS OBTAINED BY CHEMICAL PRECIPITATION•

I. M. Vasserman

Production of chemicals in the form of chemical precipitates is widely practised in the chemical industry and in the laboratory. Chemical precipitation generally proceeds at high supersaturations remote from equilibrium; such conditions are favorable to the formation of unstable precipitates with highly active surfaces due to the incompleteness of the structure and to the presence of crystal defects. Precipitates amorphous to x-rays may be obtained at very high supersaturations.

Actually it is very usual for precipitates to be true crystals in incomplete form, containing a large number of structural defects and possessing a large internal surface due to the discontinuous structure. In such cases the separation of the mother liquor from the freshly formed precipitate and the washing out of impurities trapped by the precipitate are attended by great difficulties both in the laboratory and in industry. Long ago it was noted that if fresh precipitates remain in contact with their mother liquors, the properties are improved: The total surface of the particles decreases, the crystal shape is perfected and the adsorption of impurities from the liquid is diminished. Further processing of the precipitate is thereby facilitated. This change of properties of a precipitate is known as aging and is widely discussed in the literature. The aging of a precipitate in contact with a mother liquor is a dynamic process proceeding at the interphase boundary, and is governed by the general laws of heterogeneous processes.

Our physico-chemical study of chemical precipitation has shown that in a series of cases of industrial importance, aging of fresh precipitates leads not to improvement but to deterioration of the surface properties of the precipitate. For example, in a study of chemical precipitation in the system $Ni(NO_3)_2$–Na_2CO_3–H_2O [1] it was established that the usual aging of the fresh precipitate was accompanied by a peculiar type of chemical "aging" which we called "chemoaging". This latter was accompanied by change of composition and surface properties. The simultaneous progress and interaction of the two aging processes determine the final properties of the precipitate and of the precipitate – solution system. Such an aging process bears an anomalous character and merits close investigation since when it takes place it determines the technically important properties and the quality of the precipitate.

In our previous work [1] we established the mechanism of anomalous aging. It was shown that during precipitation in the system $Ni(NO_3)_2$–Na_2CO_3–H_2O products of partial hydrolysis of Na_2CO_3 are also present (NaOH and $NaHCO_3$), that Na_2CO_3 and NaOH mainly participate in the chemical reaction of precipitation, and that the $NaHCO_3$ remains unused and passes into the mother liquor. Consequently the system, freshly formed precipitate – mother liquor, exists in presence of two salts differing in chemical composition: in the precipitate a basic salt (basic nickel carbonate) and in the liquor an acid salt (sodium bicarbonate). These salts are present in different phases, and a heterogeneous chemical neutralization reaction can proceed at their interface at relatively low speed which will depend on the conditions of precipitate/liquor contact:

$$a\mathrm{Ni(OH)_2}\cdot b\mathrm{NiCO_3} + 2x\mathrm{NaHCO_3} \rightarrow (a-x)\mathrm{Ni(OH)_2}\cdot(b+x)\mathrm{NiCO_3} + x\mathrm{Na_2CO_3} + 2x\mathrm{H_2O}.$$

• Communication II in a series on the technology of isolation of substances from solutions by chemical precipitation.

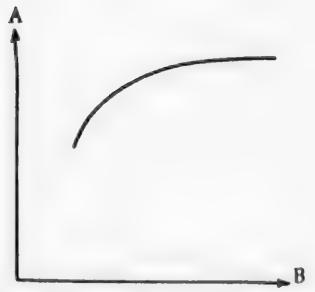

Fig. 1. Change of the pH of the system during anomalous aging of the precipitate (neutralization reaction): A) pH value; B) time (hr).

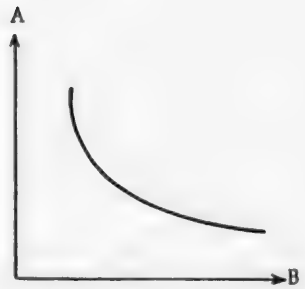

Fig. 2. Change of chemical composition (basicity) of the precipitate during anomalous aging (neutralization reaction). A) basicity of the precipitate ($OH^-_{equiv.}/Ni^{2+}_{equiv.}$) B) time (in hours).

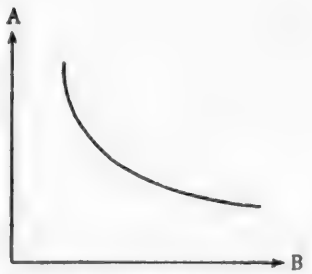

Fig. 3. Change of surface properties of precipitate (filtration coefficient) during anomalous aging (neutralization reaction). A) Filtration coefficient $K \times 10^{-6}$ (cm/sec). B) time (hr).

Fig. 4. Change of surface properties of precipitate (specific surface) during anomalous aging (neutralization reaction). A) Specific surface of precipitate expressed by adsorption of methyl violet (in mg/g); B) time (hr).

Fig. 5. Change of pH of a system during anomalous aging (hydrolysis reaction). A) pH value; B) time (hr).

This reaction alters the chemical properties of the system: The chemical composition of the mother liquor, the pH of the medium; it lowers the original chemical activity of the precipitate and its basicity and brings about the characteristic process of chemoaging. The physical properties of the precipitate (filtration coefficient and specific surface) also deteriorate due to change in the structure of the surface at which the chemical reaction takes place.

In a general form the property-changes in the system in question during aging can be represented by kinetic curves (Figs. 1 to 4).

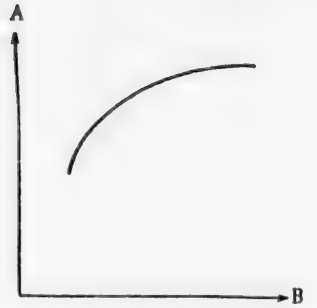

Fig. 6. Change of chemical composition (basicity) of a precipitate during anomalous aging (hydrolysis reaction). A) Basicity of precipitate ($OH^-_{equiv.}$ / $/Ni^{2+}_{equiv.}$); B) time (hr).

Fig. 8. Change of surface properties of a precipitate (specific surface) during anomalous aging (hydrolysis reaction). A) Specific surface of precipitate expressed by the adsorption of methyl violet (mg/g); B) time (hr).

Fig. 7. Change of surface properties of a precipitate (filtration coefficient) during anomalous aging (hydrolysis reaction). A) A) Filtration coefficient K $\times 10^{-6}$ (cm/sec); B) time (hr).

The system $Ni(NO_3)_2-Na_2CO_3-H_2O$ is a special case of formation of a poorly soluble basic carbonate when using a carbonate of an alkali metal as the precipitant. This case of chemoaging and anomalous aging of a precipitate is therefore of general significance for this group of precipitates.

Is anomalous aging limited to the chemoaging of a precipitate due to neutralization at its surface? Before answering this question we shall consider the case of formation of a precipitate of a poorly soluble basic salt which is easily hydrolyzed by water during contact with mother liquor, for example precipitation in the systems

$$MnSO_4-Na_2CO_3-H_2O,\ Pb(NO_3)_2-Na_2CO_3-H_2O,$$

$$Ni(NO_3)_2-Na_2CO_3-H_2O$$

and others.

The chemical reaction of hydrolysis will take place at the precipitate/water interface:

$$a\mathrm{Me(OH)_2}\cdot b\mathrm{MeCO_3}+2x\mathrm{HOH}\rightarrow(a+x)\mathrm{Me(OH)_2}\cdot$$

$$\cdot(b-x)\mathrm{MeCO_3}+x\mathrm{H_2CO_3}.$$

Consequently all that was said above about the behavior of a freshly formed precipitate of basic nickel carbonate will also be valid for the case of an hydrolyzable precipitate, i.e., chemoaging will also occur and in short the pattern of aging of the precipitate will be anomalous. Kinetic curves of change of the properties of a system containing a hydrolyzable precipitate are shown in a general form in Figs. 5 to 8.

Chemoaging, i.e., anomalous aging, of a precipitate is also bound to take place when a freshly formed precipitate reacts with gases dissolved in the mother liquor such as oxygen and carbon dioxide.

In the system $MnSO_4-Na_2CO_3-H_2O$, for example, the precipitate of basic manganese carbonate is oxidized by oxygen and its aging is anomalous. In the light of the foregoing discussion we are justified in assuming the existence of two more cases of chemoaging of freshly formed precipitates: 1) The case of a synthesis reaction between components of a complex precipitate, e.g., ferrite formation [2] when hydroxides of iron, zinc, and nickel are coprecipitated and nickel-zinc ferrite ($Fe_2O_3\cdot ZnO\cdot NiO$) is formed; 2) exchange reactions between two salts, one of which is in the solid phase and the other in solution, e.g., reaction between AgCl (solid) and KBr (dissolved) [3, 4].

Sometimes several chemical reactions are observed to proceed simultaneously on the surface of an aging precipitate. In the case of basic manganese carbonate, for example, we have neutralization of the basic salt and its hydrolysis and the action of dissolved oxygen. In such cases the complex interaction of the chemoaging reactions will govern the intermediate and end properties of the precipitate. These examples show that in a large number of cases of practical importance chemical precipitation is a complex process whose mechanism is not limited to the primary formation of the precipitate but involves the chemical substances in the system (precipitate, dissolved salts, gases) present in different phases (chemoaging of the precipitate). In all such cases the aging of the freshly formed precipitate is anomalous and affects its properties and composition.

The development of new techniques is resulting in the preparation of a large number of catalysts, luminophores and ferrites by chemical precipitation, and ever more stringent standards are being set for the properties and quality of the precipitates. It is therefore important to deepen our insight into the process of chemical precipitation and of aging of precipitates.

In this connection we may recall Tananaev's remark [5] that only close study of the chemistry of precipitation by methods of physico-chemical analysis will lead us to a rational theory of chemical precipitation. As examples we have cited some inorganic systems with which we are more familiar, but all that has been said above is applicable to the formation of precipitates by interaction of organic substances or of organic with inorganic substances during secondary reactions on their surfaces.

On the basis of the foregoing considerations we have developed general concepts of the chemoaging and anomalous aging of organic and inorganic precipitates, and have also gained an insight into the types of secondary reactions during chemical precipitation which are enumerated in the summary of this paper.

SUMMARY

1. A freshly formed precipitate in contact with its mother liquor undergoes chemical aging ("chemoaging") if the interface between the phases is the site of one or several secondary chemical reactions accompanied by change in the chemical composition and surface properties of the precipitate.

2. Secondary chemical reactions in the system precipitate – mother liquor are: reaction of a basic precipitate with an acid salt in the mother liquor (neutralization reaction), reaction of the precipitate with a neutral salt in the mother liquor (double decomposition), reaction of the components of a complex precipitate (synthesis reaction), reaction of a precipitate with dissolved gases (oxidation, carbonation, etc.), reaction of the precipitate with the water of the mother liquor (hydrolysis reaction).

3. Chemoaging of a precipitate proceeds at the same time as normal (physical) aging, and the interplay of the two modes of aging leads to anomalous aging of the precipitate.

LITERATURE CITED

[1] I. M. Vasserman and Kh. E. Brainina, J. App. Chem. 31, 11 (1958).*

[2] I. Kolthoff and L. Overhalzer, J. Phys. Chem. 43, 767, 909 (1939).

[3] I. Kolthoff and H. Jutzy, J. Am. Chem. Soc. 9, 1634 (1937).

[4] H. Jutzy and I. Kolthoff, J. Am. Chem. Soc. 5, 917 (1937).

[5] I. V. Tananaev, I. B. Mizetskaya and A. D. Vinogradova, J. Anal. Chem. USSR 8, 1, 14 (1952).*

Received November 13, 1958

* Original Russian pagination. See C. B. Translation.

EXTRATION OF FINE SUSPENSIONS FROM SOLUTIONS BY THE EMULSIFICATION METHOD

S. G. Mokrushin and V. I. Borisikhina

Ural S. M. Kirov Polytechnic Institute

In some cases liquid adsorbents have considerable advantages over solid adsorbents since they can be prepared in standard grades of adequate purity.

Shedlovskii [1] and Natanson [2] have pointed to the possibility of utilizing organic liquids as adsorbents.

Velmarn and Alekseev [3] had earlier shown that the agitation of colloidal solutions with organic liquids can enable separation of water-insoluble solid particles at the interface of the phases. Reinders [4] and Hofmann [5] indicate the role of interphase tension in the process of migration of suspended dispersed particles to the interface of the phases. A similar theory of emulsification was put forward by Rebinder [6].

Work by Mokrushin [7, 8] established the influence of gelatin additions on the process of extraction of solid, finely dispersed substances from solutions by the method of foam chromatography. In this work it was observed that small quantitites of added gelatin differ markedly in action from large quantities. Small quantities cause sensitization of the extracted solid particles so that they acquire a bifilar character. Large additions of gelatin lead to hydrophilization and to protection of the dispersed particles or to their "suppression" [9].

The purpose of the present work was to clarify the problem of the influence of the degree of dispersity of solid, finely dispersed substances on the process of their extraction from hydrosuspensions, and also to clarify the influence of additions of gelatin solution on the extraction process.

TABLE 1

Data of Screen Analyses of Metal Hydroxide Powders

Hydroxide powder	Total wt. of powder (g)	Weight of fraction (%)			Residue and losses (%)
		I	II	III	
Cobalt	3.9	31.8	33.3	33.3	1.6
Nickel	6.2	29.0	33.5	32.4	5.1
Iron	5.02	80.0	20.0	—	—

Freshly distilled benzene was selected as the organic liquid and artificially prepared fine powders of metal hydroxides were taken as adsorbates. Gelatin was added in the form of a 0.1% aqueous solution.

Powders of the hydroxides of cobalt, nickel, and iron were prepared by precipitation from aqueous solutions of the chlorides with dilute ammonia. Chloride ions were washed out by the method of decantation with distilled water and then by filtration in a funnel under a vacuum. The filtrate was tested for absence of chloride with silver nitrate solution.

TABLE 2

Data of Sedimention Analysis of the Investigated Metal Hydroxide Powders

Hydroxide powder	Particle size (cm) in each fraction		
	I	II	III
Cobalt . .	$1 \cdot 10^{-4}$—$1 \cdot 10^{-5}$	$7 \cdot 10^{-4}$— $2 \cdot 10^{-4}$	$3 \cdot 10^{-2}$—$1 \cdot 10^{-3}$
Nickel . . .	$1.5 \cdot 10^{-4}$—$3 \cdot 10^{-5}$	$1.05 \cdot 10^{-3}$—$6.7 \cdot 10^{-4}$	$5 \cdot 10^{-2}$—$1 \cdot 10^{-3}$
Iron . . .	$5 \cdot 10^{-5}$—$1 \cdot 10^{-5}$	$9 \cdot 10^{-4}$— $5 \cdot 10^{-5}$	—

TABLE 3

Relation Between Degree of Extraction of Powders and Particle Size and Amount of Gelatin Solution Added

Hydroxide powder	Particle size (cm)	0.1% gelatin solution added (ml)	4% extracted	Remarks
Cobalt . .	$3 \cdot 10^{-2}$—$1 \cdot 10^{-3}$	0.21	49.9	Benzene layer emulsified. Aqueous and benzene layers colored nearly identically.
Cobalt . .	$7 \cdot 10^{-4}$—$2 \cdot 10^{-4}$	0.21	93.3 96.6	Aqueous layer substantially transparent. Benzene layer emulsified and deeply colored; small deposit at bottom of funnel.
Cobalt . .	$1 \cdot 10^{-4}$—$1 \cdot 10^{-5}$	0.09	99.82	Benzene layer emulsified and deeply colored. Aqueous layer substantially colorless.
Cobalt . .	$3 \cdot 10^{-5}$—$1 \cdot 10^{-5}$	—	99.95 99.98	Aqueous layer colorless. Emulsion unstable. Powder located at interphase boundary.
Nickel . .	$5 \cdot 10^{-2}$—$1 \cdot 10^{-3}$	0.21	51.0	Benzene layer emulsified. Aqueous and benzene layers of approximately the same color.
Nickel . .	$1.05 \cdot 10^{-3}$—$1 \cdot 10^{-4}$	0.21	90.3	Benzene layer emulsified and deeply colored. Aqueous layer somewhat turbid.
Nickel . .	$1.5 \cdot 10^{-4}$—$3 \cdot 10^{-5}$	0.09	99.75	Aqueous layer substantially colorless. Benzene deeply colored.
Nickel . .	$3 \cdot 10^{-5}$—$1 \cdot 10^{-5}$	0	100	Aqueous layer colorless. Benzene layer emulsion unstable. Powder at interphase boundary.
Iron	$9 \cdot 10^{-2}$—$5 \cdot 10^{-3}$	0.21	60.0	Benzene layer emulsified. Color of aqueous and benzene layer roughly the same.
Iron	$5 \cdot 10^{-5}$—$1 \cdot 10^{-5}$	0	99.9	Aqueous layer colorless. Benzene layer emulsion unstable. Powder at interphase boundary.

The washed precipitates were dried with gradual rise of temperature to 100°, and they were held at this temperature until constant in weight. The dry powders were ground in a porcelain mortar and finally in an agate mortar; they were then screened through three sieves: 12,000, 8500, and 4900 meshes/cm^2. In this manner three fractions – I, II, and III – were obtained by the preliminary screening. Sedimentation analysis (Figurovskii's method) was later used for more accurate determination of particle size. Results from screen and sedimentation analyses are presented in Tables 1 and 2.

EXPERIMENTAL

75 ml of distilled water was poured into a 150 ml separating funnel and a weighed quantity of 0.1 g of the powder was introduced. After a suspension had been formed, 25 ml of freshly distilled benzene was run in. The stopper of the funnel was firmly fitted in and the mass was vigorously shaken for one min. The funnel was fixed vertically to a stand. After separation into layers, the lower aqueous layer was colorless and transparent if extraction of the powder had been complete, and the lower layer could be separated from the upper emulsified layer. But if the lower aqueous layer remained colored or cloudy, then 1-2 drops of 0.1% aqueous gelatin solution were added to the suspension and the operations of shaking and standing were repeated.

Subsequently, depending on the progress of extraction, gradually increasing quantities of gelatin solution were added until extraction was complete or had reached its maximum effectiveness. The aqueous layer was checked for completeness of extraction after standing by being poured off into a tared porcelain dish and evaporated on a water bath; the residue was then dried at 100° to constant weight, cooled in a desiccator and weighed. Results are set forth in Table 3 which shows the relation between degree of extraction of powders and the particle dimensions and on the amount of gelatin added.

It is evident from these results that the degree of extraction depends on the particle size. Maximum extraction is observed for powders of cobalt, nickel, and iron hydroxides with particle sizes of 10^{-4} to 10^{-5} cm.

Complete extraction of particles of the same hydroxides whose size was between 10^{-3} and 10^{-4} cm called for preliminary addition to the reaction vessel of the quantities of gelatin solution enumerated in Table 3. In the absence of such additions the degree of extraction was only 70% for particles in the size range of 10^{-3} to 10^{-4} cm, and still less (down to 30%) for 10^{-2} cm particles.

We see from Table 3 that gelatin promotes complete extraction although any increase in gelatin quantity over the amounts in the table has no influence and in some cases may even bring about desorption (the duplicate figures in the "degree of extraction" column relate to parallel experiments).

SUMMARY

1. The possibility is demonstrated of extraction of highly dispersed powders of cobalt, nickel, and iron hydroxides from solutions by shaking with freshly distilled benzene.

2. It is shown that the degree of extraction depends on the degree of dispersity of these powders, 100% extraction being possible for 10^{-5} cm particles.

3. It is shown that small additions of gelatin solution improve the extraction of coarser particles. 99% extraction is possible for 10^{-4} cm particles and up to 60% extraction for particles with sizes between 10^{-3} and 10^{-2} cm.

LITERATURE CITED

[1] L. Shedlovskii, Chromatography: A Collection of Papers Edited by M. M. Dubinin [in Russian] (Moscow, 1949), p. 176.

[2] É. M. Natanson, Colloid Journal 9, 6, 428 (1947).

[3] P. P. Veimarn and A. V. Alekseev, J. Russ. Chem. Soc. 46, 133 (1914).

[4] W. Reinders, Koll. Z. 13, 235 (1913).

[5] F. B. Hofmann, Z. Phys. Chem., 385 (1913).

[6] P. A. Rebinder, Colloid Journal 8, 157 (1946); Publications of the Department of Mathematics and National Sciences Acad. Sci. USSR., Chem. Series 5, 639 (1936).

[7] S. G. Mokrushin, Report of Scientific Work of Members of the D. I. Mendeleev All-Union Chemical Society 2, 26 (1953).

[8] S. G. Mokrushin, Abstracts of Proceedings of Conference on the Application of M. S. Tswett's Chromatographic Method in Chemical Analysis [in Russian] (Acad. Sci. USSR Press, Moscow, 1953), p. 14.

[9] S. M. Yasyukevich, Beneficiation of Ores [in Russian] (State Sci. Tech. Press, Moscow, 1953), p. 316.

Received August 18, 1958

THE SEPARATION OF COALS INTO FRACTIONS OF DIFFERENT DENSITIES

N. S. Goloushin

Research Institute of Geology of the Arctic

A detailed study of the composition and properties of coals is only possible by combined application of chemical and physical methods of investigation. In this connection the fractionation of coals in heavy liquids is an efficient technique.

This is because coal is a heterogeneous and complex mineral comprising various components of varying densities. These differences can be exploited for fractionation.

At the present time the separation of coals into fractions of different densities is being undertaken with the objective of obtaining a deeper insight into their nature and of solving practical problems of coal chemistry.

The first experiments on the preparation of fractions differing in ash contents, according to Lamprecht, were carried out by Drown in 1888 [1] who employed calcium chloride solutions. McCallum [2] recommended the fractionation of coals in heavy liquids in order to obtain suitable coking fractions. Simmersbach [3] fractionated coal in calcium chloride solution and carried out a technical analysis of the fractions. Since the coal had been crushed to sizes of 2-8 mm, the fractionation effect was very poor. Sulfrian [4] fractionated gas coals and examined the fractions on the same lines as Simmersbach but using more finely ground material. The coal was previously treated with a mixture of ether and alcohol in order to improve its wetting by calcium chloride solution. Lessing [5] fractionated coals in mixtures of carbon tetrachloride and ligroine. Prior to heavy-liquid separation, the coals were screened into various grain sizes.

Drakeley and Hepburn [6] investigated the distribution of ash over the various fractions with the help of a mixture of chloroform and alcohol as heavy liquid, while Wuster [7] made use of sulfuric acid, zinc chloride, carbon tetrachloride, bromoform, chloroform, and gasoline. Dunkel [8] fractionated coals in a mixture of carbon tetrachloride and xylene and obtained fractions with densities of 1.28 to 1.58. He aimed at isolating vitrain, clarain, durain, and fusain in maximum purity but did not obtain good results.

Gross [9] improved the precision of heavy-liquid classification of coals and attempted the quantitative determination of the components of the individual fractions. He concluded that coal particles below 0.5 mm in size separate in accordance with their gravity but that particles below 0.02 mm upset the process due to their low rate of fall. Gross recommended preliminary removal of the mineral constituents and he used organic liquids as heavy media.

In the opinion of Kattwinkel [10], the best heavy liquids are chlorinated hydrocarbons. Fougner [11] was the first to use a centrifuge to speed up the process of classification of coals.

Lange [12] found that with pulverization to the usual analytical degree (0.25 mm) the isolated fractions of coals have differing compositions and properties. He recommended grinding to a size of 0.03 mm and the use of a centrifuge to shorten the fractionation period.

Zetsche, Vigari and Schärer [13] and Val'ts [14] obtained sporinite concentrates by heavy-liquid fractionation of coals pulverized to less than 0.20 mm. Macrae and Wandles [15] pulverized coal in a disc mill but obtained unsatisfactory results during fractionation. They therefore designed a vacuum disintegrator.

The pulverized coal was classified by grain size and then separated into fractions. In this way they obtained fractions containing 90-98% of sporinite.

Panchenko, Popova and Kozhevnikova [16] fractionated coals and studied the composition and properties of the fractions with the objective of identifying the components responsible for sintering. Particles of 1-12 mm were fractionated in aqueous solutions of zinc chloride. The results led the authors to the conclusion that the caking constituents are not all of the microcomponents of the vitrinite group but are restricted to vitrain and the homogeneous vitrainized basic mass.

Samoilovich [17] made a combined chemical and petrographic study of Donets coals after fractionating them in mixtures of carbon tetrachloride and benzene.

Comparable results were obtained by using a constant range of heavy liquids: below 1.225, 1.225-1.250, 1.250-1.275, 1.275-1.300, 1.300-1.350, 1.350-1.400, 1.400-1.450, 1.450-1.500, and heavier than 1.500. Coal was reduced to a size of less than 0.2 mm and fractionated in heavy liquids in a conical funnel with a tap for discharge of the sunk fractions. Liquid was removed from the isolated fractions by filtration or centrifuging. The fractions were then dried, weighed, and analyzed.

Samoilovich points out that the yield of a fraction is bound up with reducing character of a coal, while the caking tendency of Donets coals is governed not so much by the quantity as by the qualitative characteristics of the gelling substance.

Ammosov [18, 19] separated a series of coals into fractions of different densities when using coal particles less than 0.25 mm in size.

Fractionation was performed in mixtures of carbon tetrachloride and benzene into the following fractions: below 1.24, 1.24-1.25, 1.25-1.26, 1.26-1.27, 1.27-1.28, 1.28-1.30, 1.30-1.35, 1.35-1.40, and heavier than 1.40. A tubular centrifuge (type TsÉ-3) was used for successive isolation (in the direction of heavy to light) of the fractions.

Each settled and floated fraction was dried initially on a glass filter at room temperature and then by heating to 75°. After a floated fraction had been dried, it was subjected to further fractionation. A balance was drawn up for each float-and-sink treatment of a coal and the separated fractions were analyzed.

Ammosov found that the yields of different fractions can serve as a basis for the grading and classifying of coals. Heavier fractions become enriched with fusainite and the lightest fractions with leiptinite. At the same time the components of the vitrinite group (comprising most of the humic coals) undergo separation. Isometamorphic coals vary in behavior during heavy-liquid separation, which in Ammosov's opinion is evidence of differences in the structure of more or less "reduced" coals.

Horton [20] fractionated a series of coals with the objective of determining the change of composition and properties of individual components in dependence on the degree of coalification. All of the samples were previously pulverized to less than 0.2 mm. Fractionation was performed in mixtures of benzene and carbon tetrachloride and with the help of a centrifuge. Centrifuging was repeated in view of the partial mixing of light with heavy components. A relation exists between yields of fractions and degree of coalification. In Horton's opinion, the coalification stage can be more accurately determined by heavy-liquid fractionation than by elemental analysis.

Nesterenko [21] studied the fractionation of Donets basin coals with special reference to the characteristics of the isolated groups of microcomponents. The coals were pulverized to below 0.25 mm. The specific gravities of the heavy liquids were selected to suit the petrographic composition of the coals. Separation was undertaken in glass cylinders with the help of mixtures of carbon tetrachloride and benzene and was commenced with the liquid of maximum density. The work enabled Nesterenko to establish the characteristics of the individual groups of microcomponents of Donets coals.

Davydkov [22] carried out fractionation of coals in order to examine the possibility of their beneficiation. Coals were fractionated with the help of a tube centrifuge using mixtures of benzene and carbon tetrachloride. Davydkov made use of special inserts (pipet-funnels) in the centrifuge tube. Their function was to prevent mixing of the fractions (the floated particles were bound to collect in the funnels).

Goloushin and Korznenevskaya [23, 24] imparted greater precision to the conditions of fractionation of coals with the help of a centrifuge using mixtures of benzene and carbon tetrachloride. The scale of densities of the heavy liquids was selected for each coal on the basis of the results of a trial fractionation. Fractionation was started from the light fractions. Components of the following concentration were isolated: vitrinities 25-97%, fusinites 100%, leiptinites 68-87%. Each of the isolated components was chemically characterized. The fractionation led to the gelling components being collected in the light and in the heavier fractions which differed in chemical properties. Yields of fractions of different densities are related to the degree of coalification of the coals.

Dormans, Huntgens, and Krevelen [25] obtained concentrates of petrographic components from coals: vitrinite and fusinite with the help of manual sorting, and micrinite and exinite by grinding (to less than 0.01 mm) and by fractionation with the help of centrifuging in aqueous solutions of zinc chloride (density 1.25-1.54). On the basis of the characteristics of the concentrates of the petrographic components, the authors determined their structural parameters and the character of the coalification.

Kröger and others [26, 27] isolated vitrinite, exinite and micrinite from glance coals and dull coals from five beds in the Ruhr basin.

The coals were crushed to nut size and then in a disc mill to 1-2 mm. They were dried in a nitrogen atmosphere at 60-65°. Further size reduction was effected by elastic pulverization in a disintegrator at approximately 18,000 rev/min in an inert gas atmosphere. The fineness of grinding for vitrinite and micrinite was 0.001-0.02 mm; for exenite it went to 0.1 mm. Fractionation was performed in jigging machines and subsequently in a rotary supercentrifuge (12,000-25,000 rev / min). Depending on the results of a trial fractionation, narrower or wider ranges of specific gravity and a smaller or larger number of repetitions of operations were selected. The suspensions were filtered through filter presses and residues of heavy liquids (carbon tetrachloride—toluene) were eliminated from the precipitate under reduced pressure (85 mm mercury) and at a temperature of 60-65°. Components of the following purity could be separated: vitrinites 99%, exinites 94-97%, micrinites 91-95%.

The coal components were analyzed for content of hydroxyl and carbonyl oxygen; determinations were made of the yield of coking products, density, heat of wetting, and caking ability; technical and elemental analyses were also performed. Data were obtained for changes of characteristics of the petrographic constituents of the coals as functions of the degree of coalification.

Alaev [28] fractionated one sample of coal with the aim of determining the reactive characteristics of the different components during combustion. The coal was reduced to particles of less than 0.02 mm so that the petrographic constituents were not (as normally) in the form of aggregates but in the form of individual particles. Fractionation was effected in a continuous centrifuge at 15,000 rev / min and the proportion of coal dust in the liquid was about 7-8% by volume.

Zabramnyi [29] fractionated two samples of coals in order to obtain data in support of his theory that long-flame lignites and gas coals cannot change into better caking fat coals by coalification.

It should be added that fractionation of coals in heavy liquids is employed for establishment of the genetic relations of rare elements, as well as for commercial enrichment [30] in order to obtain concentrates of the requisite quality from run-of-mine coals. Work along these lines has led to the characterization of the constituents of coals from various fields. This work must only be regarded, however, as the start of systematic application of the method of fractionation of coals by density. More details of the method itself are given below.

Fractionation of coals involves far-reaching loosening of the cohesion between the original coalesced particles. Pulverization of coal can only be pushed to a certain limit since extremely fine particles are difficult to examine in the form of petrographic sections, are increasingly oxidized in air, and are increasingly soluble in the heavy liquids. Flotation also becomes a disturbing factor (interfering with separation by gravity).

Particles of coal larger than 0.001 mm behave normally in respect to extractability by liquids. Extraction increases sharply when the particles are reduced to 0.001 mm or below.

According to Kröger [26, 27] pulverization of coal cannot be pushed to any desired limit since particles of less than 0.003 mm cannot be reliably differentiated under the microscope and their petrographic evaluation is therefore limited.

According to Goloushina and Korzhenevskaya [23, 24] the number of concretions in the investigated coals was over 50% when the grain size was below 0.20 mm and about 15% when the grain size was below 0.08 mm. These values indicate that grinding to normal analytical fineness (to 0.20 mm) is inadequate for the formation of good concentrates of microcomponents.

Measures against possible oxidation must be taken when coals are to be very finely pulverized. Such measures are crushing and drying in an inert gas atmosphere. Air grinding and drying should not go beyond a grain size of 0.08 mm. Coarser grinding is permissible if fractionation by density is carried out not for the purpose of preparation of good concentrates of microcomponents but for enrichment.

It may also be added that when elastic-impact grinding is practised, considerable enrichment of individual classes of coal in specific components is possible during actual grinding. Coals can be fractionated with the help of organic liquids, aqueous salt solutions, and aqueous suspensions.

Heavy liquids for coal fractionation must satisfy the following requirements: They should separate completely from coal, should have good wetting power for coal, should be inert to coal, and should have a low viscosity. Liquids with a specific gravity of 1.5 have the following viscosities (centipoises): aqueous $ZnCl_2$ solution 2.40, aqueous $ZnBr_2$ solution 1.55, aqueous $CaCl_2$ solution (specific gravity 1.40) 6.27, mixture of C_6H_6 and CCl_4 0.65, and mixture of $C_6H_4(CH_3)_2$ and CCl_4 0.64.

Aqueous solutions of salts wet coal less effectively than mixtures of organic liquids and are therefore inadequate for fractionation of finely pulverized coal. The difficulty can be eliminated by preliminary wetting of the coal with organic liquids such as a mixture of ether and alcohol.

Salts adsorbed by the coal can generally be removed only after boiling followed by washing and filtration. Moreover, organic liquids are better than aqueous solutions of salts due to their low viscosity and better wetting power.

Aqueous solutions of salts and suspensions are used at the present time for industrial beneficiation of coals. A defect of organic liquids is their solvent action on the bituminous portion of coal. Thus, for example, under fractionation conditions a mixture of benzene and carbon tetrachloride extracts from bituminous coals 0.3-1.4% of the soluble substances [23, 24] or about 10% of the bitumen content. According to Horton [20] a mixture of carbon tetrachloride and benzene is not completely removed from coal even after drying in vacuo at 100°. This is evident from the chlorine balance (0.5-0.9%) which shows that part of the CCl_4 is retained by the coal.

A mixture of benzene and carbon tetrachloride is therefore not completely inert to coal and is not completely removed after fractionation.

A mixture of carbon tetrachloride and toluene or xylene is a less powerful solvent and can therefore be recommended for fractionation of bituminous coals. Fractionation of coals is usually commenced with a liquid of maximum density. Commencement with light fractions is desirable for bituminous coals in order to minimize the solubility.

There are various approaches to the question of choice of specific gravities of heavy liquids. Apart from the objective of separation of components by fractionation of coals, some investigators [17-19] are concerned with utilizing the data on quantitative yields of fractions for characterization of coal properties. In such cases a previously prepared set of heavy liquids is used. Other workers [21, 23, 24, 26, 27] select the densities of heavy liquids according to the composition of the coal in question as revealed by a preliminary screening classification.

In order to obtain good concentrates of groups of microcomponents, it is necessary to select a range of specific gravities of heavy liquids on the basis of a trial fractionation for each of the coals concerned.

Gravity fractionation of coals is governed by the speed of settlement of the particles. The force causing movement of the particles in this case (in the earth's gravitational field) is their weight. The rate of fall of solid particles in a viscous medium can be calculated from Stokes' Law.

The theory of sedimentation analysis has been derived from Stokes' formula and a series of equations. Fractionation of coals can be effected not only on the basis of weight but also with the help of centrifugal force. When using an electric tube centrifuge (type TsÉ-3) (with a mean radius of circle of rotation of 85 mm) the centrifugal force at a speed of 1500 rev/min is 214 times greater than the acceleration of gravity, and at 3000 rev per min it is 855 times greater. This example vividly demonstrates the great acceleration of fractionation of coals

in heavy liquids when centrifugation is applied. Tube centrifuges are now used in most processes of heavy-liquid fractionation of coals. Disadvantages of the tube centrifuge are the low volume of even large diameter tubes and the partial mixing of fractions during their separation after centrifuging.

Horton [20] obtained pure concentrates of groups of microcomponents by repeating the fractionation when using the tube centrifuge. Our own data show this to be a very useful procedure. It should be noted that centrifuging over a long period is not desirable due to evaporation and change of density of the heavy liquid. Centrifuging for 7 min is usually adequate when using the TsÉ-3 tube centrifuge at 2000 rev / min. The rotary supercentrifuge [26, 27] gives more complete classification of coal fractions by density. Other centrifuges [31, 32] can also be used. The All-Union Research Institute for Coal Beneficiation, for example, fabricated an experimental laboratory centrifuge for heavy-liquid fractionation of batches of coal weighing up to 500 g. The original coals and the individual fractions must also be subjected to petrographic examination and chemical analysis.

A combination of chemical and petrographic investigation is likely to improve our knowledge of the structure of coals from different deposits.

SUMMARY

1. Separation of coals into fractions of different densities offers the possibility of study of the petrographic components, of determination of the degree of coalification in relation to the yields of fractions, of carrying out petrographic beneficiation, and of obtaining concentrates of the required quality from run-of-mine coal.

2. Isolation of good concentrates of petrographic components from a coal calls for fine pulverization, the employment of organic liquids and centrifuging. A repeat fractionation is desirable when a tube centrifuge is used.

LITERATURE CITED

[1] R. Lamprecht. Die Kohlenaufbereitung. Leipzig, A. Felix (1888).

[2] A. L. McCallum, Canad. Min. J. 130, 531 (1909).

[3] O. Simmersbach, St. u. E. 33, 2027, 2077 (1913).

[4] A. Sulfrian, Gluckauf 57, 1115 (1921).

[5] R. Lessing, Fuel 1, 610 (1922); 2, 87 (1923).

[6] T. Y. Drakeley and Hepburn, Brennstoffchemi 5, 358 (1924).

[7] R. Wuster, Gluckauf 61, 62 (1925).

[8] M. Dunkel, Z. Oberschl. V. 64, 604 (1925).

[9] W. Gross, Z. Oberschl, V. 65, 588 (1926).

[10] R. Kattwinkel, Gluckauf 63, 450 (1927).

[11] B. Fougner, Z. Oberschl. V. 66, 618, 706 (1927).

[12] T. Lange, Z. Oberschl. V. 67, 208, 281 (1928).

[13] F. Zetsche, H. Vigari, and G. Schãrer, Helv. Chim. Acta 14, 14 (1931).

[14] I. É. Bal'ts, Chem. Solid Fuels 2, 83 (1936).

[15] I. L. Macrae and A. M. Wandles, Fuel 15, 68 (1936).

[16] S. I. Panchenko, M. E. Popova, and O. I. Kozhevnikova, Trans. Eastern Research Institute for Coal Chemistry 5, 38 (1948).

[17] P. Ya. Samoilovich, Trans. DONUGI 8 (1950).

[18] I. I. Ammosov, Proc. Acad. Sci. USSR 73, 797 (1950).

[19] I. I. Ammosov, Symposium on Chemistry and Origin of Solid Combustible Minerals, Acad. Sci. USSR Press (Moscow, 1953).

[20] L. Horton, Fuel 31, 341 (1952).

[21] L. L. Nesterenko, Symposium on Chemistry and Origin of Solid Combustible Minerals. Acad. Sci. USSR Press (Moscow, 1953).

[22] N. N. Davydkov, Sci. Trans. All-Union Research Institute for Coal Chemistry 9, 36 (1953).

[23] N. S. Goloushin and E. S. Korzhenevskaya, Information Bull. Inst. Geology of the Arctic 4, 45 (1957).

[24] E. S. Korzhenevskaya and N. S. Goloushin, Trans. Inst. Geology of the Arctic, 107 (1959).

[25] H. N. Dormans, F. L Huntgens, and D. W. van Krevelen, Fuel 36, 321 (1957).

[26] C. Kröger, A. Pohl, and F. Küthe, Gluckauf 93, 123 (1957).

[27] C. Kröger, Brennstoffchemi 38, 33, 82, 102, 147, 179, 200, 231 (1957); 39, 1, 110 (1958).

[28] G. P. Alaev, Bull. Siberian Div. Acad. Sci. USSR 10, 78 (1958).

[29] D. Zh. Zabramnyi, Uzbek Chem. J. 1, 47 (1958).

[30] V. S. Kaminskii and Yu. Z. Yurovskii, Coke and Chemistry 2, 11 (1958).

[31] L. S. Zarubin, Collection of Information on Beneficiation and Briquetting of Coals 4, 31 (1957).*

[32] L. G. Demidov, ZL. 24, 183 (1958).

Received May 27, 1959

* In Russian.

THE EMPLOYMENT OF NORMAL AND DIFFERENTIAL POLAROGRAPHY FOR THE ANALYSIS OF COKE – CHEMICAL PRODUCTS

A. G. Pozdeeva, N. Kh. Cherkasov, and F. L. Kruglova

Eastern Research Institute for Coal Chemistry, Lower Tagil Metallurgical Combine

The polarographic method of analysis and investigation of organic compounds has found extensive application. Methods are now available for determination of naphthalene and pyridine bases in returned coke oven gas, of thiophene, styrene, cumarone and indene in crude benzole fractions, and of quinoline, isoquinoline and quinaldine in heavy bases [1]. We have also developed methods of analysis of pyridine bases in direct coke oven gas, in saturator mother liquor and in ammonia liquors. Apart from normal polarography, use is made in the latter case of the method of differential polarography which is known to afford several advantages [2].

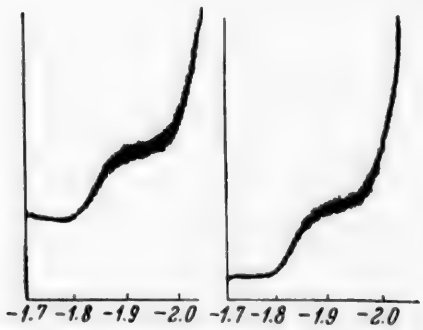

Fig. 1. Integral polarogram of pyridine bases. Concentration 3.84 g/l., $E_{\frac{1}{2}}$ = - 1.85 V (relative to a saturated calomel electrode).

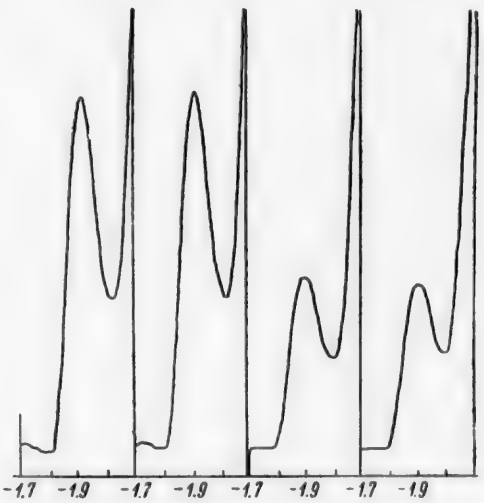

Fig. 2. Differential polarogram of pyridine bases. Concentration 3.84 g/l., $E_{\frac{1}{2}}$ = - 1.90 V (relative to the saturated calomel electrode).

The trace of the polarograms is differentiated with the help of an automatic integro-differentiating ÉP-312 polarograph [3]. A dropping mercury electrode was used as the cathode; the dropping period of the capillary was 1.5-2 sec. All of the measurements were made relative to a saturated calomel electrode in an electrolyzer with an external anode.

The pyridine homologs for the investigation were prepared by the literature method [4]. Pure pyridine was obtained from commerical pyridine by distillation in a 100-tray column; it boiled at 115.4°. Pyridine bases were also obtained for investigation in the form of a 113-180° fraction isolated from crude pyridine bases via the sulfates.

The normal polarograms were recorded during reduction of pyridine and its homologs at the dropping mercury electrode in 0.1 molar solution of calcium chloride. The following half-wave potentials (relative to the saturated calomel electrode) were determined: pyridine -1.80 V; α-picoline -1.84 V; β-picoline -1.88 V; γ-picoline -1.91 V; 2,6-lutidine -1.88 V; 2,4-lutidine -1.95 V; pyridine bases in the form of 113-180° fraction -1.90 V.

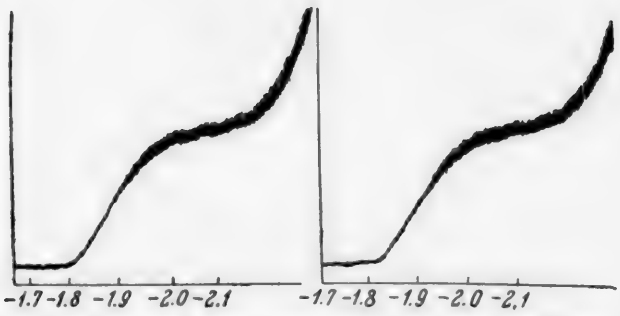

Fig. 3. Integral polarogram of pyridine bases traced at reduced speed. Concentration 3.84 g/l.

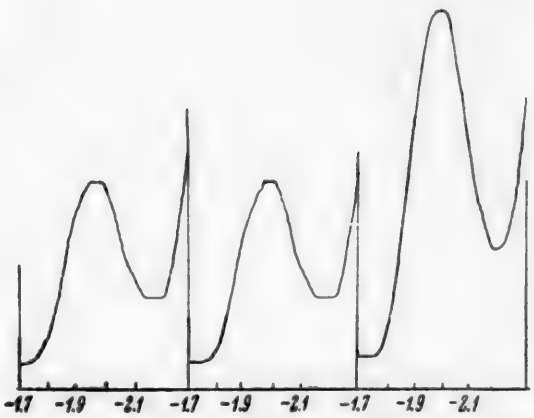

Fig. 4. Differential polarogram of pyridine bases traced at reduced speed. Concentration 3.84 g/l.

One over-all wave is obtained when solutions containing a mixture of pyridine and its homologs are polarographed (Fig. 1). Recording of the differential polarograms of pyridine bases (Fig. 2) showed that the half-wave potential of these substances on the differential curves is displaced in relation to the normal curves by 0.05 V in the direction of negative values. When normal and differential polarograms of pyridine bases are plotted at a reduced speed (Figs. 3 and 4), in both cases the half-wave potentials of the bases are shifted. Close investigation of pyridine and its homologs with the help of an electronic polarograph showed (Figs. 5 to 10) that a proportionality exists between the height of the wave or its maximum and the concentration of these substances (from 0.2 to 2.2 mg/ml). The plotted curves can therefore be utilized for quantitative analysis.

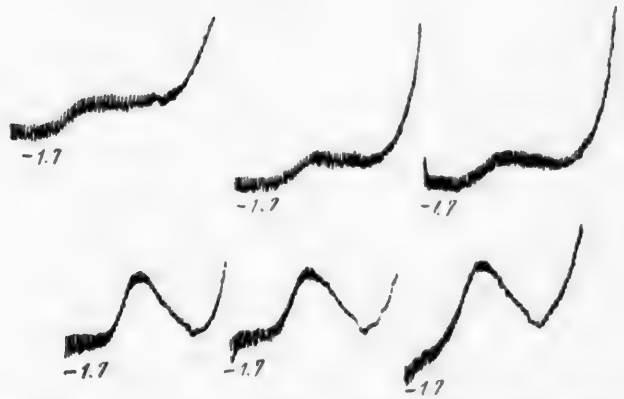

Fig. 5. Normal and differential curves of pyridine. Concentration 0.66 mg/ml.

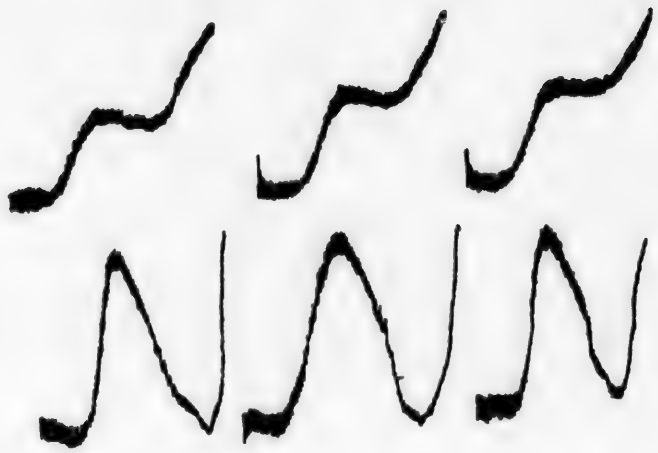

Fig. 6. Normal and differential polarograms of β-picoline. Concentration 0.68 mg/ml.

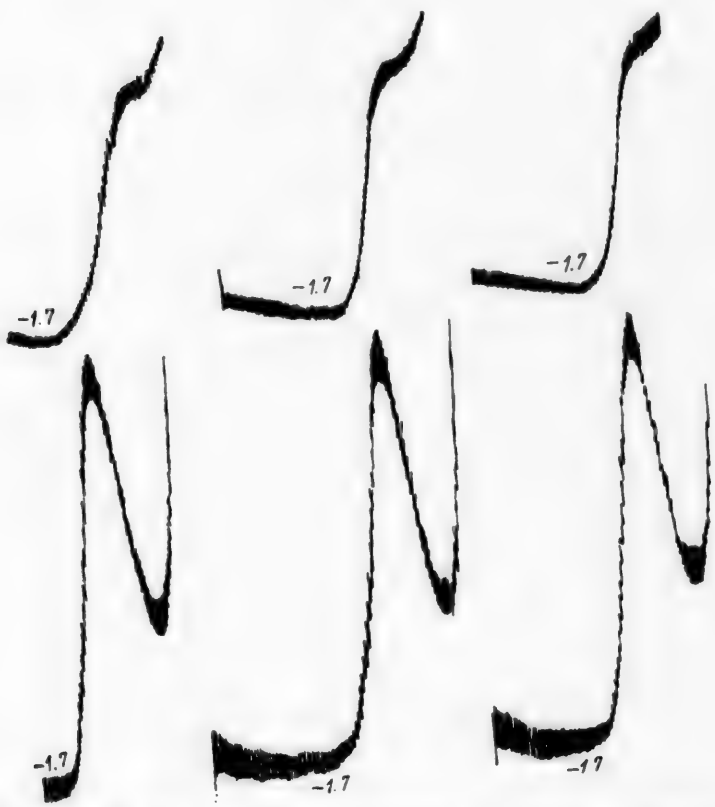

Fig. 7. Normal and differential polarograms of γ-picoline. Concentration 0.68 mg/ml.

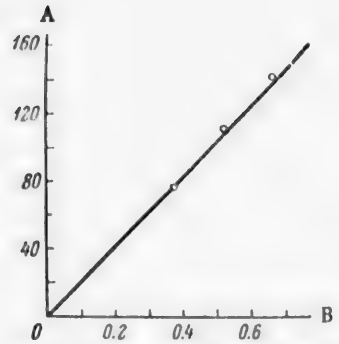

Fig. 8. Calibration graph for pyridine (based on differential polarograms). A) Height of wave and maximum (in mm); B) concentration (in mg/ml).

We know that one of the advantages of differential polarography is its higher potential resolving power in comparison with the normal method. We carried out a series of experiments to test the possibility of resolution polarography of pyridine and its homologs with the help of a differential polarographic circuit. One general maximum was always traced on the polarogram when two-, three- and multi-component mixtures of pyridines in various ratios were polarographed. This aspect evidently calls for further investigation which must be linked with a study of the mechanism of reduction of pyridine and its homologs at the dropping mercury electrode.

In our investigation we also devoted a great deal of attention to methods of measurement of the height of the maximum on the differential polarograms. This aspect has been neglected. Tsfasman [3] assumes the height of the maximum to be the distance from the derivative of the residual current to the peak.

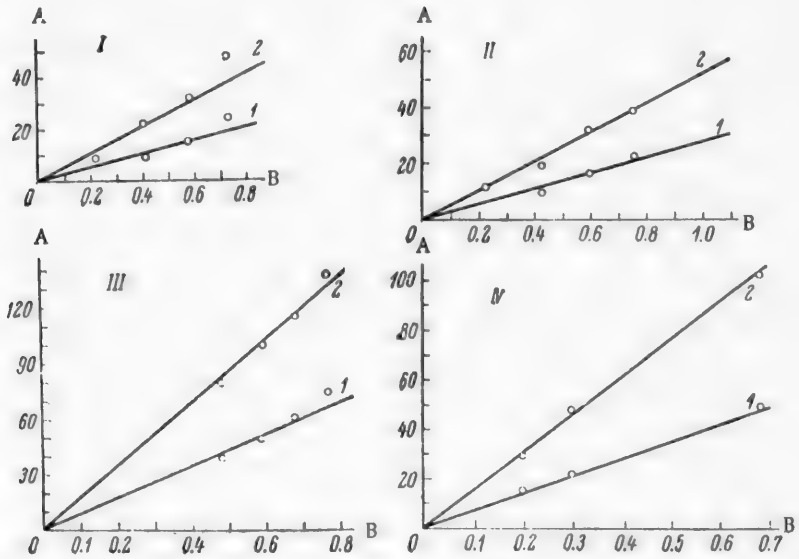

Fig. 9. Calibration diagram. I) α-picoline, II) β-picoline, III) γ-picoline, IV) 2,6-lutidine. 1) Straight line plotted from integral polarograms, 2) straight line plotted from differential polarograms.

We encountered some unusual features of the differential polarogram traces when working out a method of determination of pyridine bases in ammonia liquors. Firstly, a record could only be traced at low speed; secondly, the maximum on the polarogram is not sharp. This is due to the presence of a large quantity of ammonia in the products investigated whose reduction at the dropping mercury electrode starts at potentials very close to the diffusion current of pyridines.

The choice of method of measurement of the height of the maxima of pyridine bases in ammonia liquors was based on data obtained by polarographing artifical mixtures of ammonia and pyridine bases (Fig. 11). The height of maximum measured by this procedure was found to be directly proportional to the concentration of pyridine bases.

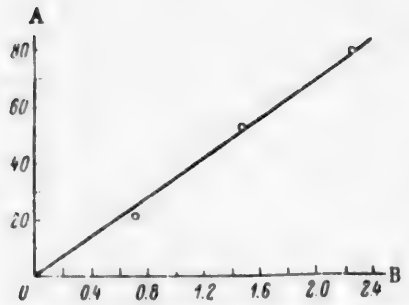

Fig. 10. Calibration graph of pyridine bases plotted on the basis of differential polarograms. A) Height of maximum (in mm), B) concentration (in mg/ml).

Several variants (Fig. 11) are possible when measurements are being made of the height of the maximum on the differential polarogram, during analysis of ammonia liquors for their content of pyridine bases, as a function of the differential curve (Fig. 11).

1. If the maximum is well-defined and has sharp boundaries between residual and limiting current, then the height is assumed to be the distance between them (I, line AB).

2. If at the maximum the derivative of the residual current is diffuse and the derivative of the limiting current is sharp, then the height of the maximum is taken as the distance EM (II). For this purpose the tangents AB and CD are drawn to the derivative of the residual current and the side of the maximum bordering on it. The distance from the vertex of the maximum to the point of intersection of these tangents is considered the height of the maximum.

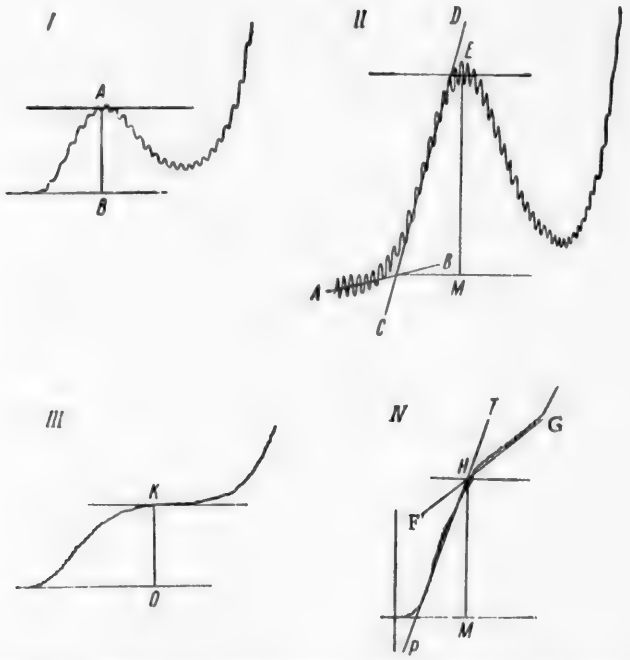

Fig. 11. Method of measurement of the height of the maximum on differential polarograms.

3. If the derivative of the limiting current on the differential polarogram is represented by a straight line (saddle absent from the maximum), then the height of the maximum is taken as the distance from the derivative of the residual current to the rectilinear part of the derivative of the limiting current – KO (III).

4. If the differential polarogram has a well-defined derivative of the residual current but the derivative of the limiting current is diffuse, then the height of the maximum is taken as the distance MH (IV). This is found by drawing the tangents PT and FG to the derivative of the limiting current and the side of the maximum abutting on it.

The distance from the derivative of the residual current to the point of intersection of these tangents is assumed to be the height of the maximum.

SUMMARY

1. Pyridine and its homologs and the pyridine bases isolated from crude pyridine bases were analyzed by the method of normal and differential polarography with the electronic polarograph. A proportionality was established between wave height, maximum, and concentration of these substances. This relation enabled the development of a series of methods of analysis of pyridine bases in coking products.

2. New methods are put forward for measurement of the height of the maximum on differential polarograms.

LITERATURE CITED

[1] Bulletin of Scientific and Technical Information of the VUKhINa, No. 1, Metallurgical Press, Sverdlovsk (1956).

[2] E. M. Skobets and V. D. Skobets, Factory Lab. 2, 167 (1957).

[3] S. B. Tsfasman, Factory Lab. 2, 131 (1956).

[4] A. G. Pozdeeva and E. M. Gepshtein, J. Gen. Chem. 22, 2065 (1952).*

Received July 12, 1958

* Original Russian pagination. See C. B. Translation.

COMPARATIVE CHARACTERIZATION OF SOME ANIONITES

A. T. Davydov and Yu. A. Tolmacheva

Chemical Research Institute of the Khar'kov A. M. Gorkii State University

The existence of a large number of diverse anionites of Russian manufacture and their extensive practical application gives rise to the necessity for comprehensive and systematic investigations of their properties. In a series of papers it was shown that the laws of anion exchange by anionites are the same as the laws governing exchange of cations [1, 2]. In recent years details have been published of the synthesis, structure and physico-chemical properties of a series of anionites [3-13], and special attention has been given to determination of the exchange constants [9-11], to the titration curves [6, 7, 10], to the adsorption series of anions [5], and to the exchange capacities as determined by different methods under various conditions [3-8, 11].

The present paper is devoted to investigation of the basicity of a series of Russian anionites, to determination of the exchange constants of some inorganic and organic anions, and to the investigation of the exchange capacity of sorbents as a function of the pH of the solutions. We studied the following anionites: DN, AN-9, EDE-10P, AV-16, AN-2F, AN-9F, TN, MMG-1, N-O, and TM.

We know from the literature [3-12] that these anionites have been systematically examined from the above aspects. To a certain extent our data fill these gaps in the quantitative characterization of Russian anionites.

EXPERIMENTAL

The anionites needed for the investigation were previously saturated with chloride ions. For this purpose the sorbents were treated with potassium chloride solutions whose concentration increased gradually from 0.25 N to 1 N. They were then washed free of excess of chloride ions. The anionites were dried at first in the air and later in a drying cupboard at 60° for two days. The specimens used had a particle size of 0.25 to 1 mm.

A first series of experiments was run for determination of the constants of exhange of chloride ions by nitrate, formate, acetate, propionate, and butyrate ions according to the equation

$$XCl + R^- \rightleftarrows XR + Cl^-. \qquad (1)$$

Weighed samples of anionites (1 g each) were covered with solutions of the appropriate sodium salts (volume 50 ml). The mixtures were shaken for 8 hr, then after 12 hr the aqueous phase was separated from the sorbent. The equilibrium solution was analyzed volumetrically for the content of chloride ions (mg-equiv. in 50 ml solution). Exchange constants were calculated from the formula

$$K = \frac{(S_m - a)(cV - a)}{a^2}, \qquad (2)$$

where a is the quantity of Cl^- ions found (in mg-equiv.) in the equilibrium solution, c is the concentration of displaced ion in the original solution (in mg-equiv./ml), V is the volume of this solution (in ml).

Simple rearrangement of equation (2) gives

$$a = S_m - K\left(\frac{a^2}{cV - a}\right), \qquad (3)$$

TABLE

Values of Capacities S_m (upper figure) and Exchange Constants K (lower figure) for the Investigated Anionites *

Anionite	System						
	$Cl^- - NO_3^-$	$Cl^- - R_1$	$Cl^- - R_2$	$Cl^- - R_3$	$Cl^- - R_4$	$Cl^- - OH^-$	S_m
ÉDE-10P	5.0	4.5	4.5	4.5	4.6	—	4.6
	0.56	1.2	1.3	1.3	1.4	—	—
AV-16	4.6	4.5	4.0	4.3	4.2	—	4.3
	0.56	1.5	1.4	1.8	1.8	0.02	—
AN-2F	3.6	3.6	3.4	3.3	3.5	—	3.5
	0.34	1.6	1.7	1.6	1.6	0.03	—
AN-9F	2.5	2.2	2.3	2.6	2.7	—	2.5
	0.28	0.64	0.72	0.58	0.53	0.002	—
AN-9	3.4	2.4	2.5	2.9	3.0	—	2.8
	0.37	0.30	0.30	0.26	0.41	—	—
MMG-1	2.9	3.0	2.8	2.9	2.8	—	2.9
	0.38	1.9	2.5	2.2	1.5	0.03	—
N-O	2.7	2.8	2.5	2.6	2.7	—	2.7
	0.19	1.0	1.0	1.1	1.4	0.03	—
DN	1.9	1.8	1.5	2.0	1.9	—	1.8
	0.27	1.7	1.4	1.6	1.6	—	—
TN	2.0	1.9	1.6	2.4	2.0	—	2.2
	0.25	2.0	2.2	1.4	1.0	0.04	—

* R_1 formate, R_2 acetate, R_3 propionate, R_4 butyrate ions.

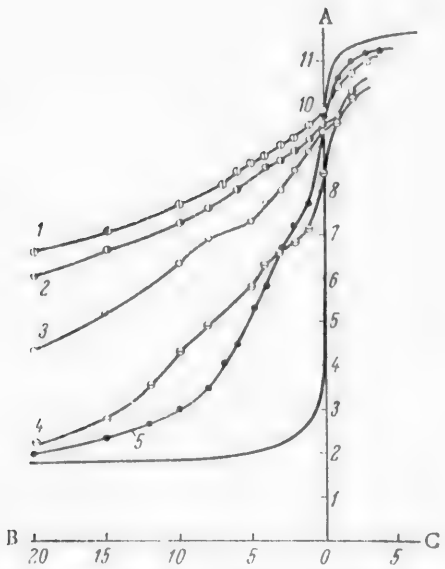

Fig. 1. Titration curves of anionites: 1) ÉDÉ-10P, 2) AV-16, 3) AN-2F, 4) AN-9F, 5) AN-9. A) pH value; B) amount of HCl (in ml), B) amount of NaOH (in ml).

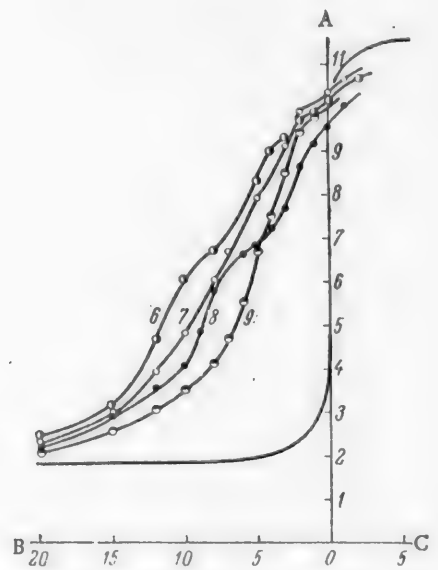

Fig. 2. Titration curves of anionites: 6) MG-1, 7) N-0, 8) DN, 9) TN. A) pH value; B) amount of HCl (in ml); B) amount of NaOH (in ml).

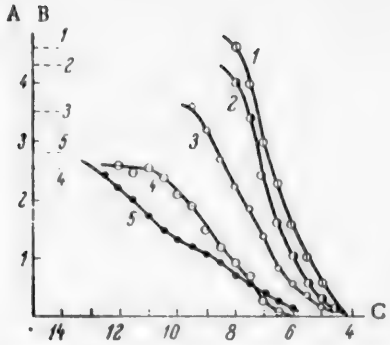

Fig. 3. Effect of pH value of medium on exchange capacity of anionites: 1) ÉDÉ-10P, 2) AV-16, 3) AN-2F, 4) AN-9F, 5) AN-9. A) Exchange capacity g; B) capacity S; B) pOH value.

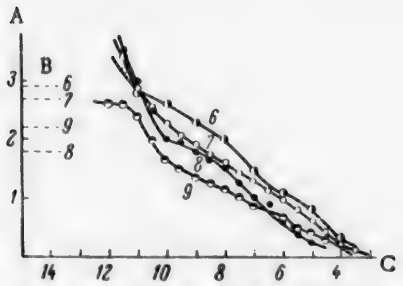

Fig. 4. Effect of pH of medium on exchange capacity of anionites: 6) MMG-1, 7) N-0, 8) DN, 9) TN. A) Exchange capacity g; B) capacity S; B) pOH value.

The value of S_m can be found from the latter by a graphical method, and then the constant K can be calculated from equation (2).

The experimental and calculated data obtained for 46 systems are presented in the table. The values S_m used for calculation of these constants by equation (2) were obtained during examination of the exchange of chloride ions with nitrate ions.

The next series of experiments served for investigation of the titration curves of the anionites and for study of the change of capacity of the sorbents as a function of the pH of the medium. These experiments were performed by the procedure described in the literature [13, 14]. Weighed samples of anionites in the hydroxyl form (0.5 g each) were placed in bottles to each of which was added 25 ml of 0.2 N sodium chloride solution, various volumes of 0.1 N HCl or 0.1 N NaOH, and enough double-distilled water to make up the volume to 50 ml. The mixtures were shaken for 8 hr; then after 12 hr the solutions were filtered and their pH values were measured with a glass electrode. Titration curves, i.e., curves of pH of equilibrium solution versus volume of added acid or alkali, were obtained in this manner. A titration curve was similarly plotted for the alkali against the acid in presence of sodium chloride but without an anionite. Titration curves of the following anionites are plotted in Fig. 1: ÉDÉ-10P, AV-16, AN-2F, AN-9F, AN-9; Fig. 2 contains the plots for MMG-1, N-O, DN, and TN.

The exchange capacity of the anionites that we investigated was calculated from the titration curves with the help of the formula

$$g = \frac{c_0 (v_1 - v_0)}{m}, \qquad (4)$$

where c_0 is the initial concentration of the solution of hydrochloric acid or alkali (in mg/equiv./ml), v_1 is the number of ml of 0.1 N HCl or NaOH solution for titration with the anionite, v_0 is the same without the anionite, and m is the weight of anionite (in g).

Figs. 3 and 4 are plots of the values of g for the various anionites as a function of the pH of the equilibrium solutions.

EVALUATION OF RESULTS

We see from the table that the constants of exchange of chloride ions with anions of organic acids differ by amounts that are within the limits of experimental error. Separation of these acids in aqueous solutions with the aid of the anionites in question would therefore hardly be possible. Comparison of the exchange constants shows that all of the anionites have less affinity for organic anions than they have for chloride anions ($K > 1$). Nitrate ions are held more firmly by the anionites than are chloride ions ($K < 1$). The anionites have a greater affinity for hydroxyl ions ($K << 1$). We know [3, 13] that their behavior does not always conform to the laws of

ionic exchange. We confirmed this on attempting with the help of equation (3) to determine the exchange constants and capacity of the anionites. The experimental data were not consistent with equation (3) which represents the straight line which cuts off on the ordinate a length numerically equal to S_m. Linearity is more closely followed during exchange of inorganic anions ($XCl-NO_3^-$) and less closely during exchange of chloride ions with anions of organic acids. It is interesting to note that for anionites AN-9 and AN-9F the exchange constants are substantially identical both for inorganic and for organic anions and are less than unity. The remaining anionites differ in their capacity to exchange ions of different natures and manifest considerably less affinity for organic anions.

We previously investigated the reciprocal exchange of halide ions with anionites TN and N-O [11] when it was found that the exchange constants for the systems $XCl-Br^-$ and $XCl-I^-$ are respectively 0.48 and 0.37 for anionite TN and 0.62 and 0.23 for N-O. On the basis of these data we can arrange the exchanging anions in the following order of magnitude of exchange constants with anionites TN and N-O:

$$OH^- > NO_3^- > I^- > Br^- > Cl^- > HCOO^- \sim CH_3COO^- \sim C_2H_5COO^- \sim C_3H_7COO^-.$$

This series is evidently also valid for the remaining anionites except AN-9 and AN-9F. The above series of univalent anions broadly confirms the series found for the anionites by other methods [5].

As previously indicated, an important property of anionites is their exchange capacity as determined from the titration curves. Nikol'skii [13] considers four types of ionites in dependence on the manner in which their exchange capacity alters with changing pH of solution. The first type are strongly basic, the second weakly basic, the third are anionites of mixed type exhibiting both acid and basic properties, and the fourth are a special type of mixed anionites characterized by continuous change of exchange capacity with changing pH of solution. Consequently the type to which a particular anionite belongs will depend on the nature of its active groups.

As we see from Figs. 3 and 4, the anionites that we investigated are of various types. Fig. 3 indicates that the exchange capacity of anionites ÉDÉ-10P and AV-16 increases rapidly with the pOH; this behavior characterizes them as strongly basic sorbents. The anionites in this diagram can be arranged in the following order of falling basicities: ÉDÉ-10P ≥ AV-16 > AN-2F > AN-9F > AN-9. This order is consistent with the literature data [12]. The exchange capacity of these anionites at certain values of pOH attains values of S_m close to the values that we found when calculating the exchange constants (see table). Anionite AN-9 is characterized by a multifunctional behavior. Even more conspicuous is the multifunctionality of the anionites whose curves of change of exchange capacity are plotted in Fig. 4. It is interesting to note that, with progressive change of pH, these curves have a trend toward higher exchange capacity values than we calculated when determining the exchange constants (see table). The calculated S_m values characterize only a part of the total capacity of the anionites which is associated with participation in anionic exchange of the predominantly more basic active groups of the anionites. The presence in the anionites of several functional groups with differing basicities is a hindrance to the classification of anionites in terms of basicity. We can only speak of a certain magnitude of activity averaged over all of the active groups of a given anionite and in a given pH region. A comparison of the curves in Figs. 3 and 4 reveals that in the investigated pH region the anionites form the following series in respect to basicity: ÉDÉ-10P > AV-16 > AN-2F > MMG-1 > N-O > DN > AN-9F > TN > AN-9.

SUMMARY

1. Determinations were made of the capacity of anionites and the constants of exchange of chloride ions with nitrate, formate, acetate, propionate, and butyrate ions in the cases of the following anionites: DN, AN-9, ÉDÉ-10P, AV-16, AN-2F, AN-9F, TN, MMG-1, N-O, and TN. It was shown that adsorption of the investigated anions falls off in the order $OH^- > NO_3^- > I^- > Br^- > Cl^-$ > ions of organic acids. Anionites AN-9 and AN-9F possess higher affinity for anions of organic acids.

2. Titration curves of the above anionites were plotted and the alteration of their exchange activity as a function of pH of the equilibrium solutions was calculated and plotted. These data show that the anionites can be arranged in the following series with respect to basicity: ÉDÉ-10P ≥ AV-16 > AN-2F > MMG-1 > N-O > DN > AN-9F > TN > AN-9.

LITERATURE CITED

[1] A. T. Davydov, Trans. Chem. Research Inst. Khar'kov State Univ. 6, 23, 139 (1946).

[2] B. P. Nikol'skii and V. I. Paramonova, Sci. Memoirs Leningrad State Univ., Chem. Series 163, 112, 121 (1953).

[3] A. B. Davankov and V. M. Laufer, Symposium on Investigations in the Field of Ion-Exchange Chromatography, Acad. Sci. USSR Press (1957), p. 12.

[4] K. M. Saldadze and Z. G. Demonterik, Loc. Cit., 106.

[5] L. S. Aleksandrova, T. B. Gapon, and K. V. Chmutov. Symposium on Theory and Practice of Application of Ion-Exchange Substances [in Russian] (Acad. Sci. USSR Press, 1955), p. 23.

[6] D. N. Ryabchikov, M. M. Senyavin, and K. V. Filipova, J. Anal. Chem. 7, 140 (1952).*

[7] D. N. Ryabchikov, M. M. Senyavin, and K. V. Filipova, J. Anal. Chem. 8, 222 (1953).*

[8] K. M. Saldadze and E. N. Fedorova, Summaries of Reports of the Conference on Chromatography, Acad. Sci. USSR Press (Moscow, 1958), p. 25.

[9] K. M. Saldadze, Symposium on Investigations in the Field of Ion-Exchange Chromatography, Acad. Sci. USSR Press (1957), p. 38.

[10] E. A. Materova and V. I. Paramonova, Symposium on Theory and Practice of the Application of Ion-Exchange Substances, Acad. Sci. USSR Press (1955), p. 5.

[11] A. T. Davydov, Yu. A. Morozova, and K. Ya. Levina, Trans. Chem. Faculty and Inst. Chem. Research of Khar'kov State Univ. 15, 19, 23 (1956).

[12] K. M. Saldadze, Z. G. Demonterik, and Z. V. Klimova, Symposium on Investigations in the Field of Ion-Exchange Chromatography, Acad. Sci. USSR Press (1957), p. 48.

[13] B. P. Nikol'skii, Symposium on Chromatography, Leningrad State Univ. Press (1956), p. 5.

[14] B. P. Nikol'skii and V. I. Paramonova, Prog. Chem. 8, 10, 1535 (1939).

Received July 25, 1958

* Original Russian pagination. See C. B. Translation.

HIGH-TEMPERATURE CERAMIC HEATERS

E. K. Keler and E. N. Nikitin

The first attempts to utilize ceramic masses as materials for high-temperature ceramic heaters were undertaken more than fifty years ago. Such serious difficulties were encountered, however, in the course of practical study of this problem that it has not yet been solved completely. The main difficulties are the unfavorable temperature coefficient of electrical conductivity, difficulties associated with starting during the ignition period, irregular distribution of current over the cross-section, and the poor heat conductance of ceramics. Serious difficulties arise in addition in the construction of electrical contacts between heating and conducting wires. Due to the negative temperature coefficient of electrical conductivity, a ceramic heater has a tendency either to overheat or to "freeze" so that current ceases to pass. Fabrication of heaters and of contacts consumes expensive and scarce materials such as yttrium oxide and platinum.

Geller [1] and Davenport et al. [2] have studied the problem of ceramic heaters. They describe the main designs of furnace elements with ceramic heaters. The former author patented an electrical contact; the second recommended the use of a contact mass of zinc oxide. Our own investigations show the latter to be unsuitable due to its volatility at temperatures above 1200°.

In the present work we made yet another attempt to fabricate high-temperature ceramic heaters developing a temperature of over 2000° in an atmosphere of air. In place of expensive and scarce materials (yttrium oxide and platinum) we made use of readily available zirconium oxide and magnesia. An electrically conductive layer of zirconium carbonitrides was applied at the places of contact. Moderate water cooling was employed to reduce oxidation of the conducting leads.

The electrical conductivity of some types of ceramics is known to increase sharply with rising temperature and to reach values characteristic of semiconducting materials. According to the theory of semiconductor physics [3] the current in a ceramic is carried to a small extent by electrons; the latter can be called free electrons to distinguish them from the remaining bound electrons. In a number of cases the logarithm of electrical conductivity is a linear function of the reciprocal temperature. It must be realized that the electrons may originate from impurities whose dissociation energy is usually lower than that of the substance itself. Foreign constituents as well as an excess of one type of ion not only sharply change the magnitude of the electrical conductivity but also govern the mechanism of conductivity. In crystalline lattices of the ionic type, an excess of electropositive atoms of metal that easily split off electrons creates an electronic current mechanism, whereas electronegative ions of oxygen or sulfur bind a certain number of valence electrons in the atom and this leads to a hole mechanism of transfer of charges. In compounds with valence bonds the character of the current carriers is governed by the number of valence electrons in the atom. If an impurity atom contains more valence electrons than are present in the surrounding substance, then an excess of electrons moves into the free zone; if the valence electrons are not captured, they are supplemented from the filled zone so that a corresponding number of holes remain in the latter. The electrical conductivity of oxides depends in great measure on the composition of the surrounding atmosphere. A reducing atmosphere (also a vacuum) favors thermal dissociation of oxides, and this leads to a bigger part being played by the electronic component of the conductivity.

Much experimental material concerning the electrical conductivity of oxides and their mixtures is presented in the monographs of Hedvall, Hauffe and Jost [4-6]. X-ray investigations show that the crystal structure of zirconium dioxide which has been stabilized by oxides of yttrium, calcium, or magnesium, does not change [7, 8].

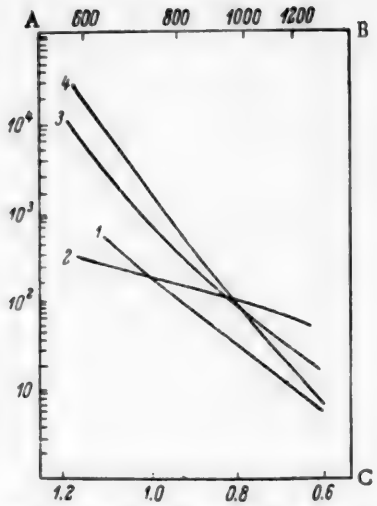

Fig. 1. Temperature dependence of the electrical conductivity of ceramic mixtures. A) Electrical conductivity (in Ω × cm); B) temperature (°C); B) reciprocal temperature ($10^3/T$). Composition of mixtures: 1) 84% ZrO_2 + 16% Y_2O_3, 2) 74% Cr_2O_3 + 26% Al_2O_3, 3) 85% ZrO_2 + 15% MgO, 4) 65% ZrO_2 + 35% CaO.

On the basis of our own measurements of thermoelectromotive force we can conclude that the hole mechanism of electrical conductivity characterizes solid solutions of zirconium dioxide. The observed thermo-emf values range from 2000 to 3000 millivolts/degree. The electrical conductivity was measured with the help of a bridge circuit at temperatures up to 1350°. The ends of platinized specimens were pressed between two platinum contacts and heating was effected in a silit furnace. Fig. 1 illustrates the change of electrical conductivity with temperature for ceramic masses with good electrical conductivity and suitable by virtue of their technical characteristics for fabrication into ceramic heaters. A zirconia–magnesia mixture has valuable ceramic qualities.

An important requirement for fabrication of ceramic heaters is a stock with homogeneous body and regular outlines. Very small flaws (pores or cracks) inevitably lead to rejection. The raw material for heaters was technical zirconium dioxide (99.2% ZrO_2) previously calcined at 1200° and pulverized in a ball mill. The pulverized mass was dried and used for preparation of blocks measuring 2 × 2 × 15 cm by the method of semidry moulding. Preliminary baking was performed at 1250°. The initial mass and the preliminary calcining temperature were so selected that the blocks could be successfully worked on a lathe. A neck with a diameter of 8 mm was cut in the middle part of the heater. Final high-temperature calcination (1700°) was effected in the suspended state. Fig. 2 is an illustration of a ceramic heater gripped between two water-cooled contacts.

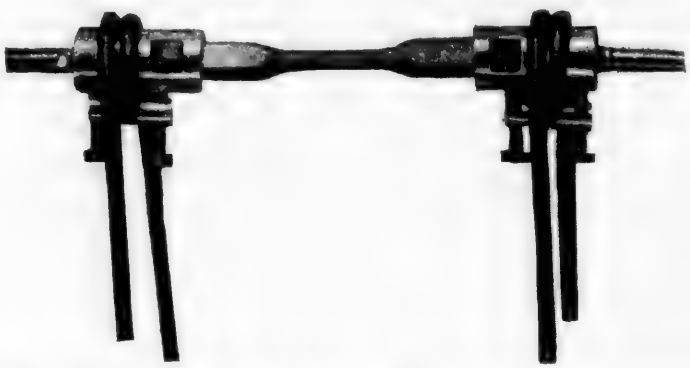

Fig. 2. Ceramic heater in test stand. The contacts are water-cooled.

The commonest cause of rejection of a heater is breakdown of the electrical contact. An imperfect contact leads to voltaic arcing with melting-out of large craters. Deposition of electrically conductive films reduces arcing but the presence of foreign materials lowers the melting point of the ceramic. Zirconium carbide and nitride are highly resistant to oxidation by atmospheric oxygen up to 1200°. Coatings of these substances are formed by high-temperature calcination in a nitrogen (or ammonia) atmosphere at the surface of the thickened portion of the heater after this has been covered with a layer of carbon black. Products of oxidation of zirconium carbide and nitride do not lower the melting point of a ceramic heater. The leads can be made from ÉI-626 alloy heat-treated at a temperature of 1350°. The life of the contacts is prolonged if they are moderately water-cooled. Heaters in the vertical position can generate a higher temperature without bending than is the case in the horizontal position.

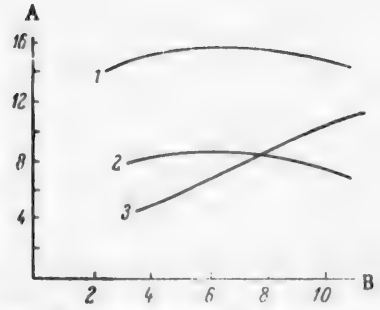

Fig. 3. Volt–ampere characteristic of ceramic heaters. A) Voltage drop along length (volts/cm); B) current density (amps./cm^2). The ceramic heater contains 85% ZrO_2 and 15% additives: 1) Y_2O_3, 2) CaO, 3) MgO.

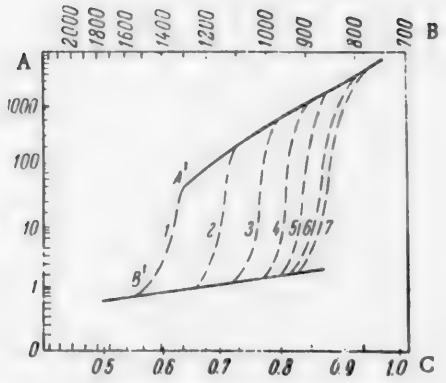

Fig. 4. Temperature dependence of the electrical resistance of a ceramic heating element with the composition 85% ZrO_2 + 15% MgO. A) Electrical resistance (in Ω × cm); B) temperature (in °C); C) reciprocal temperature ($10^3/T$). Applied voltage (volts/cm): 1) 25, 2) 35, 3) 45, 4) 70, 5) 100, 6) 120, 7) 150.

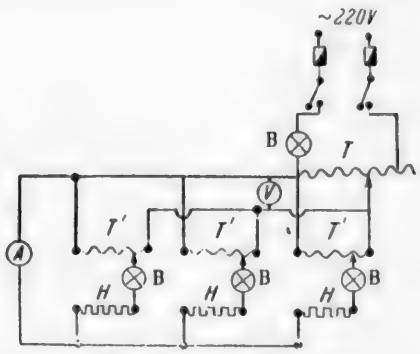

Fig. 5. Electric supply circuit of ceramic heating elements. T-autotransformer (20 amp., 250 volts), T' ditto (9 amps., 250 volts), B) set of barretter lamps (4 kW, 127 volts), ditto (100 watts, 12 volts), H-ceramic element.

The volt–ampere characteristic of a ceramic heater operating in the air is plotted in Fig. 3. The voltage drop along the length was measured with two platinum probes inserted in holes drilled in the neck of the heater. Passage of an increasing current raises the temperature of the heater and correspondingly its electrical resistance falls; the product of these two magnitudes (the voltage drop) remains nearly constant. The temperature of a ceramic heater should therefore be regulated not by the applied voltage but by means of the current.

The temperature dependence of a ceramic heater (85% ZrO_2 + 15% MgO) is plotted in Fig. 4. The linear portion at low temperatures corresponds to preliminary heating of the rod by the external heat source. Higher temperatures are accompanied by an extraordinarily rapid drop in resistance, giving the impression of electrical breakdown of the ceramic. Under the action of an external applied voltage a current starts to pass through the heater which is needed for further heating. The heater undergoes "ignition", and subsequently it serves itself as a powerful heat source. The temperature ceases to rise when the heat losses to the surrounding space – which increase as the fourth power of the difference of temperature between the medium and the heater – offset the effect of further heating. Indefinite increase in current is also prevented by a barretter resistance which is included in series in the heater circuit. The temperature of preliminary heating, required for the "ignition" of the heater, can be lowered by increasing the applied voltage. The rectilinear stretch in the region of higher temperatures corresponds to the electrical resistance of the operating heater at various temperatures of the latter. Similar relations were obtained for heaters fabricated from 85% ZrO_2 + 15% CaO and 85% ZrO_2 + 15% Y_2O_3.

The temperature gradient across the heater section when working without thermal insulation may reach 200–300°. The uneven temperature across the section is the most frequent course of cracking of the ceramic. The temperature gradient can be reduced by making the heater hollow and by using thermal insulation.

During operation a ceramic heating element requires automatic current strength regulation. The simplest device for this purpose consists of a set of barretter lamps. When the current increases the lamp-filament lights up and this creates an extra electrical resistance which counteracts further rise of current. The barretter resistance comprised a set of ordinary incandescent tungsten filament lamps with a total power of about 4 kW. The supply circuit to a furnace with three ceramic elements is represented in Fig. 5. Evenness of distribution of the load is checked with the help of three lamps B; adjustment is effected by change of the length of the winding of the 9-ampere auto-transformer arranged in series with each of the heating elements.

The temperature of a heating element, operating in an atmosphere of air and not protected by thermal insulation, reached 1950°. At higher temperatures the ceramic sagged under its own weight. The preliminary heating from an external heat source must be pushed to 900-1000°.

The working life of a heating element depends on the rate of temperature rise during the ignition period as well as on the intensity of heating. An element is designed for continous operation without frequent start-ups. Under normal conditions of use a heating element should be placed in a heat-insulated space. The maximum temperature generated by a heater then reaches 2050°. At 1800° a ceramic heating element which is thermally insultated can operate continuously for a number of days.

LITERATURE CITED

[1] R. F. Geller, J. Research Nat. Bur. Stand. 27 (6), 555 (1941).

[2] W. H. Davenport et al., J. Am. Cer. Soc. 33, 11, 333 (1950).

[3] A. F. Ioffe, Physics of Semiconductors [in Russian] (Acad. Sci. USSR Press), 1957 .

[4] J. A. Hedvall, Introduction to the Chemistry of Solids (in German), 1952.

[5] K. Hauffe, Reactions in and on Solids [in German] (1955); Ergebnisse der Exakten Naturw. 25, 193 (1951).

[6] W. Jost, Electrical Conductivity of Non-Metallic Crystals [in German] (1934).

[7] F. Hund, Z. Phys. Ch. 199, Heft 1/3, S142 (1952).

[8] F. Hund and Dürrwächter, Z. Anorg. Allg. Ch. 265, 265, 67 (1951).

Received July 4, 1958

THE TEMPERATURE OF THE VAPOR OF BOILING LIQUIDS

A. G. Bol'shakov, A. V. Kortnev and G. N. Gasyuk

When evaporating units are being designed, it is very important to correctly determine the temperature of the vapor evolved from a boiling solution. This so-called secondary vapor is utilized as heating vapor in multi-stage evaporators and also for evaporation with a heat pump. The temperature of the secondary vapor enters into the equations for calculation of the heating surfaces of evaporators and for determination of the heating vapor consumption. It therefore influences the economics of operation of evaporators.

In the majority of cases the literature (text books, handbooks, special publications) of chemical engineering [1-5] contains contradictory and even erroneous statements about the vapor temperature. At the same time this parameter plays an important part in the design and operation of evaporating plants.

Stabnikov and Molchanov [6] assume that the problem of the temperature of the vapor of a boiling solution has not been conclusively solved, but they suggest that thermal calculations of evaporation would be more accurate if we allowed for the consumption of heat for superheating of the secondary vapor from the saturation temperature to the boiling point of a solution at a given pressure.

Hausbrand and Hirsch [1] also incline to the opinion that the problem of vapor temperature has not been solved. They write: "Still unanswered is the question as to whether the vapor evolved from a solution is saturated or superheated, i.e., whether it corresponds to the boiling point of the solution or to the boiling point of the solvent, or indeed whether it is intermediate between these two." The same authors point to the conflicting views of Faraday and Gay-Lussac on this question. Faraday considered that the temperature of the secondary vapor corresponds to the boiling point of the pure solvent. On the other hand Gay-Lussac assumed it was the boiling point of the solution.

Schreber [1] concludes on the basis of his experiments that vapors have the temperature of the solvent on formation, but since they are subjected during evaporation to the action of the solution and the vessel walls they emerge from the apparatus at a temperature intermediate between the boiling points of solvent and solution.

Kasatkin [3] is of the opinion that superheating of the vapor is observed only in the immediate vicinity of the surface of the boiling solution and no longer occurs at a small distance away, i.e., the temperature of the secondary vapor is equal to the boiling point of the pure solvent at the pressure in the plant, and is uninfluenced by the concentration of the boiling solution.

An experimental unit was designed for the purpose of solving the problem of the temperature of the vapor evolved from boiling solutions. Studies were carried out with solutions of NaOH and KOH of various concentrations.

EXPERIMENTAL

Fig. 1 is a line diagram of the apparatus for determination of the vapor temperature of boiling solutions. A feature of this apparatus is the division of the vapor from the boiling liquid into two independent streams. In one of these streams is a thermometer for determination of its temperature. The other stream is used for establishment of the isothermal conditions under which the temperature of the first stream is measured.

This arrangement eliminates the possibility of cooling, condensation,or superheating of the vapor of the boiling liquid due to external conditions.

The solution is vaporized in a specially fabricated flask 1 of heat-resistant glass with a capacity of about 1.2 liters. The neck of the flask, height 130-140 mm and diameter 35-40 mm, is closed by a vapor discharging ground-glass fitting 2. To the upper part of this fitting are sealed a vapor-discharging union with an angle of 10-15° to the horizontal, for discharge of the constant-temperature stream of vapor, and a vertical tube 3 for the vapor stream whose temperature is to be measured. This tube is fitted concentrically in the neck of the flask; its middle has four holes for passage of vapor and is 30-40 mm below the level of the boiling liquid. Tube 3 terminates in a vapor-discharging union inclined at 10-15° to the horizontal and a ground-glass fitting 4 on which is suspended a mercury thermometer 5 for measurement of the temperature of the vapor and provided with screen 6.

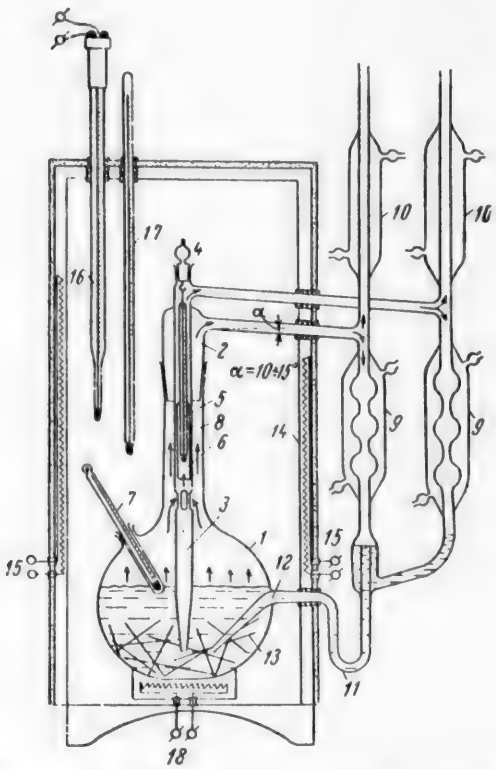

Fig. 1. Experimental apparatus for determination of the vapor temperature of boiling solutions. 1) tall-necked flask; 2) vapor-discharge fitting; 3) internal vapor outlet; 4) ground-glass fitting; 5) thermometer; 6) thermometer screen; 7) thermometer; 8) outer vapor outlet; 9, 10) condensers; 11) hydraulic seal of condensate return; 12) condensate return; 13) capillaries; 14) air thermostat; 15) heating element; 16) contact thermometer; 17) standard thermometer; 18) heating element.

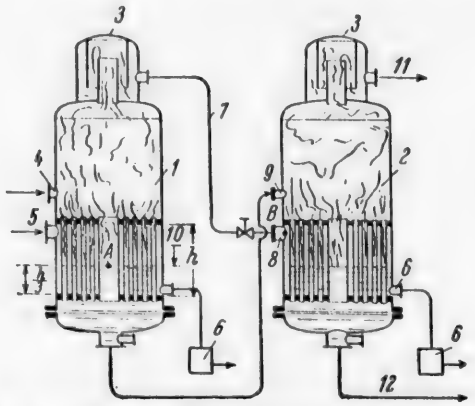

Fig. 2. Double-effect evaporator. 1) first effect; 2) second effect; 3) trap; 4) supply of feed solution; 5) inlet of heating (live) steam into the first effect; 7) steam line of secondary (exhaust) steam; 8) inlet of heating steam to second effect; 9) supply of evaporated solution to second stage; 10) level of boiling solution; 11) discharge of vapor for condensation; 12) discharge of evaporated solution; h) height of heating chamber.

The boiling point of the solution is determined with thermometer 7.

The vapor of the boiling solution, passing through internal vapor channel 3 and outer vapor line 8, is condensed in condensers 9, 10. Condenser 10 maintains atmospheric pressure in the flask without loss of vapor.

Condensate from the condensers returns to the flask via hydraulic seal 11 and connection 12. By this arrangement the concentration of the boiling solution remains substantially constant during steady-state operation. The fine capillaries 13 ensure uniform boiling.

The vaporizing apparatus 1 is placed in an air thermostate 14 with a jacket in which heater 15 is inserted. The outer wall of the thermostat is connected by contact relays to an LATR-1 autotransformer. The winding of the contact relay is connected up to the anodic circuit of a TG-1-0.3/1/3 thyratron which is controlled by the mercury contact thermometer 16.

The temperature in the thermostat is measured by standard thermometer 17.

TABLE 1

Determination of the Temperature of the Vapor of Boiling KOH Solution

Atmospheric pressure P_b (mm merc.)	Conc. of solution C_r (wt.-%)	B. p. of liquid t_{liq}	Temp. of vapor t_{steam}	$t_{liq}-t_{steam}$
760	16.2	104.5	104.0	+0.5
765	26.4	110.0	111.0	0
755	30.2	113.0	112.5	+0.5
762	36.6	120.0	120.0	0
761	42.2	128.0	128.0	0
758	46.2	135.5	135.5	+0.5
758	50.6	146.0	146.0	0
760	54.2	157.0	156.5	+0.5
762	58.3	171.0	170.5	+0.5
761	62.5	188.5	188.0	+0.5
762	68.1	216.5	216.0	+0.5

TABLE 2

Determination of the Temperature of the Vapor of Boiling NaOH

Atmospheric pressure P_b (mm merc.)	Conc. of solution C_r (wt.-%)	B. p. of liquid t_{liq}	Temp. of vapor t_{steam}	$t_{liq}-t_{steam}$
762	16.8	106.0	106.0	0
761	21.4	109.0	109.0	0
761	32.8	119.5	119.0	+0.5
765	39.2	127.5	127.0	+0.5
762	43.6	133.0	133.0	0
758	49.7	142.5	142.0	+0.5
755	53.4	147.0	147.0	0
761	58.1	156.5	156.0	0
759	61.5	163.0	162.5	+0.5
763	67.6	175.0	174.5	+0.5

The solution is kept at the boil by heating element 18 whose power is varied by an LATR-1 autotransformer.

The front side of the thermostat contains a window of transparent mica through which readings can be taken of the thermometers registering the temperature of the boiling solution and the vapor temperature. To the same side is attached a lamp for illuminating the apparatus inside the thermostat.

The test solution (or its components) is placed in the flask and brought to the boil with the help of heating element 18. At the same time the heater of the air thermostat is switched on; the temperature in the latter is held at 102-110°, to within 1°.

Tapwater is run through the condensers. Steady evaporation was indicated by constancy of the boiling points of the solution and of the steam flowing through the internal line 3. This temperature was the temperature of the vapor of the boiling solution.

Special preliminary experiments established that the increase of pressure in the vapor space of the flask did not exceed 0.3-0.4 mm mercury column over atmospheric pressure.

Experimental results on determination of the steam temperature of a boiling KOH solution and NaOH solution are presented in Tables 1 and 2.

It follows from the direct experimental data of Tables 1 and 2 that the temperature of the vapor released from boiling solutions of substances whose vapor pressure is negligibly small (salts, alkalies and some acids) is equal to the temperature of the boiling solution at all of the investigated concentrations between 16 and 68%.

These results confirm the validity of Khvol'son's observations [7] about the fallacy of the very widespread view that the temperature of vapors evolved from solutions at the boil is equal to the temperature of the pure solvent at the same total pressure.

An explanation of the differences in the readings of a thermometer placed in the vapor space and in a boiling solution has been given by Warburg [8] and by Tamman [9].

Depression of the temperature of the superheated vapor evolved from a boiling solution is substantially caused only by heat losses during its movement from the surface of the boiling liquid to the exit from the apparatus due to heat transfer by convection and radiation.

The experiments here described also confirm the validity of the recommendation of Stabnikov and Molchanov concerning allowance for the heat expended in superheating the vapor during evaporation. They also support the conclusions of Magnus [10] in a similar investigation.

For evaporator plant design, therefore, we must assume the temperature of the secondary steam to be equal to the boiling point of the solution. The necessary corrections must then be made for heat losses in the vapor lines and other parts of the plant.

For example, in the case of a two-stage evaporator the temperature of the secondary vapor entering the heating chamber of the second stage (Fig. 2) must be calculated from the formula

$$t_s = t_b - \delta t, \qquad (1)$$

where t_s = temperature of the secondary vapor (used as heating vapor in the second state); t_b = boiling point of the solution in the first stage, determined for the final concentration of the boiling solution (continuous operation) with application of a correction for the hydrostatic and hydraulic effects; δt = fall in temperature of the superheated vapor in passage from the surface of the boiling solution (point A) to the inlet to the heating chamber of the adjacent stage (point B).

The error in calculations will be the greater the higher is the boiling point of the solution and the smaller are the heat losses (these are reduced by good thermal insulation of the evaporator and of the connecting vapor lines). Thus, for example, when steam is superheated by 100°, the error in calculation of the heating surface of an evaporator and of the consumption of heating steam is more than 10% on the low side.

SUMMARY

1. It was established that the temperature of the vapor released from boiling solutions of NaOH and KOH with concentrations between 16 and 68% is equal to the boiling point of the solution of the given concentration at the total pressure in the plant.

2. Difference between the readings of the thermometer placed in the vapor space and in the boiling solution does not exceed 0.5° at boiling points of 104.5 to 216.5°, corresponding to a relative error of 0.5 to 0.25%.

3. Confirmation is obtained of the validity of the experiments of Magnus and of all those authors who assume the temperature of the vapors of boiling solutions to be equal to the boiling point of the solution itself.

4. Confirmation is obtained of the validity of the recommendation of Stabnikov and Molchanov [6] to the effect that allowance must be made for the consumption of heating steam for superheating of the secondary vapor during evaporation of solutions.

5. An error of over 10% is obtained for superheating of steam by 100° unless allowance is made for the above factor when heating surfaces are being calculated.

LITERATURE CITED

[1] E. Hausbrand and M. Hirsch, Evaporation, Condensation, and Cooling [Russian translation] (United Sci. Tech. Press, 1936).

[2] N. L Gel'perin, Evaporators [in Russian] (State Chem. Press, 1947).

[3] A. G. Kasatkin, Fundamental Processes and Equipment of Chemical Technology [in Russian] (State Chem. Press, 1955).

[4] M. A. Kichigin and G. N. Kostenko, Heat-Exchangers and Evaporators [in Russian] (State Energy Press, 1955).

[5] D. Perry, Chemical Engineering Handbook (1937), 1.

[6] V. N. Stabnikov and V. P. Molchanov, Khimstroi 10 (1933).

[7] O. D. Khvol'son, Course of Physics (1923). III.*

[8] E. Warburg, Course of Experimental Physics [Russian translation] (United Sci. Tech. Press, 1936).

[9] G. Tammnan. Textbook on Heterogeneous Equilibria [Russian translation] (United Sci. Tech. Press, 1935).

[10] H. Magnus, Pogg. Ann. 112, 404 (1861).

Received June 24, 1958

* In Russian.

GENERALIZED EQUATIONS FOR CALCULATION OF PACKED COLUMNS UNDER VARIOUS HYDRODYNAMIC CONDITIONS

V. V. Kafarov and V. S. Murav'ev

Mass transfer in packed columns is usually accompanied by movement of two-phase streams (gas–liquid, vapor–liquid, liquid–liquid).

Attempts to describe the processes of mass transfer in two-phase streams in the form of well-known equations of the type of $Nu_g = A \times Re_g^m \times Pr_g^n$, $Nu_1 = A_1 \times Re_{liq.}^{m_1} \times Pr_{liq.}^{n_1}$ or of the type of $Nu_{g(liq)} = A_2 \times Re_g^{m_2} \times Re_{liq.}^{m_3} \times Pr_g^{n_2} \times Pr_{liq.}^{n_3}$ have not hitherto led to the required results.

In our opinion, these attempts are associated with one fundamentally erroneous assumption, namely that they aim at describing a process taking place in a two-phase stream with the help of parameters characterizing single-phase streams without introducing a parameter characterizing the interaction of two-phase streams. This approach is evidently a logical consequence of the film theory of mass exchange. In a two-phase stream interaction of the moving streams is unavoidable and therefore neither Re_g nor $Re_{liq.}$ can reflect the true picture of processes taking place. It is also evident that the character of the interaction between the phases must vary in dependence on the intensity of relative movement of the phases. This leads to different hydrodynamic regimes of two-phase systems.

The main problem in the treatment of two-phase systems becomes the problem of the state of the phase interface and the associated phenomena taking place at the interface. A factor that might serve for taking into consideration the dynamic interaction of the moving streams of the phases is the previously introduced [1, 2] factor of the dynamic state of the surface $\underline{f}$. The values of $\underline{f}$ vary in dependence on the intensity of relative movement of the streams which in turn govern the various hydrodynamic regimes.

Mass transfer equations acquired the following form when the factor of the dynamic surface state is introduced:
for the gas phase

$$Nu_{gas} = A_3 \times Re_{gas}^{m_4} \times Pr^{n_4} (1 + f), \tag{1}$$

for the liquid phase

$$Nu_{liq.} = A_4 \times Re_{liq.}^{m_5} \times Pr_{liq.}^{n_5} \times (1 + f), \tag{2}$$

where

$$f = \frac{\left(\frac{\Delta P}{l}\right)_{gas\text{-}liq.} - \left(\frac{\Delta P}{l}\right)_{gas}}{\left(\frac{\Delta P}{l}\right)_{gas}} = B\left(\frac{L}{G}\right)^a \cdot \left(\frac{\gamma_{gas}}{\gamma_{liq.}}\right)^b \cdot \left(\frac{\mu_{liq.}}{\mu_{gas}}\right)^c, \tag{3}$$

The value of f (the dynamic surface state factor) is governed by the resistance in the two-phase and single-phase streams at the same gas rate [3, 4].

Using the principle here put forward, it seems to us possible to generalize the great mass of experimental material published up to now in the world literature.

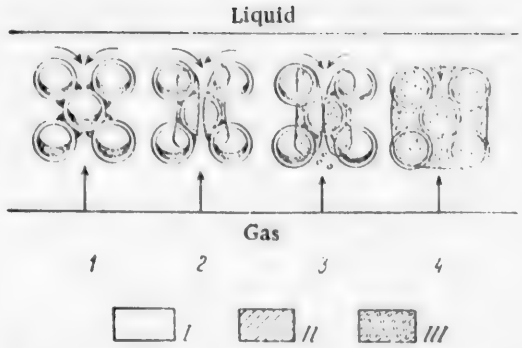

Fig. 1. Character of movement of streams in a packed column. 1) Film regime with drip/film flow of liquid, 2) intermediate regime with film/ /jet movement of liquid, 3) turbulent regime with film/jet movement and eddying of the liquid. 4) emulsification regime. I) liquid contact, II) liquid film, III) eddying of liquid film.

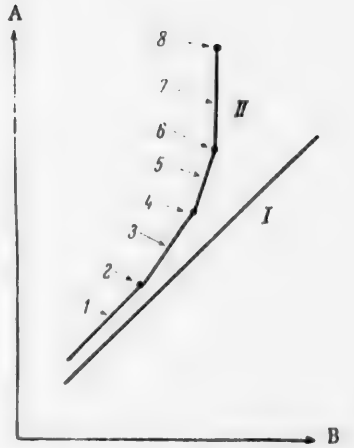

Fig. 2. Hydrodynamic regimes and transition points in packed columns. A) pressure drop $\Delta p/l$ (in mm water column/metre), B) gas rate in empty column w_0 (in metres/sec). 1) Film regime, 2) loading point, 3) intermediate regime, 4) hold-up point 5) turbulent regime, 6) point of inversion of phases, 7) emulsification regime, 8) flooding point, I) for dry packing, II) with irrigation.

Visual observations [3] on colored streams in packed columns and measurements of pressure drop as a function of the gas rate in irrigated columns enable us to reach the following conclusions.

Four characteristic forms of movement of the streams (approximately illustrated in Figs. 1 and 2) can be observed in the packing when the phases move in countercurrent. These forms of movement are the following:

1. Film interaction is observed with drop/film movement of the liquid from element to element of the packing; it occurs at low irrigation densities and low gas rates. Interaction between the phases occurs at the surface of the packing elements at individual points of contact.

2. An intermediate regime is observed with jet/film movement of the liquid which sets in from the start of slowing-down of the gas by the liquid stream (loading point). The liquid covers the packing in the form of a thin falling film and individual streams. Interaction between the phases takes place at the surface of the film and liquid streams and at points of contact of liquid with individual packing elements. The film and stream of liquid slow down the gas stream with formation of individual eddies.

3. Turbulent regime marked by film/jet movement with eddying of the liquid; it starts at very high gas rates and initiates hold-up of the liquid in the packing (hold-up point). Interaction between the phases occurs at the surface of the turbulent liquid film.

4. Emulsification regime – region of developed turbulence – sets in packed columns after the inversion point due to development of turbulence at the boundaries of each of the phases and leads to the interface of the phases being drawn into turbulent pulsations. The concept of the dispersed and continuous phases loses its meaning in this regime since the phases are being continuously reversed and at one instant the gas and at another instant the liquid becomes the continuous or the dispersed phase. During this process the phases are permeated by innumerable fine eddies.

Under these conditions we have a hydrodynamically stable system of "emulsified" liquid; gaseous eddies are continuously formed and moved and penetrate the turbulent liquid; the latter in turn becomes permeated with moving liquid eddies.

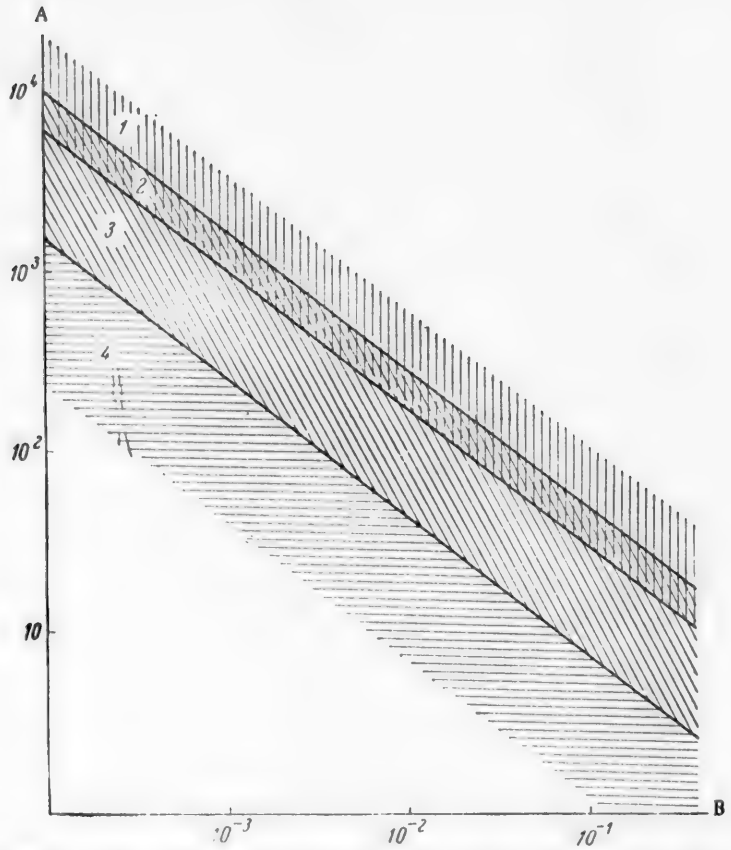

Fig. 3. φ^3 as a function of Φ for packed columns operating at various regimes. A) Value of φ^3; B) value of $\Phi = (\frac{L}{G})^{1.8} \cdot (\frac{\gamma_{gas}}{\gamma_{liq.}}) \cdot (\frac{\mu_{liq.}}{\mu_{gas}})^{0.2}$. Regimes: 1) Emulsification, 2) turbulent, 3) intermediate, 4) film.

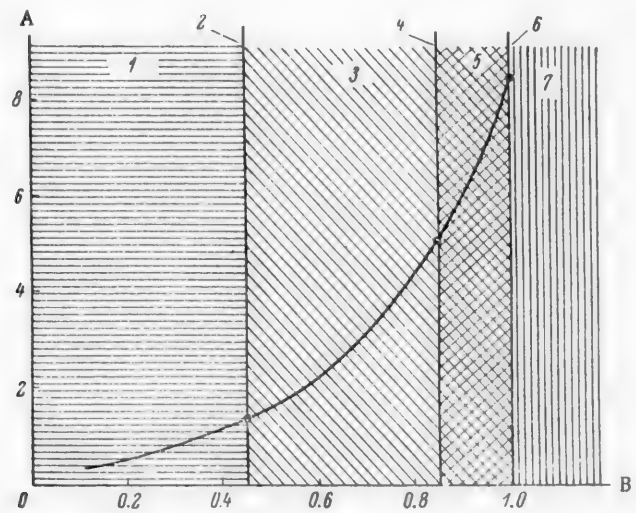

Fig. 4. Coefficient C as a function of $\frac{w_o}{w_{o,\,inv.}}$ for various hydrodynamic regimes. A) Value of C; B) value of $\frac{w_o}{w_{o,\,inv.}}$. 1) Film regime, 2) loading point, 3) intermediate regime, 4) hold-up point, 5) turbulent regime, 6) inversion point, 7) emulsification regime.

TABLE 1

Curve	System	Reference	Raschig rings
1	NH_3—water	Author's data	20 × 20 × 3
2		The same	8 × 8 × 1.5
3		[14]	25 × 25 × 3
4		[15]	25 × 25 × 3
5		[16]	25 × 25 × 3
6	NH_3—H_2SO_4	[15]	25 × 25 × 3
7	NH_3—water	[17]	8 × 8 × 1.5
8		[17]	12 × 12 × 2
9		[18]	25 × 25 × 3
10		[19]	8 × 8 × 2
11		[19]	15 × 15 × 3
12	Acetone – water	[20]	1 1/4"
13		[20]	3/4"
14		[20]	1/2"
15		[20]	3/8"
16		[18]	25 × 25 × 3
17	Ethanol – water	[18]	25 × 25 × 3
18		[21]	25 × 25 × 3
19	Methanol–water	[18]	25 × 25 × 3

TABLE 2

Curve	System	Reference	Raschig rings
1	CO_2—water	Author's data	20 × 20 × 3
2		[22]	3/8", 1/2", 3/4", 1 1/4"
3		[23]	3/8"
4		[24]	12 × 12 × 2, 20 × 20 × 3
5		[25]	25 × 25 × 3
6		[26]	15 × 15 × 2.5, 25 × 25 × 3
7	O_2—water	[27]	25 × 25 × 3
8		[28]	1", 1 1/2", 2"
9		[24]	8 × 8 × 1.5, 12 × 12 × 2, 20 × 20 × 3
10		[29]	1"
11	SO_2—water	[30]	1"
12		[29]	1"
13		[17]	12 × 12 × 3
14		[26]	25 × 25 × 3
15	Cl_2—water	[31]	5 × 25 × 3

Equations necessary and sufficient for description of the operation of packed columns under conditions of single-phase flow are the following: rate distribution equation; pressure distribution equation; equation of distribution of concentrations.

Such equations cannot be obtained under the conditions of two-phase streams; they can be replaced only by equations permitting calculation of these parameters as certain mean values (rate, pressure, and mass-transfer coefficient).

The most characteristic and critical point of operation of packed columns is the inversion point above which emulsification sets in; below the inversion point are regions of separate flow of the phases. Equations for calculation of the main working parameters of packed columns have been obtained for the inversion point and the emulsification regime: gas rate [5-8], pressure drop [4-7] and separation efficiency [6, 7, 9]. The majority of investigations

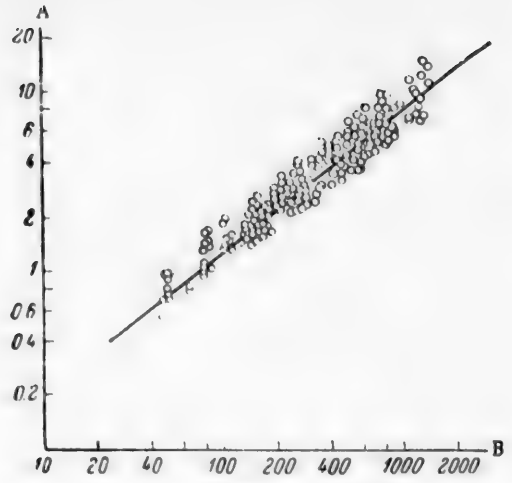

Fig. 5. Plot of $\frac{Nu_{gas}}{(1+f)Pr_{gas}^{2/3}} \cdot \frac{d_{e.s}}{d_e}$ versus Re_{gas} for all hydrodynamic regimes for readily soluble gases. A) Values of $\frac{Nu_{gas}}{(1+f)\,Pr_{gas}^{2/3}} \cdot \frac{d_{e.s}}{d_e}$; B) values of Re_{gas}. The various points correspond to the results of different authors [14-21] (see Table 1).

of the working of packed columns have been devoted, however, to analysis of their operation below the inversion point. The numerous experimental results on gas rates in packed columns published in the world literature can be generalized on the basis of the principle of corresponding states [2] if the reference velocity is taken as the velocity at the inversion point ($w_{0,inv.}$), which is unequivocally defined for gas–liquid systems by the equation

$$\lg\left(w_0^2\frac{\sigma}{gF_s}\cdot\frac{\gamma_{gas}}{\gamma_{liq.}}\left(\frac{\mu_{liq.}}{\mu_{gas}}\right)^{0.16}\right) = 0.022 - 1.75\left(\frac{L}{G}\right)^{1/4}\cdot\left(\frac{\gamma_{gas}}{\gamma_{liq.}}\right)^{1/8}. \quad (4)$$

On the basis of the pressure drop versus gas rate graph (Fig. 2) all of the previously obtained values of gas rates under various column regimes can be represented in the form of the following ratios:

turbulent regime $$\frac{w_0}{w_{0.\,Inv.}} = 1 \div 0.85, \quad (5)$$

hold-up point $$\frac{w_0}{w_{0.\,Inv.}} = 0.85, \quad (6)$$

intermediate regime $$\frac{w_0}{w_{0.Inv.}} = 0.85 \div 0.45, \quad (7)$$

loading point $$\frac{w_0}{w_{0.Inv.}} = 0.45, \quad (8)$$

film regime $$\frac{w_0}{w_{0.Inv.}} < 0.45. \quad (9)$$

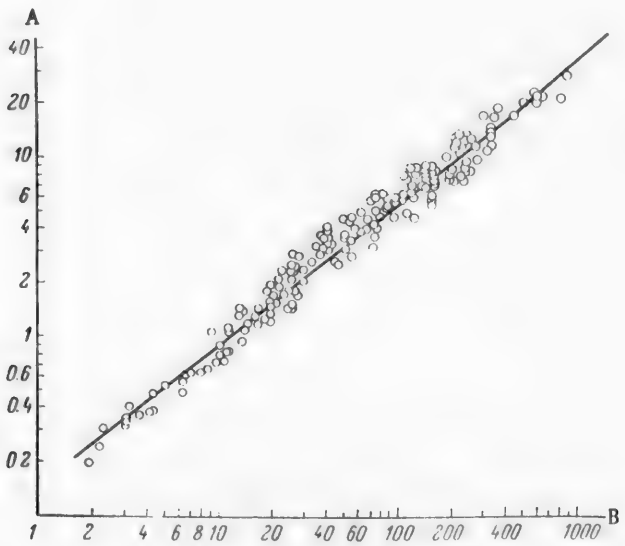

Fig. 6. Plot of $\frac{Nu_{liq.}}{(1+f)\,Pr_{liq.}^{2/3}} \cdot \frac{d_{e.s}}{d_e}$ versus $Re_{liq.}$ for sparingly soluble gases for the various hydrodynamic regimes. A) Value of $\frac{Nu_{liq.}}{(1+f)\,Pr_{liq.}^{2/3}} \cdot \frac{d_{e.s}}{d_e}$; B) value of $Re_{liq.}$. The various points correspond to the data of different authors [17, 22-31] (see Table 2).

From these ratios, $w_{o\ inv.}$ being calculated from eq. (4), it is always possible to determine w_o and consequently also the regime in which a given column is operating. Consequently ratios (7)-(9) are characteristics for the determination of operating regimes of packed columns in presence of two-phase streams.

We make use of an equation of the following general form for determination of resistance in a two-phase stream in packed columns below the inversion point [4]:

$$\frac{\left(\frac{\Delta P}{l}\right)_{gas\text{-}liq.}}{\left(\frac{\Delta P}{l}\right)_{gas}} = \left[1 + \left(\frac{L}{G}\right)^{1.8} \cdot \left(\frac{\gamma_{gas}}{\gamma_{liq.}}\right) \cdot \left(\frac{\mu_{liq.}}{\mu_{gas}}\right)^{0.2} \cdot \varphi^3\right]. \tag{10}$$

The factor φ^3 allows for the proportion of cross-section occupied by gas and liquid in a two-phase stream; it depends in turn on the set of terms $(\frac{L}{G})^{1.8} \cdot (\frac{\gamma_{gas}}{\gamma_{liq.}}) \cdot (\frac{\mu_{liq.}}{\mu_{gas}})$. In Fig. 3 in a logarithmic plot φ^3 is represented as a function of $\Phi = (\frac{L}{G})^{1.8} \cdot (\frac{\gamma_{gas}}{\gamma_{liq.}}) \cdot (\frac{\mu_{liq.}}{\mu_{gas}})^{0.2}$ for various packings and systems. The diagram is based on data of a number of investigators [3, 10-13] for all of the hydrodynamic regimes and transition points. •

The experimental data (Fig. 3) are seen to be grouped on a set of parallel lines which are expressed by the equation

$$\varphi^3 = C\left[\left(\frac{L}{G}\right)^{1.8} \cdot \left(\frac{\gamma_{gas}}{\gamma_{liq}}\right) \cdot \left(\frac{\mu_{liq}}{\mu_{gas}}\right)^{0.2}\right]^{-0.775} \tag{11}$$

with $0.13 < L/G < 15$.

By the foregoing treatment we obtained the following equation for calculation of the resistance when $0.13 < L/G < 15$:

$$\left(\frac{\Delta P}{l}\right)_{g-liq} = \left(\frac{\Delta P}{l}\right)_{gas}\left[1 + C \cdot \left(\frac{L}{G}\right)^{0.405} \cdot \left(\frac{\gamma_{gas}}{\gamma_{liq}}\right)^{0.225} \cdot \left(\frac{\mu_{liq}}{\mu_{gas}}\right)^{0.045}\right] \quad \left(\frac{\text{mm } H_2O \text{ colm.}}{\text{m}}\right) \tag{12}$$

where C = 8.4 – inversion point (2); C = 8.4-5.1 – turbulent regime; C = 5.1 – hold-up point; C = 5.1-1.81 – intermediate regime; C = 1.81 – loading point; C < 1.81 – film regime.

Fig. 4 can be used for determination of the value of coefficient C within the range of each regime.

Accordingly we obtain the values of the dynamic surface state factor:

$$f = \frac{\left(\frac{\Delta P}{l}\right)_{gas\text{-}liq.} - \left(\frac{\Delta P}{l}\right)_{gas}}{\left(\frac{\Delta P}{l}\right)_{gas}} = C\left(\frac{L}{G}\right)^{0.405} \cdot \left(\frac{\gamma_{gas}}{\gamma_{liq}}\right)^{0.225} \cdot \left(\frac{\mu_{liq}}{\mu_{gas}}\right)^{0.045}. \tag{13}$$

We have obtained numerous experimental values [14 - 21] for the different operating regimes of packed columns in connection with absorption of easily soluble gases. Results of this treatment are presented in a logarithmic plot (Fig. 5). For each experiment the factor f was calculated in accordance with the existing hydrodynamic regime.

A similar treatment of the data of various investigators [22 - 31] for sparingly soluble gases is plotted in Fig. 6.

• Due to the numerous experimental points these are not included in the diagram.

It follows from Figs. 5 and 6 that the experimental data for the different systems, packing and hydrodynamic regimes, fall on straight lines with a tangent of the angle of slope of 0.6 and 0.8.

On the basis of the relations derived and of the treatment of the experimental data, we obtain equations for calculation of the mass-transfer coefficients for various systems in packed columns for all of the hydrodynamic regimes and transition points:

For readily soluble gases

$$Nu_{gas} = 0.0315 \cdot \frac{d_e}{d_{e.s.}} \cdot Re_{gas}^{0.8} \cdot Pr_{gas}^{1/3} \cdot (1 + f), \tag{14}$$

Substituting the values

$$Nu_g = \frac{K_{o.g} \cdot d_e}{\sigma \cdot D_g}, \quad Re_g = \frac{w_g d_e \gamma_g}{F_s \mu_g g}, \quad Pr_g = \frac{3600 \mu_g g}{\gamma_g D_g}, \tag{15}$$

where $d_{e.s}$ is the equivalent diameter of a standard packing element measuring 25 x 25 x 3 mm, and selecting f for the given regime according to eq. (13), we obtain

$$\frac{K_{o.g} \cdot d_e}{\sigma \cdot D_g} = 0.0315 \frac{d_e}{d_{e.s}} \left(\frac{w_g d_e \gamma_g}{F_s \mu_g g} \right)^{0.8} \cdot \left(\frac{3600 \mu_g g}{\gamma_g D_g} \right)^{1/3} \times \times \left[1 + C \left(\frac{L}{G} \right)^{0.405} \cdot \left(\frac{\gamma_g}{\gamma_l} \right)^{0.225} \cdot \left(\frac{\mu_l}{\mu_g} \right)^{0.045} \right]; \tag{16}$$

for sparingly soluble gases

$$Nu_l = 0.23 \frac{d_e}{d_{e.s}} \cdot Re_l^{0.6} \cdot Pr_l^{1/3} \cdot (1 + f), \tag{17}$$

substituting the values

$$Nu_l = \frac{K_{o.l} \cdot d_e}{\sigma D_l}, \quad Re_l = \frac{w_l d_e \gamma_l}{F_s \mu_l g}, \quad Pr_l = \frac{3600 \mu_l g}{\gamma_l D_l}$$

and the corresponding value of f, we obtain •

$$\frac{K_{o.l} \cdot d_e}{\sigma D_l} = 0.23 \frac{d_e}{d_{e.s}} \left(\frac{w_l d_e \gamma_l}{F_s \mu_l g} \right)^{0.6} \cdot \left(\frac{3600 \mu_l g}{\gamma_l D_l} \right)^{1/3} \times \times \left[1 + C \left(\frac{L}{G} \right)^{0.405} \cdot \left(\frac{\gamma_g}{\gamma_l} \right)^{0.225} \cdot \left(\frac{\mu_l}{\mu_g} \right)^{0.045} \right]. \tag{18}$$

• In a previously published paper (Khimich. Mashinostroenie, 1959, No. 2) an approximate equation is obtained without allowance for the individual hydrodynamic regimes.

LITERATURE CITED

[1] V. V. Kafarov, J. App. Chem. 31, 5, 706 (1958).*

[2] V. V. Kafarov, Sci. Proc. Higher Schools, Chem. Series 1, 3 (1958).

[3] V. V. Kafarov, Doctoral Dissertation, Moscow D. I. Mendeleev Institute of Chemical Technology (1952).

[4] V. V. Kafarov, J. Chem. Ind. 6, 174 (1948).

[5] V. V. Kafarov and L. I. Blyakham, J. App. Chem. 23, 3, 244 (1950); 24, 12, 1274 (1951).*

[6] V. V. Kafarov, J. Chem. Ind. 5 (1953).

[7] V. V. Kafarov, Chem. Sci. and Ind. 1 (1957).

[8] V. V. Kafarov and Yu. I. Dytnerskii, J. App. Chem. 30, 11, 1698 (1957).*

[9] V. V. Kafarov and Yu. I. Dytnerskii, J. App. Chem. 31, 4, 631 (1958).*

[10] E. Mach, Forsch. Geb. Ing. Wesen, 6 Forschungsheft, 375 (1935).

[11] N. M. Zhavoronkov, J. Chem. Ind. 2-3, 12 (1944).

[12] B. R. Sarchet, Trans. Am. Inst. Chem. Eng. 38, 283 (1942).

[13] E. M. Schoenborn and W. I. Dougherty, Trans. Am. Inst. Chem. Eng. 40, 51 (1944).

[14] M. G. Molstad, I. F. Kinney, and R. G. Abbey, Trans. Am. Inst. Chem. Eng. 39, 605 (1943).

[15] T. B. Doherty and F. G. Johnson, M. S. Thesis in Eng., MIT (1938).

[16] O. E. Dwyer and B. F. Dodge, Ind. Eng. Chem. 33, 485 (1941).

[17] N. A. Prished'ko, Candidate's Dissertation, Moscow D. I. Mendeleev Inst. Chem. Tech. (1949).

[18] R. W. Houston and C. A. Walker, Ind. Eng. Chem. 42, 1106 (1950).

[19] V. I. Trofimov, Candidate's Dissertation, Moscow Inst. Chem. Tech. (1959).

[20] L. E. Hutchings, L. F. Stutzman and H. A. Koch, Chem. Eng. Progr. 45, 253 (1949).

[21] M. G. Molstad and L. F. Parsley, Chem. Eng. Progr. 46, 20 (1950).

[22] H. A. Koch, L. F. Stutzman, H. A. Blum, and L. E. Hutchings, Chem. Eng. Progr. 45, 677 (1949).

[23] H. V. Allen, M. S. Thesis in Chem. Eng., MIT (1938).

[24] I. P. Tsiparis, Candidate's Dissertation, Moscow D. I. Mendeleev Inst. Chem. Tech. (1952).

[25] Chikita, Suchata, and Kamo, Chem. Eng. (Tokyo) 18, 10, 454, 460 (1954).

[26] Chikita, Kamo, and Suchata, Chem. Eng. (Tokyo) 18, 10, 457, 460 (1954).

[27] M. G. Molstad, I. F. Kinney, and R. G. Abbey, Trans. Am. Inst. Chem. Eng. 38, 410 (1942).

[28] T. K. Sherwood and F. H. Holloway, Trans. Am. Inst. Chem. Eng. 36, 1, 39 (1940).

[29] R. P. Whitney and J. G. Vivian, Chem. Eng. Progr. 45, 5, 323 (1949).

[30] D. A. Pearson, L. A. Lundberg, F. B. West, and J. L. McCarthy, Chem. Eng. Progr. 47, 5, 257 (1951).

[31] J. E. Vivian and R. P. Whitney, Chem. Eng. Progr. 43, 691 (1947).

Received June 27, 1958

* Original Russian pagination. See C. B. Translation.

INVESTIGATION OF THE PROCESS OF FRACTIONAL DISTILLATION IN A FILLED COLUMN UNDER REDUCED PRESSURE

H. I. Gel'perin and N. N. Zelenetskii

In spite of its wide practical use, the process of vacuum distillation has not yet been investigated sufficiently. The scanty data in the literature on the influence of the working pressure and the velocity of the vapor on the efficiency of filled columns, which are commonly used for vacuum distillation, are very contradictory.

According to various data, the efficiency of filled fractionating columns decreases [1-5], remains constant [3, 6-9], increases [7, 8, 10], or passes through a maximum [11, 12] when the working pressure is lowered, and decreases [7, 8, 12, 13], remains constant [1, 3, 12], or increases [12], when the vapor velocity decreases or has two maxima at extreme values of the vapor velocity [2, 5, 8]. It should be noted in this connection that many of the investigations mentioned suffer from serious methodological deficiencies, as for example the determination of the efficiency of the column at different pressures on different control mixtures [4, 10-13] or at noncomparable vapor velocities [4, 9, 11], and the carrying out of the experiments at very low vapor velocities [1].

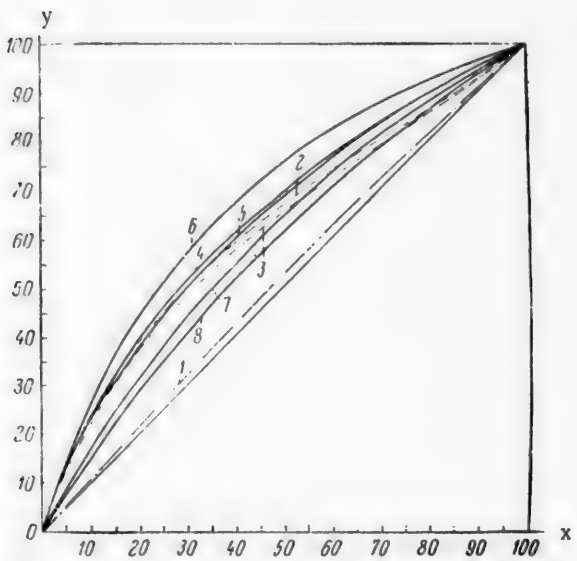

Fig. 1. Equilibrium curves for the mixtures investigated. y) concentration of lower-boiling component in the vapor (in mole %), x) concentration of higher-boiling component in the liquid (in mole %). Mixture: 1) ethylbenzene–chlorobenzene, P = 20 mm Hg; 2) n-octane–toluene, P = 20 mm Hg; 3) n-octane–toluene, P = 745 mm Hg; 4) diphenyl oxide – ethyl salicylate, P = 5 mm Hg; 5) diphenyl oxide – ethyl salicylate, P = 180 mm Hg; 6) menthol-menthone, P = 5 mm Hg; 7) menthol–menthone, P = 50 mm Hg; 8) menthol–menthone, P = 180 mm Hg.

This situation impelled the authors to undertake a comparative investigation of the process of fractional distillation in a filled column at atmospheric and various lowered pressures and with various vapor velocities.

The experiments were carried out on the following four mixtures: ethylbenzene–chlorobenzene, n-octane–toluene, diphenyl oxide–ethyl salicylate, and menthol-menthone (the second component is the lower-boiling). Among the components of these mixtures are normal and aromatic hydrocarbons, a chlorinated derivative of an aromatic hydrocarbon, an ether and an ester, an alcohol and a ketone. The first two mixtures can be used with ordinary water cooling in the pressure range from atmospheric to 20 mm of Hg, and the other two mixtures at even lower pressures.

The ethylbenzene–chlorobenzene mixture, according to data from the investigation by Hawkins and Brent [7], is close to ideal and its partition coefficient (α) increases as the pressure is lowered, from 1.10 at 760 mm Hg to 1.12 at 20 mm Hg.

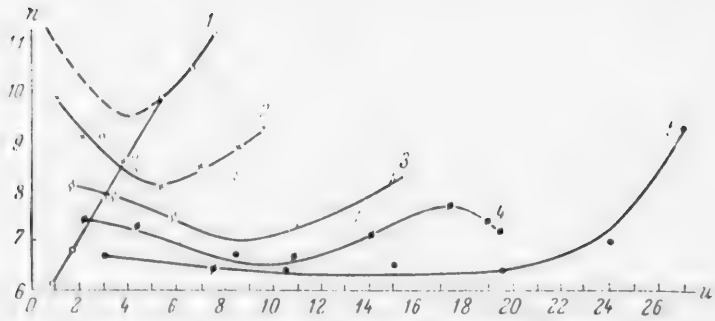

Fig. 2. Relation of efficiency of filled column (h_{fill} = 500 mm) to vapor velocity. Ethylbenzene–chlorobenzene mixture. n) number of theoretical plates; w) residue – vapor mass velocity (in ml/min). Pressure (in mm Hg): 1) 20; 2) 60; 3) 150; 4) 350; 5) 755.

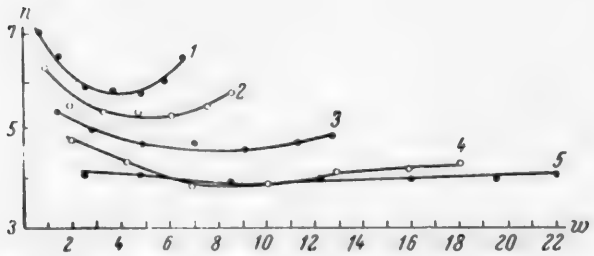

Fig. 3. Relation of efficiency of filled column (h_{fill} = 500 mm) to vapor velocity. n-Octane–toluene mixture. n) number of theoretical plates, w) residue – vapor mass velocity (in ml/min). Pressure (in mm Hg): 1) 20; 2) 60; 3) 150; 4) 350; 5) 745.

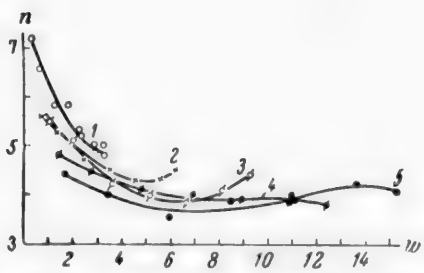

Fig. 4. Relation of efficiency of filled column (h_{filled} = 250 mm) to vapor velocity. Diphenyl oxide–ethyl salicylate mixture. n) Number of theoretical plates; w) residue – vapor mass velocity (in ml/min). Pressure (in mm Hg): 1) 5; 2) 20; 3) 50; 4) 100; 5) 180.

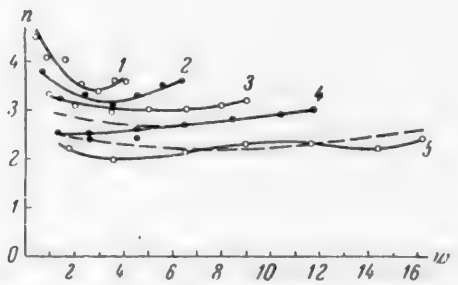

Fig. 5. Relation of efficiency of filled column (h_{fill} = 250 mm) to vapor velocity. Menthol–menthone mixture. n) Number of theoretical plates; w) residue – vapor mass velocity (in ml/min). Pressure (in mm Hg): 1) 5; 2) 20; 3) 50; 4) 100; 5) 180.

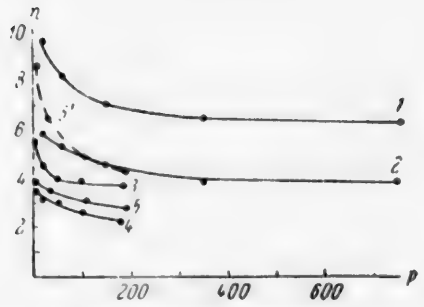

Fig. 6. Relation of efficiency of filled column to working pressure. Vapor velocity above column amounts at each pressure to 50% of the velocity at which choking of the column starts. n) Number of theoretical plates; p) working pressure (in mm Hg). Mixture and h_{fill} (in mm), respectively: 1) ethylbenzene–chlorobenzene (500); 2) n-octane–toluene (500); 3) diphenyl oxide–ethyl salicylate (250); 4) menthol–menthone (250); 5) diphenyl oxide–ethyl salicylate (another column).

Equilibrium data for the n-octane–toluene mixture at pressures of 760, 640, 400, 300, 200, 100, 50, and 20 mm Hg were obtained by Berg and Popovac [6]. They show that α at each pressure decreases with an increase in the toluene content of the mixture, and for a constant composition of the mixture increases with a decrease in pressure. Only the data obtained at 20 mm Hg deviate from the latter rule. An infraction of the regularity of the change in α with pressure, however, is not very likely. Furthermore, the authors themselves have expressed doubt of the accuracy of the experiments carried out at 20 mm Hg (indicating the unreliability of the measurement of the temperature of the phase transition in these experiments). Therefore, equilibrium data for the pressure 20 mm Hg were obtained by us by extrapolation of the data given for all the other pressures. At x = 50 mole %, α changes in the pressure range 760 mm to 20 mm Hg from 1.90 to 2.03.

For the diphenyl oxide–ethyl salicylate and menthol–menthone mixtures presented by us there are no liquid–vapor equilibrium data in the literature. A merit of the second mixture is, among others, that its components occur in several ethereal oils (and are, in particular, the main components of peppermint oil), and there the data obtained in the investigation of it are of practical value for accomplishing the rectification of these oils.

The equilibrium liquid-vapor compositions for the two mixtures mentioned were determined by us experimentally in a modified circulation apparatus of the Otmer type at pressures of 180, 50, and 5 mm Hg. It appeared that for the diphenyl oxide–ethyl salicylate mixture α decreased a trifle with an increase in the ethyl salicylate content and also increased a trifle with a decrease in the pressure (at x = 50 mole %, from 2.24 at 180 mm Hg to 2.28 at 5 mm Hg). For this mixture we noted a substantial difference in the magnitude of α at various pressures determined experimentally from that calculated from the vapor tensions given by Stell [14].

The menthol–menthone mixture appeared close to ideal and its α increased greatly with a lowering of the pressure (from 1.60 at 180 mm Hg to 3.12 at 5 mm Hg). The equilibrium curves for all the mixtures are shown in Figure 1.

The materials entering into the composition of the mixtures were purified by fractional distillation on a cap column with an efficiency of 23 theoretical plates (determined on a dichloroethane–benzene mixture), and with a separation of ethyl benzene, chlorobenzene, and toluene within limits of 0.1° (at atmospheric pressure), n-octane 0.3° (at atmospheric pressure), diphenyl oxide, ethyl salicylate, and menthone 0.5° (at 5 mm Hg).

The materials obtained had the constants given below.

	Ethyl-benzene	Chloro-benzene	n-Octane	Toluene	Diphenyl oxide (m.p.27°)	Ethyl salicylate	Methanol $[\alpha]_D^{20}=-26°$
n_D^{20}	1.4955	1.5247	1.3975	1.4963	1.5765*	1.5225	1.4492
d_4^{20}	0.8706	1.1079	0.7016	0.8674	1.0774**	1.1330	0.8924

The experiments were carried out in a glass column with an inner diameter of 30 mm, filled with glass Raschig rings 4.5 × 4.5 × 1.05 mm [15, 16]. In working with the ethylbenzene–chlorobenzene and n-octane – toluene mixtures, the height of the filling layer was 500 mm, and in the work with the diphenyl oxide–ethyl salicylate and menthol–menthone mixtures it was 250 mm.

* At 28°.

** Supercooled to 20°. The menthol used was pure, separated from Chinese peppermint oil, with m.p. 44° and $[\alpha]_D^{20} = -49°$.

All the experiments were carried out with a full trickle, for the first and second mixtures at pressures above the column of 755 (745 for the second), 350, 150, 60, and 20 mm Hg, and for the third and fourth mixtures at pressures of 180, 100, 50, 20, and 5 mm Hg. The vapor velocities at each pressure were 10, 20, 35, 50, 65, 80, and 90% of the velocity at which choking started.

The composition of the ethylbenzene–chlorobenzene, n-octane–toluene, and diphenyl oxide–ethyl salicylate mixtures was determined by measurement of their refractive index; the accuracy of such a determination was ±0.7 mole % for the first mixture and ±0.2 mole % for the second and third mixtures. The menthone content of the menthol–menthone mixture was determined by preparation of the oxime with hydroxylamine hydrochloride, with an accuracy of ±1%.

Calculation of the number of theoretical plates (n) in the column, including vaporization in the flask, was carried out for the ethylbenzene–chlorobenzene and menthol–menthone mixtures by the analytical method from the geometrical mean value of α, and for the diphenyl oxide–ethyl salicylate and n-octane–toluene mixtures by the method of McCabe and Tile.

The results of the experiments that were carried out are presented graphically in figures 2-5. • The curves for the relation of column efficiency to vapor velocity for all the mixtures and working pressures are similar in appearance – two maxima at low vapor velocity and at a vapor velocity close to choking. Some deviations from this rule appear in only four curves out of the twenty – at 20 mm Hg for the ethylbenzene–chlorobenzene mixture, at 5 mm Hg for the diphenyl oxide–ethyl salicylate mixture, and at 100 and 180 mm Hg for the menthol–menthone mixture. It must be assumed that these deviations are of a chance character and the probable course of the curves is shown by dots.

The form of the efficiency curve indicated was previously established [17-20] for distillation at atmospheric pressure. It was determined by measurement of the hydrodynamic work cycle of the filled column with a change in pressure. The results of the investigations carried out by us, which are in agreement with the data of several other authors [2, 5, 8], indicate that such a change in efficiency of the filled column with the velocity of the vapor has the nature of a general rule for any mixtures at all working pressures. Establishment of this fact is of great significance for the design of the vacuum distillation process and the apparatus for accomplishing it.

The relation of the column efficiency to the working pressure for the mixtures investigated at a vapor velocity equal to 50% of the velocity at which choking starts is shown in Figure 6. Curve 5 was constructed on the basis of the results of experiments on the diphenyl oxide–ethyl salicylate mixture carried out by us previously on another column [21], using for the calculation of the efficiency the equilibrium data determined by us for this mixture (shown in dots is curve 5', obtained for these same experiments by calculating the efficiency of the column from the value of α derived from the vapor tensions given by Stell).

As can be seen, with a lowering of the pressure the efficiency of the column in all cases rises in increasing degree. Inasmuch as the investigation was carried out on four mixtures with different partition coefficients and components that differed considerably in their chemical nature and physicochemical properties, it may be concluded that this rule should apparently hold true for all, or a majority, of liquid mixtures.

LITERATURE CITED

[1] H. Bliss, A. M. Eshaya, and N. W. Frisch. Ch. Eng. Progr. 48, 12, 627 (1952).

[2] E. Kirschbaum and A. David. Ch. Ing. Techn. 25, 10, 592 (1953).

[3] T. J. Walsh, G. H. Sugimura and T. W. Reinolds, Ind. Eng. Ch. 45, 12, 2629 (1953).

[4] N. M. Zhavoronkov, V. A. Malyusov, and N. N. Umnik. Coll. Methods and Processes of Chem. Technology, Acad. Sci. USSR Press, 45 (1955).

[5] E. Kirschbaum, W. Busch, and R. Billet, Ch. Ing. Techn. 28, 7, 475 (1956).

[6] L. Berg and D. O. Popovac, Ch. Eng. Progr. 45, 11, 683 (1949).

• Tables of results of experiments on the ethylbenzene–chlorobenzene mixture are given in [16].

[7] J. E. Hawkins and J. A. Brent, Ind. Eng. Ch. 43, 11, 2611 (1951).

[8] M. S. Peters and M. R. Cannon, Ind. Eng. Ch. 44, 6, 1452 (1952).

[9] I. N. Bushmakin and N. V. Lutugiva, J. Appl. Chem. 29, 8, 1164 (1956).*

[10] C. Capitani and E. Milani, La Chimica' l' Industria 36, 9, 671 (1954).

[11] R. T. Struck and C. R. Kinney, Ind. Eng. Ch. 42, 1, 77 (1950).

[12] M. Myles, J. Feldman, I. Wender, and M. Orchin, Ind. Eng. Ch. 43, 6, 1452 (1951).

[13] J. Feldman, M. Myles, I. Wender, and M. Orchin, Ind. Eng. Ch. 41, 5, 1032 (1949).

[14] D. R. Stell. Tables of Vapor Pressure of Individual Substances [in Russian] (IL, 1949).

[15] N. I. Gel'perin and N. N. Zelenetskii, Chem. Science and Indus. 2, 1, 91 (1957).

[16] N. N. Zelenetskii and N. I. Gel'perin, Proc. VNIISNDV. 4. Pishchepromizdat, 138 (1958).

[17] E. Kirschbaum, Destillier and Rektifiziertechnik (1940).

[18] V. V. Kafarov and B. G. Luk'yanov, J. Chem. Indus. 4, 107 (1950).

[19] V. V. Kafarov and L. I. Blyakhman, J. Appl. Chem. 23, 3, 244 (1950).*

[20] V. V. Kafarov, L. I. Blyakhman, Coll. Processes and Apparatus of Chemical Technology. GKhI, 25 (1953).

[21] N. I. Gel'perin, N. G. Krokhin, and N. N. Zelenetskii, Proc. VNIISNDV, 2. Pishchepromizdat, 127 (1954).

Received November 18, 1958

* Original Russian pagination. See C. B. Translation.

HYDRAULIC RESISTANCE OF THE GAS – LIQUID LAYER IN SIEVE APPARATUSES

I. P. Mukhlenov and É. Ya. Tarat

Lensovet Leningrad Technological Institute

The hydraulic resistance of the shelf of a sieve apparatus (ΔP) can reasonably be determined as the sum of the resistances of the dry grid (ΔP_1) and the gas–liquid layer on it (ΔP_2):

$$\Delta P = \Delta P_1 + \Delta P_2. \tag{1}$$

The resistance of the dry grid, which has been considered in our previous publications [1, 2], is calculated with sufficient accuracy by the formula

$$\Delta P_1 = 1.45k \frac{\gamma_G w_0^2}{2g} \quad \text{mm water (kg/m}^2\text{)}, \tag{2}$$

where k is the coefficient of the change in resistance of the grid in relation to its thickness [1], γ is the specific gravity of the gas (in kg/m^3), w_0 is the velocity of the gas in the openings of the grid (in m/sec), and g is the acceleration of the force of gravity (in m/sec^2).

The hydraulic resistance of the gas–liquid layer makes up the larger part of the resistance of the shelf and mainly determines the expenditure of energy in passing the gas through the apparatus.

A theoretical analysis has shown [3] that the hydraulic resistance of the gas–layer may depend in greater or less degree on many independent variables. In accordance with this, we have investigated the following functional relationship:

$$\Delta P_2 = f(w_G, h_0, \gamma_L, \mu_L, \sigma, \gamma_G, \mu_G, m, d_0), \tag{3}$$

where w_G is the linear velocity of the gas in the apparatus (in m/sec); h_0 is the height of the initial layer of liquid from which the gas–liquid layer on the grid is formed (in m); γ_L and γ_G are the specific gravities of the liquid and gas (in kg/m^3); μ_L and μ_G are the dynamic coefficients of viscosity of the liquid and gas (kg·sec/m^2 or kg·hr/m^2); σ is the surface tension of the liquid at the interface with the gas (in kg/m); d_0 is the diameter of the openings in the grid (in m); m is the distance between centers of the openings (in m).

The relationship of the hydraulic resistance of the gas–liquid layer to some of the factors entering into equation (3) has already been studied previously under the conditions of a bubbler system. Some authors assume [4-9] that the resistance of the layer is equal to its hydrostatic pressure:

$$\Delta P_2 = \gamma_L \cdot h_0. \tag{4}$$

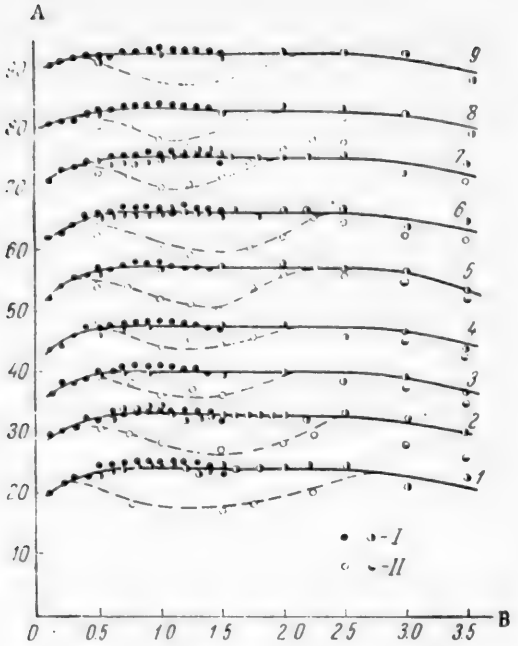

Fig. 1. Relation of hydraulic resistance of gas – liquid layer to gas velocity in a full cross section of the apparatus. Air–water system; model foam apparatus with grid 86 · 86 mm. A) Resistance of gas–liquid layer ΔP_2 (in mm water); B) gas velocity in apparatus w_G (in m/sec); Height of initial liquid layer h_0 (in mm): 1) 10; 2) 20; 3) 30; 4) 40; 5) 50; 6) 60; 7) 70; 8) 80; 9) 90; free cross section of grid S (in %): I ~ 10, II < 7.

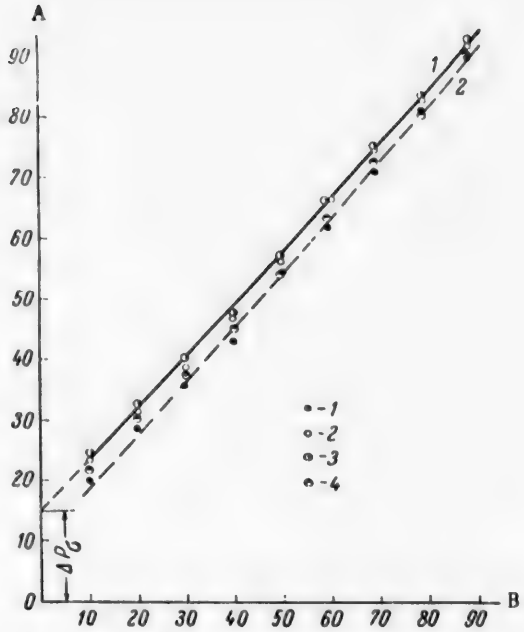

Fig. 2. Relation of hydraulic resistance of gas–liquid layer to height of initial liquid layer. Air–water system. A) Resistance of gas–liquid layer ΔP_2 (in mm water); B) height of initial liquid layer h_0 (in mm): 1) 0.1; 2) 0.5; 3) 1; 4) 3.5.

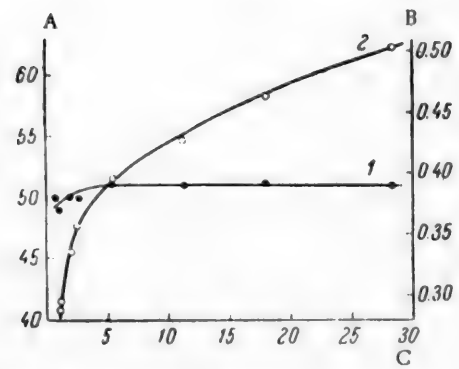

Fig. 3. Relation of hydraulic resistance of foam to viscosity of liquid. Air–glycerol solution system. A) Resistance of foam ΔP_2 (in mm water); B) specific resistance of foam $\Delta P_{spec.}$ (in mm water/mm); C) viscosity of liquid (in centipoises); mean data for various values of w_G (h_0 = 40 mm): 1) ΔP_2; 2) $\Delta P_{spec.}$

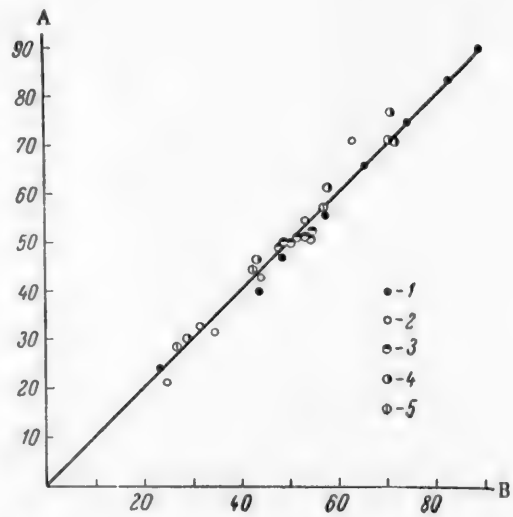

Fig. 4. Comparison of experimental and calculated data on the resistance of foam ΔP_2 in noncirculating apparatuses. A) Experimental value ΔP_2 (in mm water); B) calculated value ΔP_2 (in mm water). Air–liquid system: 1) water; 2) 20% NaCl solution; 3) glycerol solution; 4) 75% H_2SO_4 solution; 5) 90% H_2SO_4 solution.

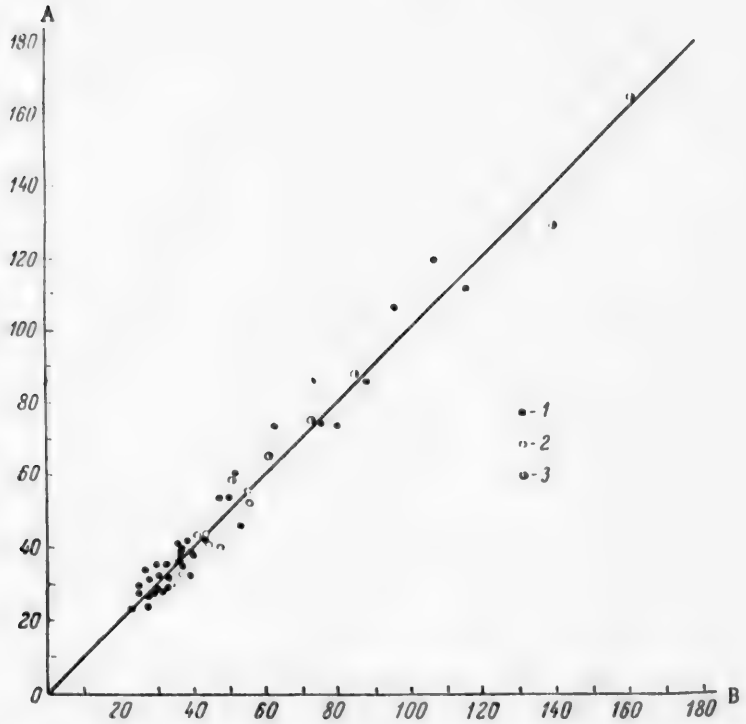

Fig. 5. Comparison of experimental and calculated data for the resistance of foam ΔP_z in circulating apparatuses. A) Experimental value ΔP_z (in mm water); B) calculated value ΔP_z (in mm water). Air–liquid system: 1) water; 2) 75% H_2SO_4 solution; 3) filter liquid from soda manufacture (NH_4Cl 160 g/l, NaCl 70 g/l, NH_4HCO_3 45 g/l, $(NH_4)_2CO_3$ 30 g/l).

In this connection many investigators inaccurately calculate the height of the initial liquid layer. Thus, Arnold, Plank, and Schoenborn [7] do not take into account the layer of liquid (h_s) that is formed above the overflow baffle as a result of the flow of liquid.• Stabnikov [4] and Zhavoronkov and Furmer [5] do not cite sufficient information required for the calculation of h_0. A more complete investigation is that by Usyukin and Aksel'rod [11], in which they develop and calculate the effect of the surface tension exerted in addition to the hydrostatic pressure of the liquid column. However, Usyukin and Aksel'rod in calculating h_0 consider the gas content of the layer as a constant; they assume the specific gravity of the gas–liquid layer to be $\gamma_p = 0.5\ \gamma_L$, which corresponds only to a particular case. Actually the ratio γ_p/γ_L may change approximately from 1 to 0.1.

The above mentioned research permitted a close calculation of the drop in pressure in the gas–liquid layer in a bubbler system with an accuracy in most cases sufficient for the design of industrial bubbler apparatuses. However, it was impossible without carrying out special experiments to determine the degree of adaptability of these data to conditions of active foam, under which sieve apparatuses work most efficiently. Therefore our experiments were carried out mainly in a foam system, i.e., at gas velocities in a cross section of the apparatus of 1.0-4.0 m/sec, under conditions where there was formed on the grid a suspended layer of liquid in the guise of a rapidly moving film and a stream of liquid, which were intimately mixed with bubbles and whirling streams of gas.

• In our publications [2, 10] it has been shown that $h_s = 3\sqrt[3]{i^2}$, where i is the intensity of the liquid flow measured in cubic meters of liquid flowing in 1 hour through an overflow baffle 1 m in length (in $m^3/m \cdot hr$).

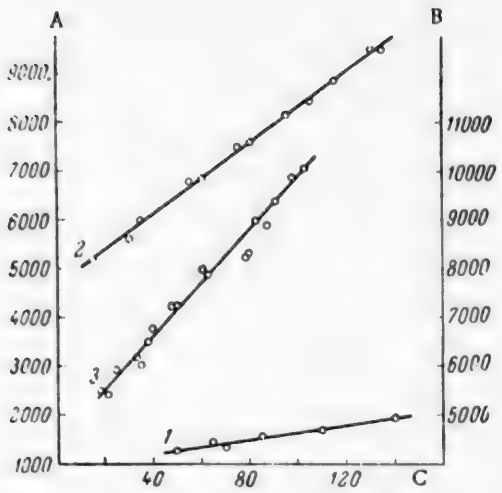

Fig. 6. Relation of coefficients of mass- and heat-transfer to hydraulic resistance of foam. A) Coefficient of mass-transfer K_M (in $kg/m^2 \cdot hr \cdot kg/m^3$); B) coefficient of heat-transfer K_H (in $Cal/m^2 \cdot hr \cdot deg$); C) resistance of foam ΔP_2 (in mm water). 1) K_M of system: CO_2 (6%)–NaOH solution (120 g/l), T = 60°, w_G = 2.0 m/sec, grid 6/3; 2) K_M of system: C_{12} (1%)–CaO suspension (100 g/l), T = 80°, w_G = 1.5 m/sec, grid 12/5; K_H for system: air–water, w_G = 1.5 m/sec, grid 6/3.

The effect of various factors on the hydraulic resistance of the gas–liquid layer has been studied by us in model foam apparatuses previously described [2]. Leakage of liquid through the openings of the grid was eliminated in the main experiments. The hydraulic resistance of the plate of the one-shelf apparatus was measured with the aid of U-shaped manometers placed in the gas stream before and after the apparatus. At the beginning the hydraulic resistance of the apparatus was measured with a dry grid, and then at the same gas velocities the resistance of the apparatus with the gas–liquid layer was measured. ΔP_2 was calculated from the difference in the first and second measurements.

The effect of structural parameters was usually investigated along with the processes.

Some investigators [4, 5] connect the hydraulic resistance of the plate with the diameter of the apparatus. In our first experiments, previously described [2], we established the independence of ΔP_2 from the diameter of the apparatus (D) when $D \geq 0.036$ m. The dimensions of the openings in the grid (d_0) and the distance between the centers of the openings (m) do not affect ΔP_2 when $d_0 \geq 3$ mm and $m/d_0 \leq 3$, i.e., when the free cross section of the grid $S > 10\%$. • [3] When the diameter of the openings is decreased from 3 to 2 and 1.5 mm, the height of the gas–liquid layer is increased a little and the hydraulic resistance rises a trifle (usually by 2-5 mm water). In practical calculations such an increase in ΔP_2 can be neglected. Zhavoronkov and Furmer [5], Mayfield and Church [8], and other investigators arrived at the same conclusion under conditions of a bubbler system. On grids with a free cross section $S < 10\%$ sometimes a small decrease in resistance is observed, with a special minimum at a gas velocity w_G = 1.3-1.5 m/sec. This decrease has previously been considered in detail [2, 10] and is illustrated in Fig. 1. However, it is comparatively small and is not characteristic of grids with $S > 10\%$, which are usually used in foam apparatuses.

The effect of the gas velocity in the apparatus (w_G) on ΔP_2 has been shown in numerous experiments. In Fig. 1 is shown the effect of w_G in experiments carried out in a noncirculating model (without overflow devices). The larger part of the experiment was carried out on a grid with $m/d_0 = 6/2$, on which the special minimum ΔP_2 at w_G = 1.3-1.5 m/sec was not observed. In other experiments various grids were used with free cross sections less than 7%. To carry out the experiments, a specific amount of water was poured onto the grid to produce a given height h_0. In the course of the experiment all of the determining parameters entering into the functional relationship (3) were maintained constant, and only w_G was changed. In different series of experiments h_0 was varied. From Fig. 1 it can be seen that the hydraulic resistance of the suspended layer of liquid (active foam) at ordinary gas velocities (w_G = 0.5-3.0 m/sec) may be considered independent of the gas velocity. All deviations of the hydraulic resistance from the mean value when the gas velocity was varied were so insignificant that in practical calculations ΔP_2 can be assumed to be independent of w_G. The hydraulic resistance of the bubbling layer at a given h_0 is only slightly less than that of the foam; under the conditions usual for a bubbler, w_G = 0.2-0.5 m/sec. ΔP_2 at 1-2 mm is less than for foam. However, the height of the gas–liquid layer (and consequently the rate of heat- and mass-transfer) under foam conditions is greater than for bubbling and increases (1.5-3 times) with an increase in w_G from 1.0 to 3.0 m/sec [2, 3, 12]. Therefore the hydraulic resistance of a gas-liquid layer of a

• The free cross section S of the grid is calculated as the ratio of the area of all the openings to the area of the cross section of the apparatus (in %).

given height is much smaller under foam conditions than with bubbling, and consequently the expenditure of energy in passing the gas through is less. In other words, at one and the same hydraulic resistance the rate of work for a sieve apparatus is much higher under foam conditions than for bubbling.

The effect of the height of the initial liquid layer h_0 has been established previously both in investigations by other authors [4, 8] and by our own experiments [2, 3, 10]. Using a typical graph for the relationship $\Delta P_2 = f(h_0)$ for the foaming of water (Fig. 2), we found the proportionality factors and obtained the equation

$$\Delta P_2 = 0.85h_0 + 15 \text{ mm water} \quad (5)$$

for foam conditions, and

$$\Delta P_2 = 0.88h_0 + 10 \text{ mm water} \quad (6)$$

for bubbling conditions.

The relation of the hydraulic resistance of the foam layer to the rate of flow of the liquid, the height of the overflow baffle, and the height of the head of foam necessary to overcome the overflow resistance (in the presence of a block of foam in the overflow opening) is fully determined by the effect of these parameters on h_0, as previously described [2, 3, 10, 12].

The effect of the physical properties of the liquid and gas on the hydraulic resistance of a foam layer was investigated [3] for the foaming of water, sulfuric acid solutions of various specific gravities, table salt solution, and glycerol. The experiments showed that the hydraulic resistance ΔP_2 is proportional to the specific gravity of the liquid (taking into account the effect of the surface tension), with the relationship being expressed by binomials of the same type as in formulas (5) and (6).

In Fig. 3 is shown the relation of $\Delta P_2 = f(\mu_L)$ for the given experiments on the foaming of air–glycerol solutions, which are very convenient for such experiments, since with an increase in the concentration of glycerol the viscosity increases greatly with only a trifling change in σ and γ_L. The experiments showed that the hydraulic resistance of the foam layer formed from a given initial layer of liquid (h_0 = const.) does not change with an increase in viscosity of the solution. The curvature of the line in Fig. 3 is fully explained by the effect of the small change in surface tension. At the same time the height of the foam layer H decreases so much when μ_L is increased that the expenditure of kinetic energy of the gas in overcoming the forces of internal friction of the liquid remains constant (independent of μ_L). Thus, the specific resistance of the foam layer

$$\Delta P_{spec.} = \frac{\Delta P_2}{H} \quad (7)$$

increases with an increase in viscosity of the liquid, as shown in Fig. 3. Consequently, an increase in the viscosity of the liquid increases the expenditure of energy in carrying out the processes of mass- and heat-transfer.

The independence of ΔP_2 from μ_L under other working conditions has been established by Noskov and Sokolov [13].

The effect of the specific gravity and viscosity of the gas on the hydraulic resistance of the foam layer should not be significant, on the basis of theoretical considerations, and first and foremost because of the fact that when there is a rapid forced movement of gas from below upward, the Archimedeanforce can not play a substantial role. This circumstance was verified [3] by passing nitrogen and hydrogen through a given layer of water in a noncirculating apparatus. The use of these gases was convenient, since the surface tensions at the water–nitrogen and water–hydrogen interfaces differ little. At the same time, the specific gravities (γ) and viscosities (μ) of nitrogen and hydrogen are very different. At a temperature of 20° γ_{N_2} = 1.16 kg/m^3, μ_{N_2} = = 175 micropoises; γ_{H_2} = 0.085 kg/m^3; μ_{H_2} = 88 micropoises.

As can be seen from the experimental data given below, the hydraulic resistance of the whole shelf of a sieve apparatus when nitrogen is passed through is only 1-3 mm water higher than when hydrogen is passed through. Such a difference can be neglected in technical calculations.

Gas velocity w_G (in m/sec)	0.2	0.3	0.5	0.8	1.0	1.3	1.5
ΔP for nitrogen at $h_0 = 42$ mm.	48	48	49	51	51	53	55
ΔP for hydrogen at $h_0 = 42$ mm. . . .	—	48	48	50	51	52	53
ΔP for nitrogen at $h_0 = 78$ mm.	85	85	84	86	88	90	92
ΔP for hydrogen at $h_0 = 78$ mm. . . .	82	82	82	83	85	87	90

The total increase in hydraulic resistance when the gas velocity is increased is caused by a rise in the resistance in the grid openings.

The effect of the surface tension σ on thehydraulic resistance of the gas–liquid layer has been noted by many investigators [4-6, 11, 13]. Usyukin and Aksel'rod [13] took into account the effect of σ in the formula proposed by them, but they incorrectly connected the surface tension with the size of the openings in the grid, which does not affect ΔP_2.

According to the generally known equation of Laplace, the pressure difference necessary to overcome the surface tension forces ΔP_σ under otherwise constant conditions is directly proportional to the surface tension:

$$\Delta P_\sigma = \alpha \sigma, \tag{8}$$

where α is the dimensional factor (1/M).

Having ascertained the effect on ΔP_2 of all the parameters entering into the functional relationship (3) with the exception of σ, we were in a position to assume that in a foam layer ΔP_σ is approximately expressed for the system water–air by the free member of equation (5), i.e., $\Delta P_\sigma = 15$. Then, when $\sigma = 74.2 \cdot 10^{-4}$ kg/m, $\alpha = \frac{\Delta P_\sigma}{\sigma} = \frac{1 \cdot 5}{74.2 \cdot 10^{-4}} \approx 0.2 \cdot 10^4\ m^{-1}$.

Verification of the factor $0.2 \cdot 10^4\ m^{-1}$ was carried out [3] by passing air through solutions of sulfuric acid, table salt, glycerol, amyl alcohol, and acetone, i.e., varying σ from 23.7 to 77 dynes/cm. The variation of the values of ΔP_σ calculated from equation (8) from the experimental values did not exceed 3 mm water, i.e., they were sufficiently accurate for technical calculations. Thus, the hydraulic resistance of the foam layer is proportional to the height of the initial liquid layer (h_0), the specific gravity of the liquid (γ_L) and its surface tension (σ):

$$\Delta P_2 = 0.85 h_0 \gamma_L + 0.2 \cdot 10^4 \cdot \sigma \text{ mm water (kg/m}^2) \tag{9}$$

For the system air–water and other systems with a surface tension close to $\sigma = 73$ dynes/cm ($74.2 \cdot 10^{-4}$ kg/m) and $\gamma_L = 1000$ kg/m^3, the calculation of equation (9) is simplified, i.e., it reduces to the form:

$$\Delta P_2 = 0.85 h_0 + 15 \text{ mm water}.^* \tag{5}$$

The applicability of the calculated equation (9) was verified by passing air through various liquids at constant temperatures in noncirculating apparatuses (without overflow devices) and apparatuses with a current of liquid along the grid (with an overflow device). Comparison of the experimental and calculated data (Fig. 4 and 5) shows the applicability of formula (9) for foam conditions. When applied to bubbling conditions, formula (9) gives results about 2-4 mm high in comparison with the experimental values.

In designing foam apparatuses, the hydraulic resistance is calculated after calculating the necessary height of the foam layer (H) and choosing the gas velocity in the apparatus (w_G). Therefore, the initial layer of liquid (h_0) can be calculated for any gas–liquid system according to the formula:

$$h_0^{0.6} = 2.3 \cdot 10^4 \frac{H \sigma^{1.3} \nu_{\text{liq.}}^{0.25}}{w_{\text{gas}}^{0.5}}\ \text{m}, \tag{10}$$

and for systems having surface tension (σ) and kinematic viscosity coefficient (ν_L) values close to those for the system air–water by the formula:

$$h_0^{0.6} = \frac{H}{0.806 w_{\text{gas}}^{0.5}}\ \text{m}, \tag{11}$$

* In equation (9) h_0 is expressed in meters, and in equation (5) in millimeters.

The total hydraulic resistance of the shelf of a foam apparatus at constant temperature of the gas, and in the absence of mass transfer is expressed by the general formula:

$$\Delta P = \Delta P_1 + \Delta P_2 = 1.45k \frac{\gamma_G w_0^2}{2g} +$$

$$+ 0.85 h_0 \gamma_L + 0.2 \cdot 10^4 \sigma \text{ kg/m}^2 \qquad (12)$$

where 1.45, k*, and 0.85 are dimensionless coefficients; $0.2 \cdot 10^4$ is a dimensional coefficient (m^{-1}); γ_G and γ_L are measured in kg/m^3; w_0 in m/sec; g in m/sec^2; h_0 in m; and σ in kg/m.

Investigation has shown [10] that for concrete systems within specific limits of working conditions of the foam apparatus in which foam formation was studied, it is possible to obtain simple relationship between ΔP_2 and the height of the foam, which are suitable for practical calculations. According to the experimental data, the resistance of the foam increases in proportion to its height. Since the structure of the foam depends on the gas velocity in the apparatus, the resistance of the foam (when its height is constant) depends on w_G. The greater the gas velocity, the less the specific gravity of the foam and the less its resistance. The relationship $\Delta P_2 = f(H, w_G)$ can be expressed by the empirical formula:

$$\Delta P_2 = xH - yw_G + z \text{ mm water } (\text{kg/m}^2), \qquad (13)$$

where H is the height of the foam (in m); w_G is the gas velocity in the apparatus (in m/sec); x, y, and z are empirical coefficients that change depending on the gas–liquid system. Within limits of variation of H from 0.05 to 0.4 m and of w_G from 1 to 3.5 m/sec, the values given below were found for x, y, and z.

System	x	y	z
Air–water	325	23	43.5
Air–75% H_2SO_4 solution	330	0	28
Air–12% NaOH solution	400	20	30
Air–salts solution**	300	5.5	16.5
Air–CaO suspension (200 g/l)	405	24	32.5

Inasmuch as the volume of the foam formed on the grid when the gas is passed through and its resistance are mutually related, the value of ΔP_2 can serve as some criterion of the work rate of the apparatus. The graphs shown in Fig. 6 for the relation of the coefficients of heat- and mass- transfer to the hydraulic resistance of the foam [10] show that the rate of heat exchange or of diffusion in the foam apparatus is proportional to the amount of energy expended in foam formation.

SUMMARY

1. In an investigation of the effect of structural and process parameters on the hydraulic resistance of the gas–liquid layer in a foam system, it was established that the structural parameters of the grid, the gas velocity in the openings of the grid and in the apparatus, the viscosity of the gas and the liquid, and the specific gravity of the gas have no effect on the hydraulic resistance of the gas–liquid layer.

2. The hydraulic resistance of a gas–liquid layer of a given height (constant) in a foam system is much less than for a bubbling system, and within limits of gas velocity (w_G = 1.0-4.0 m/sec) corresponding to those for a foam system, it decreases considerably with an increase in the gas velocity. The hydraulic resistance for the same height of the initial liquid layer is only slightly higher (by 1-3 mm) for a foam system than for a bubbling system. With the same hydraulic resistance, the rate for a foam system is much higher than for a bubbling system.

3. The hydraulic resistance of a plate of a sieve apparatus for all systems can be calculated by the formula:

$$\Delta P = 1.45k \frac{\gamma_G w_0^2}{2g} + 0.85 h_0 \gamma_{liq} + 0.2 \cdot 10^4 \sigma \text{ kg/m}^2$$

* Value (k) given in [1].

** NH_4Cl 160 g/l, NaCl 70 g/l, NH_4HCO_3 45 g/l, $(NH_4)_2CO_3$ 30 g/l.

LITERATURE CITED

[1] I. P. Mukhlenov and E. Ya. Tarat, J. Appl. Chem. 31, 4, 542 (1958).*

[2] M. E. Pozin, I. P. Mukhlenov, E. S. Tumarkina, and E. Ya. Tarat, Foam Method of Processing Gases and Liquids. (State Chem. Press, 1955)[in Russian].

[3] I. P. Mukhlenov, Doctoral Diss., Lensovet LTI (1955).

[4] V. N. Stabnikov, Proc. Voronezhskii Chem.-Tech. Inst. III-IV, 177 (1939).

[5] N. M. Zhavoronkov and I. E. Furmer, Oxygen 5, 9 (1947).

[6] E. Kirschbaum, Destillier- und Rektifiziertechnik, Berlin (1950).

[7] D. E. Arnold, E. A. Plank, and E. M. Schoenborn, Ch. Eng. Progr. 48, 12, 623 (1952).

[8] F. D. Mayfield, W. Z. Church, A. G. Green, and D. C. Lee, Ind. Eng. Ch. 44, 9, 2238 (1952).

[9] J. Jones and C. Pyle, Ch. Eng. Progr. 51, 9, 424 (1955).

[10] E. Ya. Tarat, Cand. Diss., Lensovet LTI, (1945).

[11] I. P. Usyukin and L. S. Aksel'rod, Oxygen 1 and 2, 5 (1949).

[12] I. P. Mukhlenov, J. Appl. Chem. 31, 1, 45 (1958).*

[13] A. A. Noskov and V. N. Sokolov, Proc. Lensovet LTI 39, 110 (1957).

Received May 19, 1958.

* Original Russian pagination. See C. B. Translation.

ELECTROCHEMICAL DEPOSITION OF GOLD-COPPER ALLOYS

N. P. Fedot'ev, E. G. Kruglova, and P. M. Vyacheslavov

In its decorative properties gold surpasses all other metallic platings. Therefore, in spite of their high cost gold platings are used more and more widely. In particular, gold platings are widely used for a decorative finish on articles of light and domestic industry. The thickness of the gold platings in these cases usually is 0.5-1 μ and only occasionally is increased to 2-3 μ. Nevertheless, in spite of the fact that the platings are so thin, the total consumption of gold in connection with the bulk of production is very considerable.

A great economy of gold can be achieved by increasing the hardness and the durability of the gold platings. This permits, in the case of articles that receive much wear (for example, automatic pens and pencils) maintaining the same period of service while considerably decreasing the thickness of the plating, and consequently the consumption of gold.

The hardness of gold can be considerably increased by the addition of copper, since in this way a series of solid solutions are produced. The durability of a metal is not directly related to its hardness. However, as has been shown in previous communications [1], an increase in the hardness of gold indicates an increase in its durability.

The literature data that are available do not give a complete presentation of the mechanical properties of galvanic gold-copper alloys, or of their physicochemical properties, for example their resistance to corrosion in different media (H_2S vapor, NaCl solution). Data are almost completely lacking on the conditions of deposition of gold-copper alloys, and the information in the literature cannot be considerable sufficiently basic [2, 3].

In the present investigation we have studied the technology of the deposition of gold-copper alloys and their mechanical and physicochemical properties.

EXPERIMENTAL

Investigation of Conditions for Deposition of Gold-Copper Alloys of Various Compositions

Alloys of three different compositions, containing, 60, 75, and 90% Au, were investigated.

In Table 1 are given the compositions of the electrolytes used for the deposition of these alloys.

The main factors exerting an influence on the composition of the deposits and the yield based on the current are the concentrations of gold, copper, and KCN, the cathode current density, and the temperature of the electrolyte.

Effect of potassium cyanide concentration. When the concentration of potassium cyanide in the electrolyte is increased, the gold content of the alloy increases (Fig. 1). When the KCN concentration changes by 4 g/l, the composition of the deposits changes for alloy No. 1 (60% Au) by 8%, and for the rest of the alloys by 4-6%.

The current yield at the cathode falls with an increase in the potassium cyanide concentration (Fig. 2).

Effect of gold and copper concentration. A change in the gold concentration in the electrolyte noticeably affects the composition of the deposits (Fig. 2), and the lower the gold content in the alloy, the more appreciable is the effect. Thus, when the Au concentration was changed by 0.2 g/l, for electrolyte No. 1 the composition of the deposits changed by 6%, for electrolyte No. 3 by 4%, and for electrolyte No. 4 by 2%.

TABLE 1

Composition of Electrolytes for Gold–Copper Alloys

No. of alloy and electrolyte	Composition of alloy (in %)		Composition of electrolyte (in %)		
	Au	Cu	Au	Cu	KCN
1	60	40	1.2—1.4	5—6	6—8
2	60	40	2.8—3.0	15—18	10—12
3	75	25	1.7—2.0	3.4—4.4	7—9
4	90	10	2.3—2.8	2.5—3.5	11—14

To a lesser extent, a change in the copper concentration (Fig. 3) affected the composition of the deposits. Thus, with a change of 1 g/l in the copper concentration, the composition of the deposits changed by 3-4%.

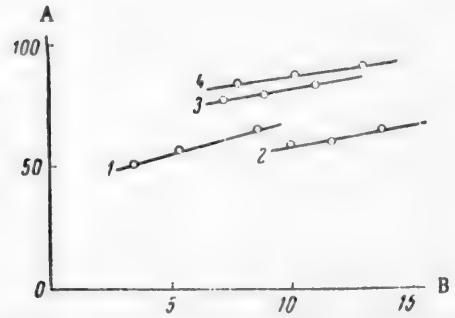

Fig. 1. Relation of composition of deposits to KCN concentration in electrolyte; A) Au content (in %); B) KCN concentration (in g/l); Au and Cu content (in g/l): 1) 1.2-1.4 and 5-6; 2) 2.8-3.0 and 15-18; 3) 1.7-2.0 and 3.4-4.4; 4) 2.3-2.8 and 2.5-3.5.

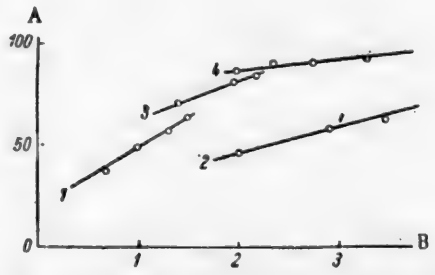

Fig. 2. Relation of composition of deposits to gold concentration in electrolyte; A) Au content of deposit (in %); B) Au concentration (in g/l); Cu and KCN content (in g/l); 1) 5-6 and 6-8; 2) 15-18 and 10-12; 3) 3.4-4.4 and 7-9; 4) 2.5-3.5 and 11-14.

Effect of cathode current density. The cathod current density within known limits (0.25-1.0 A/dm^2) showed almost no effect on the composition of the deposits (Fig. 4). An exception is electrolyte No. 2, with a high copper content. The limits of the working current density at which deposits of the necessary composition are obtained are narrower in this case (0.5-1.0 A/dm^2).

The cathode current yield when the current density is increased falls appreciably (Fig. 5) and in all cases is less than 100%, since even at comparatively low current densities (0.25 A/dm^2) the deposition process is accompanied by the evolution of hydrogen. The average values for the current yields for D_K = 0.5 A/dm^2 are within the limits 50-70%.

Effect of temperature. A decrease in the temperature of the electrolyte leads to an increase in the gold content of the plating, and this effect is more appreciable for an alloy with a lower gold content (Fig. 6). Thus, when the temperature is lowered 10°, the percentage of gold in the deposits increases for electrolyte

No. 1, by 6.6%, for electrolyte No. 3 by 3.8%, and for No. 4 by 2.3%. The cathode current yield falls appreciably when the temperature of the electrolyte is lowered (Fig. 7), and the quality of the deposits sharply deteriorates in all cases at temperatures below 40°. The deposits take on a dark coloration and become powdery.

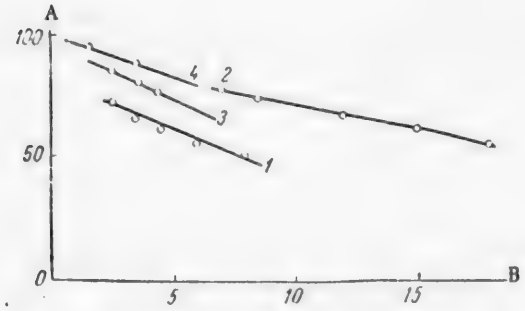

Fig. 3. Relation of composition of deposits to copper concentration in electrolyte; A) Au content (in %); B) Cu concentration (in g/l); Au and KCN content (in g/l); 1) 1.2-1.4 and 6-8; 2) 2.8-3.0 and 10-12; 3) 1.7-2.0 and 7-9; 4) 2.3-2.8 and 11-14.

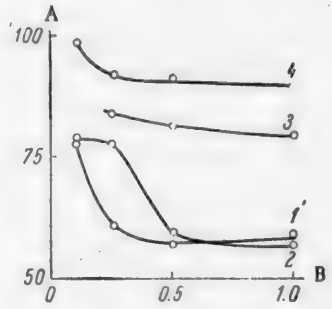

Fig. 4. Relation of composition of deposits to current density; A) Au content (in %); B) current density D_K (in A/dm²); Au, Cu, and KCN content (in g/l): 1) 1.2-1.4, 5-6, and 6-8; 2) 2.8-3.0, 15-18, and 10-12; 3) 1.7-2.0, 3.4-4.4, and 7-9; 4) 2.3-2.8, 2.5-3.5, and 11-14.

Investigation of the Anode Process

The deposition of gold—copper alloys can be carried out with insoluble (platinum or carbon), as well as soluble anodes. The soluble anodes can be partitioned or of an alloy of the appropriate composition.

Work with insoluble anodes requires frequent adjustment of the electrolyte and therefore is less convenient under industrial conditions. Work with partitioned anodes is complicated by the fact that it is necessary to work under conditions of partial passivation to maintain a constant composition of the electrolyte. Otherwise, the anode current yield will considerably exceed the cathod current yield. Therefore, we carried out an investigation of the anode process for soluble anodes of alloys with a gold content of 60, 85, and 91%.

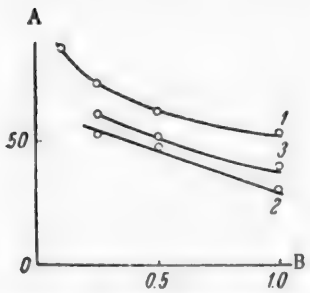

Fig. 5. Relation of cathode current yield to current density; A) cathode current yield η_K (in %); B) current density D_K (in A/dm²); Au, Cu, and KCN content (in g/l): 1) 1.2-1.4, 5-6, and 6-8; 2) 1.7-2.0, 3.4-4.4, and 7-9; 3) 2.3-2.8, 2.3-2.5, and 11-14.

Anode polarization. Anode polarization curves were obtained for two alloys that contained 60 and 85% gold, at different potassium cyanide concentrations in the electrolyte. The composition of the electrolytes corresponded to selected optimum compositions for the deposition of the corresponding alloys. The temperature of the electrolyte, as measured, was 50±0.1°. As can be seen from Figs. 8 and 9, the anode polarization curves have two inflexions and three branches.

The first branch of the curve represents the process of electrochemical solution of the alloy, the current yield for which is 100%. The first platform of maximum current corresponds to the moment when the formation of a passive film takes place on the anode.

The second branch of the curve represents the process of electrochemical solution of the anode under the conditions of partial passivation, when the current yield is less than 100% and decreases as the current density increases, approaching zero. The second inflexion corresponds to the transition of the anode to a condition of complete passivation, when the anode has not already dissolved. The current yield for this is zero.

The third branch of the curve represents the process of oxidation of the cyanides and, possibly, the evolution of oxygen. The values of the working current densities for the anodes should be within the limits of the second branch of the curve, i.e., when the anode is working under conditions of partial passivation. The position of the second branch of the curve depends greatly on the concentration of potassium cyanide in the elec-

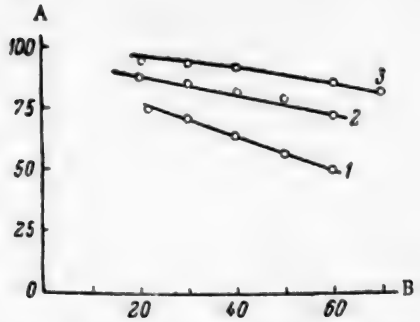

Fig. 6. Relation of composition of deposits to temperature; A) Au content (in %); B) temperature (in °C); Au, Cu, and KCN content (in g/l): 1) 1.2-1.4, 5-6, and 6-8; 2) 1.7-2.0, 3.4-4.4, and 7-9, 3) 2.3-2.8, 2.5-3.5, and 11-14.

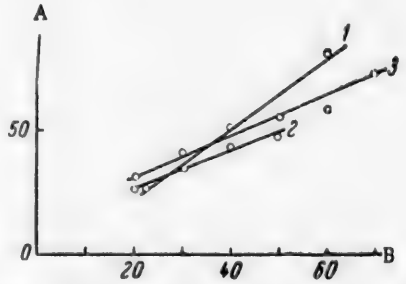

Fig. 7. Relation of cathode current yield to temperature; A) cathode current yield η_K (in %); B) temperature (in °C); Au, Cu, and KCN content (in g/l): 1) 1.2-1.4, 5-6, and 6-8; 2) 1.7-2.0, 3.4-4.4, and 7-9; 3) 2.3-2.8, 2.5-3.5 and 11-14.

trolyte. When the concentration of KCN is increased, the polarization curves are shifted in the direction of higher current density values, which may be explained by the depassivating effect of potassium cyanide on the anode process.

Current yield and permissible working current densities at the anode. The anode current yields were determined by the decrease in weight of the anodes. The relationship of the anode current yield to the current density was investigated at various concentrations of potassium cyanide and a temperature of 50 ± 0.1° for alloys of the three indicated compositions (60, 85, 91% Au).

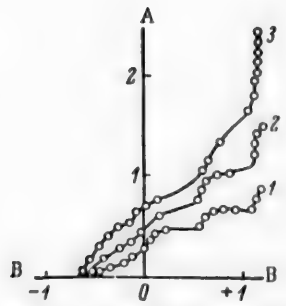

Fig. 8. Anode polarization curve for Au-Cu alloy, containing 60% gold (1.2 g/l Au and 6 g/l Cu). A) Current density D_a (in A/dm^2); B) potential (in volts). Concentration of KCN (in g/l): 1) 3.46, 2) 5.8, 3) 9.3.

Fig. 9. Anode polarization curve for Au-Cu alloy, containing 85% gold (1.95 g/l Au and 3.53 g/l Cu). A) Current density D_a (in A/dm^2); B) potential (in volts). Concentration of KCN (in g/l): 1) 3.5, 2) 7.4, 3) 11.7.

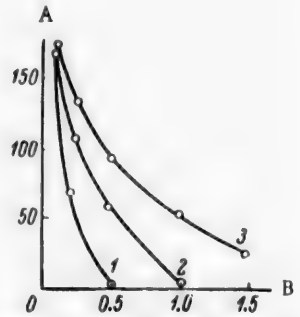

Fig. 10. Relation of anode current yield to current density for an anode containing 60% Au (1.2 g/l Au and 6 g/l Cu). A) Anode current yield (in %); B) anode current density (in A/dm^2). KCN concentration (in g/l): 1) 1.3, 2) 3.0, 3) 5.6.

The anode current yield depends to a great degree on the current density and the concentration of potassium cyanide (Figs. 10-12). in the electrolyte. When the KCN concentration is increased, the current yield is appreciably increased. When the current density increases, the current yield falls, and the lower the potassium cyanide concentration in the electrolyte, the more distinct is the effect of the current density. From the experimentally obtained curves, the permissible working current densities at the anode have been found for specific values of the anode current yield. The values of the anode current yield were taken as equal to those for the cathode when D_K = 0.5 A/ dm^2 and were found from the curves in Fig. 5.

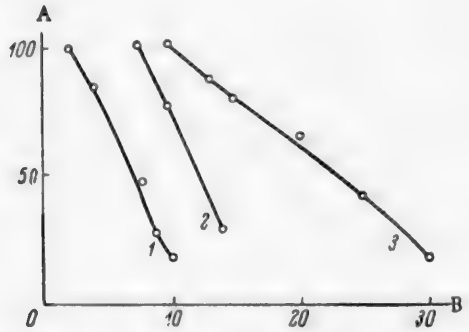

Fig. 11. Relation of anode current yield to current density for an anode containing 85% Au (1.95 g/ l Au and 3.53 g/ l Cu); A) anode current yield (in %); B) anode current density (in A/ dm^2); KCN concentration (in g/ l): 1) 3.7; 2) 7.8; 3) 11.5.

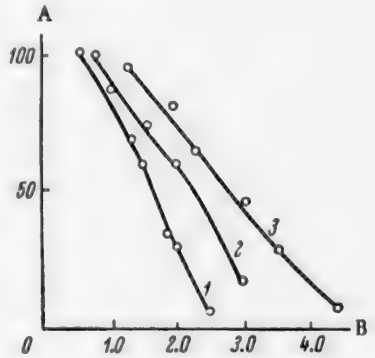

Fig. 12. Relation of anode current yield to current density for an anode containing 91% Au (2.5 g/ l Au and 3 g/ l Cu); A) Au content (in %); B) anode current density (in A/ dm^2); KCN concentration (in g/ l): 1) 10; 2) 12.0; 3) 15.7.

On the basis of the data obtained, the relation of the permissible working current density at the anode to the potassium cyanide concentration in the electrolyte was plotted (Fig. 13). When the KCN concentration in the electrolyte is increased, the permissible anode current density increases. This fact should always be taken into account in selecting the anode system, since on it depends the working stability of the electrolyte and the constancy of the composition of the deposits obtained.

INVESTIGATION

Mechanical Properties of Electrochemical Alloys of Gold and Copper

Electrolytic Au–Cu alloys containing from 30 to 100% of gold were investigated.

Microhardness. To determine the microhardness, the gold–copper alloy was deposited on polished brass plates. The thickness of the deposit was 3-4 μ. The microhardness was determined on a PMT-3 microhardness gage with a load of 20 g. Under these conditions, according to literature data [4], the base has practically no effect on the hardness number.

It is interesting to compare the microhardness of the electrolytic gold–copper alloys with rolled alloys, and also with jewelry gold.

These data are given in Table 2, in which are also shown the hardness values of pure cast gold, and of electrolytic gold obtained from different electrolytes with additives to increase the hardness.

As can be judged from Fig. 14 and Table 1, the addition of copper even in small amounts appreciably increases the hardness of gold platings. Thus, with 10% copper in the alloy the hardness is increased almost twice. The value of the microhardness for alloys containing from 30 to 70% copper is within the limits 240-270 kg/ mm^2, i.e., 2.5-3 times higher than the hardness of pure gold and approximately equal to the microhardness of jewelry gold sample 583.

TABLE 2

Relation of Microhardness of Alloys to Means of Obtaining the Alloy

Metal or alloy	Means of obtaining alloy	Microhardness H (in kg mm^2)
Gold	Electrolytic:	
	usual cyanide electrolyte	106
	with addition of	
	$K_3Co(CN)_6$	185
	$K_2Ni(CN)_4$	168
	Rolled	58
Gold–copper alloy (90%)	Electrolytic	194
	Rolled	197
Gold–copper (85%)	Electrolytic	242
	Rolled	228
Gold–copper (60%)	Electrolytic	270
	Rolled	216
Jewelry gold sample 583 (Au–Ag–Cu)	Rolled	276

For cast rolled gold the microhardness is considerably less (Table 1) in comparison with electrolytic gold. This difference is explained by the grain size, since it is known that deposits obtained from cyanide electrolytes have a very fine-grained structure, and consequently should also have a higher hardness. Probably for the same reason, electrolytic Au–Cu alloys are harder in comparison with rolled alloys.

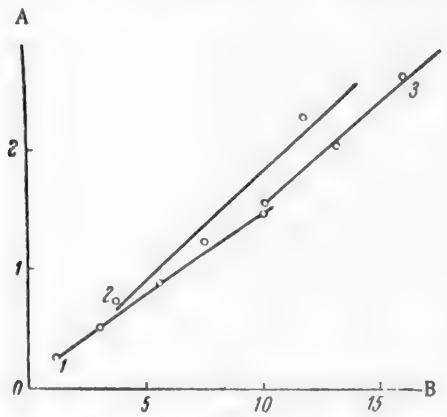

Fig. 13. Relation of permissible anode density to KCN concentration in electrolyte; A) permissible anode current density (in A/ dm^2); B) KCN concentration (in g/ l); Au and Cu content (in %); 1) 60 and 40; 2) 85 and 15; 3) 91 and 9.

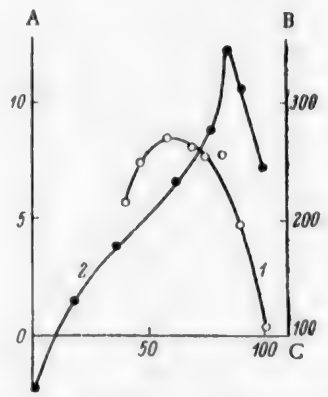

Fig. 14. Relation of microhardness and tension to composition of deposits; A) tension σ (in kg/ mm^2); B) hardness H (in kg/ mm^2); C) Au content (in %); curve: 1) microhardness; 2) tension.

Internal tension. Measurement of the internal tension was carried out by measuring the camber of a polished plate covered with the alloy. The camber was determined with the aid of an optimeter [5] especially adapted to this purpose. The plating was carried out on one side of plane-parallel polished plates 80 × 20

mm and 1 mm thick. The reverse side was isolated with ethynol, which is stable in alkaline medium, after hot drying at a temperature of 50° for 2 hours. The thickness of the plating was 3-4 μ.

As shown in Fig. 14, galvanic gold platings have rather large internal compression tensions. When the copper content in the alloy is increased, the compression tension at first increases, and then begins to decrease, changing sign on approaching the composition of pure copper. Pure copper from a cyanide bath has an expansion tension. The presence of a maximum in the tension curve can be explained by the destruction of the bond between the grains of the deposit, and by the friability, which increases on approaching 100% gold. The maximum in the tension curve corresponds approximately to the maximum in the hardness curve. This indicates that a decrease in the hardness in a given case is elicited not only by the change in the composition of the alloy, but by the destruction of the bond between the grains of the plating as a result of the compression tension.

Durability of the platings was determined on a special apparatus, the main element of which was a revolving brass cylinder with a cloth stretched on it. The sample being tested, in the form of a brass disk plated with Au–Cu alloy, was placed with a bearing surface on the cloth by means of a special holder. The durability of the plating was judged by the number of revolutions of the cylinder necessary to wear down a plating 3-4 μ in thickness to the base metal with a load of 500 g on the sample.

The results are given below in the form of comparative data with pure gold.

Durability of Electrolytic Platings

Gold content of plating (in %)	100	94	88	80	73	63	56	50	37
Durability (in % compared to pure gold)*	100	130	146	263	327	355	387	410	440

As can be seen from the above data, platings of gold–copper alloy are considerably more durable than pure gold plating. Addition of 10% copper increases the durability of the plating 1.4-1.5 times. For an alloy containing 30-40% copper, the durability is increased 3-4 times. Thus, addition of copper to gold even in small amounts may give a considerable effect in the sense of increasing the resistance of the plating to wear.

Corrosion Resistance of Gold–Copper Alloys

Testing in 3% NaCl solution was carried out by complete immersion for 30 days. In the testing process, the formation of white, flocculent corrosion products of the base metal was observed, and it was found that platings of pure gold showed a high rate of corrosion, probably as a result of their great porosity in comparison with alloy platings.

The platings themselves were little changed in external appearance after testing, with the exception of alloys with a gold content of 50% or less. The latter showed some traces of corrosion in the form of tarnish.

TABLE 3

Optimum Composition of Electrolytes, t = 45-55

Gold content in alloy (in %)	Composition of Electrolyte (in g/l)			D_K (in A/dm²)	η_K* (in %)	D_a** (in A/dm²)
	Au	Cu	KCN			
55–65	1.2–1.4	5–6	6–8	0.25 ÷ 1.0	65–70	0.9–1.2
	2.8–3.0	15–18	10–12	0.5 ÷ 1.0	—»—	1.4–1.6
75–80	1.7–1.9	3.4–4.4	7–9	0.25 ÷ 1.0	50–55	1.3–1.6
88–92	2.3–2.8	2.5–3.5	11–14	0.25 ÷ 1.0	45–50	1.7–2.3

* At D_K = 0.5 A/dm².

** Anode current density given at D_K = 0.5 A/dm².

* Average of 5-10 tests.

On the basis of the tests carried out we can say that regardless of the composition of the alloy, a plating thickness of 3 μ is insufficient to protect the base metal from corrosion under these conditions.

Tests in hydrogen sulfide atmosphere. Testing was carried out in a desiccator on the bottom of which was placed a crucible with a small amount of pyrites. Water was poured into the desiccator to create a moist atmosphere. Every day there was added to the crucible 0.1 ml of sulfuric acid, which corresponded to a concentration of hydrogen sulfide in the atmosphere of 7 mg/l. In the first days of the tests a great difference was found in the behavior of the samples. The samples that were plated with an alloy containing less than 75% gold were covered during the first days with dark spots, the amount of which was greater as the gold in the alloy decreased. After testing for a month, the following picture was observed. Samples containing 100 and 90% gold were almost unchanged in outward appearance, with the exception of the edges and sharp corners, where a noticeable darkening appeared. On plating containing 75% gold a large number of dark lines were formed, but it did not lose its luster. The rest of the samples with a gold content of less than 75% had a dark tarnish on almost the whole surface.

On the basis of all the investigations carried out, the optimum compositions for the electrolytes for deposition of gold–copper alloys were selected (Table 3).

SUMMARY

1. The composition of the deposits of gold–copper alloys depends in a great degree on the concentration of gold and copper in the electrolyte. Thus, the composition of the platings changes within the limits 2-6% when the gold concentration changes by 0.2 g/l, and within the limits 3-4% when the copper concentration changes by 1 g/l.

When the KCN concentration increases, the gold content in the plating is increased, but the cathode current yield decreases.

2. A change in the cathode current density within the limits 0.25-1.0 A/dm^2 has practically no effect on the composition of the deposits, but the current yield decreases with an increase in the current density.

3. When the temperature of the electrolyte is lowered, the gold content in the plating is increased, but the equality of the deposits distinctly deteriorates, and the cathode current yield is appreciably lowered.

4. The permissible anode working current densities should be within the limits corresponding to the conditions for partial passivation of the anode, when the current yield is less than 100% and consequently equal to that at the cathode. The values of the permissible anode current density are higher as the KCN concentration in the electrolyte becomes greater.

5. It has been shown that with a copper content of 20-40% in the alloy the microhardness and the durability of the platings are increased 2-3 times in comparison with pure gold. It has been established that deposits of pure gold and of alloy have a rather large compression tension, which decreases as the copper content of the alloy increases.

6. Comparative tests have been carried out on platings of alloys of various composition with regard to corrosion in 3% NaCl solution and in an atmosphere of hydrogen sulfide. The tests showed that with a thickness of 3 μ neither pure gold nor alloys protect the base metal from corrosion. The plating itself in NaCl solution proved to be rather resistant, especially in the case of alloys containing more than 50% gold. In an atmosphere of hydrogen sulfide only alloys containing more than 80% gold proved to be resistant.

LITERATURE CITED

[1] N. P. Fedot'ev, N. M Ostroumova, and P. M. Vyacheslovav, J. Appl. Chem. 28, 489 (1956).*

[2] Kaio, Metaloberflache 3, 62 (1956).

[3] Rospromsovet "Information Sheet" (Moscow, 1955).

[4] N. P. Fedot' ev and P. M. Vyacheslavov, ZL 7 (1952).

[5] A. A. Glikman, N. P. Fedot'ev, and P. L. Chernova, ZL 9 (1951)

Received September 19, 1958

*Original Russian pagination. See C. B. Translation.

HYDROGEN OVERVOLTAGE ON LEAD AND SOME OF ITS ALLOYS IN CONCENTRATED SULFURIC ACID SOLUTION

I. A. Aguf and M. A. Dasoyan

The question of the magnitude of the hydrogen overvoltage on lead and its alloys in sulfuric acid solution is of considerable interest in the theory of the lead storage battery. This question acquires special significance in connection with the problem of increasing the corrosion resistance of the alloy used to prepare the grid of the positive plates. As is well known, when the storage battery operates, individual components of the anode alloy, and in particular components used as alloy additives which increase the corrosion resistance, are partially transported to the cathode. The effect of these components on the operation of the negative electrode of the battery can be characterized to a notable degree by the magnitude of the hydrogen overvoltage on the respective alloys.

In the literature notice is also taken of the presence of a direct connection between the hydrogen overvoltage and the corrosion resistance of the alloy when there is anodé polarization [1, 2].

A large number of investigations have been devoted to the measurement of the hydrogenovervoltage on lead in sulfuric acid solutions.

In previous communications [3-6] it has been shown that the relation between the hydrogen overvoltage on lead and the polarizing current density is described by Tafel's equation over a wide range of current densities. The slope obtained for the semilogarithmic curve frequently proves to be anomalously high [5, 6], amounting to approximately 0,2, which is explained by the authors by the presence on the surface of the lead, of a layer of sulfate firmly bound to the surface of the metal even at considerable cathode potentials.

A high value of the prelogarithmic coefficient also was obtained for lead (0.3) by Hickling and Salt [7]. However, the method used in this work involved appreciable errors, which could explain this occurrence [8]. Measurement of the overvoltage of hydrogen on lead in very pure condition was carried out by Kabanov et al. [9]. In this work it was shown that this value does not depend on the sulfuric acid concentration in the range from 0.1 to 8 N H_2SO_4. The semilogarithmic curves obtained had a slope b = 0.125. It was also shown that the overvoltage of hydrogen on lead depends essentially on the degree of purity of the metal, increasing with an increase in the latter.

In a series of investigations carried out in recent years [10-12], it has been established that all of the data on the overvoltage of hydrogen on lead can be satisfactorily explained from the point of view of the theory of delayed discharge.

The overvoltage of hydrogen on lead in concentrated acid solutions was investigated in the work of Iofa [11]. The author showed, in particular, that the relationship of the overvoltage to the composition of the solution can be expressed by an equation similar to the one for the overvoltage of mercury [13]:

$$\eta_i = \text{const} + \left(1 - \frac{1}{\alpha}\right) \vartheta \lg [H^+] + \left(1 - \frac{\alpha'}{\alpha}\right) \vartheta \lg f_{H^+} + \left(\frac{1}{\alpha} - 1\right) \psi_1 + \frac{\vartheta}{\alpha} \lg i, \quad (1)$$

where ψ_1 is the potential of the diffuse part of the double layer; f_{H+} is the activity coefficient of the hydrogen ions; α is the transfer number for the discharge of the hydrogen ions; α' is a constant characterizing

the change in energy of solvation with concentration; $\vartheta = \frac{2.303\ RT}{F}$. Formula (1), in calculating the relationship of ψ_1 to the acid concentration, makes it possible to explain the known phenomenon of a decrease in the hydrogen overvoltage on lead when the concentration is increased in very strong solutions of sulfuric acid (> 8 N).

The effect of the condition of the electrode surface on the hydrogen overvoltage on lead was investigated in detail in recent years by Kolotyrkin, Medvedeva, and Buné [14-18]. In contrast to previous work, the polarization curves were obtained under fixed conditions where to each current density there corresponded a steady potential. The authors established the existence of two regions of straight-line relationship of η to log i, with the transition from one relationship to the other occurring in the region of potentials close to that of the nul point for the discharge of lead [19].

The indicated effect may be connected with the adsorption of anions, particularly of sulfate ions on the positively charged surface of the metal, and with the change in value of the ψ_1-potential. In conformance with this, the relationship of the hydrogen overvoltage on lead to the current density over a wide polarization range can be expressed by the equation [18].

$$\eta = a + \Delta\varphi^0 + b \lg i, \tag{2}$$

where $\Delta\varphi^0$ is the shift in the nul point for the discharge of lead as a result of adsorption.

When there is no adsorption of anions, $\Delta\varphi^0 = 0$; if the surface of the electrode is completely occupied, $\Delta\varphi^0 = \text{const}$. In both cases, obviously, there is a relationship between η and log i expressed by Tafel's equation, but with different a coefficients, which also has been observed in the investigations cited. In 1N H_2SO_4 solution, according to the data of Kolotyrkin and Buné [14], the following formulas hold true:

for high current densities ($i > 10^{-5}$ A/cm^2)

$$\eta = 1.56 + 0.12 \lg i, \tag{3}$$

for low polarizations

$$\eta = 1.40 + 0.12 \lg i. \tag{4}$$

The hydrogen overvoltage on technical grade lead at high current densities ($10^{-3} - 2 \cdot 10^{-1}$ A/cm^2), according to data obtained by Pecherskaya and Stender [20] is expressed by the equation

$$\eta = 1.33 + 0.095 \lg i. \tag{5}$$

Data on the hydrogen overvoltage on lead alloys are very few and quite contradictory. This pertains, in particular, to lead-antimony, and also lead-silver and ternary lead-antimony-silver alloys that are of importance to the storage battery industry.

In some investigations [21, 22], for example, it has been indicated that the hydrogen overvoltage on lead-antimony alloys increases with an increase in the antimony content of the alloy. This result, however, is not in agreement with practical observations and appears improbable. Careful measurements [23] have shown that the semilogarithmic curve for 8% lead-antimony alloy lies on the average 200 mv below the curve obtained for pure lead in the current density range from $2 \cdot 10^{-7}$ to $2 \cdot 10^{-3}$ A/cm^2 in 2N H_2SO_4 solution. These data are in qualitative agreement with the data obtained by Mashovets and Fateeva [24], according to which the addition to lead of 5.72% Sb lowers the hydrogen overvoltage by approximately 10 mv.

In recent years the hydrogen overvoltage on a series of lead-antimony alloys with an Sb content from 1 to 6% at high current densities (10^{-3}–10^{-2} A/cm^2) has been investigated in the work of Rüetschi and Cahan [1], who showed that with an increase in the antimony content of the alloy there is some increase in the prelogarithmic coefficient in the Tafel equation.

The hydrogen overvoltage on lead-silver alloys has been studied only in the old work of Raeder and Brun [21], who did not find any appreciable effect from the addition of silver up to a content of 50 atom-%. This result, however, as in the case of the lead-antimony alloys, is very doubtful. The overvoltage on lead-antimony-silver alloys has not been systematically studied at all.

Thus, in the contemporary literature there are no detailed data on the effect of silver on the hydrogen overvoltage on lead, nor on lead–antimony alloy. This problem, however, is of considerable practical interest in connection with the fact that silver, as numerous investigations have shown, is the only one of the available metals that substantially increases the resistance to corrosion of lead alloys when anode polarization occurs [25].

The present work was devoted to a study of the hydrogen overvoltage on a series of lead–silver and lead–antimony–silver alloys with a silver content of 1 to 10%, and also on lead and lead–antimony alloy with an antimony content of 4.5%. All the experiments were carried out in sulfuric acid solution with a specific gravity of 1.320 (11.2 N) at a temperature of 25 ± 0.02°. The metals used were of high technical grade: lead SO, antimony SuO, and silver 99.99.

Measurement of the hydrogen overvoltage was carried out in an apparatus illustrated in Fig. 1. Charging of the cell was accomplished with four 3ST70 starter batteries, connected in series and placed in circuit, by means of switch 1, with two rheostats, R_1 with a resistance of 1100 ohms, and R_2 with a resistance of 200 ohms, from which the required voltage was obtained potentiometrically. In series with the cell was connected a variable radio-resistance (R_3) of 0.1 milliohms. The presence of the three rheostats with different resistances and methods of connection made possible the smooth and accurate regulation of the current, and also guaranteed its steadiness. To measure the current, a multirange M-193 type milliammeter was used.

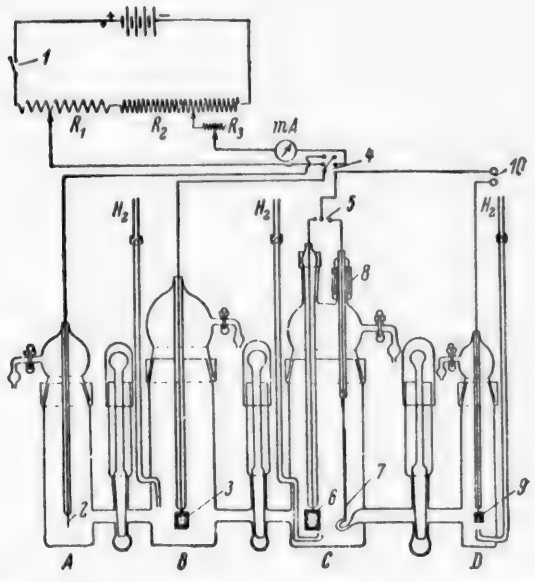

Fig. 1. Apparatus for measurement of hydrogen overvoltage.

The cell consisted of 4 vessels A, B, C, and D, connected by stopcocks. Hydrogen was introduced into vessels B, C, and D by means of special ground connections. All the ground joints and stopcocks were sealed with sulfuric acid solution of the same concentration as the acid in the cell. In vessels A and B the preliminary purification of the electrolyte was carried out by prolonged electrolysis with platinum electrodes (2 and 5). The purification was done by a cathode current density of approximately 1 mA / cm^2. At the start of the purification, the stopcock between vessels A and B was open. In this position the electrolysis was carried out for 4-5 days. After this the stopcock was closed and the further purification for 1.5-2 days was carried out while hydrogen was passed into vessel B. After the purification was ended, the stopcock between vessels B and C was opened and part of the electrolyte was carried over by the hydrogen pressure into vessel C. Then switch 4 was moved over to the lower position and switch 5 to the left-hand position. After this the stopcock was closed, and electrolysis was carried on for 5-6 hours with the platinum cathode 6 while hydrogen was passed into vessel C, to additionally purify the electrolyte. The electrode 7 under investigation, which was prepared and soldered to a sealed-in-glass platinum contact directly before beginning the experiment, was immersed in the electrolyte, turning on the current by its immersion. Switch 5 was previously moved over to the right-hand position. The place where the electrode was soldered was 5-6 cm from the level of the electrolyte in vessel C. A hermetic seal was maintained by means of the mercury trap S. The potential of the electrode under investigation was measured relative to a hydrogen electrode 9 (vessel D) in a sulfuric acid solution of the same concentration. Measurement of the potential was carried out with the aid of a semiautomatic potentiometer 10 of type P 2/ 1. The hydrogen, which was passed continuously during the whole experiment into vessels B, C, and D, was perpared by the electrolysis of 25% KOH solution and was purified from traces of oxygen and moisture by consecutively passing it through calcium chloride heated to 300°, platinized asbestos, sodium plumbite solution, and again through calcium chloride.

The electrode under investigation was cleaned directly before the start of the experiment with a steel scraper, pressed between two steel mirrors, and cut to the necessary size. The surface of the electrode was mirror-smooth, permitting us to consider that the area of the visible surface of the part of the electrode immersed in the electrolyte (7 cm^2) was equal to the true surface [26]. Before the measurements were started, the electrode was polarized for 20 hours with a current of 10^{-4} A/ cm^2. The measurements were made in the current density range from 10^{-3} to 10^{-7} A/ cm^2. The electrode was kept at each current density until a constant potential was established. The time that it was kept at the different current densities was 30 to 90 minutes. The difference in the value of the potentials for each current density between the individual experiments did not exceed 4-5 mv.

The results of the measurements are given in Fig. 2. Curve 1, which characterizes the relation between η and log i for lead, consists, as can be seen from the graph, of 4 portions.

The first portion (where i is from 10^{-3} to 10^{-4} A/ cm^2) is characterized by the equation

$$\eta = 1.438 + 0.16 \log i. \qquad (6)$$

When the current density is further lowered, the angle of slope of the curve decreases; the coefficient b takes on a value of 0.12. When $i < 5 \cdot 10^{-6}$ A/ cm^2, a sharp decrease in potential sets in (third portion of the curve).

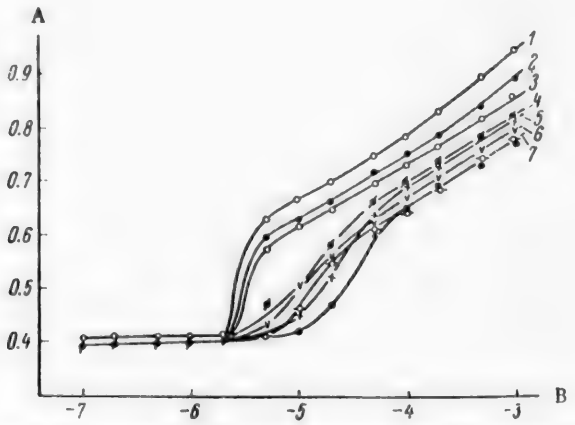

Fig. 2. Relation of hydrogen overvoltage to logarithm of current density: 1) Pb; 2) Pb + 1.01% Ag; 3) Pb + + 2.94 ÷ 9.87% Ag; 4) Pb + 4.5% Sb; 5) Pb + 4.65% Sb+ + 0.95% Ag; 6) Pb + 4.65% Sb + 3.04% Ag; 7) Pb + + 4.55% Sb + 9.47% Ag.

Further decrease in the current does not lead to a substantial change in the value of overvoltage – the curve in this last portion runs almost parallel to the abscissa axis ($5 \cdot 10^{-6}$ to 10^{-7} A/ cm^2).

To explain the character of the relationship between η and log i in the first two portions, it is necessary to direct our attention to the very high sulfuric acid concentration in which the polarization was carried out.

The high concentration of sulfate ions may result in their adsorption on the surface of the electrode not only at potentials corresponding to the positive discharge of the surface, but also at more negative potentials. We therefore may assume that when the current is gradually decreased, adsorption of the HSO_4^- ions begins and increases as the potential approached the nul point for the discharge of lead. Under these circumstances, obviously, if the curve drops from high values of i to low ones, the values obtained for the overvoltage of hydrogen at each current density will prove to be somewhat low in comparison with those that would exist in the absence of adsorption. A gradual increase in the number of adsorbed sulfate ions on the surface of the electrode as the current density decreases could, obviously, affect the magnitude of the logarithmic coefficient, causing it to increase.

This result follows directly from equation (2) if it is assumed that the value $\Delta\varphi^\circ$ in the first part of curve 1 is a function of the polarizing current density and increases in absolute value as the latter decreases.

At some value of the current density, apparently, the surface of the electrode is completely occupied by adsorbed ions. When the current density decreases further, the hydrogen overvoltage on some portion changes according to Tafel's equation with the normal scope. The equation describing the second portion of curve 1 has the form

$$\eta = 1.264 + 0.12 \log i. \quad (7)$$

The sharp decrease in the value of η at low current densities that was observed in our experiments has been described in the work of Iofa [11] and is explained, apparently, by the presence of depolarizers that are found in strong acid solutions. The value of the potential for the 4th portion of the curve, where η has little relation to i, as Iofa has shown, agrees well with the reversible potential of lead in the given solution. This result is fully confirmed by the data obtained. Actually, the reversible potential corresponding to the equilibrium

$$Pb + SO_4^{--} \rightleftarrows PbSO_4 + 2e, \quad (8)$$

measured in relation to a hydrogen electrode in a solution of the same concentration at a temperature of 25° can be calculated from the formula

$$\varphi = -0.356 - 0.088 \lg a_{\pm H_2SO_4}. \quad (9)$$

Calculation by formula (9) for 11.2 N H_2SO_4 solution gives the value $\varphi = -0.409$ v, which agrees with the value for the potential in the 4th portion of the curve under consideration, where for a change in current density from $5 \cdot 10^{-6}$ to 10^{-7} A/cm^2 the potential changes from -0.412 to 0.404 v.

Addition of 1% Ag, as seen in Fig. 1, lowers the hydrogen overvoltage. In curve 2 four portions also are observed with a difference in the nature of the relationship of the overvoltage to the current density, with the transition from the first portion of the curve to the second occurring at approximately the same potential as in curve 1. The upper branch of curve 2 is described by the equation

$$\eta = 1.378 + 0.16 \log i, \quad (10)$$

and the lower branch by

$$\eta = 1.228 + 0.12 \log i. \quad (11)$$

An increase in the silver content of the alloy up to 3% results in a further lowering of the hydrogen overvoltage. An increase in the silver concentration from 3 to about 10%, however, does not change the value of η; the η – log i curves for the alloys containing 2.94%, 4.73% and 9.87% Ag agree within the limits of error of the measurements. Curve 3, which characterizes the hydrogen overvoltage on these alloys, is described by the equation

$$\eta = 1.220 + 0.12 \log i. \quad (12)$$

It should be noted that curve 3 does not have the inflexion in the current density range from 10^{-3} to 10^{-5} A/cm^2 that is observed in the η – log i curve for lead and the alloy with 1% silver. This can be explained by the effect of the appreciable silver content in the alloy on the adsorption of sulfate ions, as a result of which the saturation of the electrode surface by the adsorbed anions is reached at a somewhat more negative potential than in the case of the Pb in the Pb = 1% Ag alloy.

As can be seen from Fig. 2, in the area of low current density the curves for lead and lead–silver alloys fully coincide, which confirms our conclusion as to the determining role of equilibrium (8) in this region.

Curves 4-7 characterize the relationship of the hydrogen overvoltage to the logarithm of the current density for lead–antimony and lead–antimony–silver alloys. All of these curves lie at lower potentials than the curves for the non-antimony alloys.

The linear portion of the curves is described by the equations given below.

Hydrogen Overvoltage on Lead–Antimony–Silver Alloys

Composition of Alloy	Tafel Equation
Pb + 4.5% Sb	$\eta = 1.210 + 0.128 \lg i$
Pb + 4.65% Sb + 0.95% Ag	$\eta = 1.203 + 0.128 \lg i$
Pb + 4.65% Sb + 3.04% Ag	$\eta = 1.186 + 0.128 \lg i$
Pb + 4.54% Sb + 4.94% Ag	$\eta = 1.170 + 0.128 \lg i$
Pb + 4.55% Sb + 9.47% Ag	$\eta = 1.170 + 0.128 \lg i$

As can be seen from the data given above and in Fig. 2, the introduction of antimony into the alloy lowers the hydrogen overvoltage. The introduction of silver up to approximately 5% into the lead–antimony alloy results in a further lowering of this value. An increase in the silver content of the alloy approximately for 5% to 9.5% causes no change in the hydrogen overvoltage in the region of linear relationship of η and $\log i$. In accordance with the data in the literature [1], the value obtained for the prelogarithmic coefficient in the Tafel equations for the alloys containing antimony turns out to be somewhat higher than the corresponding value for the non-antimony alloys. The absence of inflexions in the linear portions of the semilogarithmic curves 4-7 apparently indicates the saturation of the electrode surface by adsorbed sulfate ions in this region of potentials, which may be connected with the lowering of the overvoltage as a result of the addition of antimony and silver.

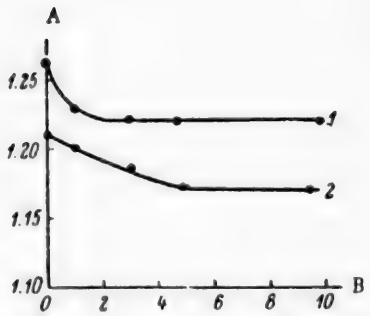

Fig. 3. Relation of hydrogen overvoltage to silver content of alloy.

It should be noted that the sharp decrease in the overvoltage and the flexure of the semilogarithmic curves occurs in the case of alloys containing antimony at higher current densities than in the case of the non-antimony alloys. This phenomenon, apparently, is connected with the depolarizing effect of the antimony ions that originate as a result of the reaction of the antimony contained in the alloy with the hydrogen that is evolved and the subsequent breakdown by the sulfuric acid of the antimony hydride formed in this process [23]. At low current densities, the curves for lead–antimony–silver alloys, as can be seen from Fig. 2, run almost parallel to the abscissa axis, like the curves for the non-antimony alloys. The value of the potential changes from -0.402 to -0.394 when the current density changes from $2 \cdot 10^{-6}$ to 10^{-7} A/cm^2. The determining role is played in this portion of the curve, as in the case of the non-antimony alloys, apparently, by equilibrium (8). Some lowering of the potential is connected, probably, with the particular effect of the process of autosolution of the antimony [27]:

$$Sb + H_2O \rightleftarrows SbO^+ + 2H^+ + 3e. \qquad (13)$$

This is the more probable, since the reversible potential corresponding to equilibrium (13) in relation to a hydrogen electrode in the same solution, calculated on the basis of data on the solubility of trivalent antimony in sulfuric acid [28], is −0.252.

The curves, characterizing the effect of silver on the hydrogen overvoltage on lead and lead-antomony alloy are presented in Fig. 3.*

In conclusion, let us stop to consider the question of the possibility of the theoretical calculation of the values of the hydrogen overvoltage on the alloys investigated, starting with the corresponding magnitudes for the separate components of the alloy. Such a calculation is possible if the electrode is considered as a multiphase system [29, 30]. Such a view can be taken, in particular, for electrodes composed of eutectic alloys. With application to the alloys investigated in the present work, the calculation of the constant a in the Tafel equation can be carried out by the following formulas [30]:

* For lead and Pb + 1% Ag alloy the values of coefficient a in Fig. 3 are taken from equations (7) and (11) for the lower branches of the semilogarithmic curve.

$$a_{Pb-Ag} = a_{Pb} - 0.12 \lg \left[\left(e^{\frac{a_{Pb} - a_{Ag}}{0.052}} - 1 \right) S_{Ag} + 1 \right], \quad (14)$$

$$a_{Pb-Sb} = a_{Pb} - 0.12 \lg \left[\left(e^{\frac{a_{Pb} - a_{Sb}}{0.052}} - 1 \right) S_{Sb} + 1 \right], \quad (15)$$

$$a_{Pb-Sb-Ag} = a_{Pb} - 0.12 \lg \left[\left(e^{\frac{a_{Pb} - a_{Sb}}{0.052}} - 1 \right) S_{Sb} + 1 \right] \times$$

$$\times \left\{ \left[\frac{e^{\frac{a_{Pb} - a_{Ag}}{0.052}} - 1}{\left(e^{\frac{a_{Pb} - a_{Sb}}{0.052}} - 1 \right) S_{Sb} + 1} \right] S_{Ag} + 1 \right\} = a_{Pb} - 0.12 \lg \left[S_{Sb} \left(e^{\frac{a_{Pb} - a_{Sb}}{0.052}} - 1 \right) \times \right.$$

$$\left. \times (1 - S_{Ag}) + S_{Ag} \left(e^{\frac{a_{Pb} - a_{Ag}}{0.052}} - 1 \right) + 1 \right], \quad (16)$$

where $a_{Pb} = 1.264$ is the experimental value of the coefficient in the Tafel equation for lead; $a_{Ag} = 0.95$ [31]; $a_{Sb} = 0.93$ [20]; S_{Ag} and S_{Sb} are the fractions of the electrode surface occupied by the silver and antimony, respectively.

The greatest difficulty in carrying out the calculation by formulas (14)-(16) is presented by the determination of the values of S_{Ag} and S_{Sb}. If we assume that the ratio of the fractions of the surface occupied by the various components of the alloy is equal to the ratio of their total surfaces, then in the case of the lead-silver alloys the equation takes the following form:

$$S_{Ag} = \frac{1}{1 + \left(\frac{\rho_{Ag} \cdot m_{Pb}}{\rho_{Pb} \cdot m_{Ag}} \right)^{2/3}}, \quad (17)$$

and in the case of the three-component lead-antimony-silver alloys

$$S_{Ag} = \frac{1}{1 + \left(\frac{\rho_{Ag} \cdot m_{Pb}}{\rho_{Pb} \cdot m_{Ag}} \right)^{2/3} + \left(\frac{\rho_{Ag} \cdot m_{Sb}}{\rho_{Sb} \cdot m_{Ag}} \right)^{2/3}}, \quad (18)$$

where ρ is the density, and m is the weight-percent of the respective metal.

The values of the constant a calculated by formulas (14)-(16) employing values of S obtained from (17)-(18) correctly reflect the character of the effect of the individual additions on the hydrogen overvoltage. However, the divergence between the calculated and the experimentally determined values considerably exceeds the error of measurement. The cause of this, apparently, is the fact that, as a result of the strong influence exerted by the alloying additive on the structure of the alloy, and also as a result of a possible inequality in the distribution of the components of the alloy, the true values of S_{Ag} and S_{Sb} do not correspond to the values calculated by formulas (17)-(18).

It can be assumed that the true value S' of the fraction of the surface of the electrode occupied by the respective component of the alloy is related to the value S by a simple ratio

$$S' = k \cdot S, \quad (19)$$

where k is the proportionality factor characterizing the effect of the corresponding additive on the structure of the surface of the alloy.

Obviously, the factor k is a function of the composition of the alloy. Employing the experimental values of the hydrogen overvoltage, it is possible to obtain empirical formulas characterizing the relationship of k to the composition of the alloy in the region of silver concentrations investigated.

In the case of the lead–silver alloys, the corresponding relationship can be represented in the form

$$k = \frac{1}{12.8 + 5.5 m_{Ag}}, \qquad (20)$$

and in the case of the lead–antimony–silver alloys

$$k = \frac{m_{Ag}}{34 + 8 m_{Ag}}. \qquad (21)^{*}$$

The data calculated by formulas (14), (16)-(21) are presented in the table.

Values of S_{Ag} and Constant a in the Tafel Equation for the Alloys Investigated

Composition of alloy	S_{Ag}	S'_{Ag}	$a_{calc.}$	$a_{expt.}$
Pb + 1.01% Ag	0.047	0.0021	1.233	1.228
Pb + 2.94% Ag	0.093	0.0032	1.221	1.220
Pb + 4.73% Ag	0.125	0.0032	1.221	1.220
Pb + 9.87% Ag	0.194	0.0029	1.224	1.220
Pb + 4.65% Sb + 0.95% Ag	0.039	0.0009	1.204	1.203
Pb + 4.65% Sb + 3.04% Ag	0.083	0.0043	1.185	1.186
Pb + 4.54% Sb + 4.94% Ag	0.113	0.0075	1.172	1.170
Pb + 4.55% Sb + 9.47% Ag	0.157	0.0135	1.154	1.170

As can be seen from the data presented above, the calculated values of constant a in the Tafel equation are in good agreement with the experimental data.

SUMMARY

1. The hydrogen overvoltage on lead, lead–antimony alloy, and also on a series of lead–silver and lead–antimony–silver alloys has been measured.

2. It has been shown that the addition of silver to the alloy up to a certain limit lowers the hydrogen overvoltage on lead and on lead–antimony alloy.

3. The relationship obtained between the overvoltage and the logarithm of the current density has been explained, by taking into account the possibility of adsorption of sulfate ions on the electrode surfaces and the effect of depolarizing processes.

4. The possibility of theoretical calculation of the hydrogen overvoltage on a series of alloys has been shown.

LITERATURE CITED

[1] P. Ruetschi and B. D. Cahan, J. Electroch. Soc. 104, 406 (1957).

[2] Otani, J. Inst. Metals 20, 158, 162 (1956).

[3] S. Glasston, J. Chem. Soc. 123, 2926 (1923).

[4] S. Glasston, J. Chem. Soc. 125, 250, 2414 (1924).

[5] B. Baars, Naturw. 63, 213 (1928).

* In deriving this formula, the value of S_{Sb} calculated by equation (15) for lead–antimony alloy was used; it was $S_{Sb} = 0.003$.

[6] T. Erdey-Gruz and H. Wick, Z. Phys. Ch. 162, 53 (1932).

[7] A. Hickling and F.W. Salt, Trans. Faraday Soc. 36, 1226 (1940).

[8] A. N. Frumkin, Acta Phys. Chem. 18, 23 (1943).

[9] B. N. Kabanov et al., J. Phys. Chem. 13, 341 (1939).

[10] Ya. M. Kolotyrkin and A. N. Frumkin, J. Phys. Chem. 15, 346 (1941).

[11] Z. A. Iofa, J. Phys. Chem. 19, 117 (1945).

[12] Ya. M. Kolotyrkin, J. Phys. Chem. 20, 667 (1946).

[13] Z. A. Iofa and A. N. Frumkin, J. Phys. Chem. 18, 268 (1944).

[14] Ya. M. Kolotyrkin and N. Ya. Buna, J. Phys. Chem. 21, 581 (1947).

[15] Ya. M. Kolotyrkin and L. A. Medvedeva, J. Phys. Chem. 25, 1355 (1951).

[16] Ya. M. Kolotyrkin and L. A. Medvedeva, Proceedings of the Conference on Electrochemistry, Acad. Sci. USSR Press, 369 (1953).

[17] N. Ya. Buna and Ya. M. Kolotyrkin, Proc. Acad. Sci. USSR 100, 295 (1955).

[18] Ya. M. Kolotyrkin and N. A. Buna, J. Phys. Chem. 29, 435 (1955).

[19] T. N. Borisova, B. V. Ershler, and A. N. Frumkin, J. Phys. Chem. 22, 925 (1948).

[20] A. G. Pecherskaya and V. V. Stender, J. Phys. Chem. 24, 856, (1950).

[21] M. G. Raeder and I. Brun, Z. Phys. Ch. 133, 15 (1928).

[22] V. Croatto and M. DaVia, Gas. Chim. Ital. 73, 117 (1943).

[23] Z. A. Iofa, B. N. Kabanov, et al., Coll. Sci.-Res. on Chem. Sources of Current 3, 36 (1938).

[24] V. P. Mashovets and V. N. Fateeva, J. Appl. Chem. 21, 448 (1948).

[25] Yu. D. Dunaev and G. Z. Kir'yakov, Trans. Inst. Chem. Sci. Acad. Sci. Kaz. SSR 3, 87 (1958).

[26] B. N. Kabanov and R. Yudkevich, J. Phys. Chem. 13, 813 (1939).

[27] N. I. Tugov and G. A. Tsyganov, Uzb. Chem. J. 2, 35 (1958).

[28] P. Rüetschi and R. T. Angstadt, J. Electroch. Soc. 105, 555 (1958).

[29] D. S. Nadezhdin, Ukr. Chem. J. 21, 305 (1955).

[30] I. A. Aguf and M. A. Dasoyan, J. Appl. Chem. 31, 2, 454 (1959).*

[31] B. N. Kabanov, J. Phys. Chem. 8, 486 (1956).

Received April 7, 1959

* Original Russian pagination. See C. B. Translation.

THE EFFECT OF SOME ORGANIC COMPOUNDS IN THE ANODIC OXIDATION OF ALUMINUM

L. Donev and L. Boyadzhiev

Central Laboratory of Technical Education for Industry (Sofia, Bulgaria)

The natural oxide film on an aluminum surface gives poor anticorrosion protection. In contrast to it, the oxide film obtained artificially possesses a numberof advantages. First, the resistance of the metal to corrosion is increased. Second, the hardness and abrasion resistance of the artificial oxide film is a valuable property. The hardness of the film fluctuates around 1500 kg/ mm^2, whereas tempered instrument steel has a much lower hardness [1]. In the way of comparison it could be mentioned that the hardness of cast aluminum is about 30 kg/ mm^2. The presence of copper, silicon and other metals causes a substantial reduction in the hardness of the film [2]. Third, the oxide film possesses good electrical insulation properties. At room temperature the resistivity of the film is about 10^9 Ω/ cm^2. The oxide layer is characterized by having a high adsorption capacity. This makes it easy to paint it with organic dyes (for example, aniline and other types) [3, 4].

The artificial oxide film can be obtained either chemically or electrochemically (anodic oxidation). The anodic oxidation of aluminum can be accomplished in electrolytes of variable composition. Some of the electrolytes used for this purpose contain sulfuric and oxalic acids, chromic anhydride, etc. The electrolyte containing 20% sulfuric acid has found the most extensive use [3, 5, 6]. The mechanism of the oxidation still remains quite obscure [7].

Two opposite processes take place when aluminum is anodically oxidized in sulfuric acid solution: formation of the oxide film and its solution in the sulfuric acid with the formation of aluminum sulfate. When the aluminum concentration in solution reaches 25 g/ liter, the electrolyte becomes unsuitable and should be replaced. According to the literature, the solution is corrected by adding ammonium sulfate, which leads to the deposition of the crystalline binary ammonium sulfate-aluminum sulfate salt. Large amounts of ammonium sulfate are consumed when this method is employed [1].

In this paper we studied the effect of a number of inhibitors on the dissolving of the oxide film in sulfuric acid during the anodic oxidation of aluminum. We had in mind the possibility of adding a small amount of an organic compound to extend the operating life of the electrolyte. Here, a thicker film is obtained in the same length of time. For this reason the time required for the anodic oxidation of aluminum can be reduced, which is an advantage in industry, where the oxidation is run on a large scale.

Despite the large number of publications on anodic oxidation in sulfuric acid solution, there is very little information as yet in the literature on the effect of inhibitors on this process.

It should be mentioned that inhibitors are usually compounds that contain elements of Groups 5 and 6. Especially active here are those that have a free pair of electrons in the outer shell [8]. For this reason we selected aniline hydrosulfate, ethyl alcohol, and glycerol as the test inhibitors.

EXPERIMENTAL

For the experiments we used A1M aluminum with the following composition: Al 99.56%, Fe 0.28%, Si 0.15%, Cu 0.01%. The oxidation was run in 20% sulfuric acid solution. The anodic current density reached 1 amp/ dm^2, and the voltage was 12 v. A thermostat was used to maintain the temperature at 20 ± 1°.

To insure constant experimental conditions, several samples were run at the same time. Since we were interested in obtaining a high concentration of aluminum sulfate in solution, the oxidations were run for 40 min. As inhibitors we investigated ethyl alcohol, glycerol, and aniline hydrosulfate. Parallel experiments were run in which control samples were oxidized in the absence of inhibitor.

Concentration of Inhibitors (in g/ liter)

Ethyl alcohol	6.84	13.68	34.20	68.4
Glycerol	10.5	21.00	52.5	–
Aniline hydrosulfate	0.5	1	2.5	5

After oxidation, the amount of aluminum in solution was determined. In addition, the corrosion resistance of the oxide film was tested by the drop method. For this we used a solution with the following composition.

Potassium dichromate	3 g
Hydrochloric acid (d 1.19)	25 ml
Water	75 ml

This solution destroys the oxide film and penetrates to the surface of the metal. The time, elapsing before the drop assumes a green color, characterizes the protective capacity of the oxide film.

All of the specimens were tested for their ability to adsorb organic dyes.

EXPERIMENTAL RESULTS

The amount of aluminum that went into solution varied from $0.745 \cdot 10^{-3}$ to $1.700 \cdot 10^{-3}$ g/ liter. The experimental results are given in the Table.

Test Results

Inhibitor	Inhibitor concentration (in g/ liter)	Amount of aluminum (in g/ liter $\times 10^{-3}$) after 20 min	Amount of aluminum (in g/ liter $\times 10^{-3}$) after 40 min
Ethyl alcohol	6.84	1.458	1.684
	13.68	1.262	1.482
	34.20	1.115	1.325
	68.4	1.037	1.258
Glycerol	10.5	1.192	1.422
	21.0	1.113	1.328
	52.5	0.975	1.176
Aniline hydrosulfate	0.5	0.957	1.177
	1.0	0.911	1.112
	2.5	0.842	1.029
	5.0	0.745	0.918

For the control specimen, oxidized in the absence of inhibitor, the amount of aluminum dissolved after 20 min was $1.457 \cdot 10^{-3}$ g/ liter, and after 40 min it was $1.700 \cdot 10^{-3}$ g/ liter.

All of the specimens withstood the test for corrosion resistance by the drop method.

The adsorption capacity of the obtained oxide film toward organic dyes proved to be the same for all of the specimens, and failed to differ from the control specimen.

From the data given above it is obvious that the addition of an inhibitor retards somewhat the dissolving of the oxide film. The addition of aniline hydrosulfate exerts the greatest inhibition, and the addition of ethyl alcohol the least. Even a small amount of aniline hydrosulfate (0.5 g/ liter) is sufficient to retard dissolving the oxide film. This inhibitor can also be used for anodic oxidation on an industrial scale. The addition of either ethyl alcohol or glycerol has little inhibiting effect.

SUMMARY

1. When aluminum was oxidized in sulfuric acid solution, in the presence of ethyl alcohol, glycerol, and aniline hydrosulfate as inhibitors, the amount of the aluminum that went into solution due to dissolving the oxide film ranged from $0.745 \cdot 10^{-3}$ to $1.700 \cdot 10^{-3}$ g/ liter.

2. The greatest retarding effect was observed when aniline hydrosulfate was used as the inhibitor, and the least when ethyl alcohol was used.

3. The adsorption cpacity of the obtained oxide films toward dyes remained the same in all cases.

LITERATURE CITED

[1] N. P. Fedot'ev and S. Ya. Grilikhes, Electrochemical Etching, Polishing, and Oxidation of Metals [in Russian] (State Scientific and Technical Press of Literature on Machine Building, 1957).

[2] R. S. Ambartsumyan (Editor), Corrosion and Protection of Metals [in Russian] (State Press of the Defense Industry, 1957).

[3] V. I. Lainer and N. T. Kudryavtsev, Principles of Electroplating [in Russian] (Metallurgical Press, 1957), vol. 2.

[4] Abstract Journal, Chemistry [in Russian] 5 (1958).

[5] R. Moshchev and Z. Vladov, Guide for the Protective Coating of Metals Based on Galvanic Principles [in Russian] (Public Light, Sofia, 1957).

[6] N. D. Tomashov and M. Zh. Tyukina, Trans. Inst. Phys. Chem. Acad. Sci. USSR 2 (1951).

[7] Ts. Mutafchiev, Applied Electrochemistry [in Russian] (Science and Art, Sofia, 1956).

[8] I. N. Putilova, S. A. Balezin, and V. P Barannik, Metal Corrosion Inhibitors [in Russian] (Goskhimizdat, 1958).

Received September 27, 1958

STUDY OF EFFECT OF COMPOSITION AND CONCENTRATION OF ELECTROLYTE SOLUTIONS ON ELECTROCHEMICAL ACTIVITY OF ION-EXCHANGE MEMBRANES

Z. P. Koz'mina, T. P. Zharinova, and G. P. Kisova

The electrochemical activity of a membrane is characterized by the change in the transference numbers of the ions in the membrane and depends both on the nature and structure of the membrane and the composition and concentration of the solution. For example, in a colloidion membrane with an average pore radius of 20 mμ the transference numbers of the ions change in 0.01N solutions for the case of the chlorides of Li, Na, K, Rb, and Cs [1], and do not change in solutions of the same concentration for the case of the chlorides of Ba, Ca, Mg, and Sr [2]. The electrochemical activity of a membrane decreases with increase in the solution concentration, in which connection membranes with a large average pore radius become electrochemically inactive at lower concentrations. Thus, for example, in a colloidion membrane with an average pore radius smaller than 65 mμ the transference numbers change in 0.01N KCl solution, but only the membranes with a pore radius smaller than 3 mμ are electrochemical-active when the concentration of the solution is 0.269 N [2].

A study of the effect of various factors on the electrochemical activity of membranes makes it possible to approach the problem of selecting rational conditions for the electrodialysis of different solutions in a more intelligent manner. It is known that the rate of change in the concentration of an electrolyte in the middle of an electrodialyzer depends, with other experimental conditions constant, on the difference in the transference numbers of ions in cathodic and anodic membranes [3]. The most efficient electrodialysis in achieved when ideally electrochemical-active membranes of opposite charge are used. In such case the difference in the transference numbers of the electrolyte ions in cathodic and anodic membranes reaches one.

In 1954, Grigorov, Kulikova, and Sharapova [4] proposed the use of membranes made of ion-exchange adsorbents for electrodialysis and developed a method for obtaining different types of ionite membranes. They prepared membranes from Cationites SBS, SBSR, and SDV-3, and from Anionites MMG-1, PE-9, and ÉDÉ-10P. In 0.01N KCl all of the cation-exchange membranes were close to ideally electrochemical-active membranes. Electrodialysis goes most efficiently with the least consumption of electrical energy when membranes made from ion-exchange adsorbents are used [4-6].

In their structure the ionite membranes differ sharply from the conventional membranes of the colloidion, ceramic, etc. type. It is possible to regard ion-exchange adsorbents as homogeneous systems, representing a sieve formed from a high-molecular compound, in which ion-exchange groups are located in individual spots. As a result, the term average pore radius, porosity, and filtration coefficient, characterizing the structure of conventional membranes, do not apply to such systems. However, due to the technology of preparation, even rigid membranes, prepared from ionites, possess a certain filtration coefficient, which is determined by the creation of empty spaces between the particles of ionite and bonding agent when they are pressed, or it could be due to the presence of pores in the bonding agent (cement). For powder membranes the greatest value of the filtration coefficient is determined by the presence of pores between the ionite particles.

In a powder membrane it is possible for the electric current to pass both through the ionite particles and through the solution, filling the pores. It is obvious that a change in the transference numbers of ions occurs mainly in the skeleton of the ionite particles.

The question of whether a change in the transference numbers of ions in a powder membrane will depend on the macrostructure of the latter has not been examined up to now, and obtaining an answer to this question was our first problem in the present investigation. We studied the transference numbers of ions in powder membranes made of SBS and SDV-3, having a different value of the filtration coefficient in 0.01N KCl solution. In a conventional rigid membrane the ion transference numbers are strongly dependent on the filtration coefficient of the membrane [2]. The effect of the nature of the electrolyte on the electrochemical activity of ion-exchange membranes was studied on the examples of the rigid membrane made from SDV-3 and the powder membranes made from SDV-3 and KM, using 0.01N solutions of LiCl, NaCl, KCl, $MgCl_2$, $CaCl_2$, and $BaCl_2$ as the test electrolytes. The effect of the electrolyte concentration on the change in the ion transference numbers in ion-exchange membranes was studied on the example of the rigid membrane made from SDV-3, using LiCl solutions.

EXPERIMENTAL

The cationites selected for preparing the membranes we re obtained in the hydrogen form by treatment with 0.5N HCl solution. From the hydrogen form the cationites were converted to the Li, Na, K, Mg, Ca and Ba forms by treatment with 0.5N solutions of the proper chlorides until alkaline to methyl orange. After this the cationite was washed with 0.01N solution of the proper chloride until the starting solution and that passing through the ionite had the same electroductivity. Then the cationites were dried, pulverized in a porcelain mortar, and sifted into individual fractions using standard Taylor screens.

The rigid membranes were prepared by the method described in the paper by Grigorov, Kulikova, and Sharapova [4].

To prepare the powder membranes, the processed resin was treated with a small amount of the proper solution and the obtained thick mass was transferred to a Plexiglas mold with a perforated bottom, which was covered with a sheet of filter paper. The mass was compressed, covered with a sheet of filter paper, and the whole was covered with a tightly fitting perforated cover. The powder membranes prepared in this manner made it possible to determine the necessary electrokinetic and structural characteristics of the membranes without disturbing their macrostructure.

The transference numbers of ions in a membrane were determined analytically with exclusion of electroosmotic transfer[2]. The current was supplied from a kenotron. The experiments on determining the transference numbers of ions in a membrane in 0.01N solution were run at a voltage of 400 v. When operating with solutions of lower concentration the voltage was increased to 1000 v. The concentration of the solutions was determined by potentiometric titration using a silver chloride electrode. The diffusion potential method, employing silver chloride electrodes, was used to determine the ion transference numbers in more concentrated solutions. The macrostructure of the powder membranes we characterized mainly by the filtration coefficient, which was determined in conventional manner [2], except that the liquid passing through the membrane was 0.01N KCl solution.

For some of the membranes the total porosity W was calculated using the equation

$$W = \frac{V - \frac{m}{d}}{V},$$

where V is the membrane volume, and m and d are respectively the weight and density of the ionite.

To calculate the average pore radius we used the equation

$$r = \sqrt{\frac{24Dd\eta}{W}},$$

where D, d, and W are respectively the filtration coefficient, thickness, and total porosity of the membrane, and η is the viscosity coefficient of the liquid.

To study the relation between transference numbers of ions in ionite powder membranes and the macrostructure of the latter, we took three fractions of Cationit SBS (<44, 62-88, and 297-350 μ), and 3 fractions of Cationit SDV-3 (<44, 44-62, and 62-88 μ). By subjecting powdered ionite SBS, with a particle size smaller than 44 μ, to a variable degree of compression we obtained several membranes with the filtration coefficient ranging from 9×10^{-9} to 3.98×10^{-8}. We prepared but a single membrane from each of the other two fractions, and the filtration coefficient was 1.52×10^{-7} and 1.2×10^{-6}. Parallel with the filtration coefficient, we determined the ion transference numbers in 0.01N KCl solution.

The data obtained by us are given in Table 1, from which it follows that the ion transference numbers in the membrane have practically the same value when the filtration coefficient is increased from 9×10^{-9} to 10^{-7}, and only for the latter membrane was some increase in the transference numbers of the chlorine ion observed. A reduction in the change of the ion transference numbers in the given membrane can be explained as due to experimental error, since with such a large filtration coefficient ($D = 1.2 \times 10^{-6}$) a slight change of the level in one of the compartments of the apparatus can cause a reduction in the concentration changes due to filtration of the solution through the membrane.

TABLE 1

Study of Transference Numbers in Powder Membranes Prepared from SBS

Fraction (μ)	D $\frac{cm^2 \times sec}{g}$	W (in %)	r(mμ)	n'_{Cl}
I — <44	$9.11 \cdot 10^{-9}$	47.5	455	0.218
	$9.67 \cdot 10^{-9}$	53.7	441	0.215
	$2.16 \cdot 10^{-8}$	47.8	492	0.217
	$3.98 \cdot 10^{-8}$	48.3	942	0.211
II — 62—88	$1.53 \cdot 10^{-7}$	—	—	0.214
III — 297—350	$1.2 \cdot 10^{-6}$	—	—	0.278

The data obtained in studying the transference numbers of ions in powder membranes made from ionite SDV-3 of different dispersity are given in Table 2, and here the filtration coefficient varied from 9×10^{-9} to 1.2×10^{-7}. The transference numbers of ions in membranes made from SDV-3, the same as in the case of the membranes made from SBS, did not change when the degree of dispersion of the ionite was reduced, and consequently, they did not change with change in the macrostructure of the membrane. The obtained results support our theory that a change in the transference numbers of ions in such membranes occurs in the particles of the ionite. Actually, the transference numbers of ions cannot change in pores, the average radius of which

TABLE 2

Study of Transference Numbers in Powder Membranes Prepared from SDV-3

Fraction (μ)	D $\frac{cm^2 \times sec}{g}$	n'_{Cl}
I — <44	$9 \cdot 10^{-9}$	0.113
II — 44—62	$2.9 \cdot 10^{-8}$	0.116
	$5.03 \cdot 10^{-8}$	0.119
III — 62—88	$1.2 \cdot 10^{-7}$	0.123

exceeds 400 mμ. However, the presence of such pores in the investigated membranes reduced the variation in the transference numbers of the ions when compared with rigid ionite membranes, since a certain amount of electricity is transported by the ions of the solution found in these pores. Because of slight changes in the total porosity of powder membranes (Table 1), a change in the ion transference numbers when compared with a rigid membrane reduced to the same value, and proves to be independent of the macrostructure of the membranes. This made it possible to study the effect of solution composition on the change in the transference numbers of ions in both rigid and powder membranes.

TABLE 3

Effect of Solution Composition on Change in Transference Numbers

Membranes	Transference number of cation	0.01N Solution					
		LiCl	NaCl	KCl	$MgCl_2$	$CaCl_2$	$BaCl_2$
Rigid membranes made from SDV-3	In the free solution, n	0.330	0.397	0.496	0.407	0.435	0.446
	In the membrane, n'	0.937	0.937	0.966	0.966	0.942	0.964
	$\frac{\Delta n}{n} \cdot 100$	185.6	136.0	94.7	137.3	116.5	116.1
Powder membranes made from SDV-3	n'	0.764	0.804	0.886	0.750	0.781	0.800
	$\frac{\Delta n}{n} \cdot 100$	131.5	102.5	78.8	84.3	81.8	79.4
Powder membranes made from KM	$\frac{\Delta n}{n} \cdot 100$	0.647 98.3	0.699 71.1	0.767 54.5	— —	— —	— —

To prepare the rigid and powder membranes in the present case we used the fractions of Cationits SDV-3 and KM having a particle size smaller than 44 μ. The obtained experimental data are given in Table 3. From an examination of the data given in this table it follows that for all of the investigated solutions the transference number of the cation in the rigid membrane made from ionite SDV-3 lies close to one. As a result, in contrast to the membranes usually used in electrodialysis, represented by colloidion, ceramic and other types of membranes, the investigated membrane proved to have the same electrochemical activity in solutions of both univalent and bivalent cations. When compared with the rigid membranes, the powder ionite membranes proved to be less electrochemically active in all of the solutions investigated. When the transference numbers of cations in powder membranes were arranged in order of increasing value, we obtained the same series as were found to hold in the case of colloidion membranes [7]:

$$n'_{Li} < n'_{Na} < n'_{K},$$
$$n'_{Mg} < n'_{Ca} < n'_{Ba},$$

Comparing the changes in the cation transference numbers in ionite membranes with their values in the free solution gives, the same as in the case of colloidion membranes, the reverse order, i.e., Li > Na > K, and Mg > Ca > Ba, corresponding to the ratios of the hydrodynamic radii of these ions in water solutions. A sharp difference in the change of the transference numbers of univalent and bivalent cations, observed when colloidion membranes were investigated, was not observed by us for either the powder ionite membranes or the rigid type. The powder membranes prepared from SDV-3 proved to be electrochemically active in all of the investigated solutions. The membranes prepared from ionite KM possess a somewhat smaller electrochemical activity (Table 3). As was indicated above, we studied the effect of electrolyte concentration on the transference numbers of ions in a membrane on the example of using LiCl solution and a rigid membrane made from SDV-3. The transference numbers of the ions were determined by the diffusion potential method. In the concentration interval from 0.005 to 0.1N we also used the analytical procedure to determine the transference numbers. The obtained results are given in Table 4.

From the data given in Table 4 it can be seen that the change in the transference numbers decreases with increase in the electrolyte concentration. However, even with a 3N solution there is a substantial change in the transference numbers of the ions in the membrane. For rigid ionite membranes to show such a high electrochemical activity in concentrated solutions is especially important when they are used for the electrodialysis of like solutions.

TABLE 4

Effect of Electrolyte Concentration on Transference Number in a Membrane Made from SDV-3

Analytical method			Based on the diffusion potential		
concentration of LiCl solution	transference number of Li in the free solution	n'_{Li}	concentration of the solution c_1	concentration of the solution c_2	n'_{Li}
0.005	0.330	0.989	0.010	0.020	0.981
0.0100	0.330	0.946	0.096	0.202	0.854
0.020	0.328	0.937	0.507	1.061	0.736
0.100	0.313	0.888	0.910	1.965	0.600
—	—	—	1.965	4.093	0.470

SUMMARY

1. The transference numbers of ions in powder ionite membranes are independent of the membrane macrostructure, which supports our theory that a change in the transference numbers of ions occurs in the particles of the ionite.

2. The transference numbers of cations in rigid membranes made from SDV-3 in 0.01N solutions of LiCl, NaCl, KCl, $MgCl_2$, $CaCl_2$ and $BaCl_2$ lie close to one. In the less active powder membranes they increase in the following order: Li < Na < K, Mg < Ca < Ba.

Comparing the changes in the transference numbers of cations in ionite membranes with their values in the free solution gave the reverse series: Li > Na > K, Mg > Ca > Ba, corresponding to the ratios of their hydrodynamic radii.

3. It was established that rigid membranes made from ionite SDV-3 possess a high electrochemical activity in concentrated solutions.

LITERATURE CITED

[1] I. I. Zhukov and Z. P. Koz'mina, Colloid J. (USSR) 8, 221 (1946).

[2] O. N. Grigorov, Z. P. Koz'mina, A. V. Markovich, and D. A. Fridrikhsberg, Electrokinetic Properties of Capillary Systems [in Russian] (Izd. AN SSSR, 1956).

[3] I. I. Zhukov, Prog. Chem. USSR 12, 265 (1943); O. N. Grigorov and Yu. S. Afanas'eva, Colloid J. (USSR) 8, 311 (1946); A. V. Markovich, Sci. Reports Leningrad State Univ., Chem. Series 108, 71 (1949).

[4] O. N. Grigorov, K. F. Kulikova, and A. I. Sharapova, Proc. Acad. Sci. USSR 94, 501 (1954).

[5] O. S. Linchevskii, Themes of Reports Delivered at the Scientific-Technical Conference on the Purification of Drinking Water [in Russian] (All-Union Scientific Research Institute for Water Supply, Sewer Systems, Hydraulic Structures, and Hydrogeological Engineering, 1955).

[6] A. G. Winger, G. W. Bodamer, R. Kunin, C. J. Prizer, and G. W. Harmon, Ind. Eng. Ch. 47, 50 (1955).

[7] L. Michaelis, J. Gen. Physiol. 10, 5, 671 (1927).

Received July 16, 1958

INTENSIFICATION OF ELECTROLYSIS PROCESSES BY INTRODUCTION OF COMPOUNDS WITH COVALENT BONDS INTO SOLUTIONS

P. P. Belyaev

Scientific Research Institute of Chemical Machine Building

Intensification of electrochemical treatments of metals, accomplished by increasing both the temperature and the electrolyte concentration, as well as by resort to mixing and increasing the current density, although carried to the limit in most cases, has still failed to reduce the duration of the operations to a matter of less than several minutes. At the same time, in installations of continuously moving cold-rolled strip, the duration of the processes should be reduced to a matter of several seconds.

Treatments, falling within a span of 10 seconds, we tentatively called rapid, and began to search for ways of speeding them up by making it easier for a given process to go, and here even the possibility of simultaneously reducing both the solution concentration and the temperature was considered.

Electrochemical cleaning of a metal surface, if it is accomplished by desorption as the result of surface overvoltage, should fall within a time interval of 1×10^{-8} seconds. If removal of foreign substance by formation of a dense separating gas (hydrogen) layer is considered, then for cleaning it is sufficient that the electrolysis continue for 1×10^{-5} seconds at a current density of 10 amp/ dm^2. In this time a gas film with a thickness exceeding 8000 A is obtained, i.e., theoretically it will be sufficiently thick to exclude the reaction of any substance in the solid state. This example shows that for rapid cleaning it is permissible to use alternating current of industrial frequency (with a half-period of 1×10^{-2} sec) for the electrolysis.

Examination of equation (1), linking the electrolysis rate with the concentration of the reactants [1], leads to the conclusion that in order to run rapid processes it is not necessary to go to concentrated solutions:

$$\tau_e = \frac{l_a \cdot S_a \cdot d_n}{S_e \cdot D_M \cdot C_c}, \qquad (1)$$

where τ_e is the time required to liberate (dissolve) one atom of the metal (in sec, l_a is the thickness of a monoatomic layer of the liberated (dissolved) metal (in cm), S_a is the face of one atom of the metal (in cm^2), d_n is the density of the metal, S_e is the face of a unit volume of the electrolyte, containing one cation of the metal (in cm^2), D_M is the maximum current density (in amp/ cm^2), and C_c is the electrochemical equivalent of the metal (in g/ amp-sec).

From the data given in Table 1 it can be seen that the fast processes can be run at electrolyte concentrations below 0.1 N. In the absence of concentration polarization, it could be possible to operate with a current density exceeding 10-100 amp/ cm^2 when the reactant concentration lies between 0.1 and 1 N.

Studies on regulating the electrolytic deposition of metal coatings by introducing surface-active colloidal substances into solutions have been made for a long time. Izgaryshev and Titov, who started these studies in the USSR in 1917 [2], considered the favorable effect exerted by additions to be due to the formation of complexes in the solution. Frumkin [3] believes that the main effect here is caused by a redistribution of the electrical state at the electrode–electrolyte boundary as the result of the additive adsorbing on the surface of the electrode.

TABLE 1

Change of Parameters in a Quasi-Crystalline Solution with Dilution of the Electrolyte

Parameters	Values of parameters							
Concentration (in mole/ liter)	10	4	2	1	0.5	0.25	0.1	0.01
Unit volume in the solution, $U_e A^3$	166	415	830	1660	3230	6640	$166 \cdot 10^2$	$166 \cdot 10^3$
Unit length in the solution, $l_e = (U_e)^{1/3} A$	5.5	7.46	9.4	11.84	14.92	18.80	25.21	55
Unit surface in the solution, $S_e = (U_e)^{2/3} A^2$	30.25	55.65	88.36	140.2	222.6	353.4	650	$3 \cdot 10^3$
Ratio:								
$\frac{U_e}{U_a}$	2.41	6.02	12.05	24.10	48.2	96.4	241	$241 \cdot 10^3$
$\frac{S_e}{S_a}$	1.80	3.51	5.24	8.35	13.25	21.0	38.7	180
$\frac{l_e}{l_a}$	1.34	1.82	2.29	2.89	3.64	4.58	6.22	13.4
Number of cations (n) in a unit layer of the solution on an electrode surface equal to 1 dm^2, degree of dissociation 100%	$3.30 \cdot 10^{16}$	$1.8 \cdot 10^{16}$	$1.13 \cdot 10^{16}$	$7.13 \cdot 10^{15}$	$4.49 \cdot 10^{15}$	$2.83 \cdot 10^{15}$	$1.53 \cdot 10^{15}$	$3.3 \cdot 10$
D_M – maximum current density (at $\tau_e = 10^{-7}$ sec (in amp/ cm^2)	527	286	281	113.5	71.5	45.1	24.5	5.27

Loshkarev [4] discovered the phenomenon of a low limiting diffusion current in the presence of a number of adsorbed substances. However, it was shown by Gorbunova and Vagramyan [5] that some surface-active substances, although they do change the electrical state, may exert a negative effect due to a local firm attachment of the adsorption product. In 1950-1951 the present author [6] expressed the theory that it is necessary for the surface-active substances used as additives to have the property of inhibiting chemical reaction of the solution with the electrode, and specifically, to inhibit its oxidation, ie., to possess the property of a selective permeability of the ions when a current is passed through the adsorption film. This same requisite was formulated by Matulis [7] in 1956 as being the ability of additive to cover the active portions of the electrode. In our studies we concentrated on investigating non-ionogeneic additives, forming secondary or covalent bonds when reacted with the metal of the solvent and with impurities, for example, fats. Preference was given to water-soluble reagents having a high heat stability. The principal characteristics of compounds with a covalent bond is their high mobility at elevated temperature and the presence of spatially oriented bonds. These properties should be retained and appear to variable degree also in complex compounds, including complexes. At the same time, fixing the non-ionogenic molecule in the complex does not necessarily lead to excluding reaction of the ionic bonds. For this reason there could be cases where the appearance of a covalent bond causes an increased stability of the electrolyte, not only in the absence of current passage, but also where it facilitates the electrolysis conditions. Kolotyrkin [8] assumes that it is possible to change the electrolysis course with compounds having a covalent bond.

In this paper we give data on the effect of adding emulsifiers of the OP-7 type, inner complexes, including Trilon B, and also glycerin and sugar. A description of the effects is given in the order usually applying in technological electroplating operations.

Electrolytic Degreasing

Kabanov and Frumkin [9] considered the influence exerted by an electric current in electrolytic degreasing as due to a change in the surface tension at the boundary of the phases, and also as due to the hydrostatic effect exerted by the liberated gas (hydrogen) bubbles.

We prescribed the following requirements for the emulsifiers that we introduced as additives: 1) facilitate a fixing of the grease particles in the liquid without causing a profound structural change in the reactants; 2) protect the surface of the metal from the oxidative action of the degreasing liquor by a semipermeable film; 3) secure a simultaneous wetting of the surface by aqueous solutions, i.e., make it hydrophilic and permeable for the ions (in particular, hydrogen) during electrolysis. The optimum case appeared when non-ionogenic additives of the polyethylene glycol ether type, known under the designation of OP, were added.

At the present time the structural formula assigned to these compounds is tentatively depicted as

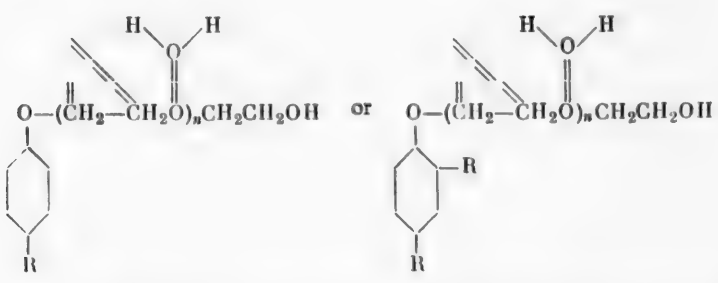

(2)

where R is an alkyl radical, containing 9-10 carbon atoms, and n, on the average, is equal to 6-7 for compound OP-7, and 10-12 for compound OP-10.

Below a certain temperature these compounds become true solutions in water, which is determined by the liquid becoming clear.

Reaction of the particles with water is considered to be through the oxygen of the glycol groups; this is shown by = =. In our opinion, adsorption of the metal can be accomplished in this case through the carbon

of the glycol groups; we have shown this by = = =; while cleavage of the grease is caused by the carbon linked to the hydrogen; this is shown by =.

In practical operation it was found that the degreasing rate rises if the introduction of an additive is supplemented by electrolysis, including the alternating current of industrial frequency (Table 2).

TABLE 2

Removal of Emulsion from Cold-Rolled Steel Strip

Emulsifier and amount used	Temp. (in °C)	Time of chemical degreasing (in sec)	Current density (in amp per dm^2)	Length of treatment (in sec)			
				direct current		alternating current	
				cathodic	anodic	direct contact	without metal contact
Without emulsifier	70	1380	8	1200	—	1200	1200
	95	1080	8	900	—	1080	1140
Sodium soap, 5 g/ liter	70	850	4	132	—	300	480
			8	120	—	260	420
	95	540	4	60	—	150	270
			8	45	—	120	240
Water glass	70	1080	4	150	150	210	1260
			8	120	120	180	1140
	95	390	4	75	60	120	900
			8	60	75	105	840
OP-7, 3 g/ liter	70	300	4	45	150	30	80
			8	15	135	15	50
	95	195	4	30	90	10	40
			8	10	70	10	35
OP-7, 5 g/ liter	70	150	4	30	90	10	60
			8	10	75	10	45
	95	105	4	15	60	5	30
			8	10	60	5	30
Nekal BX, 3 g/ liter	70	75	4	180	150	10	45
			8	180	135	10	30
	95	45	4	60	90	10	30
			8	45	75	5	30
Nekal BX, 5 g/ liter	50	45	4	150	75	10	75
			8	120	60	10	60
	95	35	4	150	75	10	75
			8	120	60	10	60
Triethanolamine, 3 g/ liter	50	1560	4	495	240	790	1680
			8	470	225	670	1620
	95	1080	4	390	150	810	1330
			8	360	120	790	1320
Triethanolamine, 5 g / liter	70	1660	4	795	135	810	1680
			8	760	125	790	1620
	95	1580	4	520	150	670	1380
			8	460	120	600	1320

A characteristic trait of the regulators with a covalent bond is a retention of the usual relationship in the change of the rate of the electrolytic process as a function of the concentration, temperature, and current density. There occurs as it were a shift of the curves in the coordinate systems.

The electrolysis of alkaline solution using alternating current of industrial frequency goes at a current density up to 10-20 amp/ dm^2 without an accumulation of either molecular hydrogen or oxygen. For this

reason the process becomes not only fast, but also explosion-proof. The time required to remove grease from cold-rolled strip using the technique of an additive and electrolysis can be reduced to 1-2 sec. Use of the indicated emulsifiers also permits obtaining rapid cleaning in water solutions when operating with ultrasonic vibrations.

Electrolytic Etching

In the electrolytic etching of metals it is also possible to effect the removal of oxides very rapidly, i.e., in a time of the order of 1×10^{-5} second. The main requisites for accomplishing purification in this case are in general the same as those that hold in degreasing. We assumed that the most complete separation of the operations of oxide removal and dissolving the base metal could be accomplished by the use of complex-formers. Experiment revealed that such a method actually does work for the removal of oxides from carbon steels in alkaline solutions when Trilon B (disodium salt of ethylenediaminotetraacetic acid) is used as the complex-former. The iron, nickel, copper, calcium and magnesium ions are seized by the additional coordination bond, giving stable inner complexes [10, 11] according to the scheme•

Fig. 1. Specimens of low-carbon steel, etched electrolytically in aqueous caustic solution.

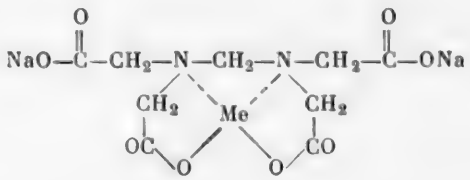

(3)

Experiments with aqueous caustic solutions of a complexon in the presence of emulsifier OP-7 confirmed the possibility of removing oxides from carbon steel (Fig. 1). A cathodic treatment is needed for this. With a current density of 0.5-4 amp/dm^2, the removal of oxide films, ranging in thickness up to 700 A, occurs in 5-10 seconds. Degreasing occurs at the same time. Consequently, intensification is accomplished via a rapid removal of oxides, combining this operation with degreasing and a complete exclusion of dissolving the base metal. Taking into consideration the fact that excess iron can be removed from solution by electrolysis in a separate operation, we obtain a purification process with a system of regenerating the solution that is very convenient in practice.

Quite efficient methods also exist for the intensification of etching in acid solutions. Included here is the addition of emulsifier OP-7 to hot sulfuric acid solutions. Here also the etching operation proceeds simultaneously with the degreasing operation.

Electrolytic Deposition of Metals

The well defined action of non-ionogenic additives was shown by the author in electrolytic tin-plating in acid solutions and in lead-coating in alkaline solutions. Trilon B functioned as an additive in the acid tin-plating solutions. Here the favorable effect after adding Trilon B (in much less than the theoretically required equimolecular amount) appeared not only in the quality of the coating, but also in the stability of the solution. Hydrolysis was retarded sharply (Fig. 2) after adding a total of only 1-10 g/liter, instead of the amount (126 g/liter) needed to tie up the tin in the complex. The stabilization lasts for several months. The current density for a dense deposition of tin on sheet iron could be expanded to a range of 1-60 amp/dm^2 instead of the 15-35 amp/dm^2 without this additive (Fig. 3). At the same time, it proved possible to establish that the addition of emulsifier OP-7 to Trilon B in a tin-plating electrolyte containing sulfuric acid

• The coordination bond is shown by a broken line

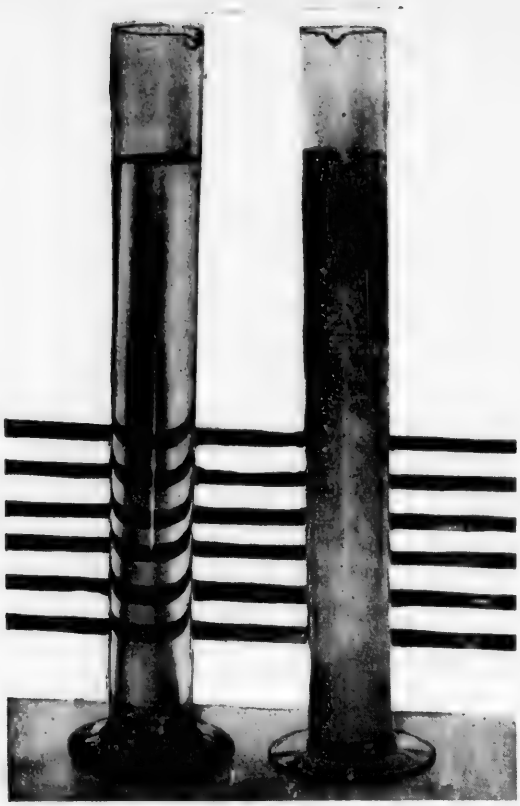

Fig. 2. Retardation of hydrolysis in a tin-plating electrolyte containing sulfuric acid. The left graduate shows a solution with stabilizer after 30 days, while the right graduate shows the same solution without stabilizer after 1 day.

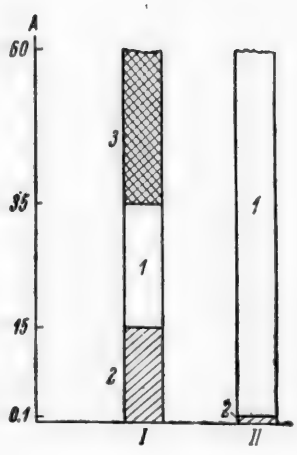

Fig. 3. Structure of electrolytically deposited tin on cold-rolled strip in acid solutions. A) current density D_K (in amp/dm^2). 1) region of uniformly dense fine-grained deposits; 2) region of powderlike deposits at low current densities; 3) region of appearance of dendritic powders and spongy deposits at extremely high current densities. I) in electrolyte without complexon; II) in electrolyte with complexon.

permits excluding all additives of a colloidal nature, eliminates the need of treating with flux prior to bonding, and yields a uniform bond, without bead formation, on cold-rolled sheet iron at a coating thickness of 2 to 3 μ. Such a layer can be deposited in a matter of 5 to 8 seconds.

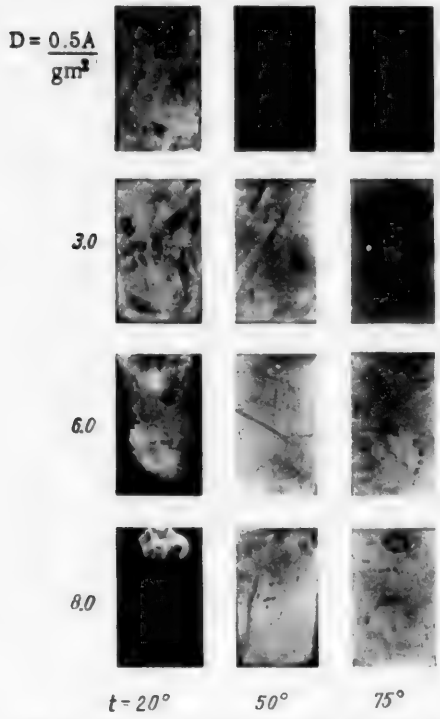

Fig. 4. Change in the structure of lead deposited electrolytically from alkaline solution with stirring.

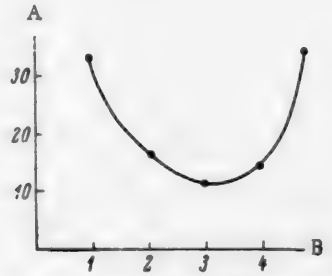

Fig. 5. Change in the porosity of a 50 μ thick lead coating deposited by electrolysis on polished steel (Class 9 purity) as a function of the cathodic current density, with stirring of the electrolyte using compressed air. A) average number of pores (per dm^2); B) cathodic current density (in amp/cm^2).

In alkaline lead-coating electrolytes it is possible to obtain dense deposition in the presence of such practically non-ionogenic additives as, for example, the phenol alcohols. These compounds are assigned the structural formula shown in scheme (4)

$$\left[\begin{array}{l} C_6H_4OH—CH_2C_6H_3 \cdot OHCH_2 \\ | \\ CH_3OH \end{array}\right]_n \left(=\!=O\!<\!\begin{array}{l} H \\ H \end{array}\right) \quad (4)$$

That these compounds show complexing properties was demonstrated by the dissolving of dry lead oxide. That the additive exerts a protective action was shown by a retarding of iron oxidation, which was revealed by determining the stationary potentials.

The dense deposition of lead was also achieved in alkaline solutions containing glycerin and sugar. The favorable influence of raising the temperature and the use of stirring is also retained in the presence of these additives. The addition of surface-active substances also permits a distinct expansion in the range of current densities that give compact coatings in electrolysis. Here the oxidative action exerted on the coating appears at both high and low current densities (Fig. 4). However, we were unable to obtain high current densities in alkaline lead-coating solutions.

In addition, we will mention that we were able to establish an increase in the porosity of the lead coating when an additive was present, both in going from the optimum value to a high current density and at low densities (Fig. 5). This again emphasizes the need for taking additional precautions to retard the action of the electrolyte on the surface being treated during electrolysis. The presence of cathodic protection of the electrode is not always sufficient.

SUMMARY

1. Processes for the electrolytic treatment of metals possess enormous possibilities in ways of speeding them up.

2. A very promising way of obtaining intensification proved to be the addition of non-ionogenic substances, possessing a well defined covalent bond, to the electrolyte.

3. The usual relationships of change in the temperature, concentration, stirring, and current density are retained when compounds with a covalent bond are present in the electrolyte, but the range of optimum processing conditions is expanded.

4. The assumption that additives regulating the electrolytic treatment of a metal must possess the ability to retard the oxidative action of the solution on the metal being treated, i.e., they must function as inhibitors, was verified.

LITERATURE CITED

[1] P. P. Belyaev, Transactions of Vilna Conference on Electrochemistry [in Russian] (Lithuanian Academy of Sciences Press, 1957), p. 151.

[2] N. A. Izgaryshev and P. S. Titov, J. Russ. Phys.-Chem. Soc. 49, 573 (1917).

[3] A. N. Frumkin, E. S. Bagotskii, Z. A. Iofa, and B. N. Kabanov, Kinetics of Electrode Processes [in Russian] (Izd. MGU, 1952).

[4] M. A. Loshkarev, Doctoral Dissertation, Inst. Phys. Chem. Acad. Sci. USSR (1948).

[5] K. M. Gorbunova and A. T. Vagramyan, Proc. Acad. Sci. USSR, No. 2, 445 (1935).

[6] P. P. Belyaev, Supplement No. 15, Scientific Research Institute of Chemical Machine Building (State Scientific and Technical Press of Literature on Machine Building, 1954); P. P. Belyaev, Supplement No. 11, NIIKhIMMASh (Mashgiz, 1951).

[7] Yu. Yu. Matulis, Transactions of Vilna Conference on Electrochemistry [in Russian] (Lithuanian Academy of Sciences Press, 1957), p. 135.

[8] Ya. M. Kolotyrkin, J. Phys. Chem. (USSR) 25, 1248 (1951).

[9] B. N. Kabanov and A. N. Frumkin, J. Phys. Chem. (USSR) 7, 539 (1933).

[10] R. Pribil Complexons in Chemical Analysis [Russian translation] (IL, Moscow, 1953).

[11] C. D. Leonard, Electroplating and Metal Finishing 7, 10, 365 (1954).

Received March 30, 1959

STUDY OF CORROSION RESISTANCE OF SHEET CAST IRON

A. S. Afanas'ev and B. Sh. Shteinberg

At the present time sheet cast iron is used essentially as roofing material. Therefore, one of its main required characteristics is its resistance to atmospheric corrosion. Bibliographical data on the resistance of sheet cast iron to atmospheric corrosion are very limited, sometimes contradictory, and do not account for the effect of various internal factors affecting corrosion (chemical composition, structure, treatment) or external factors (composition of the atmosphere, impurities). According to Bauer, Kronke, and Massing [1], atmospheric corrosion of cast iron is more uniform and weaker than the corrosion of cast steel. On the basis of the experiments described by Heyn and Bauer [3], Krenig assumes [2] that there is no significant difference between the corrosion of iron, steel and cast iron in the atmosphere or in water. Uhlig [4] gives only the data published by Friend [5], who showed that after 6 years of exposure to an industrial atmosphere the corrosion rate of cast iron containing 1% P is approximately the same as that of steel containing copper. He explains the absence of more detailed data by the fact that cast iron is ordinarily used in very large thicknesses.

It is obvious that these fragmentary bibliographical data cannot be used as the basis for determining either the conditions under which cast iron can be used or to work out means of increasing its corrosion resistance and its optimum chemical composition. It was necessary to make a systematic study by using long range (many years) corrosion experiments in order to determine the effect of the different factors on the corrosion resistance of cast iron: the composition of the atmosphere, and the composition and structure of cast iron. The results of a five year study are described below.

METHOD OF INVESTIGATION

Cast iron of different chemical compositions (Table 1) was prepared, formed into sheets, and annealed in accordance with the technique worked out by the experimental plant of the central Committee of Heavy Industry. The chemical analysis, the mechanical properties, and the microstructure of the prepared sheets were checked. Investigation of the corrosion resistance was made in the laboratory, in field installations, and under natural conditions.

Laboratory experiments were made in an automatic corrosion chamber, of the carousel type, allowing simultaneous testing of up to 160 samples in media of different degrees of aggressiveness [6, 7]. In general the experiments were made under the two following condistions: 1) Fog-rain conditions (rain for 5 minutes, interruption for 30 minutes, etc.); 2) Rain with SO_2 (rain for 5 minutes, interruption for 55 minutes, etc.); 0.1-.05% of SO_2 by volume (obtained by burning a given amount of sulfur) was introduced once every 8 hours. The first of these conditions was meant to imitate a humid atmosphere not contaminated by aggressive gases. Relative humidity, controlled by the August Psychometer mounted in the corrosion chamber, was 96-100%; the temperature was 35 ± 3°C. The second set of conditions was meant to imitate a humid industrial atmosphere strongly contaminated by sulfurous gas.

Field test were performed at two corrosion stations by exposing the samples on the roofs of buildings: Station No. 1 was located at a sea shore industrial region on the grounds of a large machine construction plant, and Station No. 2 in a central residential area of the town of Odessa. Corrosion was measured mainly by the gravimetric method. At the same time the mechanical properties of the sheets were measured, and the macro and micro aspects of corrosion determined. The products of corrosion were eliminated by cathodic

etching in an 8-10% NaOH solution and intermittent removal with a brush under a stream of water [8, 9]. Three to five samples were used for every experimental point. The experimental results were treated statistically [10]. The maximum duration of experiments in the corrosion chamber was 1000 hours; the intermediate periods were 200 and 600 hours. The chamber operated 8 hours in every 24. The rest of the time the samples remained in the chamber at the relative humidity of 100%. The maximum duration of the field tests was 4 years. The intermediate periods were 3 to 6 months. The comparison samples for the laboratory and the field experiments were made of a low alloy roofing steel (GOST 1393-47) containing 0.15% Cu, 0.20% Ni and 0.12% Cr.

TABLE 1

Chemical Composition of Cast Iron and Steel Samples

Sample No.	Chemical Composition, %									Remarks
	C	Si	Mn	P	S	Al	Cu	Ni	Cr	
0	0.10	0.15	0.41	0.018	0.047	—	0.15	0.20	0.12	GOST 1393-47
5	3.48	1.49	0.47	0.088	0.058	—	—	—	—	TU MSKhM 282-53
7	3.40	2.43	0.45	0.052	0.070	—	—	—	—	
8	3.66	0.52	0.42	0.077	0.070	0.44	—	—	—	
9	3.64	0.51	0.41	0.095	0.086	0.99	—	—	—	
10	3.56	1.63	0.63	0.084	0.052	—	0.24	—	—	
11	3.56	1.63	0.63	0.084	0.052	—	0.47	—	—	
27	3.48		0.73	0.104	0.062	—	—	—	—	Graphite-ferrite
30	3.35	2.67	0.73	0.300	0.041	—	—	—	—	
31	3.32	2.70	0.70	0.600	0.037	—	—	—	—	
35	3.36	1.57	0.44	0.112	0.070	—	—	—	—	
36	3.29	1.31	0.44	0.112	0.120	—	—	—	—	
46	3.17	0.93	0.40	0.140	0.228	—	—	—	—	Graphite-perlite
82	3.35	1.22	0.54	0.094	0.102	—	—	—	—	Graphite-ferrite
87	3.17	0.93	0.40	0.140	0.228	—	—	—	—	Graphite-perlite
88	3.17	0.93	0.40	0.140	0.228	—	—	—	—	Graphite-ferrite
91	3.26	1.59	0.20	0.25	0.38	—	—	—	—	Graphite-perlite
92	3.38	1.12	0.25	0.128	0.300	—	—	—	—	
+1	3.29	1.68	0.38	0.094	0.103	—	0.14	—	—	
+2	3.48	1.65	0.43	0.104	0.108	—	0.48	—	—	
+3	3.45	1.68	0.67	0.105	0.089	—	0.20	—	—	graphite-ferrite
+5	3.29	1.37	0.44	0.070	0.110	—	0.10	—	—	
+7	3.29	1.51	0.40	0.070	0.108	—	0.30	—	—	
+8	2.91	1.31	0.44	0.066	0.120	—	0.08	—	—	

Experiments under natural conditions were made on experimental roofs in Odessa, which were investigated periodically. Furthermore we investigated over 100 cast iron roofings produced at different plants and exposed to different climatic conditions (southern and central USSR, Middle Asia, and Siberia) in atmospheres of different degrees of aggressiveness – in towns and industrial areas. Characteristic sheets taken from roofs were subjected to metallographic and chemical analysis. These data characterize only the general resistance of cast iron in different atmospheres and do not give data on the effect of variations in manufacturing conditions or conditions of installation and use.

Electrochemical study. The first series of experiments (A) consisted in drawing curves of the variation of potential as a function of time, $\varphi = f(\tau)$, for the samples of the main types of sheet cast iron and roofing steel; the curves were drawn up to the time when the potential became stationary. The second series of experiments (B) consisted in drawing curves of the variation of potential as a function of the density of current, $\varphi = f(I_D)$, during cathodic and anodic polarization. All the experiments were performed in water which was being continuously saturated with oxygen. The saturated calomel electrode served as reference electrode. In the A series the first measurement was made as soon as possible after the beginning of the experiment (10 to 20 seconds afterward); after this initial measurement further measurements were made every 2 minutes. In experiments of the B series the polarization was started after the value of φ was stabilized (30 to 40 minutes after the beginning of the experiment). The

density of the current on the sample was measured every 2 minutes after the potential was measured. The density of the current varied from 0.01 to 15 ma/ cm^2 of the visible surface of the sample. In each experiment the density of the current first rose from zero to a maximum value and then dropped back to zero. The electrode potential, φ, was measured by using the ordinary PPTV-1 potentiometer.

RESULTS OF CORROSION EXPERIMENTS

Corrosion resistance of sheet cast iron in atmospheres of different degrees of aggressiveness. Figure 1 represents the results of laboratory corrosion experiments for sheet cast iron and roofing steel under the two sets of conditions. The figure shows that the resistance of cast iron is about three times higher than the resistance of roofing steel (even of low alloy steel) under the fog-rain test without SO_2. These data are in good agreement with the results of the observations made on cast iron roofs located in a noncontaminated town atmosphere.

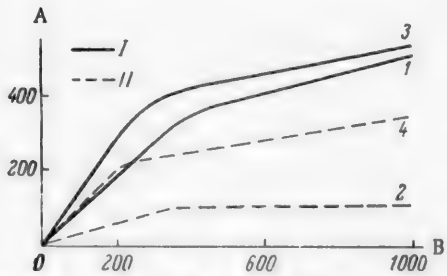

Fig. 1. Corrosion of sheet cast iron and roofing steel in laboratory tests. A) Loss of weight, in g /m^2, B) duration of test, in hours. I) with SO_2, II) without SO_2. 1, 2) sheet cast iron (sample No. 5), 3, 4) roofing steel (sample No. 0).

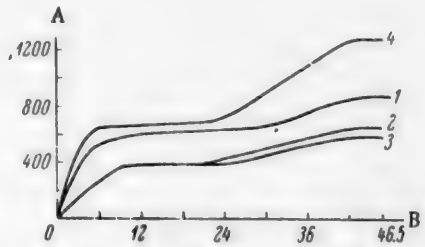

Fig. 2. Corrosion of sheet cast iron and roofing steel in the atmosphere. A) Loss of weight, in g/ m^2, B) duration of test, in months. Sheet cast iron: 1) without Cu (sample No. 5), 2) with 0.24% Cu (sample No. 10), 3) with 0.47 Cu (sample No. 11); roofing steel: with 0.15% Cu (sample No. 0).

Sheet cast iron roofs on buildings housing animals in the Odessa region were found to be covered by only a thin layer of rust after 4-5 years of exposure [7]. The introduction of SO_2 leads to the increase of the corrosion intensity of cast iron and steel. The relative increase of corrosion intensity is larger in the case of cast iron than in the case of steel. Under the effect of SO_2 the weight loss of cast iron is only slightly higher than that of steel. The results of laboratory corrosion tests imitating rain containing SO_2 are in good agreement with the results obtained after several years of exposure in field tests (Figure 2). Atmospheric corrosion of cast iron and steel is particularly intense during the first 6 to 9 months when the initial period of testing occurs during fall-winter. The weight losses of cast iron are approximately 15% lower than for steel. On further exposure the corrosion intensity of cast iron and steel decreases sharply and the relative loss of weight of the two metals remains the same during the first 2 years of exposure. After this period the corrosion of steel is more intense (up to 3.5 years) and then decreases again. The corrosion rate of cast iron increases after 2.5 years of exposure but not as much as that of steel. This increase of corrosion rate continues also up to 3.5 years of exposure, and then decreases again. At this point the loss of weight of cast iron is about 30% lower than that of steel. Taking into account the difference in densities of all the samples of cast iron and steel, which is approximately 10% (7.1 against 7.8), and the experimental error (up to 3%), the decrease of thickness of the sheets as the result of atmospheric corrosion must be considered as approximately equal in all cases during the first two year period. After two years the calculated decrease in thickness is smaller for cast iron than for steel.

A layer of rust appears a few days earlier on cast iron than on steel. This is due to at least 3 factors: 1) the difference in the natural protective layers on cast iron and steel, 2) greater irregularity of surface of sheet cast iron, which favors condensation of humidity on the surface [11, 12], 3) possibly the fact that the

potential of the surface of cast iron is more electronegative than that of roofing steel. The primary light brown loose layer of rust spreads over the whole surface of cast iron samples during the first few days of the experiment. As the time progresses the surface layer becomes more dense, its color changes to dark brown, and the rust becomes more difficult to detach from the surface of the metal. The removal of rust in all the experiments was more difficult in the case of cast iron than in the case of steel. Apparently, this can be ascribed to the fact that silicon, whose concentration in cast iron is high, passes into the rust and acts as if it were a binder. The corrosion of cast iron in the atmosphere is uniform. However, it is less uniform than on steel. After the removal of corrosion products corresponding to the same exposure time the surface of cast iron samples appears more irregular than the surface of steel samples. It is important to note that after 3.5 years of exposure steel samples as well as cast iron samples of identical average thickness (0.68 mm) were perforated by small holes, and this in spite of the fact that the first lost 1283 g/ m^2 while the second lost 889 g/ m^2. As

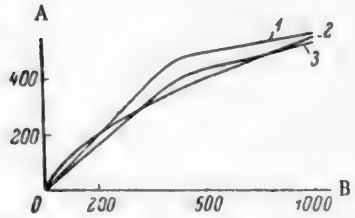

Fig. 3. Laboratory corrosion tests of sheet cast iron with different structures. A) loss of weight, in g/ m^2, B) duration of test, in hours. 1) ferrite-cementite, 2) ferrite, 3) pearlite and pearlite-ferrite.

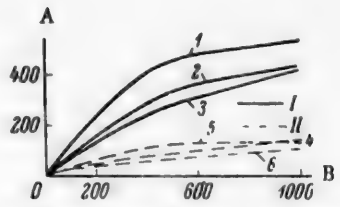

Fig. 4. Laboratory corrosion tests of cast iron with different concentrations of phosphorus. A) loss of weight, in g/ m^2, B) duration of test, in hours. I) with SO_2, 2) without SO_2. 1) Sample No. 7, 0.05% P, 2) Sample No. 30, 0.30% P, 3) Sample No. 31, 0.60% P, 4) Sample No. 7, 0.05% P, 5) Sample No. 30, 0.30% P, 6) Sample No. 31, 0.60% P.

a consequence one must consider that the corrosion resistance of sheet cast iron (TU MSKhM 282-53) in the atmosphere of a sea shore industrial region is equal to that of steel roofing (GOST 1393-47) containing 0.15% Cu, 0.20% Ni and 0.12% Cr.

Effect of structure of resistance of cast iron to atmospheric corrosion. The structure of sheet cast iron prepared according to TU MSKhM 282-53 specifications is represented by graphite flakes distributed in a ferrite field. Up to 15% pearlite is admissible. To examine the effect of different deviations from this structure on corrosion resistance, cast iron sheets corresponding to the TU chemical composition were sorted out and subjected to different heat treatments to obtain the following structures: ferrite (F), pearlite (P), ferrite-cementite (FC) and pearlite-ferrite (PF). The samples were subjected to the laboratory experiments under ordinary conditions of rain containing SO_2. The results of the experiments are represented in Figure 3. The probable relative error for the 600 and 1000 hour exposure tests reaches 1%. It can be seen that the difference in the structure of cast iron has little effect on its corrosion resistance. Cast iron having the ferrite-cementite structure is somewhat less resistant.

Effect of the Chemical Composition on Corrosion Resistance of Cast Iron

Effect of phosphorus. Samples of cast iron containing 0.05, 0.30 and 0.60% phosphorus were prepared. The concentration of all the other elements was about the same. The concentration of Si did not exceed that prescribed by the TU MSKhM 282-53 specification; it varied from 2.5 to 2.7%. The results of the experiments relative to cast iron samples containing different concentrations of phosphorus are represented in Fig. 4. Under the conditions of rain containing SO_2, cast iron containing higher percentages of phosphorus (0.3 to 0.6%) is somewhat more corrosion resistant. The same result was obtained in the case of fog-rain conditions. The only exception is the result of the 1000 hour test of samples containing 0.3% phosphorus. Field tests gave the

same results. Thus, laboratory and field tests indicate that an increased concentration of phosphorus, up to 0.3-0.6%, renders cast iron somewhat more resistant to atmospheric corrosion.

Effect of sulfur. We investigated samples of cast iron containing 0.07, 0.12 and 0.23% sulfur. High concentration (0.23%) of sulfur was achieved by introducing pyrite into the molten metal. After ordinary heat treatment the sheets had a pearlite structure with graphite inclusions in globular form. Figure 5 shows that the increase in the concentration of sulfur from 0.07 to 0.12% leads to some decrease of the resistance of cast iron to corrosion under conditions of the experiment. This result is in agreement with the results published earlier concerning steel [13]. However, further increase in the concentration of sulfur, to 0.23%, increases the resistance. The results of the laboratory experiments are in agreement with the results of field tests not only in the case of the sample described above but also for specially prepared samples containing 0.30 and 0.38% S (Figure 6).

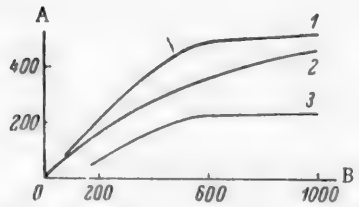

Fig. 5. Laboratory corrosion test of sheet cast iron with different concentrations of sulfur. A) loss of weight, in g/ m^2, B) duration of test, in hours. 1) Sample No. 36, 0.12% S, 2) Sample No. 35, 0.07% S, 3) Sample No. 46, 0.23% S.

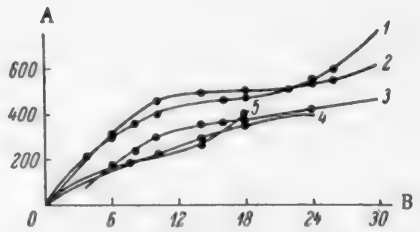

Fig. 6. Atmospheric corrosion of cast iron with different concentrations of sulfur. A) loss of weight, g/ m^2, B) duration of test, in months. 1) Sample No. 35, 0.07% S, 2) Sample No. 36, 0.12% S, 3) Sample No. 46, 0.23% S, 4) Sample No. 92, 0.30% S, 5) Sample No. 91, 0.38% S.

A high concentration of sulfur in cast iron (0.23% and higher)considerably decreases the rate of the second stage of graphitization. Therefore, as noted before, this type of cast iron acquires the pearlite structure containing globular graphite as the result of annealing under the ordinary conditions of manufacturing sheet cast iron. In order to check whether the pearlite structure containing globular graphite increases the corrosion resistance, some of the samples were annealed so as to achieve a ferrite structure, and these samples together with pearlite samples and ordinary sheet cast iron containing 0.1% S were subjected to laboratory corrosion tests. The results of these tests show that the corrosion resistance of cast iron containing 0.23% S and having a ferrite or pearlite structure is about the same, although cast iron with a pearlite structure is about the same, although cast iron with a pearlite structure manifests a somewhat higher resistance to corrosion under laboratory conditions. At the same time cast iron containing 0.23% S with either pearlite or ferrite structure has a higher corrosion resistance than ordinary ferrite cast iron containing 0.1% S.

Effect of addition of aluminum. Aluminum of the AO type was added to cast iron in proportions up to 0.44 and 0.99%. Because of the graphitizing action of aluminum, the concentration of Si was reduced to 0.61%. This allowed us to obtain sheet cast iron of the same structure as ordinary sheet cast iron by the same process. The concentration of the other components remained the same. The addition of 0.44 and 0.99% Al decreased the corrosion resistance of cast iron in both types of tests. Analagous results were obtained in field tests (Figure 7). After 9 months,samples containing 0.99% Al lose more weight than cast iron not containing Al. As the duration of the test increases, the discrepancy between the samples with and without aluminum widens, and after 3 years of exposure cast iron containing aluminum loses 32% more weight than aluminum-free cast iron. The behavior of cast iron containing 0.44% Al is somewhat different. During the first 9 months it loses less weight than aluminum-free cast iron. However, on further exposure it shows the same weight loss as aluminum-free cast iron, and then its loss of weight becomes higher. Also, corrosion of cast iron containing aluminum is

much more irregular, and as a result sheets of cast iron containing aluminum become perforated after 2.5 years of exposure instead of 3.5 years. The effect of aluminum on corrosion resistance was for practical purposes identical at both corrosion stations.

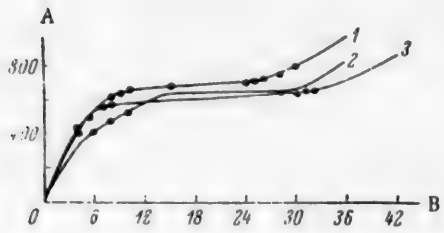

Fig. 7. Effect of the concentration of aluminum on the corrosion of cast iron in the atmosphere. A) loss of weight, g/ m^2, B) duration of test, months. 1) Sample No. 9, 0.99% Al, 2) Sample No. 8, 0.44% Al, 3) Sample No. 5, without Al.

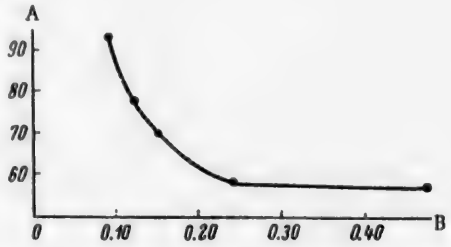

Fig. 8. Effect of the concentration of copper on the corrosion of cast iron in atmosphere. A) relative corrosion, %, B) amount of Cu, %.

Effect of addition of copper. First we tested cast iron containing 0.24 and 0.74% Cu. The concentration of the other elements remained the same as in the TU specifications. Copper was introduced into the molten metal before the forming of the sheet. Further treatment was the same as for ordinary cast iron sheets, and we obtained sheets whose structure and mechanical properties were the same. The results of the field test pursued for several years with samples containing different concentrations of copper are presented in Figure 2. Figure 2 shows that addition of small amounts of copper considerably increases the corrosion resistance. Of particular

TABLE 2

Effect of Copper on Corrosion of Cast Iron

Sample No.	Conc. of Cu, %	Loss of wt. g/ m^2	Relative corrosion, %
5	0.00	737	100.0
+8	0.08	667	90.5
+5	0.10	659	89.4
+1	0.14	616	83.6
+3	0.20	593	80.5
+7	0.30	592	80.3
+2	0.48	584	80.0

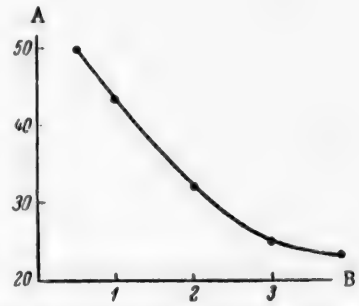

Fig. 9. Variation of the beneficial effect of 0.2% Cu on the corrosion resistance of cast iron as a function of the duration of the test in the atmosphere. A) Increase of corrosion resistance, %, B) duration of test, years.

interest is the fact that this effect ceases when the copper concentration is increased from 0.24 to 0.47%. To determine the optima copper concentration we prepared a series of samples containing 0.08, 0.10, 0.14, 0.20, 0.30, 0.48% Cu and subjected them to corrosion tests. The results of the 400 hour laboratory tests in rain containing 0.05% SO_2 are presented in Table 2.

The concentration of copper inducing maximum corrosion resistance of cast iron was found to be 0.2%. The same result was obtained in field tests (Figure 8). The beneficial effect of 0.2% copper is greatest for cast iron exposed to atmospheric conditions (the corrosion rate decreases by a factor of 2 after 1-1.5 years of exposure). As the duration of field tests increases, the beneficial effect of 0.2% copper decreases (Figure 9). It is

quite probable that this decreased effect may be related to the fact that the samples were exposed to a sea shore atmosphere; the effect of small additions of copper is somewhat different under these conditions. According to Tomashev [14], the slowing down of the corrosion rate of copper steels is explained by the onset of anodic passivity due to the presence on the corroding surface of additional effective local cathodes made of finely dispersed copper resulting from secondary deposition (from the corrosion products). The necessary conditions for the onset of anodic passivity consist not only in the supply of an oxidizing agent (oxygen) at an adequate rate but also in the absence of anodic activators (chlorine ions), which destroy the passive state on the iron's surface. Therefore, in a sea shore atmosphere, containing a high concentration of chlorine ions, the advantage of copper steels as compared to ordinary steel is less than far inland. It is probable that in our experiments the concentration of chlorine ions in the rust was increasing. This explanation is in agreement with the experimental fact that steel containing 0.15% copper and cast iron containing 0.2% copper, exposed simultaneously over a period of 4 years, shows that regardless of the conditions of exposure the loss of weight of cast iron samples is about 50-60% that of steel. According to various authors [1, 2, 15-17] the optima concentration of

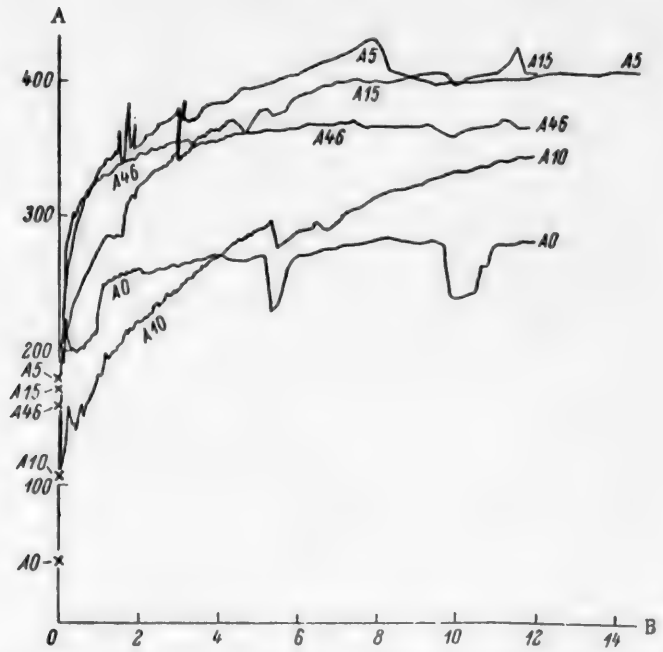

Fig. 10. Variation of electrode potential as a function of time for different samples of cast iron and steel (Series A). A) electrode potential, mV, B) time, hours.

copper in copper steels is from 0.20 to 0.35%. These data were confirmed relatively recently by Vedenkin [13]. For the optima concentration of copper in cast iron we obtained a value close to that found for steel. Addition of 0.2% Cu to cast iron, which leaves the mechanical properties of sheet cast iron almost unaltered, and does not complicate the manufacturing process, provides at the same time a large economic advantage as the result of increased resistance. Consequently an obligatory requirement of not less than 0.2% copper in cast iron is included in the project of GOST specifications for corrugated cast iron roofing.

RESULTS OF ELECTROCHEMICAL MEASUREMENTS

The curves representing the variation of the electrode potential as a function of time ($\varphi = f(\tau)$) are represented in Figure 10. This figure shows that under the conditions of the experiment the initial value of φ is more negative for cast iron than for steel. In the case of steel φ acquires a stationary value after 3-4 hours and there are only a few separate swings of the curve toward more noble values of potential after 5.5-10

hours, indicating the growth and rapid destruction of the protective layer. In the case of cast iron the value of φ becomes stationary after 3-4 hours only for sample No. 46, containing 0.23% S; this value is more positive than for samples No. 5 and 15. For these samples the value of potential is stabilized only after 9-10 hours. For cast iron sample No. 10 (0.24% Cu) the value of potential remains more positive than for the steel sample (No. 0) during the first 4 hours of the experiment, but becomes more negative after this period. Cast iron sample No. 10 is characterized by a continuous loss of nobility of the potential. Even after 12 hours the value of the potential does not become stabilized although it is more positive than that of the other two cast iron samples.

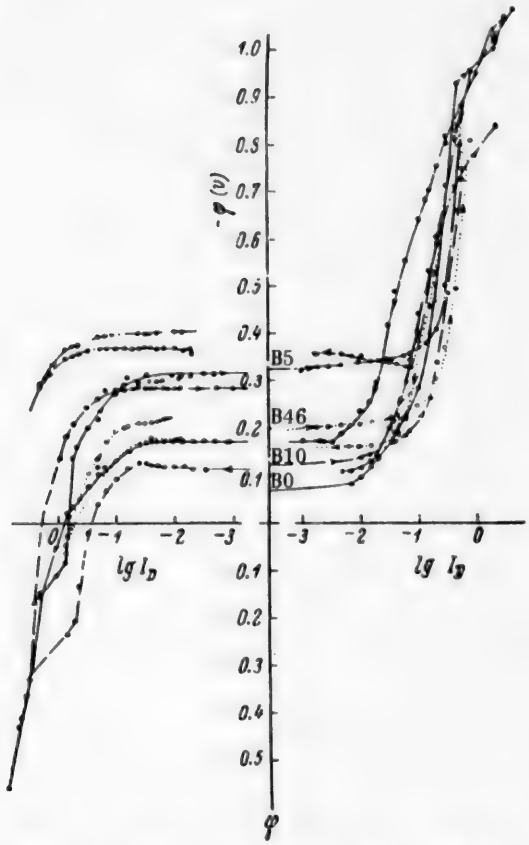

Fig. 11. Polarization curves for different samples of cast iron and steel (Series B).

The results of the experiments of the B series (polarization curves) are given in Figure 11. The hydrogen overpotential is relatively high for steel (about 0.5 volt). For cast iron samples No. 5 and 46 the value of the hydrogen overpotential is considerably lower than for steel (approximately 30%). Consequently, the corrosion of cast iron with hydrogen depolarization in acid media must proceed at a higher rate than for steel. This conclusion is confirmed by direct measurements. For small current densities the forward and reverse curves of potentials of cast iron do not change appreciably; this means that a "corrosion potential" is established (according to Tomashev). In the presence of an excess of oxygen the final potential of cast iron is very close to its initial value. Samples containing 0.24% Cu (sample No. 10) and 0.23% S (No. 46) manifest somewhat more positive potentials than the other cast iron samples. When anodic polarization is weak the value of the potential remains close to the potential of the corroding metal. Cast iron samples No. 10 and 46 undergo anodic polarization much easier than the other samples. Cast iron containing 0.24% Cu is polarized anodically and cathodically much easier than the other type of cast iron. Therefore, the electrodes of local surface elements must also become polarized. This must explain the greater chemical resistance of these samples of cast iron, a result which was shown by gravimetric measurements (Figure 2).

CONCLUSIONS

1. Corrosion resistance of TU MSKhM 282-53 sheet cast iron to atmosphere not contaminated by aggressive gases is 2.5-3.5 times greater than that of GOST 1393-47 roofing steel containing 0.15% Cu, 0.20% Ni, and 0.12% Cr. This result was demonstrated gravimetrically.

2. In industrial atmospheres, contaminated by aggressive gases, the corrosion resistance of cast iron as well as steel is much lower. The relative reduction of corrosion resistance of cast iron is considerably greater than that of steel. As a result corrosion resistance of TU cast iron sheets in industrial atmospheres becomes close to that of roofing steel containing 0.15% Cu.

3. Corrosion resistance of sheet cast iron is very little affected by its structure. Sheet cast iron with ferrite, pearlite, and ferrite-pearlite structures manifest approximately identical corrosion resistance.

4. Corrosion resistance of sheet cast iron is somewhat increased (up to about 10%) by increasing the concentration of phosphorus to 0.3-0.6%.

5. The resistance to corrosion in industrial atmospheres is increased (by 25%) by the addition of 0.23% or more sulfur.

6. Addition of 0.5-1.0% Al decreases the corrosion resistance of cast iron (by 15-30%).

7. Addition of a small amount of copper leads to a considerable increase of corrosion resistance of cast iron. Optima concentration of copper was found to be 0.2%. A decrease of weight loss due to the addition of 0.2% Cu is 43% for a sea shore industrial atmosphere (i.e., the resistance increases by about a factor of 2) when the duration of the test is 1.0-1.5 years. When the test time is increased, the relative increase in the weight loss drops to 32% after 2 years, to 25% after 3 years, and to 23% after 4 years. The addition of 0.2% Cu does not appreciably alter the mechanical properties of cast iron sheets and does not complicate the manufacturing process, while it has a large economic advantage.

8. The variation of electrode potentials as a function of the time and the polarization curves of sheet cast iron in water saturated with oxygen show the following: a) the electrode potential of cast iron containing copper is more noble than the potential of copper-free cast iron, b) cast iron containing copper is polarized cathodically and anodically with greater ease than copper-free cast iron. Therefore, its local elements operate much less intensely. This explains its higher resistance.

LITERATURE CITED

[1] O. Bauer, O. Krõhnke, and G. Massing, Die Korrosion metalischer Werkstoffe, I. Leipzig (1936).

[2] V. O. Krenig, "Corrosion of Metals," State Division of Scientifical and Industrial Institute of the People's Commissariat of Heavy Industry (GONTI NKTP) Press, Moscow-Leningrad (1938).

[3] E. Heyn and O. Bauer, Mitteilungen a.d. Materialprüfungsmat. 26, 1 (1908); 28, 62 (1910).

[4] H. H. Uhlig, The Corrosion Handbook, John Wiley Publ. N. Y., and Chapman and Hall, Publ., London (1948).

[5] J. N. Friend, Iron and Steel Inst. 18, 61 (1929).

[6] A. S. Afanas'ev, Second Conference on Corrosion of Metals, Academy of Sciences USSR Press, Moscow-Leningrad (1940), p. 195.

[7] B. Sh. Shteinberg, "Cast Iron Sheet," State Machine Press, (Moscow, 1956).

[8] A. S. Afanas'ev, Dnepropetrovsk Metallurgy Institute 25, 3 (1951).

[9] A. S. Afanas'ev, Foreign Literature 2, 217 (1957).

[10] G. V. Akimov, "Theory and Methods of Investigation of Corrosion of Metals", Academy of Sciences USSR Press, (Moscow, 1945).

[11] G. V. Akimov, "Fundamentals of the Study of Corrosion and Protection of Metals", State Metallurgy Press (Moscow, 1945).

[12] N. D. Tomashov, Progress in Chemistry 19, No. 6 (1950); "Atmospheric Corrosion of Metals" Acad. Scien. USSR Press (Moscow, 1951) Collection of articles.

[13] S. G. Vedenkin, "Problems of Sea Water Corrosion," Collection of articles, Acad. Sci. USSR Press, (Moscow, 1951).

[14] N. D. Tomashov, "Problems of Sea Water Corrosion", Collection of articles Acad. Sci. USSR Press, (Moscow, 1951).

[15] D. Buk, Trans. Am. Electroch. Soc. 39, 109 (1921).

[16] O. Bauer, Stahl u. Eisen 41, 37, 61 (1921).

[17] K. Deaves, Stahl u. Eisen 46 (1926).

Received April 4, 1958

STUDY OF THE ELECTROCONDUCTIVITY IN THE SULFONATION OF NAPHTHALENE

E. I. Matrosov

Scientific Research Institute of Organic Intermediates and Dyes (Rubezhan Branch)

The sulfonation of aromatic hydrocarbons is one of the more important processes in organic synthesis.

A study of the electroconductivity of systems, the composition of which is determined by the ratio of the components during sulfonation, can be of definite interest for determining the possibility of controlling the process.

Since we were unable to find any data in the literature on the electroconductivity of such systems as applied to the sulfonation of naphthalene, we set ourselves the task of studying the electroconductivity of the systems: sulfuric acid–water, naphthalenesulfonic acid–water, and sulfuric acid–naphthalenesulfonic acid–water. Our study was made at 140°, and the main results are given in the present paper.

EXPERIMENTAL

Pure 2-naphthalenesulfonic acid was obtained by repeated recrystallization of the technical product from aqueous hydrochloric acid solution, followed by drying of the product in a vacuum-oven. The quality of the obtained acid was judged by analysis for total acidity, and for moisture content using the Fischer method. Chemically pure sulfuric acid was used in the study.

The electroconductivity was measured using the following scheme: a ZG-10 sound generator, a fEO-5 electronic oscillograph (as the null-instrument), and a R-38 bridge. The frequency used in the measurements was 10 kc.

Taking into consideration the fact that the studied systems have a high conductance and are melts, we used a conductometric cell with a high constant (about 100 cm^{-1}) and electrodes, fitted on sleeves.

The measurements were made at 140°. An oil (transformer oil) bath, equipped with a stirrer, thermometer, and a sensitive heater, served as the thermostat. The temperature in the bath was maintained constant to ± 0.1°. For the systems in which the components reacted with each other naphthalenesulfonic acid with a high content of sulfuric acid) we used a special method of measuring: The change in the electroconductivity with time was determined, and then by extrapolation we found the desired value of the electroconductivity at zero time, i.e., at the moment of mixing the components, and here the components, having been thermostated, were mixed at the measurement temperature.

RESULTS OF EXPERIMENTS AND THEIR DISCUSSION

Two-component systems. The electroconductivity of the two-component systems: sulfuric acid–water and naphthalenesulfonic acid–water, was measured at 140° in the concentration range of 85-100 and 85-94%, respectively. The limits of studying these systems were set, on the one hand, by the high vapor pressure of water in the system at the investigation temperature (true for both acids), and on the other hand , by the high hygroscopicity (for naphthalenesulfonic acid), which did not permit investigating the acid at concentrations exceeding 94%. The obtained data are summarized in Tables 1 and 2.

The conductance of such systems is due to their ionization, which proceeds according to the equations

$$H_2SO_4 + H_2O \rightleftarrows H_3O^+ + HSO_4^-$$
$$C_{10}H_7SO_3H + H_2O \rightleftarrows H_3O^+ + C_{10}H_7SO_4^-. \quad (1)$$

The high conductivity shown by sulfuric acid when compared with naphthalenesulfonic acid (more than an order of magnitude) is due to the anomalous conductance of the bisulfate ion in sulfuric acid.

TABLE 1

Electroconductivity of System Naphthalenesulfonic Acid–Water at 140°

Composition of naphthalenesulfonic acid (in wt. %)	$\varkappa(\Omega^{-1} \cdot cm^{-1})$
85.25	0.08703
86.07	0.07605
86.95	0.06511
88.58	0.05061
90.78	0.03709
92.98	0.02606
93.85	0.02245
94.71	0.01928

TABLE 2

Electroconductivity of System Sulfuric Acid–Water at 140°.

Composition of sulfuric acid (in wt. %)	$\varkappa(\Omega^{-1} \cdot cm^{-1})$
88.15	0.7907
90.06	0.7662
91.86	0.7305
92.59	0.7269
93.98	0.6906
94.90	0.6581
95.68	0.6336
96.25	0.6101
98.12	0.4992
99.76	0.3142

An abnormally high mobility of the bisulfate ion [1] was obtained when the transport numbers of the ions of alkali metal sulfates in sulfuric acid were determined, which compares with the mobility of the hydrogen ions in aqueous solutions, and is explained by the successive transfer of a proton along the long chains of the sulfuric acid molecule.

The slow stage of such chain transfer of a proton by sulfuric acid molecules

$$HSO_4^- + H_2SO_4 \rightleftarrows H_2SO_4 + HSO_4^- \quad (2)$$

will be the rotation of the individual molecules of the sulfuric acid chains with respect to each other [2], since the molecule, releasing the proton, and the molecule that arises as the result of receiving it, have a different orientation.

Taking into consideration the fact that sulfuric acid at room temperature is a highly associated substance with long chainlike particles, formed as the result of hydrogen bonding [3], the diffusion of hydroxonium ion in such medium, possessing a quasi-crystalline structure, will be greatly retarded, and the conductance of such a system will be determined mainly by the Grotthus mechanism of chain conductance.

With increase in the temperature this conductivity should obviously rise sharply, due to a cleavage of the acid molecule chains into individual units or even into individual molecules [3], and in this way increase their ability to rotate, which in essence limits the entire conductance process. This circumstance is supported by the large difference (approximately by an order of magnitude) in the conductance of sulfuric acid at room temperature (χ = 0.010133 $\Omega^{-1} \cdot cm^{-1}$ at 25° [4]) and at the investigation temperature.

The values of the electroconductance for naphthalenesulfonic acid show that the ionic mechanism of conduction prevails here. As a result, a difference in the mechanisms of conduction (usual ionic transfer and a Grotthus chain transfer) of the two acids is responsible for such a large difference in their electroconductance.

Three-component systems. In studying the three-component systems (sulfuric acid–naphthalenesulfonic acid–water) we kept the water content constant and varied the ratio of naphthalenesulfonic acid to sulfuric acid from 0 to 100 mole%.

The experimental data are plotted in Fig. 1.

From the data, plotted in the coordinates (conductance of the system vs composition) it can be seen that quite concave curves are obtained as either acid is replaced by the other. Actually, this deviation of the experimental electroconductance–composition curve from linearity (assuming additivity in the system) is due to a difference in the mechanisms of conduction shown by sulfuric acid and naphthalenesulfonic acid. As a matter of fact, replacing sulfuric acid by naphthalenesulfonic acid, i.e., when both acids are simultaneously present in the system, results in a rupture of the Grotthus conduction chains, due to the fact that in naphthalenesulfonic acid medium the bisulfate ion apparently possesses the conventional mechanism of ionic conduction. Consequently, replacing naphthalenesulfonic acid by sulfuric acid (left branch of the curve) results in the electroconductance of the mixture increasing but slightly, since the Grotthus mechanism under these conditions apparently appears only very slightly or is completely absent. In other words, at a constant water content, the contribution made by sulfuric acid to the total conductance of the ternary mixture decreases with increase in the amount of sulfonic acid in the system. For this reason, replacing sulfuric acid by naphthalenesulfonic acid (right branch of the curve) leads to a sharp decrease in the electroconductance of the ternary mixture, which is caused by a substantial decrease in the mobility of the bisulfate ion due to rupture of the Grotthus conduction chains.

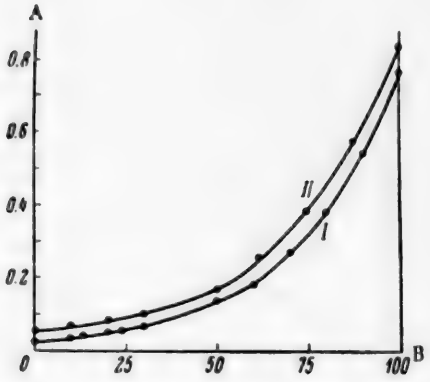

Fig. 1. Electroconductivity of the three-component system (sulfuric acid–naphthalenesulfonic acid–water) at 140° and a constant water content. A) Specific electroconductance $\varkappa(\Omega^{-1} \cdot cm^{-1})$, B) extent of replacing naphthalenesulfonic acid by sulfuric acid (in %). Water content (in mole %): I) 50; II) 60.

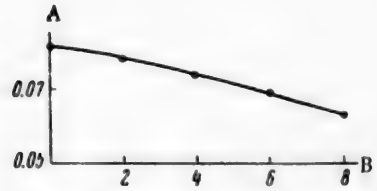

Fig. 2. Electroconductivity of the four-component system (sulfuric acid–naphthalenesulfonic acid–water–naphthalene) at 140°, a constant acid content (10 mole % of sulfuric acid and 30 mole % of naphthalenesulfonic acid), and a mutual exchange of water and naphthalene ranging from 0 to 8 mole %. A) specific electroconductance $\varkappa(\Omega^{-1} \cdot cm^{-1})$, B) extent of replacing water by naphthalene (in %).

Possible utilization of the conductometric method to control the stage of naphthalene sulfonation. It is possible to regard the process for the sulfonation of naphthalene as a process for the simultaneous replacement of naphthalene by water and of sulfuric acid by naphthalenesulfonic acid in the four-component system: sulfuric acid–naphthalenesulfonic acid–naphthalene–water. For this reason the total effect of changing the electroconductivity in the sulfonation process will be determined mainly by the superimposition of the two opposing factors, each of which is determined by the magnitude of the change in the conductance of the system deriving from an equimolecular mutual replacement of its components: naphthalene by water, and sulfuric acid by naphthalenesulfonic acid.

The effect of changing the electroductivity by the mutual replacement of sulfuric acid by naphthalenesulfonic acid can be determined from the initial portion (left branch) of the curve for the electroconductivity of the three-component systems (Fig. 1).

The effect of changing the electroconductivity by the mutual replacement of naphthalene by water can be determined from the slope of the curve for the electroconductivity of the four-component systems (Fig. 2). In obtaining this curve we kept the ratio of the acids constant ($C_{10}H_7SO_3H$ = 30 mole %; H_2SO_4 = 10 mole %), while the mutual replacement of water for naphthalene was varied from 0 to 8 mole %. This ratio of the components corresponds to the composition of the reaction mixture at the end of sulfonation.

The following values were calculated:

$$\left(\frac{\Delta\chi}{\Delta y}\right)_{av.} = \frac{\sum_{i=1}^{n}\left(\frac{\Delta\chi}{\Delta y}\right)_i}{n} = +2.12 \cdot 10^{-3}$$

$$\left(\frac{\Delta\chi}{\Delta x}\right)_{av.} = \frac{\sum_{i=1}^{n}\left(\frac{\Delta\chi}{\Delta x}\right)_i}{n} = -1.97 \cdot 10^{-3},$$

where χ is the specific electroconductance, x is the percent replacement of sulfuric acid by naphthalenesulfonic acid, and y is the percent replacement of naphthalene by water.

The obtained data indicate that the changes in the electroconductivity from a mutual replacement of the components (sulfuric acid by naphthalenesulfonic acid and naphthalene by water) are practically the same in value and are of opposite sign. For this reason the electroconductivity at the end of sulfonation should remain practically constant, which was confirmed by directly measuring the electroconductivity in the sulfonator. In all of the cases that we studied, beginning from a certain point in the reaction, the electroconductivity remained constant with time.

As a result, the conductometric method cannot be used as a continuous control method for the sulfonation of naphthalene.

The present work is of definite practical interest, since the idea of using the conductometric method to control sulfonation processes is highly intriguing.

SUMMARY

1. Values were obtained for the electroconductivity of sulfuric acid (100-85% H_2SO_4) and of naphthalenesulfonic acid (94-85% $C_{10}H_7SO_3H$) at 140°.

A large difference in the conduction shown by the two acids is explained by the presence of a chain mechanism of conduction in sulfuric acid solutions.

2. The shape of the experimental curve obtained when investigating three-component systems (sulfuric acid–naphthalenesulfonic acid–water) is explained as due to rupture of the bisulfate ion conduction chains when sulfuric acid is replaced by naphthalenesulfonic acid.

3. Based on the obtained data, it follows that the present method cannot be used as a continuous control method in the sulfonation of naphthalene, due to the fact that toward the end of reaction the electroconductivity does not change with reaction progress.

LITERATURE CITED

[1] R. J. Gillespie and S. Wasif, J. Chem. Soc. 1, 209 (1953).

[2] R. J. Gillespie and S. Wasif, J. Chem. Soc. 1, 221 (1953).

[3] V. M. Kudryavtseva, Bull. Acad. Sci. USSR, Phys. Ser., B. 131 (1931).

[4] R. J. Gillespie and S. Wasif, J. Chem. Soc. 1, 204 (1953).

Received July 5, 1958

RESIDENCE TIME OF THE REACTANTS IN THE CONTACT ZONE IN HETEROGENEOUS CATALYTIC SYNTHESIS OF VINYL ACETATE*

E. N. Rostovskii and S. N. Ushakov

The time that reactants stay in the catalysis zone is one of the most important factors in determining the results of a heterogeneous catalytic process. In this paper, we present some experimental data that characterize the effect of the contact time on the synthesis of vinyl acetate from acetylene and acetic acid. The molecular ratio of acetylene to acid in these experiments was approximately 20 : 1. In an earlier paper [1] the effect of the contact time was discussed for a different case (ratio of the reactants 5 : 1), but a detailed examination has not been made up to now, and studies relating to an investigation of the indicated factor are not reported in the literature.

The time that reactants stay in the catalysis zone is to a certain degree of conditional value, since only an approximate estimate can be made of the real path taken by the reactant stream. In the experiments given below, to determine the residence time (designated further by τ), we took into account the porosity of the catalyst.

For the calculations, we used the formula

$$\tau = \frac{V_\Delta - V_d}{U},$$

where V_Δ is the total volume of the contact area (in liters), calculated from the bulk weight of the catalyst; V_d is the volume (in liters), occupied by the actual catalyst, and determined from the true density of the catalyst; and U is the volume of the reacting gas (in liter/ sec), entering per second at the temperature and pressure prevailing in the contact area.

Such a method for calculating the residence time [2, 3] is not general, and the correction for the volume occupied by the actual catalyst is at times completely neglected, which leads to a smaller real value for the calculated contact time.

EXPERIMENTAL

The catalyst was prepared by precipitating zinc acetate on activated granular carbon Ag, prepared from anthracite. This carbon, sold commercially [4], is basically recuperative. The conditions used to impregnate the zinc salt were essentially the same as used before [5]. The obtained catalyst was characterized by its density, porosity, and chlorine absorption capacity. The apparent density (δ) was determined by filling the voids not occupied by the catalyst granules with mercury in a Tyulyukov apparatus [6], while the true density (d) of the previously ground specimen was determined by the Honig method [7].

The determination results are given in Table 1.

* Communication III.

The catalytic reaction was run under the earlier described condtions [5, 8] by passing the mixed vapors of acetic acid and acetylene through a layer of the catalyst. The reaction temperature in the first series of experiments was 200° when measured in the middle of the catalyst layer. The temperature of the mixture entering the contact zone was 165°. The amount of catalyst and the rate of the entering acetylene varied in the different experiments, which led to a difference in the values of the contact time of the reactants. The weight ratio

TABLE 1

Characteristics of the Catalyst

Designation of carbon sample	Amount of zinc acetate, in %	Density (in g/cm^2)			Porosity, in %	Static activity toward chlorine, in wt. %
		gravimetric Δ	apparent δ	true d		
AG (1)	7.6-8	0.55	0.917	1.86	50.5	35.5

of acetylene to acetic acid was maintained at 9 : 1, which corresponded to 20.6 moles of acetylene per mole of acid. The same as in previous experiments, the degree of conversion was established analytically, by removing samples from the gas stream and then analyzing them for the amount of free acid and by saponification. The volume of gas passed through the contact was calculated as the arithmetical mean of the entering and escaping volumes. This change was small due to the low initial concentration of acid under the given conditions. In addition, the association of the acetic acid molecules, due to hydrogen bonding, was taken into consideration, representing, based on the determinations made by Batschinski [9], a substantial value even at 200°. For the used ratio of the reactants, the acetic acid vapors in the original mixture occupied a volume (taking association into consideration) of about 3%.

TABLE 2

Results of Experiments on the Catalytic Conversion of Acetic Acid

Amount of catalyst (in g)	Amount of acetylene (in liter/hr)	τ (in sec)	K(in %)
7	10	1.97	60
14	10	3.92	82
21	10	5.87	98
28	10	7.82	99
14	12	3.21	72
14	6	6.56	99
21	12	4.84	90

The results of these experiments at 200° are given in Table 2, where the amount of acetylene entering the vaporizer, based on its volume at 20° and atmospheric pressure, is also shown. From 192 to 761 liters of acetylene was passed per hour per liter of catalyst. The contact time is designated τ, while the degree of acetic acid conversion (in %) is designated by K.

Table 2 shows that for a catalyst of the given activity, at 200°, and a residence time of the reactants in the catalysis zone of about 6 seconds (independent of whether the time of contact is determined by the relative amount of catalyst or by a corresponding change in the feed rate of gas), it is possible to achieve close to = 100% conversion of the acetic acid. To determine the actual character of the conversion of the acid we ran an experiment in which the reaction products were trapped, and then a material balance was made. The reaction temperature and ratio of the reactants corresponded to those given above. The contact time was 7.8 seconds. Based on analysis, the conversion of the acid was 99%. The experiment lasted 18 hours. The reaction mixture after catalysis was subjected to a three-stage cooling. The excess acetylene was collected separately. The condensate analyzed 94.0% vinyl acetate, 1.4% acetic acid, and about 4% acetylene. The fractions isolated by fractional distillation analyzed very close to these amounts of the compounds. The yield of vinyl acetate was 97% of the theoretical. We were unable to isolate either ethylidene diacetate or acetic anhydride. It should be mentioned that in some other experiments, in which the concentration of acetic acid in the vapor phase was considerably higher [1], it was possible to detect small amounts of acetic anhydride, formed from ethylidene diacetate.

The rate of a heterogeneous catalytic reaction corresponds to the total process, including a number of consecutive stages: diffusion, sorption of the individual components, chemical reaction, desorption, etc., and for this reason the dependence on the concentration of the reactants bears a complex character. However, under the conditions of the discussed synthesis of vinyl acetate, in the presence of small concentrations of both acetic acid and vinyl acetate, and a temperature that assures substantial speeds for the desorption processes, it is possible for the rate of the process to obey simpler rules in a comparatively narrow concentration range. The synthesis experiments in which the reaction medium was diluted with nitrogen confirmed this postulation – for the same degree of conversion, the residence time was directly proportional to the original concentration.

The formation of vinyl acetate is an exothermic reaction. For this reason it was important to have a more accurate idea of the temperature along the catalyst layer. To accomplish this, we used a special movable thermocouple. Its hot junction was placed between two asbestos plugs, the size of which corresponded to the internal diameter of the glass jacket of the thermocouple. These plugs, fencing off small sections in the jacket tube, permitted obtaining a more accurate reading of the temperature by moving the thermocouple along the catalyst layer. Measuring the temperature in this manner revealed that in the first quarter of the catalyst layer the temperature rose from 165 to 200°, and then it remained for the most part around 200°. As was shown by later study, it is important to mention that as the catalyst aged this front of heating to the desired temperature gradually shifted in the same direction as the gas stream, i.e., toward the end of the layer. As a result, the operating length of the catalyst layer gradually became shorter.

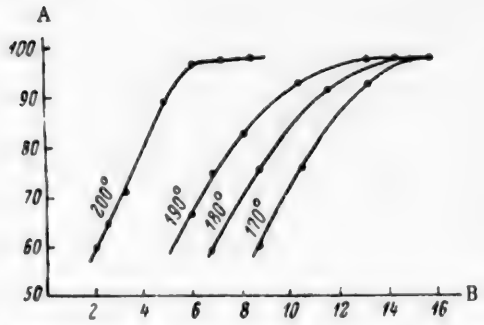

Relation between the degree of acetic acid conversion and the residence time of the reactants in the catalysis zone and different reaction temperatures. A) degree of conversion (in %); B) residence time (in sec).

To determine the effect of the residence time of the reactants in the catalysis zone at different temperatures we ran experiments at 170, 180, and 190°, under conditions similar to those described above for a temperature of 200°.

The obtained results are plotted in the Figure.

From the Figure it can be seen that with a sufficiently long contact time it is possible to obtain a high conversion at different (in the examined temperature range of 170 to 200°) temperatures. The residence time of the reactants depends on the initial activity of the catalyst, and can be less than that indicated in the Figure.

SUMMARY

1. A study of the effect of the residence time of the reactants in the catalysis zone, under the conditions of the vapor-phase heterogeneous-contact synthesis of vinyl acetate in the temperature range 170-200°, revealed that with the proper contact time it is possible to achieve a very high conversion of acetic acid and a high yield of vinyl acetate.

2. A decrease in the degree of conversion, caused by using a low catalysis temperature, can be eliminated by suitably increasing the contact time.

3. At a constant synthesis temperature, changing either the rate of the gas stream or the amount of charged catalyst has practically the same effect on the degree of conversion, provided the residence time of the reactants is maintained constant.

LITERATURE CITED

[1] L. A. Arbuzova, S. N. Ushakov, and E. N. Rostovskii, J. Applied Chem. (USSR) 31, No. 11, 1704 (1958).*

[2] V. F. Frankenberger and F. Dyurr, Prog. Chem. (USSR) 1, 85, (1932).

* Original Russian pagination. See C. B. Translation.

[3] A. A. Balandin, Bull. Acad. Sci. USSR, Div. Chem. Sci., 1, 21 (1942).

[4] A. S. Smirnov, Technology of Hydrocarbon Gases [in Russian] (Gostoptekhizdat, Moscow-Leningrad, 1946), p. 395.

[5] S. N. Ushakov, E. N. Rostovskii, and I. A. Arbuzova, J. Applied Chem. (USSR) 13, 1629 (1940).

[6] M. M. Dubinin, Physicochemical Principles of Sorption Technics [in Russian] (ONTI, 1935), p. 263.

[7] P. Honig, Kolloidchem. Beih. 22, 345 (1926).

[8] S. N. Ushakov, I. A. Arbuzova, and E. N. Rostovskii, J. Applied Chem. (USSR) 20, 1013 (1947).

[9] A. I. Batschinski, Bull. Soc. Imperial des Naturalistes de Moscou 17, 188 (1903).

Received June 14, 1958

STUDY OF THE POLYMERIZATION OF HEXAFLUOROBUTADIENE

A. L. Klebanskii and O. A. Timofeev

The broad development of the chemistry of fluorocarbon compounds in recent years is due to their remarkable properties, including high heat stability, complete chemical inertness, and several others. In their physicochemical properties the fluorocarbon compounds are sharply different from the hydrocarbons.

In going from olefins to fluorocarbon olefins it is noted that the latter are much more reactive than the corresponding olefins. Ethylene and its homologs, although they are capable of addition reactions, do not react with a number of polar compounds, whereas the completely fluorinated olefins react very easily with these compounds (addition of ammonia, amines, alcohols, hydrogen sulfide, mercaptans, and sodium bisulfite).

All of this shows that in fluorocarbon olefins the ability for dynamic polarization in the reaction with various polar reagents is much more strongly expressed than in the case of the corresponding olefins.

This same difference in the properties also appears in the different relative activity of olefins and fluorocarbon olefins toward polymerization. As is known, ethylene is much less active than tetrafluoroethylene in polymerization reactions.

In going from ethylene to diolefins with a conjugated system of double bonds there is a sharp increase in both the reactivity and diversity of reaction. The high reactivity of compounds with a conjugated system of double bonds is based on the ability to shift the electron density within the molecule with but a slight expenditure of energy (conjugation effect).

The effect of conjugation in fluorocarbon diolefins with a conjugated system of double bonds has received very little study. The single known representative of this class of compounds is hexafluorobutadiene, which was studied but slightly in this respect. The numerous data existing on the reactivity of hexafluorobutadiene give basis to assume that it is quite different from butadiene. Actually, there is nothing in the literature on its efficacy in diene synthesis reactions. Hexafluorobutadiene is capable of dimerization [1], but in this case derivatives of the fluorocyclobutene series are formed, in contrast to dienic hydrocarbons with a conjugated system of double bonds, which form derivatives of the cyclohexene and cyclooctadiene series. Information on the polymerization of hexafluorobutadiene is absent in the scientific literature. In the patent literature it is indicated [2] that the polymerization of hexafluorobutadiene is run at a pressure of 10,000-20,000 atm and at temperature of 70°.

A study of the reactivity of hexafluorobutadiene and, in particular, its activity in polymerization is of substantial theoretical interest in elucidating the influence of the structure on the properties and relative reactivity of this class of compounds when compared with the diolefin hydrocarbons and their derivatives.

EXPERIMENTAL

Starting materials. The hexafluorobutadiene, obtained by the Miller method [3], was subjected to successive chemical purification (packed column containing 5% NaOH solution, U-shaped tube with soda lime, and packed column with concd. sulfuric acid), and then was fractionated through a precision column (50 theoretical plates), where the fraction boiling at 6° was collected. For a better removal of impurities the hexafluorobutadiene was subjected to partial polymerization in emulsion, followed by distillation of the unreacted monomer, which had b. p. 6° and d_4^{20} 1.5553, corresponding to the data given in the literature for pure hexafluorobutadiene [2, 3].

Experimental procedure. The emulsion polymerization of hexafluorobutadiene was run in calibrated glass ampuls, having a volume of 8 ml. The previously tared ampuls were filled with emulsifier solution and then weighed.

The emulsifier solution was prepared as follows (amounts in g): Esteramine* 5.00, water 241.75, hydrochloric acid (36%) 3.25.

The formula was used in most of the experiments, except in those cases where the effect of some factor on the polymerization rate was studied. The pH of the aqueous phase was 3.0.

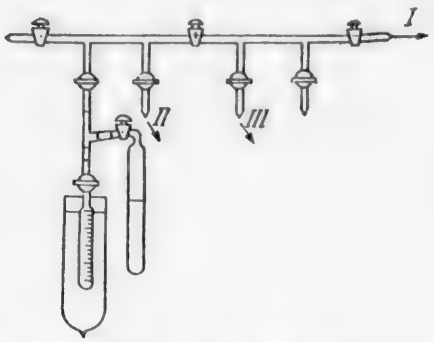

Fig. 1. Scheme of loading hexafluorobutadiene into ampul. Outlets: I) to vacuum pump, II) to vacuum gage, and III) to system for nitrogen purification.

After charging the emulsifier solution, the ampul was cooled in a Dewar flask to −20°, then the calculated amount of initiator solution (2% $K_2S_2O_8$ solution) was added from a microburet, the ampul reweighed, and then by means of a T-tube with ground-glass fittings it was connected to the vacuum setup. The holder containing the hexafluorobutadiene was connected to the vacuum setup at the same time (Fig. 1). The ampul was cooled in a transparent Dewar flask to −70°, and then the entire system was alternately evacuated and filled with oxygen-free nitrogen three times, followed by the addition of the calculated amount of hexafluorobutadiene to the ampul. The amount added was controlled dilatometrically. After adding the proper amount, both the ampul and the hexafluorobutadiene holder were disconnected from the system, and the ampul was weighed to determine the amount of hexafluorobutadiene added. The ampuls were sealed with cooling in Dry Ice, and then were placed in a thermostat equipped with a contrivance for shaking the ampuls. The temperature in the thermostat was kept constant to ± 0.1°.

At the end of the process the ampuls were removed from the thermostat, cooled in a Dewar vessel to -70°, weighed, and opened. The degree of polymerization was based on the dry weight of polymer.

In our work we used technically pure nitrogen (containing 0.01% O_2), which was purified further to remove oxygen by passage through a system of columns filled with copper turnings and saturated ammonium chloride solution in 12% ammonia solution, then freed of ammonia by passage through 10% sulfuric acid, and finally it was dried by passing through U-shaped tubes filled with calcium chloride.

The composition of the polymer was determined from the amount of fluorine contained in it after combustion of a known weight of the polymer with metallic sodium and sodium peroxide.

The thorium-alizarin method [4] was used to determine the amount of fluorine.

We ran some preliminary experiments on the polymerization of hexafluorobutadiene under various conditions.

The catalytic polymerization of hexafluorobutadiene did not go when dispersions of the alkali metals (lithium, sodium, potassium) were used.

We tried to polymerize hexafluorobutadiene at low temperatures (−80°), using $AlCl_3$ to incite reaction, but negative results were also obtained here.

The negative results obtained using ionic exciting agents points out the inertness of hexafluorobutadiene toward polar chemical reagents, which apparently is due to the small mobility of the π-electrons in the molecule.

*Esteramine has the formula $-(C_2H_5)_2N-CH_2-CH_2-OCOC_{11}H_{23}-$, and is the ester of diethylaminoethanol and lauric acid.

The polymerization of hexafluorobutadiene in homogeneous mass and in dispersed phase, using various initiators (benzoyl peroxide, azobisisobutyronitrile, isopropylbenzene hydroperoxide, tert-butylcumene hydroperoxide), also gave negative results. Consequently, as the main direction of study we selected the polymerization of hexafluorobutadiene in emulsion, which usually assures obtaining both a rapid polymerization rate and high-molecular weight polymers.

As is known, the mechanism of emulsion polymerization is based on the colloidal solution of the monomer in the micelles of the emulsifier, with subsequent expansion and continuation of the process of chain growth in the polymer-monomer particles. As was shown by Medvedev [5], the process of initiation and polymerization in this stage takes place in the adsorbed layer of the emulsifier, in contrast to the process of initiation in the initial stage of polymerization, where the process obviously takes place on the surface or within the micelles. From what has been said above, it follows that the nature of the emulsifier should exert a large influence on the polymerization rate in emulsion.

We tested both anion-active and cation-active emulsifiers: Nekal (sodium diisobutylnaphthalenesulfonate), sodium salts of the Petrov contact, resin soap, sodium oleate, Sapamine (diethylaminoethylamide of oleic acid), and Esteramine (ester of diethylaminoethanol and lauric acid).

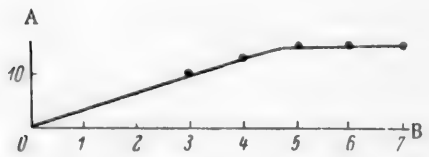

Fig. 2. Relation between the polymerization rate and the emulsifier concentration. A) Extent of polymerization (in %); B) emulsifier concentration (in % on the monomer).

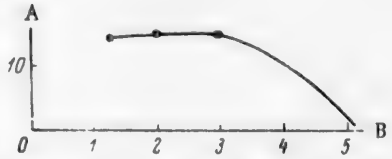

Fig. 3. Relation between the polymerization rate and the pH of the aqueous phase. A) extent of polymerization (in %); B) ph.

Only the cation-active emulsifier, Esteramine, forms stable emulsions in the initial stage. It should be mentioned that a relatively stable emulsion is formed only in the initial stage of the process and with stirring, but as the polymeric particles are formed they deposit from the emulsion with the formation of dispersions, and this is apparently due to the slight solubility of the monomer in the polymeric particles and an inadequate adsorption capacity of the polymeric particles relative to the colloidal particles of the emulsifier.

Based on the results obtained in the emulsion polymerization of hexafluorobutadiene, we examined the effect of various basic factors on the polymerization of hexafluorobutadiene.

The polymerization of hexafluorobutadiene was run at a water: monomer ratio of 2.5 : 1, a temperature of 50°, and at a pH of 3 for the aqueous phase; as initiator we used potassium persulfate [1], while Esteramine was used as the emulsifier (5%), except in those cases where the effect of some factor was studied.

Effect of emulsifier concentration. In harmony with the stated concept that the mechanism of emulsion polymerization is via colloidal solution, it could be expected that the polymerization rate will rise with increase in the emulsifier concentration, but only up to a certain limit, corresponding to the complete micellar solution of the monomer. Further increase in the emulsifier concentration should exert very little influence on the rate of the process, which is confirmed by the obtained data (Fig. 2).

The optimum concentration of Esteramine is 5%. Increasing the emulsifier concentration further is without effect on the polymerization rate; decreasing the concentration leads to a reduction in the rate of the process.

Effect of pH of aqueous phase. For hexafluorobutadiene an emulsifier will be effective in strongly acid medium, where hydrolysis is slight. Decreasing the acidity of the medium results in a reduction of the emulsifying ability due to the hydrolysis process predominating, which is confirmed by the experimental results. The polymerization is greatly inhibited when the pH is increased from 3 to 7 (Fig. 3).

Effect of the water : monomer ratio. A satisfactory polymerization rate was obtained with a water : monomer ratio of 2.5 : 1. Increasing this ratio leads to a reduction in the rate. It is possible that this is also due to dilution, which leads to a reduction in the concentration of the micelles, functioning as reaction centers. Decreasing the water : monomer ratio reduced the stability of the emulsion (Fig. 4).

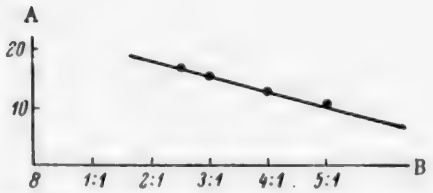

Fig. 4. Relation between the polymerization rate and the water : monomer ratio. A) extent of polymerization (in %); B) water : monomer ratio.

Fig. 5. Ratio between the polymerization rate and the nature of the initiator. A) extent of polymerization (in %); B) time (in hours). I) potassium persulfate; II) azobisisobutyronitrile; III) Isopropylbenzene hydroperoxide; IV) tert-butylcumene hydroperoxide.

Effect of the nature of the initiator. As initiators we tested both water-soluble compounds (potassium persulfate) and initiators soluble in organic media (isopropylbenzene hydroperoxide, tert-butylcumene hydroperoxide, azobisisobutyronitrile), all tested at a concentration of 0.6 mole %. Here the organic peroxides were quite inactive (Fig. 5). Apparently the low activity shown by the organic hydroperoxides is linked with their poor efficiency under the indicated polymerization conditions (acid medium).

As was indicated by certain authors [6-9], the formation of an active complex between the monomer molecule and the peroxide molecule precedes the formation of the initial active centers. The mechanism of complex formation is linked with the polarization of the molecules forming the complex. Together with a low activity in the polymerization process, hexafluorobutadiene is apparently also less inclined than other dienic compounds to enter into coordination with the initiator molecule, and this is responsible for a slowing up of the polymerization process.

Effect of oxidation-reduction systems. We studied the following known oxidation-reduction systems (in g):

I		II	
1) $K_2S_2O_8$	— 1.00	1) $K_2S_2O_8$	— 1.00
2) $FeSO_4$	— 0.05	2) $FeSO_4$	— 0.05
3) $Na_4P_2O_7$	— 0.15	3) $Na_4P_2O_7$	— 0.15
4) Invert sugar	— 1.00	4) Dihydroxymaleic acid	— 0.30

III		IV	
1) $K_2S_2O_8$	— 1.00	1) $K_2S_2O_8$	· 1.00
2) $FeSO_4$	— 0.05	2) Hydroquinone	- 0.05
3) Dihydroxymaleic acid	— 0.30	3) $KHSO_3$	— 0.25

The components of the oxidation-reduction system were taken on the basis of 100 g of monomer (Fig. 6).

It was found that oxidation-reduction systems, facilitating a more rapid decomposition of the initiator, speed up the polymerization at the start, and then the polymerization process is sharply retarded

Effect of initiator concentration. As can be seen from Fig. 7, the polymerization rate increases as the initiator (potassium persulfate) concentration is increased.

Effect of polymerization temperature. The polymerizations were run at temperatures ranging from 50- to 70°. As can be seen from Fig. 8, the polymerization rate increases with temperature increase. However, the formation of oily low-molecular polymerization products were observed at a temperature of 70°.

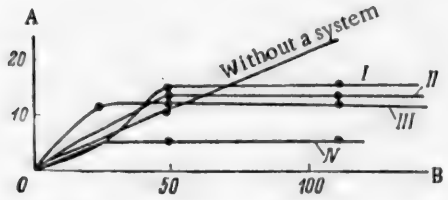

Fig. 6. Relation between polymerization rate and nature of oxidation-reduction system. A) extent of polymerization (in %); B) time (in hours). The figures on the curves correspond to the numbers of the systems.

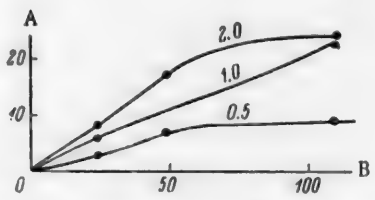

Fig. 7. Relation between the polymerization rate and the initiator ($K_2S_2O_8$) concentration. A) extent of polymerization (in %); B) time (in hours). The figures on the curves correspond to the initiator concentration.

After studying the effect of all of the above enumerated factors on the polymerization of hexafluorobutadiene, we settled on the following formula and conditions for running the process: hexafluorobutadiene 100 g, water 241.75 g, Esteramine 5.00 g, hydrochloric acid (36%) 3.25 g, and potassium persulfate 1.00 g; pH of aqueous phase 3.0; polymerization temperature 50°; time 120 hr; yield 23%.

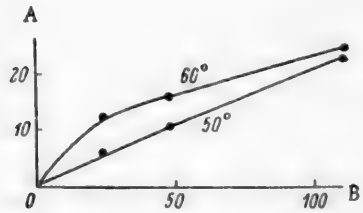

Fig. 8. Relation between polymerization rate and the temperature. A) extent of polymerization (in %); B) time (in hours).

The hexafluorobutadiene polymer was obtained as a clear powdery substance with m. p. 131°. Attempts to mold it at a pressure of 150-300 kg/ cm^2, either at room temperature or at the melting point, failed to yield a strong polymer. The obtained disks were characterized by being brittle and weak.

The solubility of the polymer in different solvents was examined, and here we were unable to find a solvent in which the polymer would dissolve. Because of its insolubility, the molecular weight of the polymer could not be determined by either the osmometric or the viscosimetric method.

Attempts were made to increase the strength of the polymer by hot rolling with fillers (active silica), the latter taken in amounts up to 50% on the weight of polymer. However, here also the strength of the polymer could not be improved.

SUMMARY

1. It was established that in going from fluorocarbon olefins to fluorocarbon diolefins with a conjugated system of double bonds a substantial reduction in reactivity is observed as regards polymerization, which is apparently due to the small mobility of the π-electrons in the hexafluorobutadiene molecule.

2. It was established that the polymerization goes only in emulsions containing the cation-active emulsifier Esteramine, and in the presence of initiators, causing excitation of the reaction by the radical mechanism.

3. In contrast to the polymer from tetrafluoroethylene, the hexafluorobutadiene polymer is characterized by a low melting point (131°) and low strength; it is insoluble in most organic solvents.

LITERATURE CITED

[1] M. Prober and W. Miller, J. Am. Chem. Soc. 71, 2, 598 (1949).

[2] U. S. Patent 2,567,956 (1951).

[3] W. Miller, R. Ehrenfeld, J. Phelan, M. Prober, and S. Reed, Ind. Eng. Ch. 39, 3, 401 (1947).

[4] S. Gericke and B. Kurmies, Z. Anal. Chem. 132, No. 5, 335 (1951).

[5] A. P. Sheinker and S. S. Medvedev, J. Phys. Chem. (USSR) 29, No. 2, 250 (1955).

[6] S. Kamenskaya and S. Medvedev, J. Phys. Chem. (USSR) 7, 922 (1940).

[7] L. Gindin, A. Abkin, and S. Medvedev, J. Phys. Chem. (USSR) 21, No. 11, 1269 (1957).

[8] J. W. Breitenbach, A. Springer, and E. Abrahamczik, Oesterr. Chem.-Ztg. 41, No. 9, 182 (1938).

[9] P. Khomikovskii and S. Medvedev, J. Phys. Chem. (USSR) 22, 1027 (1948).

Received August 9, 1958

SIMULTANEOUS SYNTHESIS OF BUTADIENE AND NORMAL BUTYL ALCOHOL FROM PROPYLENE AND FORMALDEHYDE

M. I. Farberov, A. M. Kut'in, A. F. Frolov, and T. P. Vernova

Yaroslavl Technological Institute and Institute of Monomers for Synthetic Rubber

Investigations on the technical synthesis of dienes from olefins and aldehydes have been conducted in our laboratory for a number of years [1]. The synthesis of butadiene from propylene and formaldehyde has been done on a pilot plant scale, where the results obtained in the laboratory were confirmed.

When the simpler olefins are reacted with aqueous solutions of formaldehyde in the presence of dilute sulfuric acid solution (1–5%) the main reaction products, obtained in yields ranging from 75 to 93% of the theoretical, are alkyl-1,3-dioxanes, together with small amounts of diols and cyclic alcohols [1, 2]. In our laboratory catalysts were developed and conditions selected under which the alkyldioxanes are converted to dienes in 80–90% yield. For example, 4-methyl-1,3-dioxane, the principal product when propylene is reacted with formaldehyde, can be converted to butadiene by passage over calcium-phosphate catalyst at 375–400° in the presence of steam. Besides butadiene, the other reaction products obtained here include small amounts of allylcarbinol [1].

Further study revealed that the amount of allylcarbinol (III) can be increased substantially [3] if the process is run under milder conditions (at lower temperatures and shorter contact time), resulting in a relatively low conversion of the methyldioxane (I). Thus, at 350° and a contact time of 0.4 sec, the conversion of (I) in one pass is 60%, but the molar yields of butadiene and allylcarbinol, based on reacted (I), prove to be approximately the same (Fig. 1). Increasing the contact time leads to a sharp reduction in the yield of (III). The curves for the yield of (III) pass through a maximum ("kinetic hump"), characteristic for consecutive reactions, insofar as allylcarbinol apparently suffers sequential dehydration to butadiene.

The effect of temperature on the yield of (III) in mole percent, based on passed (I), is shown in Fig. 2; in all cases the curves showing the relation between the yield of (III) and the "nominal" contact time have a characteristic maximum.

In order to obtain a better accounting of the results we ran a number of material balance experiments. The results of a typical material balance experiment are given in Table 1; these results show that under the chosen conditions the weight ratio of (III) to butadiene, when the yield is based on decomposed (I), is even slightly greater than one.

Both allylcarbinol (III) and undecomposed methyldioxane (I) distill from the aqueous condensate as close boiling azeotropes with water, and the former can be used for a number of syntheses. The most practical direction for the technical utilization of (III) is its conversion to 1-butanol (V) by hydrogenation. 1-Butanol (V) is a very important product in basic organic synthesis, and only a few methods exist for its production on an industrial scale. The hydrogenation of (III) goes easily and in quantitative yield; here it is expedient to hydrogenate the aqueous azeotrope, and not pure (III).

The formaldehyde, obtained by cleavage in the reaction, was determined in the condensate, and was found to be 16.9 g, or 25.8 wt. %, based on decomposed (I).

The mechanism for the reactions described above we consider to be the following.

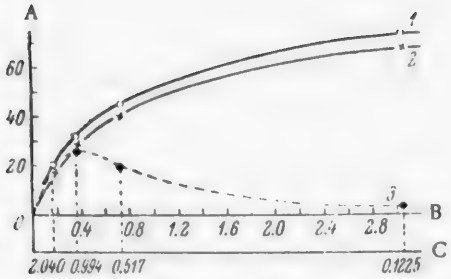

Fig. 1. Contact cleavage of methyldioxane on catalyst KCD at 350° and dilution of methyldioxane (MD) with steam in a 1:2 ratio by weight. A) Yield of allylcarbinol (in mole % on methyldioxane passed through); B) contact time (in sec); C) feed rate of methyldioxane (in ml/ml of catalyst/hr). 1) Conversion of MD to unsaturated hydrocarbons; 2) yield of C_4H_6 based on MD passed through; 3) yield of allylcarbinol based on MD passed through.

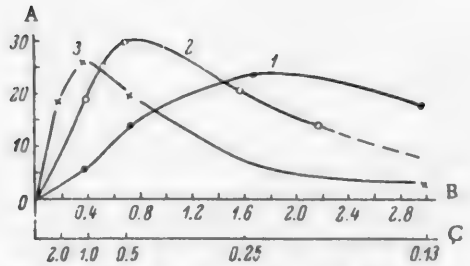

Fig. 2. Effect of temperature on yield of allylcarbinol when methyldioxane is diluted with steam in a 1:2 ratio by weight. Designation of the coordinates is the same as in Fig. 1. Temperature (in °C): 1) 300, 2) 325, 3) 350.

The catalyst (a mixture of calcium phosphates) possesses both hydrolyzing and dehydration properties. Thus, using a catalyst of this type in our laboratory, under conditions close to those described in this paper, we were able to hydrolyze methylal to methanol and formaldehyde in better than 80% yield. Using the same catalyst, and approximately the same conditions, it is possible to quantitatively dehydrate trimethylcarbinol to isobutylene. As a result, the first stage of the reaction is the hydrolysis of methyldioxane (I) in the presence of steam to 1,3-butanediol (III), with the simultaneous cleavage of formaldehyde. The butanediol then suffers dehydration with the cleavage of either one or two molecules of water to yield allylcarbinol (III) and butadiene (IV), respectively. The reactions for the formation of (III) and (IV) are consecutive, as is evidenced by the characteristic maximum on the kinetic curves expressing the relation between the yield of allylcarbinol and the contact time. Propylene is formed as the result of cracking.

TABLE 1

Material Balance Experiment on the Contact Conversion of Methyldioxane (I). Temperature 325°, space velocity 0.55 ml/ml of Catalyst/hr, Dilution with Steam 1:2 (based on a liquid volume ratio). 107.8 g (1.058 moles) of Methyldioxane (I) Was Passed During the Experiment, and the Amount That Reacted Was 65.6 g (0.643 mole).

Product	Obtained (in g)	Yield (in mole %)		Yield (in wt. %)
		on passed (I)	on decomposed (I)	on decomposed (I)
Butadiene	16.0	28.0	46.0	24.0
Propylene	1.4	3.1	5.1	2.1
Allylcarbinol	17.6	23.1	38.0	26.8
Unreacted methyldioxane	42.2	39.2	–	–
Carbon on catalyst	0.4	0.5	0.9	0.6
Unaccounted losses	–	6.1	10.0	–
Total	–	100	100	–

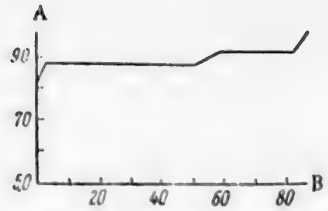

Fig. 3. Fractional distillation of condensate (material balance experiment) and isolation of methyldioxane and allylcarbinol as the azeotropes. A) Temperature (in °C); B) weight of fractions (in g).

Consequently, these transformations are depicted by the following scheme:

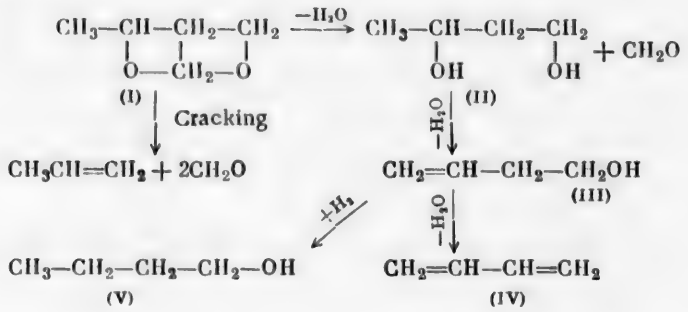

Separation of the reaction products. The contact cleavage of methyldioxane under the above described conditions yields a gas, composed mainly of butadiene with a small amount of propylene, and an aqueous condensate. This condensate contains unreacted (I), (III), and formaldehyde. It is possible to remove (I) and (III) from the condensate as their azeotropes with water (Fig. 3), the data for which are given in Table 2.

TABLE 2

Data on the Azeotropes of Methyldioxane (I) and Allylcarbinol (III) With Water [1, 4].

Product	B. p. at 760 mm (in °C)	Composition of azeotrope (in wt.%)		
		water	(I)	(III)
Methyldioxane (I)	115.3	—	—	—
Allylcarbinol (III)	114—115	—	—	—
Azeotrope with water: (I)	88.3	23.25	76.75	—
(III)	92.7	40.4	—	59.6

TABLE 3

Boiling Point and Composition of Azeotropes of Allylcarbinol (III) With Hydrocarbons [4].

Azeotrope (III)	B.p. at 760 mm (in °C)	Amt. of (III) in azeotrope (in wt.%)
With benzene	78.6	4.05
With toluene	103.6	33.6
With isooctane	91.0	21.0

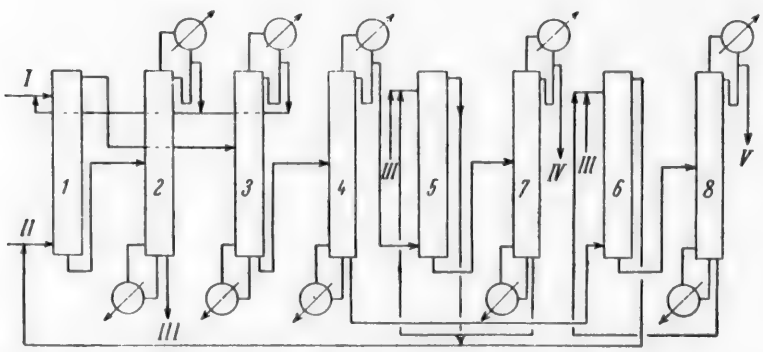

Fig. 4. Technological scheme of continuous process for separation of mixtures of allylcarbinol and 4-methyl-1,3-dioxane. I) Starting mixture, II) toluene, III) water, IV) allylcarbinol—water azeotrope, V) methyldioxane—water azeotrope.

The residue after distilling off the water azeotropes of (I) and (III) from the aqueous condensate represents dilute (7–8%) formaldehyde solution. The formaldehyde can be returned to the process (for condensation with propylene) as standard 37% solution by concentration under pressure [5].

To isolate pure (I) and (III) from the distillate (mixture of azeotropes with water) is quite difficult due to the close boiling points, not only of the substances themselves, but also of the azeotropes (Table 2). Investigation revealed that allylcarbinol (III) forms azeotropic mixtures with hydrocarbons like benzene, toluene, and isooctane (2,2,4-trimethylpentane), while methyldioxane (I) does not form azeotropes with these compounds [4] (Table 3).

On this basis, the following separation technique is proposed, consisting of the following operations: extraction of (I) and (III) from the aqueous solution with an azeotrope-former (toluene), which also functions as a solvent; fractional distillation of the extract, taking the azeotrope of (III) with toluene as the main fraction and leaving a solution of (I) in toluene as the residue; removal of (III) from the azeotrope by washing with water; removal of (I) from the toluene solution by washing with water; isolation of (I) and (III) from the aqueous solutions.

With such a technique we were able to take the starting mixture, containing 20–22% of (III), 40–45% of (I) and 35–40% of water, and isolate pure (I) and (III) as their water azeotropes in practically quantitative yields.

A continuous process for the isolation of (I) and (III), using toluene, can be accomplished by the scheme shown in Fig. 4.

The starting mixture, a water solution of (I) and (III), is fed in the top of extraction column 1, while toluene is fed at the bottom of the column. Water, containing about 4% of (I) and (III), is removed at the bottom of column 1. Up to 95% of (I) and (III) goes into the toluene solution. The water solution from the pot of column 1 enters rectification column 2, and here the water azeotropes of (I) and (III), removed at the top of the column, are recycled (returned to column 1), while the waste water is discarded. The toluene solution with extracted materials passes in succession through rectification columns 3 and 4, and here a small fraction of water azeotropes of (I) and (III) is removed in the first column and recycled, while the azeotrope of (III) with toluene is removed in the second column. The obtained azeotrope, and also the solution of (I) in toluene, are washed separately with water in columns 5 and 6. The obtained water solutions are then distilled through rectification columns 7 and 8 to yield the water azeotropes of pure (I) and (III), respectively. The toluene from columns 5 and 6 is recycled back to column 1.

Water azeotropes of pure methyldioxane (I) and allylcarbinol (III) can be obtained in this manner. Azeotrope (I) is returned to the contact process, while azeotrope (III) is used for hydrogenation to butanol.

EXPERIMENTAL *

The catalyst ("KSD"), standard for the conversion of alkyldioxanes to dienes, was a mixture of calcium phosphates [1].

Technical 4-methyl-1,3-dioxane, purified further by distillation, had the following constants: B.p. 114–116°, 1.4165, d_4^{20} 0.9741.

Literature data for the pure product [2]: b.p. 115.3° n_D^{20} 1.4159, d_4^{20} 0.9758.

The space velocity, based on methyldioxane, was expressed in milliliters of liquid passed through per milliliter of catalyst per hour.

The "nominal" contact time was calculated using the equation:

$$\tau = \frac{v_k \cdot 273 \cdot P}{v_g \cdot T \cdot 760},$$

* N. K. Shemyakina and G. V. Novikova assisted in the experimental portion of the work.

where τ is the contact time (in sec), v_k is the catalyst volume (in ml), and here the free space of the contact layer was taken equal to 65% of the bulk volume of the catalyst, v_g is the volume of the gases (in ml/sec), including the methyldioxane and water vapors, P is the pressure (in mm of Hg), and T is the absolute temperature during reaction.

Method of analysis. The amount of butadiene, collected during reaction and in the blowing of the condensate, was determined by bromination [6]. The amounts of allylcarbinol (III) and unreacted methyldioxane (I) were determined in the fraction that distilled from the condensate up to 96°. Here the amount of (III) was determined by the bromide-bromate method [6]; in individual cases this determination was checked by the phthalization method [7]. (I) was determined by hydrolysis in the presence of hydroxylamine salts [8]. The amount of formaldehyde in the condensate was determined by the Romijn iodometric method. The amount of unsaturates in the gas was determined by absorption in 84% H_2SO_4 in an Orsat apparatus; the difference between the amount of unsaturated hydrocarbons in the gas and the amount of butadiene was taken to be propylene.

Material balance experiments. In running the material balance experiments, the products from a number of experiments, run under the same conditions, were combined. The condensate was fractionated through a laboratory column with an efficiency of 45 theoretical plates. In addition, the amounts of (I) and (III) in the respective azeotrope fractions were determined analytically.

The amount of "carbon" on the catalyst was determined from the amount of carbon dioxide in the contact gas and in the recovery gases.

Allylcarbinol was isolated from its water azeotrope by salting out, followed by drying over potassium carbonate, and fractionation through an efficient column. The constants of the product were: b.p. 114.2–115° (760 mm), d_4^{20} 0.8453, n_D^{20} 1.4212. Acetate: b.p. 124.7–125.2°, d_4^{20} 0.9302, n_D^{20} 1.4206. Literature data [9]: b.p. 112–113.5° (755 mm), $d_4^{17.5}$ 0.8379, $n_D^{17.5}$ 1.4146; acetate: b.p. 125°, d_4^{20} 0.934.

Hydrogenation of allylcarbinol. The allylcarbinol–water azeotrope (isolated by azeotropic distillation with toluene) taken for reaction analyzed 57.4% of (III), 0.14% of (I), and 42.46% of water. The hydrogenation was run over copper-chromite catalyst, reduced in a rocked autoclave [10]. The charge placed in the autoclave was 6 parts of catalyst, 60 ml of methanol, 154 g (1.23 moles) of azeotrope (III) and hydrogen up to a pressure of 80 atm at 18°. The hydrogenation was run with heating for 1.5 hours. The temperature at the end of reaction was 140°. The hydrogen consumption was 28.2 liters (N.T.P.) (1.26 moles). The hydrogenation products were filtered from the catalyst and fractionally distilled. The yield of n-butyl alcohol was quantitative.

The obtained 1-butanol had b.p. 117–117.5°, d_4^{20} 0.8095, n_D^{20} 1.3999. Literature data [11]: b.p. 117.4°, d_4^{20} 0.80978, n_D^{20} 1.3993.

SUMMARY

1. A detailed study of the conditions for the contact cleavage of 4-methyldioxane (main product from the reaction of propylene with formaldehyde) made it possible to effect the simultaneous synthesis of butadiene and allylcarbinol in approximately equal weight amounts. The yield of desired products was 84%, based on decomposed methyldioxane.

2. It was pointed out that a practical technical use for allylcarbinol is to quantitatively hydrogenate it to n-butyl alcohol.

3. In our process we offer the technique of azeotropic distillation in the presence of toluene as one of the ways to separate allylcarbinol from unreacted methyldioxane.

4. As the result of our work we propose a technical process for the simultaneous synthesis of butadiene and normal butyl alcohol from propylene and formaldehyde. •

• The method is protected by a Soviet Author's Certificate [11].

LITERATURE CITED

[1] M. I. Farberov, Ya. I. Rotshtein, G. I. Kishinskii, and A. M. Kut'in, Monograph, New Method of Synthesis of Dienes of Divinyl Series (Moscow Chemical Industry Press, 1952).

[2] M. I. Farberov, Ya. I. Rotshtein, A. M. Kut'in, and N. K. Shemyakina, J. Gen. Chem. 27, 2806 (1957).*

[3] M. I. Farberov, A. M. Kut'in, T. P. Vernova, and N. K. Shemyakina, Scientific Reports of the Higher School, Vol. 1, No. 1, 149 (1958).

[4] A. F. Frolov and G. V. Novikova, Scientific Memoirs of Yaroslavl Technological Institute 2, 113 (1957).

[5] M. I. Farberov and V. A. Speranskaya, J. Applied Chem. (USSR) 28, 222 (1955).*

[6] A. I. Gulyaeva and co-workers, Analysis of Products in the Production of Divinyl From Alcohol (Moscow, 1950).**

[7] P. Elving and Benj. Warshowsky, Anal. Chem. 19, 1006 (1947).

[8] M. I. Farberov and N. K. Shemyakina, J. Gen. Chem. 26, 2749 (1956).*

[9] I. Heilbron and H. M. Bunbury, Dictionary of Organic Compounds [Russian translation] (Moscow, 1949).

[10] H. Adkins, E. E. Burgoyne, and H. J. Schneider, J. Am. Chem. Soc. 72, 2626 (1950).

[11] Soviet Author's Certificate No. 16,487, May 3, 1955.

Received December 29, 1958

* Original Russian pagination. See C. B. Translation.

** In Russian.

PREPARATION AND INVESTIGATION OF METHYL ACRYLATE – METHACRYLIC ACID POLYMER

A. Ya. Drinberg, B. M. Fundyler, and E. A. Volynskaya

Polyacrylates and poly(methyl methacrylates) surpass other types of polymers in their mechanical and dielectric properties and resistance to aging [1]. However, important differences exist between acrylate polymers and the polymeric esters of methacrylic acid. In its character, the chain of an acrylate polymer is much more flexible than the chain of a methacrylate polymer, due to the fact that it does not contain methyl groups, which are the reason for the appearance of stiffness because of limited rotation [2]. For this reason acrylic acid esters possess considerable interest for the synthesis of copolymers. Polymeric acrylates and methacrylates cannot be used alone as film formers because of their poor coating adhesion properties. One of the most effective and promising ways of modifying the properties of polymers in the desired direction is to introduce new functional groups into the polymer or copolymer molecule. In particular, the introduction of carboxyl groups into the chain of saturated polymers gives many possibilities of converting the latter into a three-dimensional state, and in this manner opens up prospective ways of obtaining mechanically stronger, heat-resistant materials, showing excellent adhesion to metals, wood, and plastics [3, 4].

The information on the copolymers of methyl acrylate with unsaturated acids like acrylic acid and maleic anhydride is limited to the copolymerization constants [5, 6].

There is no information in the literature on the copolymer of methyl acrylate with methacrylic acid.

The preparation of methyl acrylate-methacrylic acid copolymers, and an investigation of coatings based on them, is the subject of the present communication.

Several procedures exist for the preparation of carboxyl-containing copolymers [7–10]. The simplest and most rational technique is to copolymerize the monomers. The most active monomer in the binary systems butadiene–methacrylic acid [11], styrene–methacrylic acid [12] and ethylacrylate–methacrylic acid [10] is methacrylic acid. Because of this, the polymer formed in the first stages of the process is quite rich in methacrylic acid, and the chemical composition of the copolymer changes with change in the degree of polymerization.

It seemed of interest to study the change in the content of carboxyl groups in the copolymer as a function of the starting composition of the monomers and the time of copolymerization.

In our work we used the method of copolymerization in solution, using benzoyl peroxide as the initiator.

The reaction was run using a 40% concentration of the monomers. Acetone and cyclohexanone were used as the solvents. The amount of benzoyl peroxide added was 0.2% on the weight of the monomers.

Freshly distilled methyl acrylate (b.p. = 69 – 75°, d_{20} = 0.9080, n_D^{20} = 1.4015 and methacrylic acid (b.p. = = 55 – 57° (5 – 6 mm), d_{20} = 1.0152, n_D^{20} = 1.4300) were taken for reaction.

To determine the relation between the content of carboxyl groups in the copolymer and the time and temperature of the process, we subjected a mixture of methyl acrylate, containing 10% methacrylic acid,* to copolymerization.

* In all cases the amount of acid is given in % on the weight of methyl acrylate.

TABLE 1

Copolymer Composition as a Function of the Time of Copolymerization

Expt. No.	Time of copolymer (in hr)		Acid number of copolymer (in mg of KOH/ g)		Amt. of methacrylic acid found in the copolymer (in %)		Amt. of methyl acrylate (in moles/ mole of acid)	
	80°	90°	80°	90°	80°	90°	80°	90°
0	0	0	64.7	63.5	11.0	10.8	9.1	9.2
1	2	0.75	125	81.8	23.8	14.4	4.2	7
2	2.25	1	115	76.9	21.5	13.4	4.65	7.45
3	3	1.25	77	74.9	13.5	13.0	7.4	7.7
4	3.25	1.5	63	75.3	10.7	13.05	9.35	7.65
5	3.5	2	66.5	65	11.35	11.1	8.8	9
6	3.75	2.5	66.0	64.7	11.3	10.95	8.85	9.1
7	4.25	3.5	64.5	60.0	11.0	10.1	9.1	9.86
8	5.25	5.5	64.5	60.5	11.0	10.2	9.1	9.86
9	7.25	—	62.0	—	10.5	—	9.55	—

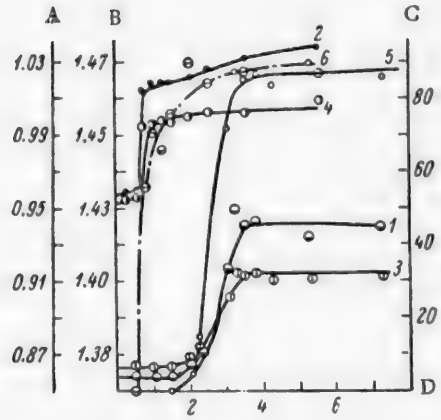

Change in the refractive index, specific gravity, and yield of copolymer as a function of the reaction time. A) Specific gravity (1, 2) d_{20} (in g/cm^3); B) refractive index (3, 4) n_D^{20} C) yield (5, 6) of copolymer (in %); D) reaction time (in hr). Temperature (in °C): 1, 3 and 5—80; 4 and 6—90.

TABLE 2

Relative Viscosity of Copolymer as a Function of the Time and Temperature of the Copolymerization Reaction

Expt. No.	Flow time of copolymer solution (in sec)		Relative viscosity*	
	80°	90°	80°	90°
1	—	20.0	—	1.26
2	19.8	19.4	1.709	1.225
3	—	19.0	—	1.201
4	19.2	18.8	1.6255	1.19
5	17.22	20.0	1.488	1.26
6	18.5	19.5	1.593	1.23
7	17.6	19.8	1.518	1.25
8	17.3	20.0	1.492	1.26
9	17.3	—	1.492	—

* Flow time of cyclohexanone at 80° is 11.6 sec, and at 90° it is 15.8 sec.

The experiments were run in sealed glass ampuls, heated in a thermostat at 80° in the case of acetone, and at 90° in the case of cyclohexanone. It should be mentioned that the copolymerization of methyl acrylate with methacrylic acid did not go in sealed ampuls when the thermostat temperature was below 80°.

The copolymerization reaction was controlled by the change in the refractive index and specific gravity of the copolymerizate. The kinetics of the reaction were studied by analysis of the copolymer, its yield, amount of reacted methacrylic acid, and change in the relative viscosity of a 1% solution of the copolymer in cyclohexanone.

To isolate the copolymer, the reaction mixture was diluted with acetone until a 10% solution was obtained, and then the copolymer was precipitated by the addition of 3—4 volumes of petroleum ether. This operation was repeated. Then the copolymer was dried at 50—60°.

The analysis results are shown in the Figure.

TABLE 3

Composition and Yield of Copolymers as a Function of the Component Ratio in the Starting Mixture and the Reaction Conditions

Starting mixture		Reaction temp. (in °C)	Reaction time (in hr)	Copolymer		Amt. of methyl acrylate per mole of acid (in moles)		Yield (in %)
amt. of methacrylic acid (in %)	K_n* (in mg of KOH/ g)			amt. of methacrylic acid (in %)	K_n (in mg of KOH/ g)	in starting mixture	in copolymer	
5.55	34.2	60—65	6	10.65	62.7	18	9.4	28
			16	9.43	56.2	18	10.7	49.2
12.00	69.5	60—65	6	20.8	112.0	8.3	4.8	30
			11	19.6	106.85	8.3	5.1	50
14.60	83.0	60—65	6	28.9	146.00	6.8	3.46	30
5.95	36.5	80	3	6.55	39.85	16.7	15.2	60
12.00	69.8	80	3	14.95	84.6	8.3	6.67	60

* K_n is given on the basis of a 100% mixture of monomers.

TABLE 4

Physicomechanical Properties of Coatings Prepared From Methyl Acrylate—Methacrylic Acid Copolymer

Drying temp. (in °C)	Drying time (in hr)	Adhesion	Impact strength in kg/cm)	Bending (in mm)	Hardness	Water resistance	Aging at 150° (in hr)
120	1.5	Good	50	1	0.860	First evidence of corrosion appeared after 18 days	160 *
60	2				0.460	The film became cloudy after 2 hours	160

* Indicates the exposure time in which the coating failed to change its physicomechanical properties.

The data shown in the Figure indicate that the reaction for the copolymerization of methyl acrylate with 10% methacrylic acid at 80 and 90° has an induction period, the duration of which is 1.5 hr in the first case, and 30 min in the second case.

The isolated copolymers were analyzed for methacrylic acid content, which was determined by titration with alkali in the presence of phenolphthalein. The mixtures taken for polymerization, the filtrates, and the copolymers were analyzed. The results of investigating the rate of change in the content of carboxyl groups in the copolymer are given in Table 1.

Copolymers rich in methacrylic acid are obtained in the intial stages of copolymerization. The polymers obtained at the higher temperature are characterized by a lower content of carboxyl groups, and their composition approaches that of the starting mixture. This is explained by the higher activity of the methacrylic acid monomer (for a given temperature) and the fact that the relative activities of the monomers approach one [13] as the temperature is raised, and this results in obtaining copolymers with a more homogeneous composition, close to the ratio of the monomers in the starting mixture. As reaction progresses the amount of methacrylic acid in the polymer decreases and gradually approaches its content in the starting mixture. As a result, running the copolymerization of

methyl acrylate with methacrylic acid at 80° leads to the formation of copolymers with a heterogeneous content of carboxyl groups, while more homogeneous copolymers, with a ratio of the components close to their ratio in the starting mixture, are obtained at the higher temperature (90°).

The change in the relative viscosity of the copolymers was investigated. The change in the relative viscosity of the copolymer as a function of the time and temperature of synthesis is shown in Table 2.

A decrease in the relative viscosity with reaction progress, especially noticeable in the first stages of the copolymerization process, is observed for the copolymers obtained at 80°. This is explained by the heterogeneous composition of the copolymers obtained under these conditions. Copolymers with a high content of methacrylic acid have a more rigid chain structure, responsible for a higher viscosity at the same solution concentration.

Subsequent minor change in the average acid number (K_n) of the copolymer results in but slight change of the relative viscosity. The copolymers obtained at 90° have a more homogeneous composition, as evidenced by the change in K_n of the copolymers with time (in this case the change in the relative viscosity of the copolymers is hardly noticeable). A smaller relative viscosity for the copolymers obtained at the higher temperature, but having nearly the same K_n, is apparently due to the fact that raising the temperature facilitates the rate of chain rupture and thus a reduction in the average molecular weight.

To determine the effect of monomer ratio on copolymer composition, we copolymerized mixtures of methyl acrylate with 5.5, 12.0, and 14.6% methacrylic acid at 60–65° in acetone medium, and at 80° in cyclohexanone medium. The concentration of the monomers was 40%, and the amount of benzoyl peroxide added was 0.2%.

In Table 3 we have given the amount of methacrylic acid (in %) in the starting mixture and the composition of the copolymers, and also the yield of copolymers as a function of the reaction conditions.

Depending on the ratio of the components, copolymers of different composition are obtained. Methacrylic acid is the more active monomer. Up to a reaction temperature of 70° and independent of the reaction time, the amount of methacrylic acid that copolymerizes with methyl acrylate is twice that present in the starting mixture. Raising the reaction temperature leads to obtaining copolymers in which the ratio of the components is close to that in the starting mixture. Here both the rate of the process and the yield of copolymers increases.

Copolymers of methyl acrylate with methacrylic acid are soluble in acetone, cyclohexanone and ethyl cellosolve. Aromatic hydrocarbons can be used as diluents.

To test the methyl acrylate–methacrylic acid copolymer in coatings we prepared 14% lacquers in ethyl cellosolve. As hardener we used hexamethylenediamine, which was taken in the ratio of 1 mole per mole of methacrylic acid.

The physicomechanical properties of the coatings were evaluated on the basis of the following criteria: impact strength, bending coefficient, hardness, adhesion, water resistance, and aging at 150° [14].

The tests were run on one-layer coatings that had been prepared from a copolymer with K_n equal to 85.6.

The results of the physicomechanical testing of the coatings are given in Table 4.

The tests revealed that coatings prepared from methyl acrylate–methacrylic acid copolymer, hardened with hexamethylenediamine, show good adhesion to steel, and a high hardness, mechanical strength and elasticity, and good aging stability.

SUMMARY

1. Using the solution method to synthesize the copolymer of methyl acrylate with methacrylic acid in either acetone or cyclohexanone medium, with a variable ratio of the components in the reaction mixture and at different temperatures, it was established that the copolymerization of methyl acrylate with methacrylic acid goes through an induction period, the time of which depends on the reaction temperature.

2. Depending on the ratio of the components, copolymers with a variable content of methacrylic acid were obtained.

3. The reaction temperature exerts an important effect on the composition of the copolymers. At 70° the amount of methacrylic acid that copolymerizes with methyl acrylate is twice that contained in the starting mixture.

Running the copolymerization at 90° leads to the formation of products with a more homogeneous composition, in which the ratio of the components is close to that in the starting mixture.

4. Coatings prepared from methyl acrylate–methacrylic acid copolymer, using hexamethylenediamine as the hardener, show good adhesion to steel, good impact and bending strength, and a high hardness. The coatings failed to suffer a change in their physicomechanical properties when exposed for 160 hours to a temperature of 150°.

LITERATURE CITED

[1] C. T. Kautter, Kunststoffe 45, 4, 131 (1955).

[2] J. T. Clarke, Monograph "Monomers" [Russian translation] (IL, Moscow, 1953), Vol. 2, p. 27.

[3] A. A. Berlin, Soviet Author's Certificate No. 73,019, April 24, 1947; Soviet Author's Certificate No. 73,440, April 24, 1947.

[4] H. R. Dittmar and H. M. Cadot, U.S. Pat. 2,557, 266, June 19, 1951; C. A. 45, 8294e (1951).

[5] F. Sabbioni, Ricerca scient 25, Suppl. 59 (1955).

[6] F. R. Mayo, F. M. Lewis, and C. Walling, J. Am. Chem. Soc. 70, 1529 (1948).

[7] German Patent 914,326, July 1, 1954.

[8] U.S. Patent 2,681,327, June 15, 1954; U.S. Patent 2,626,248, January 20, 1953.

[9] C. S. Marvel, T. R. Fukuto, James W. Berry, W. K. Taft, and B. G. Labbe, J. Pol. Sci. 8, 599 (1952).

[10] H. P. Brown and C. F. Gibbs, Ind. Eng. Ch. 47, 5, 1006 (1955).

[11] Rubb. Age 66, 2, 173 (1949).

[12] Electronics 22, 10, 110 (1949).

[13] T. Alfrey, J. J. Bohrer, and H. Mark, Copolymerization [Russian translation] (IL, Moscow, 1953) p. 109.

[14] S. V. Yakubovich, Testing of Lacquer-Paint Materials and Coatings [in Russian] (Goskhimizdat, 1952).

Received July 8, 1958

LACQUER COATINGS BASED ON COLLOIDAL DISPERSIONS OR CARBON BLACK IN CELLULOSE ACETATE PHTHALATE ESTERS

L. V. Rozental' and G. I. Burdygina

All-Union Motion Picture Scientific Research Institute

Of the cellulose esters of dibasic organic acids [1–5] that have been studied up to now, the cellulose acetate phthalate esters [1, 3, 5] have attracted the greatest attention. A valuable technical property of cellulose acetate phthalate esters is their solubility, not only in many organic solvents, but also in dilute alkalies. Reaction with the latter yields water-soluble cellulose acetate phthalate salts:

$$C_6H_7O_2\begin{vmatrix}-OOCCH_3\\-OOCCH_3\\-OOCC_6H_4\\|\\COOH\end{vmatrix} + NaOH \rightarrow C_6H_7O_2\begin{vmatrix}-OOCCH_3\\-OOCCH_3\\-OOCC_6H_4\\|\\COONa\end{vmatrix} + H_2O.$$

According to the data in a number of patents, lacquer coatings based on cellulose acetate phthalate show high water resistance. Together with this, they are easily removed by rinsing with dilute alkali solutions. The surface-active properties of cellulose acetate phthalate esters are far superior to those of other alkali-soluble polymers. As our investigations revealed, cellulose acetate phthalate esters are much more efficient dispersing agents for carbon black than carboxymethyl cellulose, polyvinyl alcohol, "Povimal" and OK lacquer (condensation product of p-cresylglycol and p-hydroxybenzoic acid). At the same time, although, according to the data of Klimova and Bershtein [5], the heat stability of cellulose acetate phthalate esters is limited, still it is substantially better than the stability of casein, used in practice as a binder for carbon black, the solubility of which shows substantial change with time because of its spontaneous tanning.

Our purpose in the present study was to establish the conditions for obtaining easily removed lacquer coatings (antihalo and protective coatings on movie film) from cellulose acetate phthalate and its colloidal dispersions containing carbon black.

EXPERIMENTAL

We synthesized cellulose acetate phthalate by two procedures: 1) phthalization of diacetylcellulose in pyridine solution with subsequent precipitation of the cellulose acetate phthalate with hot hydrochloric acid solution [1], and 2) phthalization of diacetylcellulose (in acetone solution) by heating under pressure, followed by precipitation of the cellulose acetate phthalate with water [6].

The second procedure is more convenient and permits easy regulation of the number of phthalate groups in the cellulose acetate phthalate and also the viscosity (Tables 1 and 2). •

• A study of the conditions for the synthesis of cellulose acetate phthalate was made with the assistance of O. K. Smirnova, N. I. Grineva, and L. I. Egina.

TABLE 1

Effect of Water Content in Phthalization Mixture on Number of Phthalate Groups in Cellulose Acetate Phthalate

Amounts charged into autoclave (in g)				Synthesis temperature (in °C)	Pressure (in atm)	Time (in hr)	Content of phthalate groups in cellulose acetate phthalate (in %)
acetyl-cellulose	phthalic anhydride	acetone	water				
240	240	240	9	150—152	6.5—7	4	17.5—18
240	240	240	15	150—152	6.5—7	4	21.9—21.8
240	240	240	20	150—152	6.5—7	4	22.5—22.6

TABLE 2

Effect of Content of Phthalate Groups in Cellulose Acetate Phthalate on the Viscosity and Ease of Rinsing Lacquer Coating From Triacetate Film

Content of phthalate groups in cellulose acetate phthalate (in %)	Viscosity of 10% solution of cellulose acetate phthalate in alcohol—acetone mixture (in centipoises)	Extent of removing lacquer coating from film by rinsing with water after swelling in solution with pH = 9.3
17.5—18.0	23.2	Not rinsed off
—	17.6	Rinsed with difficulty
—	13.0	
—	9.3	
21.9—21.8	6.5	Easily rinsed
22.5—22.6	5.6	

TABLE 3

Mechanical Properties of Triacetate Film With Carbon Black Coating

Specimen	Tensile strength (kg/mm^2)	Elongation (in %)	Number of double bends
Film without coating	9.8	23	90
Film with carbon black coating 5μ thick*	8.6	27.7	151

* The thickness of the coating was purposely increased to 5μ in order to obtain a better idea as to its influence on the mechanical properties of the film.

Cellulose acetate phthalate containing 22—23% of phthalate groups is readily soluble in organic solvents and in dilute alkalies. Decreasing the content of phthalate groups in cellulose acetate phthalate causes the viscosity to increase, while the solubility in alkalies decreases. This makes it more difficult to rinse off the lacquer coatings (backings), prepared from it, from triacetate film (Table 2).

To prepare the colloidal dispersions, we used specially oxidized carbon black. The average diameter of the elementary particles of this carbon black was about 350 A, and the specific surface, when determined (after oxidation) by the kinetic method, was about 230 m^2/g. *

The special carbon black contained a large amount of volatiles (up to 18%), representing a complex of oxygen with surface carbon atoms [7]. This complex facilitates a more rapid wetting and dispersing of the carbon black, and also increases the colloidal stability of the carbon black dispersion in the binder. The latter is explained by some authors as due to the fact that the surface-oxide complex, surrounding each carbon black particle, functions as a bonding link between the carbon black and the surrounding binder, in which it is distributed [8].

A comparative study of ordinary channel and special (oxidized) carbon blacks, suspended without binder in alcohol—acetone mixture, revealed that the suspension of oxidized carbon black had a much higher stability (Fig. 1).

*The samples of oxidized carbon black were graciously supplied to us by P. A. Tessner (All-Union Scientific Research Institute of Gases).

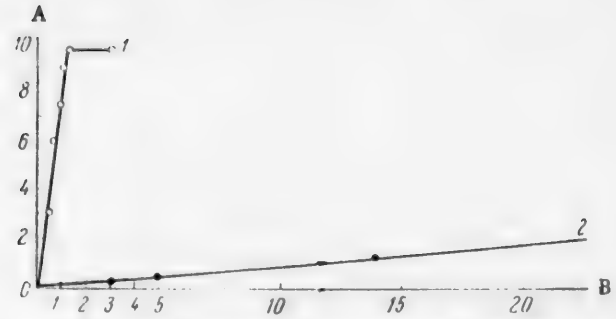

Fig. 1. Effect of nature of carbon black on its sedimentation rate in alcohol–acetone mixture. A) Height of deposit during sedimentation (in cm), B) time (in min). Carbon black: 1) channel, 2) oxidized (special).

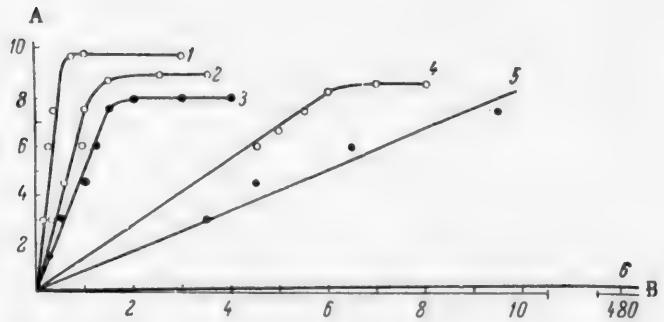

Fig. 2. Effect of the medium on the sedimentation rate of channel carbon black. A) Height of deposit during sedimentation (in cm), B) time (in min). Medium: 1) acetone, 2) water, 3) alcohol–acetone mixture (55:45), 4) dioxane + 20% water, 5) dioxane, 6) methyl cellosolve.

We estimated the stability of the suspensions by the sedimentation rate of the carbon black (height of carbon black deposit during sedimentation in a graduate cylinder).

When applied to carbon black with such a small size of the elementary particles (of the order of 350 A), the dispersion process reduces only to their complete disaggregation with the formation of a protective envelope of the binder around each particle. Because cellulose acetate phthalate has quite good surface-active properties, its use as a binder does not require the addition of special dispersing agents for the carbon black. The conditions under which the carbon black is dispersed are important here. The use of a ball mill to disperse carbon black in a solution of a cellulose acetate phthalate does not give a sufficiently complete disaggregation of the carbon black even if the process is run for 5–7 days.

A completely different picture is observed if the carbon black is dispersed in plasticized cellulose acetate phthalate without solvent, which permits running this process on powerful rolls with friction. Here the extremely high mechanical action exerted on the mass causes a complete disaggregation of the carbon black. • The absence of carbon black aggregates, visible under the microscope, when the dispersion is deposited on the film can serve as a criterion of the complete disaggregation of the carbon black.

• I. M. Alekeseeva assisted in studying the conditions for the dispersion of carbon black in plasticized cellulose acetate phthalate.

The use of water and alkali insoluble plasticizers (dibutyl phthalate) to plasticize cellulose acetate phthalate leads to obtaining lacquer coatings that do not rinse from the film. An easy rinsing of lacquer coatings from the film is achieved by using triacetin (glyceryl triacetate), and also the monomethyl ester of diethylene glycol, as plasticizers.

In choosing a dispersion medium we took into consideration the compatibility limits of the obtained dispersion in a given medium with water. Dispersions of carbon black in cellulose acetate phthalate, containing anhydrous organic solvents as the dispersion medium, when deposited on the film cause a strong deformation of the latter. This is especially pronounced when the dispersion is deposited on nitrocellulose film, which is associated with the fact that practically suitable solvents for cellulose acetate phthalate cause nitrocellulose to either swell or dissolve. Here the lacquer coating is so firmly bound to the nitrocellulose film that it is impossible to completely remove it by rinsing with alkaline solutions.

Increasing the amount of water in the dispersion lessens the effect of the latter on the film and facilitates the rinsing of the lacquer coating from the film by reducing the strength of their bonding.

Of the solvents for cellulose acetate phthalate the best dispersion medium is the monomethyl ether of ethylene glycol (methyl cellosolve). Relatively more stable suspensions are obtained when ordinary channel carbon black (without binder) is suspended in methyl cellosolve (Fig. 2). In these experiments we took channel carbon black for the express purpose of showing more clearly the influence of the medium on suspension stability.

Dispersions of the special carbon black in cellulose acetate phthalate, containing methyl cellosolve together with more volatile solvents (acetone) and diluents (alcohol) as the dispersion medium, are compatible with water in amounts up to 15%, with retention of the colloidal stability of the dispersion for 3 days. Further increase in the compatibility of the dispersion with water can be achieved only by neutral neutralization of the cellulose acetate phthalate with its partial conversion to the water-soluble ammonium salt. Neutralization of approximately 50% of the free carboxyl groups in cellulose acetate phthalate with ammonia permits increasing the amount of water in the dispersion to 30%, with a retention of its colloidal stability for more than 30 days. Here the water resistance of the lacquer coating is impaired slightly.

Damage to the dry lacquer coating (backings) on the film occurs when the friction load on the glass rod in the Derstuganov apparatus [9] exceeds 300 g. Improved resistance of the lacquer coating to abrasion damage can be achieved by putting a wax coat on top of the carbon black coating. Lacquer coatings, obtained by depositing a dispersion of carbon black in cellulose acetate phthalate on the film, hardly impair the mechanical properties of the film, and even in the presence of a wax coat are easily rinsed from the film by water, provided the film is swelled for a short time in alkaline solution with pH = 9.3.

A secondary chain structure can be seen on the photomicrographs of the lacquer coating, which is characteristic for all types of channel carbon blacks. According to the data of Pechovskaya, Pupko, and Dogadkin [10], the sharpness of these secondary structures is determined by the size of the elementary particles and nature of the carbon black.

SUMMARY

Lacquer coatings based on cellulose acetate phthalate are easily rinsed from nitrocellulose and triacetate films by dilute alkaline solutions.

In dispersing carbon black in cellulose acetate phthalate it is possible to obtain completely stable colloidal dispersions without resort to special dispersing agents and stabilizers. The stability of these dispersions and their adhesion to films both depend on the content of phthalate groups in the cellulose acetate phthalate, the number of its free carboxyl groups neutralized by ammonia, the properties of the carbon black, the degree of its disaggregation in the dispersion process, and finally, the composition of the dispersion medium.

LITERATURE CITED

[1] C. Malm and C. Fordyce, Ind. Eng. Ch. 32, 405 (1940).

[2] N. I. Nikitin and F. I. Korchemkin, Bull. Acad. Sci. USSR, Div. Chem. Sci. 2, 245 (1940).

[3] C. Malm, L. Genung, and W. Kuchmy, Anal. Chem. 25, 2, 245 (1953).

[4] S. N. Ushakov, O. M. Klimova, and S. G. Lyubetskii, J. Applied Chem. (USSR) 29, 3 (1956).*

[5] O. M. Klimova and V. A. Bershtein, J. Applied Chem. (USSR) 29, 1849 (1956).*

[6] U.S. Patent 2,183,982.

[7] V. V. Kel'tsev and P. A. Tessner, Properties, Manufacture, and Uses of Carbon Black [in Russian] (Gostoptekhizdat, 1952).

[8] L. J. Venuto, Paint Manufacture 24, 227, 265 (1954).

[9] G. V. Derstuganov, J. Scientific and Applied Photography and Cinematography (USSR) 1, 3 (1956).

[10] K. Pechkovskaya, S. Pupko, and B. Dogadkin, Colloid. J. (USSR) 12, 367 (1950).

Received February 4, 1957

*Original Russian pagination. See C. B. Translation.

APPLICATION OF CHROMATOGRAPHIC METHOD FOR INVESTIGATION OF CHANGES IN THE CARBOHYDRATE COMPLEX OF SUGAR BEET DURING PROLONGED STORAGE

O. V. Braun

The problem of determining the true content of sucrose and the amount of raffinose in the beet before refining is of major significance for the national sugar industry, since the majority of the sugar factories in the country operate for a considerable time in the winter, and some operate even in the spring (March). Undoubtedly, during such long storage certain processes occur in the beet, changing the structure of the root, and in particular the carbohydrate complex and the technological qualities of the fresh material; losses in sugar are also considerably increased during refining.

A considerable loss, found on determining sugar in the beet by various methods, is explained by the presence of optically-active substances, the amount of which is not constant, but varies within the wide limits according to the conditions under which the beet is grown and stored [1-4].

In spite of its simplicity, the polarimetric method of determining sucrose content has some substantial defects; as the content of optically-active substances increases in the beet and in the products of sugar industry, the total polarization is taken as the sucrose content, while chemical methods indicate that its content is considerably smaller [5-8].

It has been established that a smaller deviation from the true sucrose content is obtained only when the dextro-rotation of raffinose coincides with the levo-rotation of a number of nonsugars.

The main purpose of our investigation was the evaluation of the accepted industrial method of determing sucrose content in the beet, the study of the effect of other optically-active sugars on the determination of true sucrose content, and the study of changes in the carbohydrate complex in the beet during prolonged storage.

The accepted scheme of investigation of the beet and of the products of the sugar industry is based upon a combination of simultaneous determination of sugars by methods of direct polarization, inversion of polarization with two enzymes and chromatography. Such investigations and comparisons of sugar analyses are made for the first time in our industry.

The investigation has been carried out in two directions: 1) on beets of experimental "kagats" in the beet-planting zone of the Il'ich sugar factory, Iagotinsky district, Kiev region (1955 harvest), for which the beets were stored in three kagats; 2) on beets in the beet-planting region of the Dubno beet-stock location, Rovenskaya region (1955 and 1956 harvest).

In order to be able to compare changes which take place in the beet during storage in experimental kagats, great attention was paid to the homogeneity of the beet investigated. Fresh beets (1955 harvest) were treated without storage in September. Beets from one kagat were treated in January, 1956; from two others, in the beginning of March, 1956.

During treatment of experimental beet, samples were constantly taken for analysis. All samples selected were studied immediately.

A similar study for beets was also carried out during the production period 1956-1957. The method of investigation in this case was analogous to that of the preceding production season.

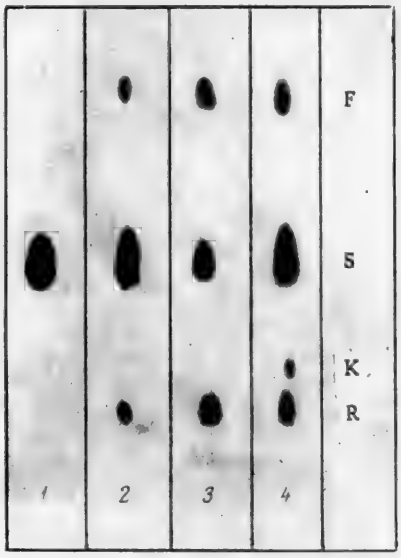

Fig. 1. "Ascending" chromatograms of sugars in the beet from beet-planting zone, Il'ich Iagotinskii Sugar Factory (Kiev region), 1955 harvest. 1) September 2) January 3) Controls 4) March R) Raffinose K) Kestose S) Sucrose F) Fructose

In the present paper, we give the results of a chromatographic study of the carbohydrate complex of beet during prolonged storage. This method was discovered by the Russian botanist M. S. Tsvet in 1903. The chromatographic method makes it possible to separate complex mixtures into component parts for analysis, and further to analyze the separate components in pure form [9, 10]. The method of chromatographic analysis is based on differential adsorption of substances which differ chemically from each other in their composition and structure.

Distribution chromatography is the name of the method for components of a mixture, based on the difference in component distribution between two nonmiscible liquids. A solution of the mixture to be studied in one of these liquids is placed on the bearer (paper), and is washed by second liquid. Chromatographic analysis is superior to the usual method of qualitative analysis and allows one to separate very small amounts of various substances in a relatively simple way.

Because of the large number of analyses and of their simplicity, we have chosen "ascending" chromatography, for which we used the special chromatographic paper number 2, of Leningrad paper factory. Out of a large number of mixtures used, we chose the mixture of n-butyl alcohol : acetic acid : water, in the ratio 5:1:2, for the moving solvent. This solvent separates sugars quite well, does not separate into layers, is sufficiently stable, and may be supplemented by simple addition, which is a very significant factor in carrying out analyses under factory conditions [11-22].

For developing chromatograms we used an α-naphthol reagent, made up of 0.5 g α-naphthol and 10 g orthophosphoric acid per 100 ml ethyl alcohol. This developer is most sensitive to minimal concentrations of ketosugars and disaccharides, but is toxic. Too, it does not stain aldosugars on chromatograms, and therefore cannot be used for development of glucose, galactose, and mannose; it makes chromatograms fragile; spots developed with this reagent decolorize rapidly and therefore need immediate fixation. When α-naphthol is used, development of chromatograms takes place in 3-5 minutes at a temperature of 90-100°. The spots are violet.

For development of aldosugars, we used a benzidine developer, consisting of 0.5 g benzidine, 20 ml glacial acetic acid and 80 ml ethyl alcohol. Development takes place in 10-15 minutes at a temperature of 100-105°. The spots are an intense yellow, and are relatively stable.

2.2 - 2.8% of dry substances were present in the original digests. The chromatograms were set up simultaneously, by placing 5 to 6 drops on them (during investigation of September samples).

Using a "descending" flow, and applying numerous drops of solution to the paper, drying it between applications, it was possible to obtain the spots of raffinose and kestose on chromatograms; these could not be developed when single drops of solution and the "ascending" flow were used.

The volume of a drop of original solution, which was placed on the chromatogram with a micropipette was 1 to 3 μl (microliters).

As chromatographic containers, we used 1 and 2 liter glass cylinders, firmly stoppered with corks to which were attached strips of paper with applied drops of solution. The separation of sugars on the chromatogram was carried out for 24-28 hours. By this time the solvent on the paper rose for 280-300 mm. The chromatograms were sprayed, using a glass atomizer. This resulted in rapid and even distribution of solvent on the paper.

Identification of sugars was carried out on the basis of previously-run experiments using pure solutions, for determination of corresponding R_f values, where R_f stands for coefficient of the movement rate, determined by

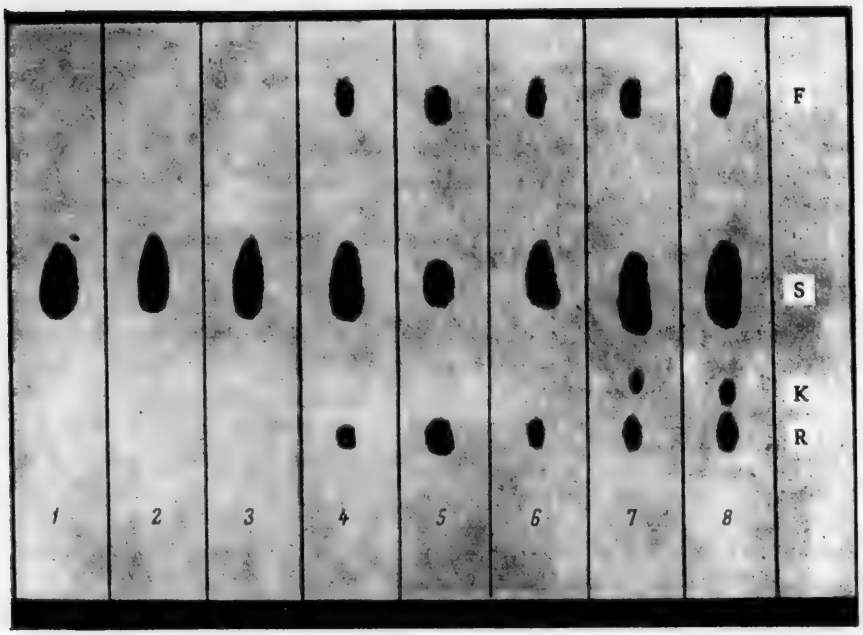

Fig. 2. "Ascending" chromatograms of beet sugars from the beet-planting zone of the beet-supply point Dubno (Rovenskaya region), 1955 harvest. 1) September 2) October 3) November 4) December 5) Controls 6) January 7) February 8) March; R) Raffinose K) Kestose S) Sucrose F) Fructose.

Fig. 3. "Ascending" chromatograms of beet sugars from the beet-planting zone of the beet-supply point Dubno (Rovenskaya region), 1956 harvest. 1) September 2) October 3) November 4) December 5) Controls 6) January 7) February 8) March; R) Raffinose K) Kestose S) Sucrose F) Fructose.

the ratio of the distance moved by a component of the mixture to the distance moved by the solvent; identification was also done by chromatographing pure samples simultaneously with the experimental solutions.

R_f values under the conditions of our experiments are given below.

Sugars	For individual sugar	For sugars of artificial mixture
Raffinose	0.09	0.09
Kestose	0.11	0.11
Sucrose	0.15	0.145
Galactose	0.16	—
Glucose	0.20	0.21
Arabinose	0.25	—
Fructose	0.26	0.25

For determination of the R_f of kestose, we carried out the following experiment. Chromatograms of a freshly-prepared 6% solution of pure sucrose were made. A single spot was developed on the chromatogram. After the solution stood for 20 days at a temperature of 19-21°, it was again applied to paper and, after developing with α-naphthol developer, threespots were clearly seen: sucrose, fructose (above sucrose) and a third component, the R_f value of which is very close to the R_f of raffinose, but is somewhat higher. Because of its location on chromatogram this component was identified as kestose. In further experiments during identification of sugars, the component having an R_f of 0.11 was taken to be kestose. During determination of the R_f of kestose in the above solution by a benzidine developer, a glucose spot was also developed, located between sucrose and fructose.

Thus, having made preliminary experiments in determining the R_f values of sugars in pure solutions, and having obtained sufficient experience in the work, we started the investigation of beet sugars in relation to the length of storage of fresh material.

Using chromatography with "descending" flow, as well as application of several drops (5-6) of solution on the same spot, we succeeded in establishing that raffinose is present in September in all beet samples of the 1955 harvest.

Figure 1 is a photograph of an "ascending" chromatogram of beet sugars from the zone of beet-planting of Il'ich Iagotinskii sugar factory (Kiev region), from the 1955 harvest. In the September sample the sucrose spot is clearly seen in the chromatogram. Parallel to this, we set up experiments with repeated application of drops of the digest, using a "descending" flow, as well as separation of sugars by "ascending" flow, with intermediate drying and secondary separation. In this way, we established the presence of raffinose in the beet studied in September.

In September, an analogous experiment was carried out using beets obtained from the beet-supply point Dubno, Rovenskaia region (Fig. 2). Using the multiple drop method for applying the digest to paper, and "descending" flow, a raffinose spot was found on the chromatogram. An invert sugar was also found in the digest after multiple drop application (a fructose spot was found, when developed with α-naphthol reagent). The amount of raffinose and fructose in sugar beet is not great in September, as is shown by the size of the spot and intensity of its color on the chromatogram.

During industrial processing, the raffinose passes from the beet into the extract, and affects to a great degree the technological indicators of results in different stations of the factory. It may be supposed that the absolute amount of raffinose depends on the conditions under which the beet was grown, and on other factors [1, 4]. Comparative experiments show that there is much less raffinose in the beet of the left bank of the Ukraine than in the beet of Western regions of the Ukraine, in analogous periods.

As a result of cold and rainy growing seasons (without frosts), significant amounts of raffinose are formed in the beet, affecting the polarimetric determination of sugar in the beet and in the products of the beet-sugar industry to a great degree.

In the chromatogram of a digest made in January (Fig. 1), it can be seen that a significant accumulation of raffinose and invert sugar took place in the beet. Considerable amounts of raffinose are formed in the beet as a result of long storages, particularly during unfavorable conditions, as a result of the activity of microorganisms.

The process of raffinose formation in the beet during long storage is accompanied by the process of kestose trisaccharide formation, the latter being also dextro-rotatary, but considerably less so than raffinose (specific rotation of raffinose $[\alpha]D^{20} = +123.1°$, specific rotation of kestose $[\alpha]D^{20} = +26.61°$). The kestose consists of two

fructose residues and one of glucose. Kestose is a new sugar. According to the communication of De Whalley kestose was found by Blanchard and Albon, and later by Bacon and Edelman, during observation of the inversion of sucrose by the chromatographic method [12, 23, 24]. It is supposed that kestose is synthesized during inversion of sucrose [23].

The experiments with the multiple drop method show that kestose is present in the digest in January. Consequently, the formation of kestose took place in the beet during storage, during inversion of sucrose as a result of microorganism activity. The kestose, as well as raffinose, passes from the beet into industrial products. Since kestose is easily hydrolyzed by invertase, it is a fermenting sugar. By their presence in beet, raffinose and kestose, being dextro-rotatary, give a fictitious sucrose content when the latter is determined by the polarimetric method.

As can be seen from the chromatograms, considerable changes in the composition of the carbohydrate complex are taking place in the sugar beet.

In the chromatogram shown in Fig. 1 (September) and in that shown in Fig. 2 (September, October, and November), the raffinose has not been spotted. However, using the method of multiple drop application, with drying between applications, and "descending" flow, raffinose was found in all digest samples studied. Still, using the same method for the study of digests in 1956, in September and October (Fig. 3), we found no raffinose; in November a raffinose spot appeared, even though in the latter case it could not be detected in single drops of digest. This indicates that raffinose is not always present in fresh beet (or is present in such small amounts that it cannot be detected even by such a sensitive method as chromatography), while it is accumulated in considerable amounts during beet storage.

We did not find any kestose in any of the numerous samples of beet which we took for investigation in September, October, and November. However, using the multiple drop method, we succeeded in establishing that ketose is present in the beet(Jan. sample)of the beet-planting zone factory, in the 1955 harvest; in the beet of the beet-planting zone of Dubno point (Rovenskaya region), 1955 harvest, kestose was also found in the digests of January samples; in the beet of 1956 harvest of the same point, kestose was found in December by the same method (Figure 3).

It is characteristic that invert sugar (the fructose spot) was found in all samples studied from the beet of the 1955 harvest; however, in the beginning months of invert sugar production, such insignificant amount was present that its presence was established only through the method of multiple application of drops from the digest studied. In the first months of storage (September-October), the invert sugar was not found in samples of the 1956 harvest.

CONCLUSIONS

1. In the process of long storage of sugar beet, the following changes took place in the carbohydrate complex (sugars having practical significance): break-down of sucrose, formation or accumulation (or both processes simultaneously) of raffinose, formation and accumulation of kestose, accumulation of invert sugar.

2. The method of distribution chromatography on paper is simple and can very well be used in practice in research and factory laboratories, as a supplementary method for determining the composition of the carbohydrate complex in beet and in products of sugar industry.

LITERATURE CITED

[1] B. A. Rubin, Storage of Sugar Beet. 3rd Edition, Pishchepromizdat, (1946).*

[2] A. I. Oparin, N. N. D'iachkov, and I. V. Glazunov, Laboratory Study of Processes Taking Place in Storage of Sugar Beet. UNIS Press, Kiev (1931).*

[3] P. M. Silin, Questions in Technology of Saccharide Substances. Pishchepromizdat 157 (1950).*

[4] M. I. Nakhmonovich, Chemical Composition of Sugar Beet. Pishchepromizdat (1940).*

[5] I. M. Litvak and M. A. Kokhan, Sakharnaia Prom. 11, 52 (1956).

[6] M. Z. Khelemskii, L. E. Fleishman, and A. K. Vorokhova, Tr. TsINS, II, 49 (1953).

[7] G. S. Benin and S. F. Skorbilin, Tr. TsINS IV, 163 (1956).

* In Russian.

[8] M. I. Barabanov and V. F. Beznosenko, The Study of Changes in the Carbohydrate Complex of Beet Sap During its Storage, by Means of Paper Chromatography. KTIPP, Kiev 7 (1955).*

[9] V. V. Rachinskii, Usp. Khim. XIX, 4 (1950).

[10] V. S. Asatiani, Usp. Khim. 22, 3, 29 (1953).

[11] P. V. Golovin, Tr. KTIPP 10, 3 (1950).

[12] A. K. Kartashev and V. A. Serdiuk, Tr. TsINS IV, 194 (1956).

[13] V. V. Rachinskii, E. I. Kniaziatova, and B. E. Kravtsova, Biokhimia 17, 5, 551 (1952).

[14] V. V. Rachinskii, Izv. Timiriazevskoi Sel'khoz. Akad. 2, 193 (1958).

[15] V. V. Rachinskii and T. B. Gapon, Chromatography in Biology. AN SSSR Press, M. (1953).*

[16] T. B. Gapon and E. N. Gapon, Doklady AN SSSR 60, 401 (1948).

[17] I. R. Rominskii and A. S. Sushkova, Biokhimia 19, 3, 261 (1954).

[18] N. P. Silina, Sakharnaia Prom. 8, 41 (1956).

[19] H. C. S. De Whalley, The International Sugar Journal 617, 127 (1950).

[20] H. C. S. De Whalley, The International Sugar Journal 618, 151 (1950).

[21] S. M. Partridge, Nature 158, 270 (1946).

[22] R. Brown, Anal. Chem. XXIV, 2, 384 (1952).

[23] H. C. S. De Whalley, The International Sugar Journal 641, 126 (1952).

[24] N. Albon, D. Y. Bell, P. H. Blanchard, D. Gross, and J. T. Rundell. J. Chem. Soc. 24 (1953).

Received February 3, 1958

* In Russian.

ON CERTAIN CATALYTIC CONVERSIONS OF ETHYLENE GLYCOL

B. N. Dolgov and V. I. Ivanskii

Work on the catalytic conversion of ethylene glycol can be divided essentially into three groups. The first of these has as its purpose the study of the catalytic dehydration of ethylene glycol (a) [1-4]; the second is concerned with the study of the catalytic dehydrogenation of ethylene glycol (b) [5]; the third is concerned with the study of the catalytic oxidation of ethylene glycol (c) [6, 7]:

$$\left.\begin{array}{l} CH_2OH{-}CH_2OH \xrightarrow{-H_2O} CH_2{-}CH_2 \longrightarrow CH_3CHO \\ \qquad\qquad\qquad\qquad\quad \diagdown O \diagup \\ 2CH_2OH{-}CH_2OH \xrightarrow{-H_2O} CH_2OH{-}CH_2{-}O{-}CH_2{-}CH_2OH \\ 2CH_2OH{-}CH_2OH \xrightarrow{-2H_2O} O\begin{array}{l}\diagup CH_2{-}CH_2 \diagdown \\ \diagdown CH_2{-}CH_2 \diagup\end{array}O \end{array}\right\} \quad (a)$$

$$\left.\begin{array}{l} CH_2OH{-}CH_2OH \xrightarrow{-2H_2} CHO{-}CHO \\ CH_2OH{-}CH_2OH \xrightarrow{-H_2} CH_2OH{-}CHO \end{array}\right\} \quad (b)$$

$$\left.\begin{array}{l} 2CH_2OH{-}CH_2OH + 2O_2 \longrightarrow 2CHO{-}CHO + 2H_2O \\ 2CH_2OH{-}CH_2OH + O_2 \longrightarrow 4HCHO + 2H_2O \\ 2CH_2OH{-}CH_2OH + 5O_2 \longrightarrow 4CO_2 + 6H_2O \\ 4CH_2OH{-}CH_2OH + O_2 \longrightarrow 2\begin{array}{l}CH_2{-}O \diagdown \\ \quad\vert \qquad\quad CH{-}CH_2OH + 4H_2O \\ CH_2{-}O \diagup\end{array} \end{array}\right\} \quad (c)$$

Aluminum oxide, silica-alumina, orthophosphates, and other materials are usually used as catalysts for the dehydration of ethylene glycol. Dehydrogenation of ethylene glycol takes place in the presence of copper and nickel. Oxidation of ethylene glycol is carried out over CuO, SeO_2, and Ag.

The best studied of these reactions is the dehydration of ethylene glycol as a consequence of a tendency to split out water from the two neighboring hydroxyl groups (intramolecular and intermolecular elimination of water). The mechanisms of the dehydrogenation and oxidation of ethylene glycol still require further study. In a practical sense, the dehydrogenation and oxidation of ethylene glycol are, in our opinion, of considerably greater interest than the dehydration of ethylene glycol.

The aim of the present work was to investigate the possibility of converting ethylene glycol to a diketone.

The catalytic conversion of ethylene glycol to a diketone should include both dehydration and hydrogenation reactions as separate stages of the ketonization reaction. As a result of the experiments described below, ethylene glycol has actually been converted to biacetyl [2,3-butanedione] and other products.

EXPERIMENTAL

Catalysts. Copper promoted with 5% thorium oxide was the first catalyst used in this study of ethylene glycol conversion; this catalyst has been successfully used in experiments on the ketonization of monohydric alcohols, which were carried out in the laboratory of the association of organic chemistry instructors, LGU [Leningrad State University]. Ethylene glycol was passed over this catalyst at a temperature of 200 to 360° and a space rate of from 30 to 300. This showed that up to 9.6% biacetyl is formed per pass under optimum condi-

tions (temperature of 335-340° and ethylene glycol feed rate of 20 ml per hour). However, although this experiment showed that it is possible in principle to convert ethylene glycol to a diketone, it was also found during the experiment that copper-thorium catalyst suffers from substantial disadvantages, since it was rapidly deactivated at the optimum experiment temperature, and the yields of diketone were small. It was thus necessary to find a more effective catalyst, one which is free from these disadvantages. We were guided by the following considerations. Considering that Al_2O_3 has been successfully used for the dehydration of ethylene glycol and CuO has been used for dehydrogenation (preparation of glyoxal), and assuming that the ketonization process combines these reactions, we hoped to find that a catalyst containing Cu and Al_2O_3 as required components would be an effective catalyst.

TABLE 1

Activity of Nickel/Silica and Copper/ Silica Catalysts (t = 320°)

Catalyst	Yield (in %)		
	biacetyl	fraction boiling to 100°	condensate, based on ethylene glycol charged (100 g)
$Cu \cdot ThO_2 + 20\%\ Na_2SO_4$	6.8	13.2	85
$Cu \cdot ThO_2 + 10\%\ Na_2SO_4$	9.6	18.0	80
$Cu \cdot ThO_2$	9.8	17.2	76
$Cu \cdot SiO_2$ (70% Cu, 30% SiO_2)	6.6	12.6	88
Cu · Ni	0.5	8.0	45
$Cu \cdot SiO_2$ (80% Cu, 20% SiO_2)	4.8	13.0	68
$Cu \cdot SiO_2$ (60% Cu, 40% SiO_2)	4.2	10.2	81
$Cu \cdot Ni \cdot SiO_2$ (80% Cu, 5% Ni, 15% SiO_2)	1.8	7.3	71
$Cu \cdot Ni \cdot SiO_2$ (60% Cu, 10% Ni, 30% SiO_2)	6.9	13.0	58
$Cu \cdot Ni \cdot SiO_2$ (50% Cu, 7% Ni, 43% SiO_2)	9.0	17.0	74

TABLE 2

Activity of Nickel/Silica-Alumina and Copper/ Silica-Alumina Catalysts

$t_{Cu} = 320°$, $t_{NiO} = 360°$

Catalyst	(Yield (in %)		
	biacetyl	fraction boiling to 100°	condensate, based on ethylene glycol charged (100°)
$Cu \cdot Al_2O_3 \cdot SiO_2$ (42% Cu, 15% Al_2O_3, 43% SiO_2)	12.2	21	84
$NiO \cdot Al_2O_3 \cdot SiO_2$ (45% NiO, 30% Al_2O_3, 25% SiO_2)	2.6	36	80
$Cu \cdot MnO \cdot Al_2O_3 \cdot SiO_2$	8.5	24	72
$Cu \cdot Al_2O_3 \cdot SiO_2$ (70% Cu, 10% Al_2O_3, 20% SiO_2)	12.5	38	82
$NiO \cdot Al_2O_3 \cdot SiO_2$ (70% NiO, 10% Al_2O_3, 20% SiO_2)	1.6	28	74
$Cu \cdot Al_2O_3 \cdot SiO_2$ (60% Cu, 15% Al_2O_3, 25% SiO_2)	15.1	30.8	84
$NiO \cdot Al_2O_3 \cdot SiO_2$ (60% NiO, 15% Al_2O_3, 25% SiO_2)	4.1	44.4	82

The following catalysts were tested: $Cu \cdot SiO_2$, $Ni \cdot SiO_2$, $Ni \cdot Cu \cdot SiO_2$. The activities of these catalysts were compared with respect to biacetyl yield, calculated on the original ethylene glycol, and with respect to the yield of products boiling below 100° (Table 1). These catalysts proved to be less active than $Cu \cdot ThO_2$, therefore, they were abandoned, and further work was centered on catalysts of the type of copper/ silica-alumina and nickel/ silica-alumina (Table 2).

The most active catalyst for the ketonization of ethylene glycol was Cu · Al_2O_3 · SiO_2, (the yield of biacetyl was 15% based on the original ethylene glycol): the yield of products boiling below a temperature of 100° was 30.8% (based on the original ethylene glycol) at a temperature of 320° and a space rate of 50. The catalyst having the composition NiO · Al_2O_3 · SiO_2 was also active (the yield of products boiling below 100° was 44.4% based on the original ethylene glycol); however, it gave lower yields of diketone. Both catalysts had high strength, were stable toward overheating, and their activity remained completely unchanged over prolonged operation (300 hours).

Catalytic apparatus. The catalytic apparatus comprised the usual vertical electric furnace containing a quartz tube filled with the catalyst. The temperature in the furnace was measured using a millivoltmeter (chromel–alumel thermocouple).

Cu · Al_2O_3 · SiO_2 catalyst. The ethylene glycol was freshly distilled, b. p. 197°, n_D^{20} = 1.4305. The experiments were carried out with an ethylene glycol feed rate of 20 ml per hour and at temperature of 250, 275, 300, 320, and 340°. The optimum temperature was 315-320°. The condensate was given a preliminary distillation under vacuum, and the low-boiling fraction (up to 100°) was distilled in an ordinary fractionation column. The high-boiling fraction was subjected to a second vacuum distillation. Data on the composition of the products are presented in Table 3.

The basic products of the reaction were biacetyl, acetaldehyde, methyl alcohol, ethyl alcohol, butyraldehyde, ethyl acetate, acetic acid, and ethylene glycol diacetate. These products were identified by means of their physical constants; chromatography was used to resolve the mixtures. The infrared spectrum of the ethylene glycol diacetate was obtained. The catalyst was purged with a stream of air after each experiment.

TABLE 3

Composition of the Products Obtained Over Cu · Al_2O_3 · SiO_2 as a Function of Temperature

Temp. (in °C)	Amt. (in % of ethylene glycol charged, 100 g)		Condensate composition (in wt. %)												
	gas	condensate	acetaldehyde	acetone	butyraldehyde	methyl alcohol	ethyl alcohol	biacetyl	methyl ethyl ketone	ethyl acetate	acetic acid	ethylene glycol diacetate	unreacted ethylene glycol	water	residue
250	5	95	4.8	—	—	—	2.7	—	—	2.7	1.1	—	65.0	18.0	3.7
275	8	92	5.4	0.8	—	—	0.8	—	—	5.2	2.0	—	53.0	27.0	4.1
300	13	87	6.3	2.1	1.6	2.0	4.4	6.4	0.8	3.2	2.8	—	24.0	39.0	4.4
320	16	84	2.7	2.5	3.6	5.0	3.1	17.6	1.8	0.5	4.0	15.5	11.0	26.0	5.0
340	22	78	3.9	—	5.1	0.6	2.0	2.5	1.8	—	8.7	7.4	2.0	51.0	12.8

NiO · Al_2O_3 · SiO_2 catalyst. The experiments were carried out at an ethylene glycol feed rate of 25 ml per hour and at temperatures of 250, 275, 300, 320, 340, and 360°.

The optimum temperature was 360°. Treatment of the condensate was the same as in the case of the copper-containing catalyst.

Data on the compositions of the products are presented in Table 4.

The major reaction products were ethyl alcohol, acetaldehyde, butyraldehyde, ethyl acetate, and biacetyl. The products were identified. The catalyst was purged with a stream of air after each experiment.

TABLE 4

Composition of the Products Obtained Over $NiO \cdot Al_2O_3 \cdot SiO_2$ as a Function of Temperature

Temperature (in °C)	Amt. (in % of ethylene glycol charged, 100 g)		Condensate composition (in wt. %)								
	gas	condensate	acetaldehyde	butyraldehyde	ethyl alcohol	biacetyl	acetone	ethyl acetate	unreacted ethylene glycol	water	residue
250	2	98	—	—	—	—	—	—	82.0	12.5	3.2
275	6	94	—	—	—	—	—	—	82.0	13.0	3.0
300	6	94	1.7	—	2.3	1.0	0.8	1.5	75.0	12.0	2.5
320	10	90	6.1	1.6	6.8	1.2	1.0	2.7	64.0	14.0	2.1
340	18	82	10.3	8.4	15.5	4.8	2.0	11.4	16.0	24.5	1.6
360	39	61	—	16.6	7.1	2.2	—	2.4	2.0	48.0	17.8

Product Identification

1. Biacetyl: b. p. 88°, $n_D^{20} = 1.3921$, $D_4^{20} = 0.9795$.

Literature data: $n_D^{20} = 1.3927$, $D_4^{20} = 0.975$.

o-Phenylenediamine derivative of biacetyl:

m. p. 185°.

Literature value: m. p. 185-186°.

Mixed melting point, 186°.

Biacetyl–nickel dimethylglyoxime derivative:

Found: nitrogen 19.37%.
Calculated: nitrogen 19.11, 19.21%.

2. Acetaldehyde. Acetaldehyde 2,4-dinitrophenylhydrazone:

m. p. 146°.

Literature value: m. p. 147°.

Mixed melting point, 146°.

3. Methyl alcohol. 3,5-Dinitrobenzoate derivative:

m. p. 107°.

Literature value: m. p. 107°.

Mixed melting point, 106°.

4. Ethyl alcohol. 3,5-Dinitrobenzoate derivative:

m. p. 93°.

Literature value: m. p. 94°.

Mixed melting point, 93°.

5. Butyraldehyde. 2,4-Dinitrophenylhydrazone derivative:

m. p., 123°.

Literature value: m. p. 123°.

Mixed melting point, 123°.

6. Ethyl acetate: b. p., 77°, n_D^{25} = 1.3710, D_4^{20} = 0.902.

Literature values: n_D^{25} = 1.3700, D_4^{20} = 0.9005.

Saponification equivalent, 86.

7. Acetic acid: Neutralization equivalent, 61.

p-Nitrobenzoate derivative of acetic acid:

m. p., 77.5°.

Literature value: m. p. 78°.

Mixed melting point, 78°.

8. Ethylene glycol diacetate: b. p. 190°, n_D^{20} = 1.4162, D_4^{20} = 1.1062.

Literature values: n_D^{20} = 1.4150, D_4^{20} = 1.1040.

Saponification equivalent, 288.

The figure shows the infrared spectrum of the ethylene glycol diacetate; the band at 1729 cm^{-1} corresponds to the valence vibration frequency of an ester carbonyl group (C = O); the bands at 1242 cm^{-1} and 1174 cm^{-1} correspond to valence vibrations of the C–O group in acetates.

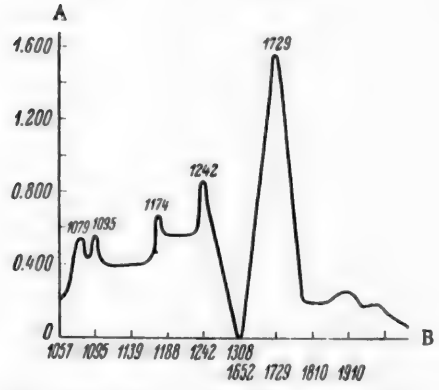

Infrared spectrum of ethylene glycol diacetate obtained in the present work. Catalyst: Cu · Al_2O_3 · SiO_2; 75-78° (9 mm) fraction. A) Intensity, B) frequency (in cm^{-1}).

9. Acetone. 2,4-Dinitrophenylhydrazone derivative:

m. p. 127°.

Literature value: 126°.

Mixed melting point, 127°.

10. Methyl ethyl ketone. 2,4-Dinitrophenylhydrazone derivative: m. p. 112°.

Literature value: m. p., 112°.

Mixed melting point, 111°.

Identification of the carbonyl compounds was carried out after separation of these compounds as the 2,4-dinitrophenylhydrazone derivatives using a chromatographic column.

Series 32 aluminum oxide containing 8% moisture was used as the adsorbent; the solvent was CCl_4; the eluent was CCl_4 containing 4% absolute ether. Recrystallization was from ethyl alcohol.

DISCUSSION OF RESULTS

That biacetyl was obtained from ethylene glycol merits the greatest attention. The highest yield of biacetyl (calculated as per cent of the original ethylene glycol) was obtained within a narrow temperature interval, 315-320° (Cu · Al_2O_3 · SiO_2 catalyst), and at a strictly fixed ethylene glycol rate of feed to the catalyst (20 ml/ hour). When the temperature deviated from this range toward lower temperatures, there was an increase in dehydration, an increase in the amount of unreacted ethylene glycol, and an increase in the acetaldehyde content of the condensate. When the temperature deviated from the indicated range toward higher temper-

atures, there was again an increase in ethylene glycol dehydration, an increase in the amount of high-boiling products, and tar formation. Thus, the optimum conditions for the preparation of biacetyl lie within a narrow "gap", which is characterized by an increase in the dehydrogenation activity of the catalyst and a decrease in the dehydration activity.

The increased amount of acetaldehyde in the condensate obtained at temperatures of 275 and 300°, together with the increase in dehydration, permitted us to conclude that the dehydration reaction has an intramolecular character:

$$CH_2OH—CH_2OH \xrightarrow{-H_2O} \begin{matrix} CH_2 \\ | \\ CH_2 \end{matrix}\!\!>O \rightarrow CH_3CHO.$$

The increased tar formation, the increased condensation of the products of the partial decomposition of ethylene glycol, and the increase in dehydration indicates that we are also dealing with intermolecular dehydration of ethylene glycol.

$$CH_2OH—CH_2OH + HOCH_2—CH_2OH + HOCH_2—CH_2OH \text{ , etc.}$$

The mechanism by which biacetyl is formed from ethylene glycol is complex and multistage.

The authors wish to extend their thanks to G. M. Murashov and K. P. Katkova.

SUMMARY

1. Biacetyl was prepared from ethylene glycol over copper/ silica-alumina, nickel/ silica-alumina, and certain other catalysts.

2. Optimum conditions were found for preparing biacetyl from ethylene glycol in the presence of these catalysts. For copper/ silica-alumina catalyst (60% Cu, 15% Al_2O_3, 25% SiO_2), the temperature was 315-320°, and the space rate was 50. For nickel/ silica-alumina catalyst (60% NiO, 15% Al_2O_3, 25% SiO_2), the temperature was 360°, and the space rate was 50.

3. The composition of the products obtained from the reaction was studied. In addition to the biacetyl, ethylene glycol diacetate, methyl ethyl ketone, butyraldehyde, acetaldehyde, methanol, ethyl alcohol, acetic acid, acetone, and ethyl acetate were found and identified.

LITERATURE CITED

[1] V. N. Ipat'ev, J. Russ. Phys. Chem. Soc. 35, 542 (1903).

[2] V. N. Ipat'ev and N. A. Klyukvin, Ber, 58, 4 (1925).

[3] V. N. Ipat'ev and V. Leontovich, J. Russ. Phys. Chem. Soc. 35, 606 (1903).

[4] T. E. Zalesskaya, Transactions of the Kiev Conference, June 25, 1952. Division of Physico-Mathematical and Chemical Sciences AN UkrSSR, Kiev, Izd. AN UkrSSR, 281 (1953).

[5] F. Sweiz, Arch. ang. Wiss u. Techn., 22, 4, 120 (1956).

[6] Ind. Eng. Ch. 43, 786 (1951).

[7] Ch. Rev. 33, 257 (1943).

Received July 15, 1958

THE EFFECT OF CERTAIN PHYSICOCHEMICAL FACTORS ON THE YIELD OF γ-HEXACHLORANE FROM THE PHOTOCHEMICAL CHLORINATION OF TETRACHLOROCYCLOHEXENES

L. S. Pereslegina and A. I. Finkel'shtein

Isomers of 3,4,5,6-tetrachlorocyclohexene are intermediate products in the production of the γ-isomer of 1,2,3,4,5,6-hexachlorocyclohexane (γ-HCCH)—an important insecticide — by the photochemical chlorination of benzene. Methods for the separation of tetrachlorocyclohexenes (TCCH) and the physicochemical properties of these compounds have been described in detail in papers by Orloff and co-workers [1, 2]. The work described in these papers showed that the valuable product in the commercial production of hexachlorane, γ-HCCH, is obtained only from two of the 2,4,5,6-tetrachlorocyclohexene isomers, which these authors designated as the α- and γ-isomers (α-TCCH and γ-TCCH).

In this connection, it appeared to be of interest to investigate the effect of different physicochemical factors on the yield of γ-HCCH during the chlorination of α-TCCH, since this would yield additional data on the mechanism of the chlorination of benzene.

Synthesis of the α- and γ-TCCH was carried out as described in the references cited above [1, 2]. 314 g of α-TCCH with an m. p. of 32-33° and 4.5 g of γ-TCCH with an m. p. of 88-89° were obtained. Investigation of the infrared absorption spectra* showed that these compounds were identical to those described in the papers by Orloff and co-workers.

TABLE 1

Temp. (in °C)	Wave length (in A)	Transmission through neutral light filter (in %)	Content of γ-HCCH in mixture of α- and γ-HCCH (in %)
50	3650	100	9.7
50	3650	42	9.0
50	4047	100	9.1
50	4358	100	9.8
50	4358	100	9.7
50	5461	100	9.6
50	5461	100	9.7
50	5461	100	8.6
50	5461	23	9.1
50		23	9.3
50	Polychromatic	42	9.8
50	radiation	42	9.8
50		42	9.9

* Investigation of the infrared absorption spectra was carried out with an IKS-11 spectrophotometer with an NaCl prism.

The apparatus pictured schematically in Figure 1 was used in the investigations. A PRK-2 mercury lamp served as the source of the incident radiation; the lamp was connected in the usual circuitry. The monochromatic radiation was obtained through the use of the standard collection of light filters. The reactor, which was constructed of molybdenum glass, was placed in a thermostatted bath which had a small window of BS-1 glass. During the reaction, the solution was stirred vigorously by means of a stirrer powered with an electric motor. The chlorine content of the reaction mixture was determined by chemical analysis. The chlorination was carried out in solution in carbon tetrachloride (5 g of α-TCCH in 150 ml of CCl_4 and 2 g of γ-TCCH in 60 ml of CCl_4). Analysis of the resulting products for content of α- and γ-HCCH was accomplished chromatographically [3]. The analyses took into account only the α- and γ-HCCH contents of the mixture. Products with a greater or lesser degree of chlorination were disregarded.

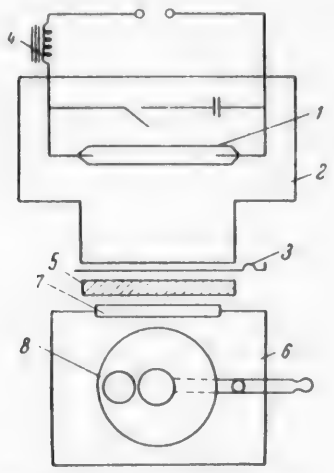

Fig. 1. Chlorination apparatus. 1) mercury lamp, 2) housing, 3) sliding diaphragm, 4) choke coil, 5) light filter, 6) thermostatted bath, 7) BS-1 glass window, 8) reactor.

Table 1 presents the results of the study of the effect of the wave length and intensity of the exciting radiation on the yield of γ-HCCH from the photochemical chlorination of α-TCCH. Other factors (temperature, 50°, and chlorine concentration, 2.6-2.8%) were held constant.

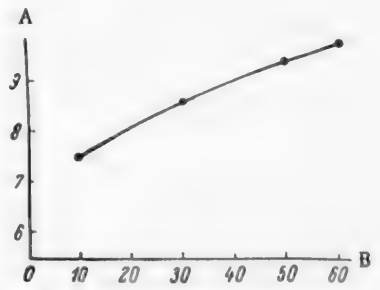

Fig. 2. Temperature dependence of α-HCCH yield during chlorination of α-tetrachlorocyclohexene. A) yield of γ-HCCH (in %), B) temperature (in °C).

TABLE 2

Temp. (in °C)	Chlorination time	Conc. of dissolved chlorine (in %)		Degree of chlorination (wt. increase in % of theoretical)	Content of γ-HCCH in mixture of α- and γ-HCCH (in %)
		before chlorination	after chlorination		
10	4 hr 05 min.	3.0	3.0	86.2	7.8
10	3 hr 30 min	3.0	3.7	94.4	6.7
10	3 hr 30 min	3.17	3.0	98.7	7.8
10	2 hr 30 min	5.7	5.2	104.3	7.0
10	2 hr 45 min	5.8	5.2	97.5	7.4
10	2 hr 30 min	6.0	6.0	114	8.1
10	15 min	10.7	10.7	110	7.8
10	34 min	10.8	10.8	126	7.2

As may be seen from Table 1, a change in the wave length of the incident radiation in the range 3650-5461 A and the variations made in the intensity of the radiation had no appreciable effect on the yield of γ-HCCH during the photochemical chlorination of α-TCCH. The observed deviations did not exceed the possible experimental error and were not systematic. Therefore, polychromatic radiation was used in further work.

As may be seen from Tables 2-4, a change in the concentration of dissolved chlorine within the limits 2.5-10% had no effect on the yield of γ-HCCH. However, when the concentration of chlorine in solution was decreased greatly (0.6-0.8), there was some decrease in the yield of γ-HCCH.

TABLE 3

Temp. (in °C)	Chlorination time (in min)	Conc. of dissolved chlorine (in %)		Degree of chlorination (wt. increase in % of theoretical)	Content of γ-HCCH in mixture of α- and γ-HCCH (in %)
		before chlorination	after chlorination		
30	60	2.7	2.6	93.7	7.9
30	63	3.0	2.7	97.5	7.8
30	70	2.7	2.7	95.0	10.0
30	70	2.8	2.7	99.3	8.7
30	75	3.3	3.2	88.8	9.0
30	10	5.6	5.1	100.0	9.3
30	12	5.5	5.3	105.5	8.3
30	15	5.6	5.3	119.0	8.4

TABLE 4

Chlorination temperature (in °C)	Chlorination time (in min)	Conc. of dissolved chlorine (in %)		Degree of chlorination (wt. increase in % of theoretical)	Content of γ-HCCH in mixture of α- and γ-HCCH (in %)
		before chlorination	after chlorination		
50	5 min	2.8	2.6	69.0	9.3
50	5 »	2.8	2.6	126	10.3
50	9.5 »	2.8	2.6	105	9.1
50	18 »	2.8	2.6	123	10.4
50	36 »	2.7	2.0	126	9.6
50	10 »	2.7	2.7	92	9.6
50	4 hr 30 min	0.4	0.8	57.6	8.2
50	3 hr	5.0	1.0	78.0	9.0
50	4 hr 40 min	0.7	1.1	103	8.3

TABLE 5

Chlorination temperature (in °C)	Chlorination time	Conc. of dissolved chlorine (in %)		Degree of chlorination (wt. increase in % of theoretical)	Content of γ-HCCH in mixture of α- and γ-HCCH (in %)
		before chlorination	after chlorination		
10	2 hr 30 min	3.2	3.6	85	35.3
50	14 hr 30 sec	3.0	3.0	100	35.8

The effect of chlorination temperature is shown in Figure 2. As seen from Figure 2, an increase in temperature caused a very definite increase in the yield of γ-HCCH from the photochemical chlorination of α-TCCH. It is interesting to note that in the photochemical chlorination of benzene, the yield of γ-HCCH decreases somewhat with an increase in temperature. This could be associated either with a decrease in the formation of γ-TCCH or with a decrease in the yield of γ-HCCH by chlorination of γ-TCCH as the temperature is increased.

In order to clarify this question, we carried out photochemical chlorination of γ-TCCH at temperatures of 10 and 50°. It was found that the yield of γ-HCCH remained constant within the limits of experimental error (Table 5).

Hence, it is clear that the decrease in the yield of γ-HCCH during the total chlorination of benzene is associated with a decrease in the extent of formation of γ-TCCH relative to other intermediate products as the temperature is increased.

TABLE 6

Wave number (in cm^{-1})	Intensity, by visual evaluation	Wave number (in cm^{-1})	Intensity, by visual evaluation
257	2	1036	0.5
340	0.5	1114	0.5
387	1	1141	1
471	2	1201	1
674	1	1237	0
718	1	1266	1
830	0.5	1650	2
899	0.5	2885	2

Note: The spectra were obtained with an ISP-51 spectrophotometer; exciting radiation, 4358 A; CCl_4 solution.

Table 6 presents the Raman spectrum of α-TCCH taken during the course of the work. As may be seen from the table, the line characteristic of the C = C bond had a wave number of 1650 cm^{-1} and a significant intensity, while in the infrared absorption spectra it could be detected only at higher α-TCCH concentrations (20% solution in CCl_4 with a cell thickness of 0.5 mm).

SUMMARY

1. It was shown that the wavelength and intensity of the radiation have no effect on the yield of γ-HCCH from the photochlorination of α-tetrachlorocyclohexene; an increase in temperature increased the yield of γ-HCCH; chlorine concentration in the range of 1-10% had no effect, but the yield of γ-HCCH decreased at concentrations below 1%.

2. It was shown that the slight decrease in the yield of γ-HCCH with an increase in temperature in the photochemical chlorination of benzene is associated with a decrease in the formation of γ-TCCH.

3. The Raman spectrum of α-tetrachlorocyclohexene was obtained.

The authors expressed their deep appreciation to N. A. Gol'dberg and G. M. Strogina for valuable discussion and consulation and to A. K. Ermolaeva and Z. N. Lapshina for assisting in the work.

LITERATURE CITED

[1] H. D. Orloff, A. J. Kolka, G. Callingaert, M. E. Griffing, and E. R. Kerr, J. Am. Chem. Soc. 75, 4243 (1953).

[2] G. Callingaert, M. E. Griffing, E. R. Kerr, A. J. Kolka, and H. D. Orloff, J. Am. Chem. Soc. 73, 5224 (1951).

[3] GOST 7854-55.

Received July 1, 1957

RECOVERY OF ORGANOMERCURY COMPOUNDS FROM SPENT ACTIVATED CARBON SATURATED WITH ORGANOMERCURY COMPOUNDS BY EXTRACTION WITH ORGANIC SOLVENTS

I. F. Zemskov and G. I. Sidel'nikova

Previous work by the present authors established that when gas-air mixtures or water containing organomercury compounds, for example, diethylmercury or ethylmercury chloride, are filtered through a layer of activated carbon, the organomercury compounds are adsorbed on the carbon [1].

Our experiments showed that the capacity of certain activated carbons for these organomercury compounds is comparatively high [1]. For example, with a gas-air mixture containing 20-30 mg/m^3 of diethylmercury vapor, the capacity of the sorbent under flow conditions is as high as 20-30% by weight [1]. Therefore, in the production of diethylmercury and ethylmercury chloride, it would appear quite possible to use activated carbon to remove such organomercury compounds from waste gas-air mixtures and water.

However, diethylmercury and ethylmercury chloride are volatile, highly toxic products [2-4]. Prior to regeneration of the sorbent by removal of the mercury compounds, the carbon will also be a source of highly toxic fumes. Consequently, the problem associated with the use of activated carbon or other solid sorbents for the removal of diethylmercury and ethylmercury chloride from air-gas mixtures and waste water can be considered solved if it is found to be possible to render the spent sorbent harmless or to recover the mercury compounds from the sorbent.

The organomercury compounds can be distilled from the sorbent by heating; therefore, it is possible to recover them by thermal treatment of the spent sorbent at a temperature of 500-600° in the absence of air, but such treatment decomposes most of the organomercury compound to metallic mercury and hydrocarbons [5-7].

It is also known that organomercury compounds are partially soluble in a number of organic solvents, for example, isopropyl alcohol, dichloroethane, etc. [3, 4].

The aim of the present work was to determine whether it is possible to recover organomercury compounds from the spent sorbent by means of organic solvents.

We selected this method of regeneration for study, since the method does not cause decomposition of the organomercury compounds, an attribute which is frequently extremely desirable.

The regeneration experiments were carried out with commercial activated carbon in which the content of organomercury compounds, calculated as mercury, was about 17% by weight of the carbon; about 70% of the organomercury compounds was diethylmercury, and about 30% was ethylmercury chloride.

Prior to sorption of the organomercury compounds, the activated carbon was first promoted with gaseous chlorine (to a chlorine content of 4% by weight of the carbon).

The amount of compound in the spent sorbent was determined by heat treatment of the sample being studied at a temperature of 600° for 2 hours in the absence of air; the organomercury compounds distilled from the sample. The mercury remaining in the sample after the heat treatment was determined spectroscopically.

At times, two samples were tested in parallel: 1) spent sorbent without additional subsequent treatment; 2) chlorinated spent sorbent.

In the latter case, the spent sorbent was additionally treated with gaseous chlorine to convert the mercury compounds to mercurous chloride. The amount of chlorine used was usually a 7-fold excess over that required to convert all of the mercury to mercurous chloride (Hg_2Cl_2).

The degree of recovery of mercury compounds* from the spent sorbent was calculated by means of the formula

$$\gamma_i = \frac{a - b}{a},$$

where a is the content of mercury compounds in the sample before treatment, and b is the content of mercury compounds in the sample after treatment.

EXPERIMENTAL

Determination of the solubility of DEM and EMC in different solvents. As was mentioned above, the spent sorbent was saturated with DEM and EMC.

The literature contains no quantitative data on the solubility of DEM and EMC in organic solvents; therefore, in the initial stages of the work it was necessary to determine the solubilities of DEM and EMC in certain organic solvents. The following solvents were tested: isopropyl alcohol, dichloroethane, carbon tetrachloride, and water. The experiments showed that at room temperature (20°), freshly prepared DEM is readily miscible with isopropyl alcohol, dichloroethane, and carbon tetrachloride, even at a volume ratio of solvent to DEM of 1 : 3. However, the solubility of DEM decreased sharply on "aging"; thus, for example, the solubility of DEM in isopropyl alcohol at a temperature of 20° was 12 g per 100 g of solvent 9 months after preparation of the DEM.

The solubility of DEM in water was 0.05 g per 100 g at 20°.

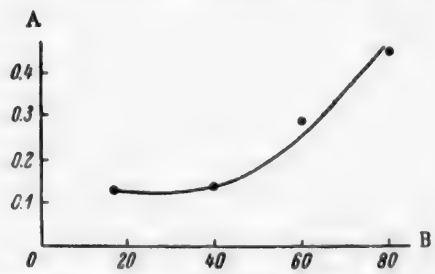

Fig. 1. Solubility curve for EMC in i-C_3H_7OH. A) solubility (in g/100 g of solvent); B) temperature (°C).

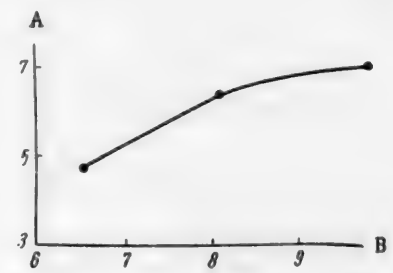

Fig. 2. Vapor–solution equilibrium curve. A) concentration of DEM in the vapor (in g/liter), B) concentration of DEM in solution (in g/liter).

Solubility data for EMC are presented in Table 1 and in Figure 1.

The next stage of the work was devoted to a determination of the variation in DEM content of the vapor with its content in the solvent, isopropyl alcohol, at the boiling point of the solvent and atmospheric pressure.

The results are presented in Table 2 and Figure 2.

Selection of the solvent for the recovery process. The next series of experiments had as its aim the determination of the relative rate of removal of DEM and EMC from spent sorbent by the solvents mentioned above.

*Diethylmercury – DEM, ethylmercury chloride – EMC.

The laboratory experiments on the removal (recovery) of the mercury compounds from spent sorbent were carried out in a Soxhlet apparatus.

A weighed amount of spent sorbent was placed in a Soxhlet thimble, and the solvent was placed in the flask. During the extraction, the mercury compounds were washed from the spent solvent by condensed solvent dripping from the condenser and went into solution; the solution overflowed into the flask through the siphon.

TABLE 1

Solubility of EMC

Solvent	Temp. (in °C)	Solubility of EMC (in g per 100 g of solvent)	Solubility of EMC calc. as metallic mercury
Isopropyl alcohol	17	0.17	0.13
	40	0.17	0.13
	60	0.365	0.285
	80	0.574	0.445
Dichloroethane	17	0.17	0.13
Carbon tetrachloride	20	0.026	0.02
Water	20	0.065	0.05

TABLE 2

Dependence of the Content of DEM in the Vapor Phase on Its Content in Solution

DEM content (in g/liter of solvent)		DEM content, calc. as metallic mercury (in g/liter)	
in flask	in vapor	in flask	in vapor
6.5	4.7	5	3.6
8.1	6.5	6.25	5
9.8	7.25	7.5	5.6

After the extraction, the degree of recovery of the mercury compounds from the spent sorbent was determined from the content of the mercury compounds in solution and in the sorbent.

Two series of experiments were carried out: 1) with unchlorinated spent sorbent; 2) with sorbent which was chlorine-treated after becoming spent.

TABLE 3

Degree of Recovery of Mercury Compounds from Spent Sorbent

Solvent	Degree of recovery (in %)	
	unchlorinated spent sorbent	chlorinated spent sorbent
Isopropyl alcohol	91	75
Dichloroethane	82	—
Carbon tetrachloride	48	5.6
Water	—	49

TABLE 4

Variation in Recovery with Solvent–Sorbent Ratio

Volume of solvent in flask (in ml)	Amt. of spent sorbent (in g)	Ratio of volume of solvent to wt. of spent sorbent	Degree of recovery of mercury compounds (in %)
250	11	22.7	90.8
250	18.23	13.7	82
250	28.51	8.8	82.5
150	26.5	5.65	62

The following materials were tested as solvents: isopropyl alcohol, dichloroethane, carbon tetrachloride, and water. The conditions were the same in all cases. The ratio of the volume of solution to the weight of sorbent was 25 ml/g, and the amount of condensate per gram of sorbent was 12 ml.

The results of the tests are presented in Table 3.

As may be seen from Table 3, under the same experimental conditions, the best recovery was with isopropyl alcohol as the solvent; therefore, all further experiments were carried out with isopropyl alcohol.

Determination of the minimum solvent-sorbent ratio. An attempt was made to determine the minimum amount of isopropyl alcohol required per gram of spent sorbent (Table 4).

Table 4 presents the data from all four experiments; the same amount of solvent was circulated through the sorbent (140 ml per g of carbon), but the ratio of the amount of solution in the flask to the weight of sorbent differed.

These experiments showed that the degree of recovery of mercury compounds from the spent sorbent depends on the solvent-sorbent ratio. However, this dependence becomes small at solvent-sorbent ratios greater than 9 ml per g of carbon.

It was found that it is not necessary to pass through the sorbent more than 60-70 ml of alcohol per gram of spent sorbent, since an equilibrium between the composition of the solution in the flask, the condensate, and the amount of mercury compounds remaining on the carbon is established when the amount of alcohol is greater (Figure 3).

Figure 3 shows the relationship between the degree of recovery and the volume of solution passed through the sorbent.

The ratio of the volume of alcohol in the flask to the weight of sorbent was 22.7 ml of alcohol per g of carbon.

It was calculated on the basis of these data that 5.5 m^3 of isopropyl alcohol would be required for the recovery of 100 kg of mercury.

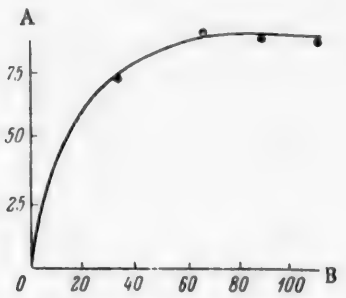

Fig. 3. Dependence of degree of recovery of organomercury compounds from spent sorbent on the solvent-sorbent ratio. A) degree of recovery (in %), B) ratio of volume of solution in flask to initial weight of sorbent (in ml/ g).

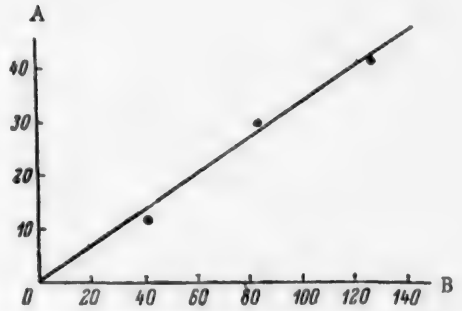

Fig. 4. Dependence of conversion of DEM to EMC on contact time of solution with carbon. A) conversion of DEM to EMC (in %), B) contact time (in min).

Reuse of the mother liquor as the solvent. Use of the mother liquors as solvents is desirable, since it reduces the amount of fresh solvent required in the recovery process.

When the hot mother liquors were cooled to room temperature, a silvery crystalline precipitate usually formed, and if the solution was filtered, the content of mercury compounds decreased in comparison with the content in the original mother liquor (Table 5).

The melting point of the precipitate was 187.3°, which corresponds to the melting point of EMC.

Experiments were carried out in which the mother liquor was reused, the spent sorbent being charged to the Soxhlet thimble, while the mother liquor from the preceding experiment was charged to the flask.

As Table 6 shows, the degree of recovery changed very little when the mother liquor was used from 2 to 5 times with removal of the EMC from the solution.

Interaction of DEM with chlorine adsorbed on activated carbon under recovery conditions. The amount of precipitate obtained from the mother liquor was usually significantly greater than the total amount of EMC on the sorbent as shown by thermal treatment of the sorbent. It was noted that the amount of precipitate usually depended on the time of contact of the solvent with the spent sorbent- the greater the amount of condensate circulated through the spent sorbent, the greater the amount of precipitate. For example, when 200 ml of condensate per gram of sorbent was passed through the sorbent, up to 50% of the total amount of mercury recovered from the sorbent was present in the precipitate as EMC, and when 100 ml of condensate was circulated per gram of sorbent, only 25% of the mercury precipitated.

TABLE 5

Content of Mercury Compounds, Calculated as Mercury, in the Flask Solution and its Filtrate

Total amount of mercury compounds, calculated as mercury (g mercury/ g solution)	
flask solution	filtrate
5.0	3.1
5.0	3.7
5.3	3.6

Since not all of the chlorine of the sorbent interacts with DEM vapors during the sorption of mercury compounds, as confirmed by analysis of the mercury compounds in the sorbent by the thermal method, it was assumed that chemical interaction of the DEM with the promoter, chlorine, occurred (in the alcoholic solution) with the formation of EMC during recovery of mercury compounds from spent sorbent with a hot solvent.

In order to confirm this assumption, an experiment was carried out in which fresh, chlorinated carbon was charged to the thimble, and a solution of DEM in isopropyl alcohol was charged to the flask to simulate the solvent.

The results of this experiment are shown graphically in Figure 4; it may be seen that the greater the amount of solution circulated through the carbon, the greater the amount of mercury in the precipitate.

This is a plus factor, since it opens up the possibility of separating valuable mercury derivatives from the solution,of using the filtrate for further recovery operations, and of decreasing, thereby, the amount of fresh solvent required in the operation.

TABLE 6

Recovery of Mercury Compounds from Spent Sorbent with Different Solvents with Subsequent Reuse of the Mother Liquors

Expt. No.	Solvent	Mercury content of original solution (in g)	Mercury content of solution after recovery (in g)	Amt. of mercury recovered (in g)	Wt. of spent sorbent (in g)	Mercury content of spent sorbent (in g)	Degree of recovery of mercury compd. (in %)
1	CCl_4	0	0.833	0.833	10	1.73	47.5
2	Mother liquor from Expt. 1	0.833	1.81	0.97	9.41	1.63	59.5
3	$C_2H_4Cl_2$	0	1.25	1.25	10.01	1.52	82.4
4	Mother liquor from Expt. 3	1.25	2.812	1.56	9.75	1.815	86
5	i-C_3H_7OH	0	1.469	1.469	11	1.62	90.8
6	Filtrate from Expt. 5	0.85	2.37	1.52	11	1.75	87

Recommended commercial recovery system. The investigations described above permitted us to form a number of conclusions; and we can, therefore, suggest a plant-scale system for the recovery of mercury compounds from spent sorbent.

This plant-scale system is shown in Figure 5. The equipment consists of the following basic components: a condenser for solvent vapors, 1, a leaching tank, 2, a vessel for the evaporation of solvent, 3, a heat-exchanger for cooling the mother liquor, 4, a vacuum filter for filtration of the mother liquor, 5, a vacuum pump, 6, and a centrifugal pump, 7, for transferring the filtrate from the vacuum filter to the evaporation tank.

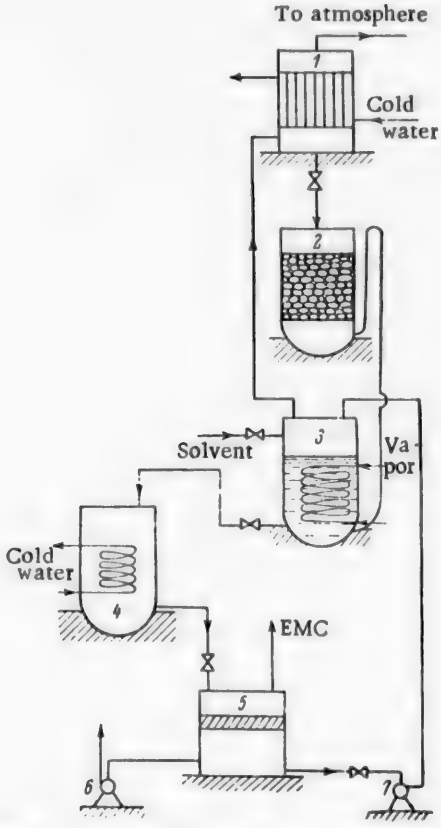

Fig. 5. Recovery system. The reference numbers are identified in the text.

The spent sorbent is charged to the leaching tank 2. The solvent is charged to vessel 3. As the solvent is evaporated in vessel 3, the vapors rise into condenser 1, where they are condensed, and the condensate flows to leaching tank 2 where it washes the organomercury compounds from the spent sorbent. As only the leaching tank becomes completely filled with solvent, the solvent flows through the overflow pipe (siphon) to vessel 3, the leaching vessel is again filled with solvent, and the cycle continues until leaching of the mercury compounds from the sorbent is concluded.

Periodically, the frequency depending on the enrichment of the mother liquor in the tank with EMC, part of the solution is transferred from vessel 3 to cooler 4, where the solution is cooled, and part of the EMC is precipitated. The cooled solution is transferred from cooler 4 to the vacuum filter, where the EMC is separated from the solution and removed from the system, and the filtrate is transferred by pump 4 to vessel 3. Since a certain amount of the alcohol is lost, the loss is made up from time to time by the addition of pure solvent to vessel 3.

SUMMARY

1. It was shown that mercury compounds can be recovered from spent activated carbon by extraction with organic solvents.

2. Isopropyl alcohol, dichloroethane, carbon tetrachloride, and water were tested as solvents, and isopropyl alcohol was found to be the best.

3. The degree of recovery of mercury compounds from spent sorbent can be as high as 91-92%.

4. The consumption of alcohol in the absence of recycle of stripped solvent is from 5 to 5.5 m^3 per 100 kg of recovered mercury.

5. After removal of the mercury compounds from the mother liquor, the latter can be used in subsequent recovery operations, thus reducing the consumption of isopropyl alcohol.

6. It was established that if chlorine is available in the spent sorbent, it can react with the organomercury compounds during treatment of the spent sorbent with hot solvent converting the DEM to EMC. This same reaction can occur if the mother liquor is passed through chlorine-containing activated carbon.

7. The solubility of chlorine-containing organomercury compounds varies with the temperature, increasing with an increase in temperature. This makes it possible to separate chlorine-containing organomercury compounds from the hot, saturated solution by cooling the solution; the chlorine-containing organomercury compound separates as a crystalline precipitate which can be separated from the mother liquor by filtration.

LITERATURE CITED

[1] I. F. Zemskov et al., Development of a Method for the Purification of Air and Industrial Gases from Vapors of Mercury and Organomercury Compounds. NIIOGAZ [State Scientific Research Institute of Gas Purification for Industry and Sanitation] (1957).*

* In Russian.

[2] N. V. Lazarev, Harmful Chemical Substances in Industry, Goskhimizdat (1951).*

[3] M. V. Alekseeva, B. E. Andronov, S. S. Rurvits, and A. S. Zhitkova, Determination of Harmful Substances in the Air of Industrial Locations, Goskhimizdat (1954).*

[4] F. C. Whitmore, Organic Mercury Compounds, Khimteoretizdat (1938).**

[5] L. G. Markarova and A. N. Nesmeyanov, Synthesis Methods in the Field of Organometallic Compounds of Mercury, Moscow (1945).*

[6] J. Schmidt, Organometallic Compounds, Moscow (1938).*

[7] S. M. Mel'nikov, Mercury, Metallurgizdat (1951).*

Received September 1, 1958

* In Russian.

** Russian Translation.

DEPENDENCE OF THE EXTENT OF CYCLOHEXANE DEHYDROGENATION ON FEED RATE AND CATALYST PARTICLE SIZE (0.5% Pt ON Al_2O_3)

N. F. Kononov, Kh. M. Minachev, and N. I. Shuikin

An understanding of the role of macrokinetic factors, i.e., mass and heat transfer processes, under reaction condtions over solid catalysts contributes to a more rational selection of operating conditions for carrying out such reactions in industry. If the rates of mass and heat transfer are small as compared to the reaction rate, inequalities in concentration and temperature arise across the cross-section of the catalyst bed, and these are particularly marked when the processes are accompanied by an appreciable heat effect. The activity, stability, and selectivity of many catalysts depend to a significant extent on the nature of the temperature distribution in the catalyst bed.

A considerable amount of work by both Soviet and foreign investigators has been devoted to the investigation of the effect of these macro factors on industrial processes. Of the investigations in this field by foreign authors, the work of Corrigan [1] may be mentioned; Corrigan studied the effect of particle size of silica-alumina catalyst on the cracking rate of isopropylbenzene. This author showed that the degree of isopropylbenzene conversion depends to a considerable extent on catalyst particle size. Dzis'ko [2] established the effect of the degree of grinding of MgO catalyst on the step-wise process of ethyl alcohol dehydration. Hettinger, Keith, et al. [3], in an investigation of the conversion of methylcyclohexane and n-heptane at a temperature of 480° over 0.6% Pt on Al_2O_3, determined the dependence of depth of conversion of these hydrocarbons on the particle size of the catalyst. Voitekhov [4], in a study of the kinetics of benzene hydrogenation and cyclohexane dehydrogenation over Pt on C at 260° and atmospheric pressure, came to the conclusion that with a known feed composition it is possible to eliminate the effect of hydrodynamic factors and heat transfer, which hinder the determination of the true kinetic constants.

The authors of the present article have suggested [5, 6] an active and stable platinum catalyst for reforming narrow gasoline fractions, and have worked out the process conditions, 460°, 20 atm., v = 1 hour^{-1}, and H_2 : HC* = 7.5.

Since under commercial conditions, gasoline reforming processes are carried out over a fixed catalyst bed at comparatively low space rates (1-2 hours^{-1}), and, consequently, since the productivity based on reactor volume is not high, it seemed to be of interest to carry out a series of experiments to investigate the effect of raw feed rate and catalyst particle size on the depths of conversion of individual hydrocarbons which enter into the composition of gasoline fractions; these experiments were carried out with the aim of studying possible improvement of the reforming process. The temperature was measured at various points across the cross-section and along the length of the catalyst bed under conditions such that there was a continuous transfer of heat through the walls of the reactor. From the temperature gradients across the cross-section of the bed it is possible to estimate the intensity of the heat transfer process, while the fractions of hydrocarbon conversion taking place in the upper and lower parts of the catalyst bed may be estimated from the temperature gradient along the length of the bed.

The present communication reports the results of experiments on the dehydrogenation of cyclohexane

* Ratio of the number of moles of H_2 to the number of moles of hydrocarbon.

over 0.5% Pt on Al_2O_3 at a temperature of 450-460°, a pressure of 20 atm., H_2 : HC of 7.5, and with various cyclohexane feed rates and different catalyst particle sizes.

EXPERIMENTAL

Feed materials. The cyclohexane was a commercial product containing 2% benzene * and having n_D^{20} 1.4270 and d_4^{20} 0.7805. The hydrogen was GOST 30-22-45 electrolytic hydrogen containing 99.7% H_2. The catalyst (0.5 Pt on Al_2O_3) was prepared by the method described by us previously [7]. The surface area of the catalyst was determined by the dynamic method [8] using benzene adsorption, and was 190 m^2/g.

Apparatus. The experiments were carried out in a flow-type apparatus which included (Figure 1) a tubular reactor set in a block, 1; the reactor was equipped with an electric heater. The temperature in the Duralumin block was controlled within ±1° by means of an electronic potentiometer. The catalyst tube, which was constructed of stainless chrome-nickel steel and which had a diameter of 25 mm and a height of 800 mm,

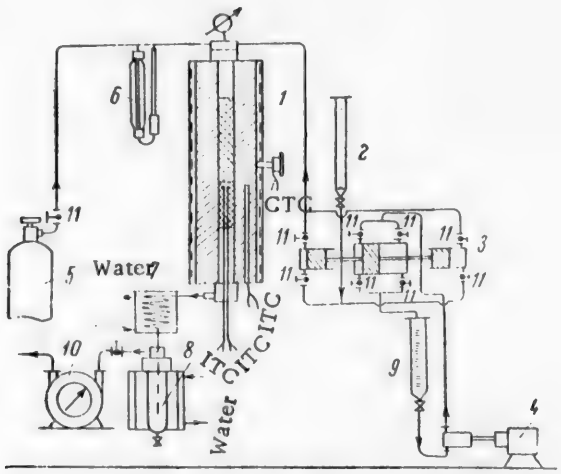

Fig. 1. Apparatus diagram. 1) reactor, 2) vessel, 3) plunger feed pump, 4) pump, 5) cylinder, 6) gas flow meter, 7) condenser, 8) separator, 9) oil vessel, 10) gas meter, 11) needle valve, CTC)control thermocouple, ITC) indicating thermocouple.

was press-fitted in the block. The cyclohexane was fed from vessel 2 by means of a plunger-type feed pump, which was powered by oil pumped by pump 4. Use of the plunger-type pump permitted cyclohexane feed rates as low as 6 ml/hour. Hydrogen was fed to the reactor from cyclinder 5 through flow meter 6. The reaction products passed from reactor 1 into condenser-cooler 7 and then into gas-liquid separator and receiver 8. Measurements of the temperature in the catalyst bed and in the reactor block were carried out by means of Chromel-Copel thermocouples. The hot junction of the thermocouple was placed directly inside the reactor. For this purpose, a Copel-Chromel cone with teflon packing was pressed into the bottom of the reactor. Chromel and Copel wires were welded to the upper and lower bases of the cone. The disposition of the hot thermocouple junctions in the catalyst bed is shown in Figure 2 (a, b, and c) for the different series of experiments.

Experimental method. The catalyst, in an amount of from 9 to 24 ml, was placed in a container - a cylinder with perforated walls and bottom - which was then inserted into the reactor; a layer of Al_2O_3

*Removal of the benzene from the cyclohexane was unnecessary. The benzene content of the feed was taken into account in determinations of the extent of cyclohexane conversion.

having the same particle size as the catalyst was placed on top of the catalyst. The amount of aluminum oxide was 250 ml, and the height of the bed was 50 cm. This layer of aluminum oxide served to preheat the hydrogen and cyclohexane vapors to the temperature of the experiment. This layer also served to prevent channeling of the gas-vapor mixture.

Before the experiments were carried out, it was necessary to determine the catalytic activity of Chromel (containing 80% Ni) and Copel (40% Ni) alloys, from which the thermocouple junctions and leads were constructed, for the conversion of cyclohexane under reforming process conditions. The results of the investigation showed that there is almost no dehydrogenation of cyclohexane in the presence of these Ni alloys. Measurement of the amount of cyclohexane fed was made in weight units, g of material/ g catalyst/ hour, so that the experiments would be carried out under comparable conditions. Before starting the cyclohexane feed, hydrogen flow was established, and the temperatures in the center, at the periphery, and along the catalyst bed were adjusted to the same value. The benzene content of the catalyzate was determined by refractive index [9], since the catalyzate consisted only of benzene and cyclohexane. The gaseous effluent consisted of almost pure hydrogen. At the conclusion of each series of experiments with different cyclohexane feed rates, an experiment was carried

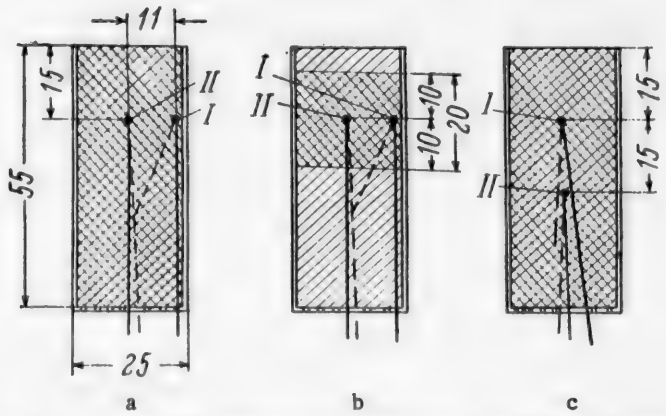

Fig. 2. Location of thermocouple junctions I and II in the catalyst bed.

out at the feed rate of the first experiment to check the activity of the catalyst, which remained close to its initial value in the majority of cases. Material loss did not exceed 2-3%.

Series I experiments. The first series of experiments was carried out at a temperature in the center of the bend (Figure 2, a) of 450-460° and feed rates of from 1 to 3 hours^{-1}. The catalyst was used in the form of cylinders having dimensions of 4 × 4 mm.* The weight of the catalyst was 16.94 g, and the volume was 24.4 ml. The results of the experiments are shown in Table 1. As may be seen from the data of Table 1, the extent of the conversion of cyclohexane to benzene varied insignificantly with a change in the feed rate from 1 to 3 hours^{-1}, and it reached the equilibrium value for this temperature and pressure region [11]. The temperature gradient between the center and the periphery of the catalyst bed was rather considerable, being 12.17 and 18.5°, respectively, at rates of 1.2 and 3 hours^{-1}. The temperature in the block changed from 485 to 567° with this change in feed rate.

The experiments of Series II were carried out under the same conditions as those of Series I, except that a smaller amount of catalyst (6.16 g instead of 16.94 g) was used in order to decrease the cyclohexane mass rate of flow; this could not be accomplished when using the former amount of catalyst owing to a significant increase in the temperature of the Duralumin block. The location of the thermocouple junctions is

* The ratio of the diameter of the tube to the diameter of the catalyst pellet ($D_T : D_g$) was made greater than 6 in order to decrease flow inequalities of the reaction mixture. This has been recommended in the paper by Boreskov and Slin'ko [10], for example.

shown in Figure 2, b. The results of the experiments are presented in Table 2. As the data of Table 2 show, an increase in the rate from 1 to 12 hours^{-1} resulted in a decrease in the benzene content of the catalyzate from 86.2 to 56.0% (Experiments 25 and 30). The temperature gradient across the catalyst bed was somewhat greater than in the experiments of Series I. Thus, in the latter series of experiments at a rate of 1 hour^{-1} (Experiment No. 12, Table 1), the temperature difference between the junction was 13°, while in Series II at the same feed rate and cyclohexane conversion (Experiment No. 25, Table 2), this difference was 15°.

TABLE 1

Temperature Distribution in the Catalyst Zone During Dehydrogenation of Cyclohexane Over 0.5% Pt on Al_2O_3 at 20 atm and H_2 : HC = 7.5

Expt. No.	Temp. (in °C)		Temp. diff. between Junction I and II (in °C)	Wt. rate (in hours^{-1})	Benzene content of catalyzate (in %)
	at periphery (Junc. 1)	in center (Junction II)			
11	464	453	11	1.04	88.5
12	465	452	13	1.0	86.2
13	464	452	12	1.02	87.0
14	466	450	16	1.94	81.8
15	476	459	17	1.88	85.0
17	475	458	17	1.96	86.0
18	478	460	18	2.96	84.0
20	480	461	19	3.01	84.5

The Series III experiments were carried out with the aim of studying the change in temperature along the catalyst bed using a suitable arrangement of the thermocouple junctions (Figure 2, c). The experimental conditions remained as before. The amount of catalyst was 16.87 g. The feed rate was varied from 1 to 6.6 hours^{-1}. The Duralumin block was replaced by a block of aluminum bronze with a melting point of about 900°. The results of the experiments are presented in Table 3. As the data of Table 3 show, as the feed rate was increased, the temperature gradient along the catalyst bed passed through a maximum of 25° (Experiment No. 36), and then fell to 10° (Experiment No. 40).

TABLE 2

Temperature Distribution in the Catalyst Zone During Dehydrogenation of Cyclohexane Over 0.5% Pt on Al_2O_3 at 20 atm and H_2 : HC = 7.5

Expt. No.	Temp. (in °C)		Temp. diff. between Junctions (in °C)	Wt. rate (in hrs^{-1})	Benzene content of catalyzate (in %)
	at periphery (Junc. I)	in center (Junction II)			
25	470	455	15	1	86.2
26	477	460	17	2	83.4
27	483	463	20	3	76.0
28	483	468	24	6	72.0
30	484	458	26	12	56.0

The experiments of Series IV were carried out with the aim of studying the effect of the size of the catalyst pellets on the degree of cyclohexane conversion. Samples of Catalyst No. 2 were prepared by the same method as Catalyst No. 1, which was used in the preceding series of experiments. The catalyst was used in the

TABLE 3

Temperature Distribution in the Catalyst Zone During Dehydrogenation of Cyclohexane Over 0.5% Pt on Al_2O_3 at 20 atm and H_2 : HC = 7.5

Expt. No.	Temp. (in °C) at top of bed (Junction I)	Temp. (in °C) at bottom of bed (Junction II)	Temp. diff. between Junctions I and II (in °C)	Wt. rate (in hrs^{-1})	Benzene content of catalyzate (in %)
34	450	465	15	1	85.5
35	460	475	15	1	82.2
36	453	478	25	1	82.6
37	450	471	21	3	76.5
38	452	470	18	4	75.0
40	448	458	10	6.6	72.0

form of cylindrical pellets with dimensions of 2 × 2 and 6 × 6 mm. The weights of catalyst having a volume of 24.4 mm were 16.8 and 13.08 g, respectively, for these sizes. The locations of the thermocouple junctions remained the same as in the experiments of Series III (Figure 2, c). The results of the experiments are presented in Figure 3 and Table 4.

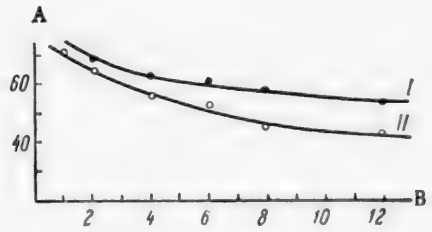

Fig. 3. Effect of feed rate on the depth of conversion of cyclohexane over 0.5% Pt on Al_2O_3. A) benzene content of catalyzate (in %), B) weight rate (in $hours^{-1}$). Pellet size (in mm): I) 2 × 2, II) 6 × 6.

The experimental results shown in Table 4 show that Catalyst No. 2 were less active than Catalyst No. 1, which was used in the preceding series of experiments. The effect of catalyst pellet size on the degree of cyclohexane conversion was appreciable, although not especially significant, and increased with an increase in feed rate. The temperature distribution along the catalyst bed was approximately the same as in the Series III experiments, although the values of the temperature gradients were less; this is explained by the lower extent of the conversion of cyclohexane.

DISCUSSION OF RESULTS

The temperature distribution across the cross-section of the catalyst bed is determined by the heat of reaction and by the heat-transfer conditions. The work of Bakhyrov and Boreskov [12] has shown experimentally that the transfer of heat in a direction normal to the direction of gas flow through a bed of granular material is due to : 1) convective transfer by the gas through the granular material (λ_c), 2) the intrinsic thermal conductivity of the granular material and the gas (λ_T), and 3) radiation between the grains (λ_{rad}). Hence, the overall coefficient of heat transfer is

$$\lambda_{ov} = \lambda_c + \lambda_T + \lambda_{rad}. \quad (1)$$

Gel'perin [13] has shown that the temperature drop across the cross-section of a catalyst bed in a cylindrical tube depends on the intensity of heat evolution or absorption and on the over-all heat transfer coefficient according to the equation:

$$\Delta t = \frac{Q \cdot R^2}{4\lambda_{ov}}, \quad (2)$$

where Q is the amount of heat supplied to (or taken from) a unit volume of catalyst (in kcal/ m^3 · hour) and R is the radius (in meters) of the catalyst tube (in our case, the distance between thermocouple junctions). Thus, λ_{ov} can be evaluated from experimental data. From the data of Experiment 13 (Table 1), the value of λ_{ov} is [Equation (2)] $\frac{0.2 \cdot 0.85 \cdot 54.4 \cdot 10^6 \cdot 0.011^2}{4 \cdot 24.4 \cdot 12} =$ = 0.96 kcal / m/ degree/ hour, where 0.2 is the amount of cyclohexane (moles/ hour), 0.85 is the degree of conversion of cyclohexane, 54.4 kcal / mole is the heat of reaction at 460°, 0.011 is the distance between thermocouple junctions (in meters), and 24.4 is the volume of catalyst (in ml).

TABLE 4

Effect of Feed Rate and Pellet Size of the Catalyst, 0.5% Pt on Al_2O_3, on the Depth of Dehydrogenation of Cyclohexane at 450-460°, 20 atm , and H_2 : HC = 7.5

Feed rate (in $hours^{-1}$)	Benzene content of catalyzate (in %) at indicated pellet size (in mm)	
	2 × 2	6 × 6
1	75.4	70.2
2	67.8	64.0
4	62.4	55.6
6	60.6	53.5
8	58.4	46.2
12	54.0	42.6

The thermal conductivity of the granular material and the gas-vapor mixture, λ_T, was determined by the method proposed in the paper cited above [12], and was found to be 0.3 kcal /.m/ degree/ hour.* The heat transfer by radiation between the catalyst pellets was calculated by the method due to Damkëller, [14] (λ_{rad} = 0.2 kcal / m/ degree/ hour). Thus, the convective component of the overall heat transfer coefficient is, according to the data of Experiment No. 13 (Table 1), λ_c = 0.46 kcal / m/ degree/ hour.

At the same time, λ_c, calculated by the equation proposed in the paper by Bakhurov and Boreskov [12] is 0.029 kcal./ m/ degree/ hour:

$$\lambda_c = 575 \cdot w_{rp} \cdot d_e \cdot c_p \gamma \qquad (3)$$

[where w_{rp} is the gas-vapor flow rate referred to the cross-sectional area of the tube (in m/ second), d_e is the equivalent diameter of the catalyst grains (in meters), c_p is the heat capacity of the gas-vapor mixture (in kcal / kg/ degree), and γ is the density of the mixture (in kg /m^3)]. Since the change in the temperature gradient was very small when the flow rate and, consequently, Q were changed by a factor of 3 (Experiment No. 20, Table 1), an appreciable increase in λ_c would be expected, since λ_T and λ_{rad} remained practically constant. In actual fact, the value of λ_{ov} as calculated by Equation (2) from the data of Experiment No. 20 was 1.89, and, consequently, λ_c was 1.39. A value for λ_c of 0.088 was obtained by using Equation (3). Such a marked divergence between the experimental and calculated values is apparently associated with the difference in the conditions under which the experiments were carried out. Equation (3) for determining λ_c was obtained analytically by the authors of reference [2] with the assumption that laminar gas flow is disturbed during flow of the gas around a grain. Experimental confirmation of Equation (3) was obtained by passing air at comparatively high rates (W_f = 0.5 m/ second) through a granular bed. Measurement of the temperature distribution in the cross-section of a catalyst bed under actual process conditions where there is a considerable heat effect and a change in volume has not yet been accomplished, either in the cited work [12] or in the work of other authors.

The value of λ_c depends on the nature of the movement of the gas stream. It would be expected that evenat low Reynolds numbers (Re), when a stream of gas flows through a bed of finely granular material, the gas flow would not be completely laminar. Thus, it was indicated in the Boreskov article [15] that turbulent flow begins at a Reynolds number as low as 10. Voitekhov, in the work cited above [4], observed a turbulent region of reactant transfer at Re ≈ 2 during the dehydrogenation of cyclohexane over Pt on C. When side processes involving a significant change in volume take place, an additional diffusional effect caused by the reactions arises and is directed normal to the surface of the catalyst. The values of the Reynolds number calculated by the equation of Zhavoronkov [16] for the conditions of Experiments Nos. 12 and 20 (Table 1) were 2.28 and 6.8, respectively. Thus when turbulent flow arises at low linear rates (in Experiment No. 12, W_f = = 0.003 m/ second), calculation of λ_c by Equation (3) can lead to results which are too low.

* The comparatively high value of λ_T was due to the high thermal conductivity of hydrogen.

It should be remarked that in the experiments of Series I the Reynolds number varied from 2.2 to 6.8 with an increase in cyclohexane flow rate from 1 to 3 hours^{-1}, while in the Series II experiments, an increase in the rate from 1 to 12 hours^{-1} was accompanied by a change in Re of only from 0.6 to 7.8. The latter is explained by the decrease in catalyst volume with no change in the cross-sectional area. Correspondingly, the temperature gradients in the Series II experiments at equal degrees of cyclohexane conversion were somewhat higher than in the Series I experiments (for example, Experiment No. 12, Table 1, and Experiment No. 25, Table 2).

The picutre is different with regard to the temperature distribution along the catalyst bed. The magnitude of the temperature gradient depends in a given case on the fractions of cyclohexane dehydrogenation taking place in the upper and lower layers of catalyst. From the results of the experiments of Series III, it can be concluded that at feed rates of from 1 to 4 hours^{-1}, cyclohexane conversion is essentially complete in the upper catalyst layers where there is the greatest absorption of heat, as indicated by the considerable temperature difference between the thermocouple junctions (Table 3). With a further increase in the feed rate, the underlying layers of catalyst participate more in the dehydrogenation of cyclohexane, and the temperature gradient is correspondingly decreased. It should also be pointed out that in the experiments of Series IV, in which the effect of particle size of the catalyst on the depth of cyclohexane conversion was studied, the magnitude of the temperature gradient along the axis of the catalyst bed depended on the dimensions of the catalyst pellets. Thus, in spite of the lower degree of conversion and the lower intensity of heat input per unit volume of catalyst with a pellet size of 6 × 6 mm, the temperature drop along the axis of the bed was lower than for the catalyst with a pellet size of 2 × 2 mm, which indicates that in the first case, deeper layers of the catalyst took part in the dehydrogenation of cyclohexane at equal feed rates.

Thus, it can be concluded that the dehydrogenation of cyclohexane under catalytic gasoline reforming conditions is not an isothermal process even in laboratory flow-type apparatus. The temperature gradient between the center and the periphery of a catalyst bed in a catalyst tube of small diameter (25 mm) reaches an appreciable value (up to 15°), even at low weight rates of flow (1 hour^{-1}). With an increase in the cyclohexane feed rate by a factor of 2 or more, the increase in the temperature gradient takes place more slowly than the increase in the amount of heat supplied, as is indicated by the increase in λ_c. The temperature gradient along the axis of the catalyst bed is high; at low feed rates, it drops with an increase in the rate, since the lower layers of catalyst begin to take part in the dehydrogenation.

It should be noted that the role of hydrogen, which is fed to the reactor in large excess to maintain catalyst activity [17], is not limited to this function. The stream of hydrogen or recycle gas flowing through the catalyst bed promotes heat transfer. The presence of a temperature gradient over the cross-section of the catalyst bed and the dependence of the degree of cyclohexane conversion on the dimensions of the catalyst pellets suggest that the dehydrogenation of cyclohexane over 0.5% Pt on Al_2O_3 at 450-470° and 20 atm proceeds in a diffusion region.

It is evident that reforming of gasoline fractions carried out under commercial conditions in adiabatic reactors at feed rates of up to 2 hours^{-1} is not sufficiently efficient with respect to the dehydrogenation cycloparaffins with six-membered rings. However, since this reaction proceeds at a higher rate than paraffin dehydrocyclization and hydrocracking reactions and at a higher rate than the dehydroisomerization of cycloparaffins with five-membered rings [17], to state that it would be expedient to carry out the reforming of even basically naphthenic fractions at an increased feed rate would still be premature. For a definitive judgment on this question, similar experiments should be carried out to study the dependence of the depth of conversion of hydrocarbons of other classes present in gasoline fractions on the feed rate and particle size of the catalyst.

SUMMARY

1. For the dehydrogenation of cyclohexane in the presence of 0.5% Pt on Al_2O_3 at 450-470°, 20 atm H_2 : HC = 7.5, and feed rates of from 1 to 6 hours^{-1}, it was shown that the degree of conversion of cyclohexane varies insignificantly at the feed rates investigated.

2. The increase in the temperature gradient between the center and the periphery of the catalyst bed with an increase in the cyclohexane feed rate takes place comparatively slowly as a consequence of an acceleration of the heat transfer process. The presence of a temperature gradient along the axis of the catalyst

bed indicates that it is predominantly the upper layers of catalyst which participate in the dehydrogenation of the cyclohexane at the cyclohexane feed rates investigated.

3. It was shown that the depth of cyclohexane conversion decreases with a change in the pellet size of the 0.5% Pt on Al_2O_3 catalyst from 2 × 2 to 6 × 6 mm.

4. A model apparatus was constructed, which will permit a study of heat transfer processes in catalyst bed during the conversion of the individual hydrocarbons in gasoline fractions under catalytic reforming conditions.

LITERATURE CITED

[1] T. E. Corringan, Ch. Eng. Progr. 49, 603 (1953).

[2] V. A. Dzis'ko, Coll. "Heterogeneous Catalysis in the Chemical Industry", Goskhimizdat, Moscow (1955).*

[3] W. P. Hettinger, C. D. Keith, I. L. Gring, and I. W. Teter, Ind. Eng. Ch. 47, 719 (1955).

[4] A. A. Voitekhov, Sci. Reports Moscow State Univ. 164, 33 (1953).

[5] Kh. M. Minachev, N. I. Shuikin, M. A. Ryashentseva, and N. F. Kononov, Bull. Acad. Sci. USSR, Div. Chem. Sci. 1229 (1957).

[6] Kh. M. Minachev, N. I. Shuikin, N. F. Kononov, I. L. Garanin, and M. A. Ryashentseva, Bull. Acad. Sci. USSR, Div. Chem. Sci. 1472 (1957).

[7] N. I. Shikin, Kh. M. Minachev, L. M. Feofanova, E. G. Treshchova, T. P. Yudkina, and A. E. Agronomov, Bull. Acad. Sci. USSR, Div. Chem. Sci. 501 (1955).

[8] A. M. Rubinshtein and V. A. Afanas'ev, Bull. Acad. Sci. USSR, Div. Chem. Sci. 1294 (1956).

[9] N. D. Zelinskii and G. S. Pavlov, J. Russ. Chem. Soc. 58, 1309 (1926).

[10] G. K. Boreskov and M. G. Slin'ko, J. Chem. Ind. 1, 19 (1955).

[11] A. A. Vvedenskii. Thermodynamic Calculations of Processes of the Fuel Industry, Gostoptekhizdat, Moscow–Leningrad (1949).*

[12] V. G. Bakhurov and G. K. Boreskov, J. Appl. Chem. 20, 721 (1947).

[13] N. I. Gel'perin, J. Chem. Mach. Ind. 3 (1940).

[14] G. Damkëller, Prog. Chem. 8, 732 (1938).

[15] G. K. Boreskov, J. Chem. Ind. 8, 221 (1947).

[16] N. M. Zhavoronkov, J. Chem. Ind. 10, 294 (1948).

[17] Kh. M. Minachev and N. F. Kononov, Proc. Chem. 26, 176 (1957).

Received July 21, 1958

* In Russian.

IDENTIFICATION OF BRANCHED OCTENES OBTAINED BY ALKYLATION OF TERTIARY BUTYL CHLORIDE WITH 2-BUTENE

M.M. Ketslakh, D. M. Rudkovskii, and F. A. Éppel'

For the purpose of identifying the branched octenes obtained during the alkylation of tertiary butyl chloride with 2-butene [1], the present authors worked out a method for the analysis of isomeric octanes by means of their tin points; this method permits the determination of the composition of binary mixtures with an accuracy of ±0.3% [2].

The essence of this method lies in the fact that in a binary mixture, the tin points (critical solution temperature of stannic iodide) of the intermediate compositions fall on a straight, or almost straight line joining the tin points of the hydrocarbons forming the mixture. This regularity makes it possible to use the tin point method for the quantitative analysis of binary mixtures through the use of the appropriate curves.

Moreover, the hydrocarbon of the greatest interest to us, 3,4,4-trimethyl-2-pentene, was synthesized from pinacolone and ethyl iodide by Grignard synthesis; until our investigation, there were no spectroscopic data in the literature, but we obtained its Raman spectrum [3] and determined the tin point [2]. The necessity for the development of the special methods of analysis arises from the closeness of the properties of certain branched olefins, which makes their identification by physical properties difficult.

It should be pointed out that 3,3,4-trimethyl-1-pentene was also found along with 3,4,4-trimethyl-2-pentene in the products of the Grignard synthesis. It is obvious that a change in the hydrocarbon skeleton takes place during dehydration of 2,2,3-trimethyl-3-pentanol in an acid medium [4]. The presence of two different isomers in the product of the reaction of pinacolone with ethyl iodide became apparent when the product was twice distilled in a column with efficiency of 20 theoretical plates (Figure 1).

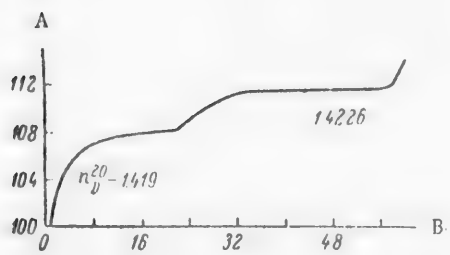

Fig. 1. Distillation curve of the products from the Grignard synthesis. A) temperature (in °C), B) amount (in ml). C) Literature data: n_D^{20} 1.414 for 3,3,4-trimethyl-1-pentene, 1.4235 for 3,4,4-trimethyl-2-pentene.

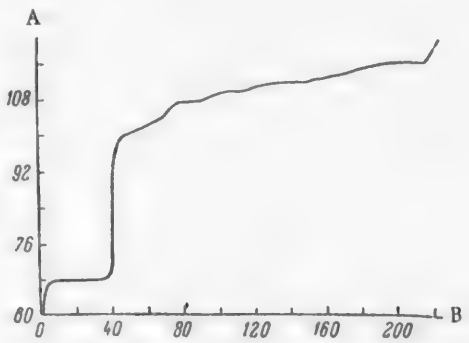

Fig. 2. Distillation curve from Experiment No. 44. A) temperature (in °C), B) amount (in ml).

Analysis of the fractions boiling at 107.5-109° and 110.5-111.7° by Raman spectroscopy showed that the first fraction consisted chiefly of 3,3,4-trimethyl-1-pentene, while the second was a mixture of the latter with a hydrocarbon having a frequency characteristic of β-unsaturation and which appeared to be 3,4,4-trimethyl-2-pentene. For a more complete identification of the latter, the synthesis product was hydrogenated over nickel at a temperature of 200°, and the hydrogenated product was distilled in a column having an efficiency of approximately 56 theoretical plates. Pure 2,2,3-trimethylpentane having the following constants was isolated: d_4^{20} 0.7164, n_D^{20} 1.40307, b. p. 109.6-109.9°, which correspond to the literature values (b. p. 109.84°, d_4^{20} 0.7161, n_D^{20} 1.4030). Fractionation of the above unsaturated fractions in a superfractionation column isolated 3,4,4-trimethyl-2-pentene, which had physicochemical properties corresponding to the pure olefin (b. p. 111.9°, d_4^{20} 0.7388, n_D^{20} 1.4232).

This 3,4,4-trimethyl-2-pentene was used as a standard with which to compare the alkylation products.

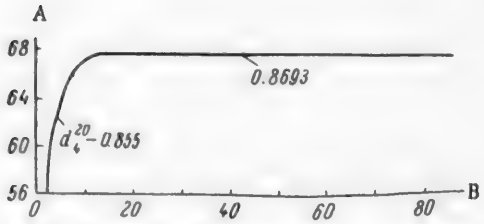

Fig. 3. Curve from the second distillation of the fraction boiling up to 72°. A) temperature (in °C), B) amount (in ml). C) Literature data: d_4^{20} for tertiary butyl chloride, 0.843; for secondary, 0.8707.

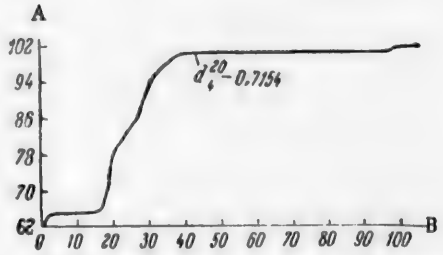

Fig. 4. Curve from the second distillation of the 72-100° fraction. A) temperature (in °C), B) amount (in ml). C) Literature data: d_4^{20} for 2,4,4-trimethylpentene, 0.7150.

For identification of the olefins obtained by the interaction of tertiary butyl chloride with 2-butene, the reaction products were washed, dried, and preliminarily distilled from a flask fitted with a Vigreux column into a fraction boiling up to 120° and a residue; the fraction boiling up to 120° was then distilled in a column having an efficiency of 33 theoretical plates, and fractions boiling to 72, 72-100, 100-103, 103-108, 108-110, 110-113, 113-115, and 115-120° were collected.

Similar fractions from a series of experiments carried out under optimum conditions (similar to Experiment No. 44, Figure 2) were combined and again distilled in the same column. The predominant products in the fractions were investigated in detail. Intermediate fractions, which were obtained in small amounts, were identified from their physical constants and by Raman spectroscopy. Thus, in the fraction boiling up to 72°, the major product was secondary butyl chloride (Figure 3). It was identified in the 67.5-67.7° fraction. Chlorine was determined by Carius' method; d_4^{20} was also determined.

Chlorine: found, by the Carius method, 38.6 wt. %; calculated for secondary butyl chloride, 38.4 wt %.

The data obtained are in good agreement with the literature and the calculated values, and they show that the fraction boiling up to 72° consisted chiefly of secondary butyl chloride and a small amount of tertiary butyl chloride (94% secondary butyl chloride and 6% tertiary butyl chloride, as calculated from the physical constants).

According to the physical constants and distillation curve (Figure 4), the fraction of reaction products boiling in the range 72-100° was a binary mixture of secondary butyl chloride and 2,4,4-trimethyl-1-pentene (19% secondary butyl chloride and 81% 2,4,4-trimethyl-1-pentene). The latter was identified by Raman spectroscopy in the 100-101.5° fraction. This was confirmed by hydrogenation of the fraction. Pure isooctane was obtained (n_D^{20} 1.3918; tin point, 194.6°; literature data: n_D^{20} 1.3919, tin point determined with pure isooctane, 195°).

It was necessary to establish the absence of dimethylhexenes in the fraction boiling at 100-103° (Figure 5). The approximate composition of the fraction was established by Raman spectroscopy – 90% 2,4,4-trimethyl-1-pentene and 10% 2,4,4-trimethyl-2-pentene. For a more precise determination of the composition, the

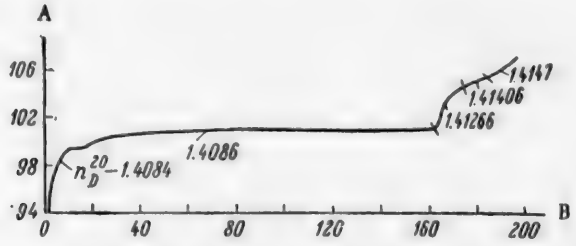

Fig. 5. Curve from the second distillation of the 100-103° fraction. A) temperature (in °C), B) amount (in ml). C) Literature data: n_D^{20} for 2,4,4-trimethyl-1-pentene, 1.4086; for 2,4,4-trimethyl-2-pentene, 1.4160.

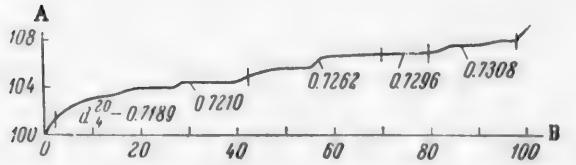

Fig. 6. Curve from the second distillation of the 103-108° fraction. A) temperature (in °C), B) amount (in ml).

fraction was again distilled (Figure 5); the two main fractions (99-100 and 100-101.5°) obtained from this distillation were hydrogenated, the physical constants of the resulting octanes were hydrogenated, the physical constants of the resulting octaneswere determined, and an analysis was carried out by Raman spectroscopy. The analytical data showed that this was pureisooctane (n_D^{20} 1.3918). The purity of this isooctane was confirmed by its tin point, which was found to be 194.6° (tin point of isooctane 195°). The composition of the intermediate fractions was established by means of the physfcal constants and by Raman spectroscopy. No dimethylhexenes were detected in the fraction. A more precise composition of the fraction is 86% 2,4,4-trimethyl-1-pentene and 11% 2,4,4-trimethyl-2-pentene.

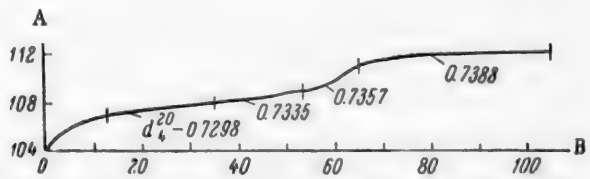

Fig. 7. Curve from the second distillation of the 108-110° fraction. A) temperature (in °C), B) amount (in ml). C) Literature data: d_4^{20} for 3,4,4-trimethyl-2-pentene, 0.7392; for 3,3,4-trimethyl-1-pentene, 0.729.

The distillation curve for the 103-108° fraction (Figure 6) shows that this fraction was a complex mixture.

The octenes boiling within this range have physical properties which are closely similar – 2,4,4-trimethyl-2-pentene (boiling point, 104.8°, d_4^{20} 0.7212, n_D^{20} 1.4160), 3,4,4-trimethyl-1-pentene (boiling point, 104°, d_4^{20} 0.719, n_D^{20} 1.412); and 3,3,4-trimethyl-1-pentene (boiling point, 105°; d_4^{20} 0.729, n_D^{20} 1.414). All of these olefins may be obtained in the alkylation of tertiary butyl chloride with 2-butene. Identification of these olefins was carried out by Raman spectroscopy in the 104-106° fraction, after which the olefins were hydrogenated and again distilled; this produced isooctane and 2,2,2-and 2,3,3-trimethylpentanes, the structures and amounts of which were established by Raman spectroscopy and by determination of the tin points. The remaining fractions were identified in the same manner. The composition of the fraction was (in %): 2,4,4-trimethyl-1-pentene, 19; 2,4,4-trimethyl-2-pentene, 18; 3,4,5-trimethyl-1-pentene, 33; 3,4,4-trimethyl-2-pentene, 12; and 3,3,4-trimethyl-1-pentene, 18.

Analysis of the individual fractions of the 108-110° fraction (Figure 7) was by Raman spectroscopy; for confirmation, the fraction boiling at 107-111° was distilled into one-degree fractions, which were hydrogenated and analyzed. The compositions of the hydrogenated fractions were confirmed by their physical constants and tin points. The analytical data established the following composition for this fraction (in %): 3,4,4-trimethyl-2-pentene, 71; 3,4,4-trimethyl-1-pentene, 11; and 3,3,4-trimethyl-1-pentene, 18

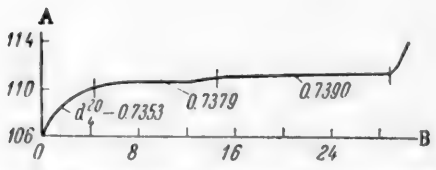

Fig. 8. Curve from the second distillation of the 110-113° fraction. A) temperature (in °C), B) amount (in ml). C) Literature data: d_4^{20} for 3,3,4-trimethyl-1-pentene, 0.729; for 3,4,4-trimethyl-2-pentene, 0.7392.

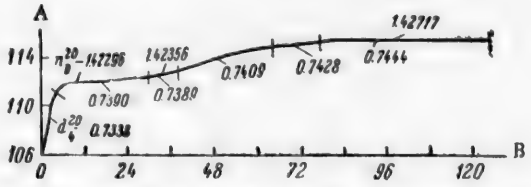

Fig. 9. Curve from the second distillation of the 113-115° fraction. A) temperature (in °C), B) amount (in ml). C) Literature data: for 3,4,4-trimethyl-2-pentene, d_4^{20} is 0.7342 and n_D^{20} is 1.4235; for 2,3,4-trimethyl-2-pentene, d_4^{20} is 0.7434 and n_D^{20} is 1.4274.

The olefin fraction boiling at 110-113° was the predominant fraction of the reaction products (Figure 2). According to Raman spectroscopy data, it was a binary mixture containing 90% 3,4,4-trimethyl-2-pentene and 10% 3,3,4-trimethyl-1-pentene. However, its distillation curve and physical constants show that this fraction was more complex.

The Raman spectrum and the physical constants of the major fraction were determined for a more complete identification. The fraction was then hydrogenated, the tin points and physical constants of the hydrogenated product were determined, and the Raman spectrum was obtained. The tin point was 145.5°, and the value of d_4^{20} was 0.7165 (literature data for 2,2,3-trimethylpentane; d_4^{20} 0.7161, tin point, 145.5°). The data are in agreement with the values for 2,2,3-trimethylpentene [1]. The compositions of the intermediate fractions were determined by means of their physical constants and by Raman spectroscopy. The analytical data established that this fraction had the following composition (in %): 3,4,4-trimethyl-2-pentene, 79; 3,3,4-trimethyl-1-pentene, 13; and 2,3,4-trimethyl-2-pentene, 8.

The distillation curves for the 113-115 and 115-120° fractions show that here we are dealing chiefly with two products – 3,4,4-trimethyl-2-pentene and 2,3,4-trimethyl-2-pentene. The physical constants of these hydrocarbons differ sharply, and it was possible to determine the composition of the individual fractions and then the overall composition of the entire fractions.

Thus, for example, the determination of the physical constants of the 111.4-112.4, 112.4-113, and 115.4° fractions (Figure 9) and of the 115-116 and 116-116.6° fractions (Figure 10) indicated that almost pure 3,4,4-trimethyl-2-pentene and 2,3,4-trimethyl-2-pentene were present. However, for more complete identification, the major fractions were hydrogenated, and the hydrogenated products were analyzed by Raman spectroscopy and by tin points.

All of the data obtained confirmed the presence of hydrocarbons having the proposed structure.*

The following compositions for these fractions were established by the analytical data: 113-115° fraction, 43% 3,4,4-trimethyl-2-pentene and 57% 2,3,4-trimethyl-2-pentene; 115-120° fraction, 73% 2,3,4-trimethyl-2-pentene and 27% 3,4,4-trimethyl-2-pentene.

Thus, secondary butyl chloride, 2,4,4-trimethyl-1-pentene, 2,4,4-trimethyl-2-pentene, 3,4,4-trimethyl-1-pentene, 3,4,4-trimethyl-2-pentene, 3,3,4-trimethyl-1-pentene, and 2,3,4-trimethyl-2-pentene were identified in the products of the alkylation of tertiary butyl chloride with 2-butene.

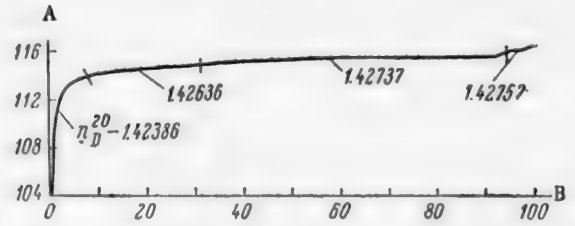

Fig. 10. Curve from the second distillation of the 115-120° fraction. A) temperature (in °C), B) amount (in ml).

The amount of hydrocarbons identified in each individual case was calculated from the analysis of the fractions and from their yields.

LITERATURE CITED

[1] M. M. Ketslakh, D. M. Rudkovskii, and F. A. Éppel', J. Appl. Chem., 32, 8 (1959).*

[2] M. M. Ketslakh and F. A. Éppel', J. Anal. Chem., 5, 3, 151 (1950).

[3] Ya. É. Shmulyakovskii and S. N. Aleksandrov, Proc. Acad. Sci. USSR, 82, 6, 931 (1952).

[4] A. D. Petrov, Synthesis and Isomeric Transformations of Aliphatic Hydrocarbons, Izd. AN SSSR, 19 (1947).**

Received (second submission) March 2, 1959

* According to the literature, n_D^{20} for 2,3,4-trimethyl-2-pentene is 1.4274, and for 3,4,4-trimethyl-2-pentene, 1.4235.

* C. B. Translation.

** In Russian.

ON THE CONVERSION OF HIGHER PHENOLS TO PHENOL, CRESOLS, AND XYLENOLS

M. K. D'yakova, A. B. Vol'-Épshtein, M. N. Zharova, and E. A. Zasukhina

Institute of Mineral Fuels AN SSSR

The growing requirement of the national economy for phenol, cresols, and xylenols has created the very real problem of expanding the sources of these compounds. One of the possible routes for the production of additional amounts of these phenols is the conversion of higher phenols to lower.

As a study of the literature shows, the most effective method of solving this problem is the use of destructive hydrogenation.

The thermal cracking of high-boiling phenols is accompanied by considerable coke formation. Senseman [1] has shown that cracking of phenols (boiling at 207-290°) from medium-temperature coal tar in a steel tube at 650° and atmospheric pressure results in a yield of 25% (36% with recycle) of phenols with a boiling range of up to 207°; however, coke formation was high, leading in individual experiments to complete coking of the apparatus. Very similar results were obtained by Zabavin [2] during the cracking of peat phenols with a boiling range of 200-255°.

Jones and Neuworth [3] and Katkovskii, Fridman, and Dorskaya [4] showed that cracking of higher phenols from coal tar (boiling range 230-300°) and from peat tar (boiling at 200-260°) in the presence of steam leads to a sharp decrease in coke formation (down to 0.8-1.0% calculated on the raw feed); however, condensation reactions are considerably increased. When the higher phenols from coal tar were processed with steam under optimum conditions, the yield of lower phenols did not exceed 15-30%, and the amount of undistillable residue was 40%.

Lower phenols have not been detected during the cracking of α- and β-naphthols [3].

A number of Soviet investigators have studied the processing of basically cresol-xylenol fractions by hydrogenation [5-7]. Kalechits and Salimgareeva [8] obtained 6.5% phenols boiling up to 230° by the destructive hydrogenation of the total phenols from the primary tar of Cheremhov coal in an autoclave over an iron catalyst (temperature, 482°; pressure, 336 atm ; time, 3 hours). As these same investigators have shown [9], the structure of the higher phenols subjected to hydrogenation has a considerable effect on the yield of low-boiling phenols. Bicyclic phenols of the naphthol series are unsuitable as a raw material for the production of lower phenols. Higher phenols with aliphatic side chains are the best raw material for the production of lower phenols.

Orchin and Storch [10] have reported the results of isolated experiments on the destructive hydrogenation of higher coal tar phenols from Pittsburgh coal without a catalyst and at a temperature of 450-475°, a pressure of 85-106 atm , and a reaction time of 2.5-3 hours. The yield of lower phenols boiling up to 233° was 32% per pass.

A high yield of low-boiling phenols (up to 65%) was obtained by Nadenik [11] by destructive hydrogenation of a narrow pyrocatechol fraction in a flow-type apparatus. The process was carried out at atmospheric

pressure and a temperature of 440° over an MoO_3/ Cr_2O_3/ Al_2O_3 catalyst; the catalyst was regenerated every 75 hours, since the yield of lower phenols had decreased sharply.

Very encouraging results were obtained by Perna and Pelčik [12], who subjected to destructive hydrogenation phenols from brown coal generator tars with a boiling range of 230-270°. The experiments were carried out using various catalysts in an autoclave at temperatures of 455-480°, an initial hydrogen pressure of 30-40 atm , and a time of 30-45 minutes.

Under optimum conditions (475°, 30 atm , WS_2/ V_2S_3 catalyst, and the addition of 25 ml of a concentrated aqueous solution of ammonia per 125 ml of raw material), the yield of phenols boiling to 225° was 57.3% per pass with 16% unconverted phenols.

The authors pointed out that the yield of lower phenols increased in the presence of an aqueous solution of ammonia and especially of pyridine, while the addition of an aqueous solution of sodium hydroxide decreased the yield of lower phenols and high coke formation.

Kubička [13], using a flow-type apparatus with a reactor volume of 200 ml, carried out the destructive hydrogenation of the total phenols in the middle oil from a lignite tar without preliminary separation of the phenols; 86% of the middle oil boiled at 360° or lower. These phenols comprised 34.6% of the oil and consisted of 20% phenol and cresols, 19.2% xylenols, and 60.8% higher-boiling phenols, including 22.6% pyrocatechol fraction. Under the conditions used (temperature, 550°; pressure, 70 atm ; feed rates of 100 ml of raw feed and 100 liters of hydrogen per hour), the per-pass yield was 26.4% phenols boiling up to 225°, calculated on the higher phenols in the raw feed; 56.2% of the original phenols remained unconverted.

The authors remarked on the absence of coke formation when the reaction was carried out in a reactor constructed of a nickel-free, high-chromium-content steel. In order to eliminate the harmful effect of the walls of a reactor constructed from steel containing a significant amount of nickel, lining of the reactor with copper foil was recommended.

The present investigation was devoted to the hydrocracking of the higher phenols in Cheremkhov tar and its liquid-phase hydrogenation products to phenol, cresols, and xylenols.

EXPERIMENTAL

Raw material. The phenols investigsted were separated from distillates boiling up to 320° from Cheremkhov medium-temperature tar and the liquid product of the hydrogenation of its heavy fraction. Separation of the phenols was accomplished by repeated treatment of the distillates with a 10% solution of sodium hydroxide, subsequent removal of the resulting phenolates from the neutral oil by means of benzene, and decomposition of the latter with a 30% solution of sulfuric acid. The resulting phenols were distilled under vacuum in a fractionation column equivalent to 12 theoretical plates; the fractions obtained from the distillation were subjected to the hydrogenation process.

As a rule, the amount of impurities in all of the higher phenol fractions amounted to 10%, of which the major portion was neutral oils. The content of bases in the tar phenols did not exceed 0.8%, while the acid content was 3% of the weight of the raw material. The water-soluble phenols comprised 12% of the weight of the phenols. The phenols from the product of Cheremkhov tar hydrogenation contained 0.1% bases, 0.8% acids, and 3.4% water-soluble phenols.

Experimental method and catalysts. Hydrogenation of the phenols was carried out in a half-liter stirred autoclave and in a flow-type apparatus with a reactor volume of 100 ml.

The catalysts used in the autoclave experiments were: ferric oxide on a brown coal semicoke, WS_2, VS_2, WS_2/ silica-alumina, WS_2/ NiS/ Al_2O_3, MoO_3/ Al_2O_3, and a silica-alumina cracking catalyst. The initial pressure in the autoclave was 20-40 atm , the operating pressure was 100-140 atm , and the length of an experiment was 30-120 minutes. A series of experiments was carried out with the addition of water or a concentrated aqueous solution of ammonia to the raw feed. The charge of raw material to the autoclave was 85 g.

Hydrogenation of the higher phenols in the flow apparatus was carried out over 50 cc of Fe_2O_3/ Al_2O_3 catalyst containing 1% iron; the temperature was 475-525°, the pressure was 15-100 atm , the space rate was 1.2 liters per liter of catalyst per hour, and the hydrogen feed rate was 1000 liters per liter of raw feed. The liquid hydrogenation products were distilled in a column into three fractions: a phenol fraction boiling to 185°, a cresol fraction boiling at 185-205°, a xylenol fraction boiling at 205-230°, and a residue. The hydrogenation products from certain experiments were distilled from a flask fitted with a Vigreux column. The phenol content of the fractions boiling up to 165° at 10 mm Hg (approximately 280° at atmospheric pressure) was determined by refractive index, while the phenol content of the higher-boiling fractions was determined gravimetrically. Coke formation during the autoclave hydrogenation experiments was determined by direct determination of the solid material, while in the flow experiments, coke formation was calculated from the amount of carbon dioxide formed by combustion of the coke deposited on the catalyst at a temperature of 500-550°; The carbon dioxide was absorbed in a 33% solution of potassium hydroxide. The material balance on the process was calculated on the basis of the higher phenols in the feed.

EXPERIMENTAL RESULTS

In order to determine the optimum conditions for the destructive hydrogenation of higher phenols, the effects of the fractional composition of the raw material, various catalysts, and the addition of water and of an aqueous solution of ammonia were investigated in autoclave experiments.

As shown by the data presented in Table 1, the chemical structure of the higher phenols, which is related to the fractional composition, has a decisive effect on the degree of conversion; the yield of lower phenols decreased with an increase in the boiling range of the phenol fractions. The best results were obtained with phenols boiling in the range of 230-255°. The content of these fractions in the higher coal tar phenols was about 35%, while the content in the higher phenols of the coal tar hydrogenation product was about 30%.

This dependence of yield on composition, which was observed during the destructive hydrogenation of tar phenols, higher phenols of the liquid hydrogenation product, and also β-naphthol, is in agreement with the

TABLE 1

Hydrogenation of Narrow Fractions of Phenols from Cheremkhov Tar, Its Liquid Hydrogenation Product, and β-Naphthol. (Temperature, 475°; initial hydrogen pressure, 40 atm ; maximum pressure, 120-190 atm ; time, 60 minutes; catalyst, iron on lignite semicoke (10,927))

Boiling range of phenol fractions (in °C)		Av. no. rings per molecule	Yield of hydrogenation products (in % of higher phenols in raw feed)							phenols in Cheremkhov tar hydrogenation product
			phenols with b.p. (in °C)			unconverted phenols	neutral oil + water	coke	gas + loss	
at 10 mm Hg	at atmospheric pressure		to 185	185–205	205–230					
Cheremkhov tar phenols										
117—138	230—255	1.36	0.4	2.8	30.4	37.3	23.8	—	5.3	53.7
138—160	258—300	1.53	—	2.9	9.9	22.5	17.8	29.2	17.7	16.5
160—200	—	—	—	1.4	3.8	15.0	21.3	38.5	20.0	6.1
Phenols in Cheremkhov tar hydrogenation product										
117—135	232—249	1.47	1.7	4.0	15.4	43.0	28.0	—	7.9	37.1
135—144	250—257	1.68	0.6	3.8	8.5	55.6	22.6	—	8.9	29.1
144—165	258—277	1.63	0.8	2.6	5.3	34.6	46.8	—	9.9	13.3
165—200	270—305	1.67	0.1	2.1	5.3	41.7	37.0	—	13.8	12.9
β-naphthol		2.00	—	—	13.5	23.5	62.1	—	0.9	17.7

data of D'yakova and Davtyan [14]. An investigation of the chemical structure of these phenols showed that the content of bicyclic phenols of the naphthol series and of indanol increased with an increase in the boiling range of the higher phenols, while the amount of monocyclic phenols decreased. The tar phenols contained a greater amount of monocyclic phenols than did the corresponding phenol fractions of the liquid hydrogenation product, and, therefore, the yield of phenol, cresols, and xylenols from the tar phenols was higher than from the phenols of the liquid hydrogenation product. The formation of phenols from β-naphthol was small under the conditions used.

Our results are in agreement with the investigations of Kalechits and Salimgareeva [9]

Data on the effect of a number of catalysts on the degree of conversion of higher phenols boiling at 107-138° at 10 mm Hg are presented in Table 2. These data show that not one of the catalysts tested gave high conversion to lower phenols. The per-pass yield of lower phenols over the various catalysts varied from 15.8 to 23.6% calculated on the higher phenols in the starting material, or from 21.5 to 47.5% on the converted phenols. The best results were obtained in the presence of WS_2/ V_2S_3 and WS_2/ silica-alumina; closely similar results were obtained with commercial catalyst 10,927 (iron on lignite dust).

Optimum conditions for the hydrogenation of the higher phenols in an autoclave were: a temperature of 475°, an initial hydrogen pressure of 30-40 atm , and a run time of 30-60 minutes. A decrease in the process temperature to 450° (5% iron catalyst) led to a sharp decrease in the yield of lower phenols; an increase in temperature to 500° caused the appearance of coke and an increase in gas formation. The highest yield of lower phenols was obtained at a temperature of 475°. A decrease in the initial pressure to 20 atm somewhat increased the formation of lower phenols at the expense of a decrease in the yield of neutral oils, but, like an increase in temperature above 475°, it caused the formation of coke. An increase in the initial pressure above 40 atm led to an undesirable excessive reduction of the phenols in the raw materials.

TABLE 2

The Effect of the Catalyst on the Hydrogenation of Phenols Boiling at 107-138° at 10 mm Hg (220-275° at Atmospheric Pressure) in the Product of Cheremkhov Tar Hydrogenation (Phenol content in raw material, 94.7%; 30% boiled up to 230°; hydrogenation temperature in autoclave, 475°; initial pressure, 40 atm ; maximum pressure, 125-145 atm ; run time, 30 minutes)

Catalyst	Yield of hydrognation products (in % of higher phenols in raw material)						Yield of lower phenols (in %)	
	lower phenols with b.r. of (in °C)			unconverted phenols	neutral oil + water	gas + loss	of higher phenols	of converted higher phenols
	to 185	185—205	205—230					
Without catalyst	0.3	0.2	11.4	67.3	12.3	8.5	17.0	36.5
V_2S_3 2%	0.1	1.1	13.0	60.0	20.2	5.6	20.3	35.5
WS_2 1% + V_2S_3 1%	0.8	3.2	12.5	65.2	16.9	1.4	23.6	47.5
WS_2 + silica-aluminum 2%	1.1	3.4	12.0	64.0	17.0	2.5	23.6	46.0
10,927 (iron) 5%	0.5	3.1	12.5	62.2	18.2	3.5	23.1	42.7
5% 10,927 + 5% silica-aluminum	1.7	2.9	6.5	48.4	31.5	9.0	15.8	21.5

Our experiments did not confirm the literature data with respect to an increase in the yield of lower phenols during destructive hydrogenation of high-boiling phenols in the presence of water or an aqueous solution of ammonia [12, 15]. In experiments with phenols boiling at 117-135° at 10mm Hg and obtained from the liquid product from the hydrogenation of tar, it was shown (Table 3) that when the hydrogenation is conducted in the presence of iron catalyst at a temperature of 475° with the addition of water or aqueous ammonia,

the per-pass yield of lower phenols is decreased (from 17.8 to 3.6-7.5%), the yield of neutral oils is decreased, and the amount of unconverted higher phenols is increased.

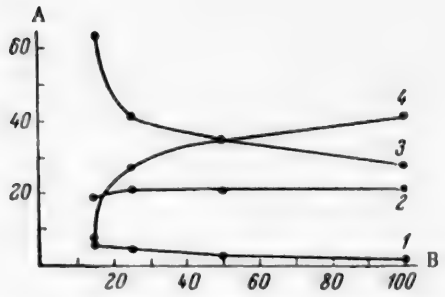

Fig. 1. Effect of pressure on the hydrogenation of phenols boiling at 117-138° at 10 mm Hg obtained from the liquid product of Cheremkhov tar hydrogenation. Temperature, 475°; catalyst, Fe_2O_3/ Al_2O_3 (1% Fe), 50 cc; space rate, 1.2 liters per liter of catalyst per hour; hydrogen feed rate, 1 liter/ minute. A) yield (in wt %), B) pressure (in atm). 1) coke formation, 2) lower phenols boiling up to 230°, 3) unconverted phenols, 4) neutral oil.

An increase in the temperature of the process to 525° along with the addition of aqueous ammonia increased the formation of lower phenols; however, the results were no better than those obtained by hydrogenation at 475° without the addition of water or ammonia; along with an insignificant increase in the yield of lower phenols, there was a substantial increase in the formation of neutral oils, which, on the whole, unfavorably changes the balance of the process.

A similar effect occurred with phenols boiling over a broad temperature range (from 230 to 320°) obtained from tar or its hydrogenation product when the hydrogenation of the phenols was carried out in the presence of aqueous ammonia.

A narrow fraction of the tar phenols, b.p. 117-138° at 10 mm Hg, and a narrow fraction of phenols from the tar hydrogenation product, b.p. 117-135° at 10 mm Hg, were hydrogenated in the flow apparatus over a fixed bed of Fe_2O_3/ Al_2O_3 (1% iron).

The basic experiments were carried out at a temperature of 475° and a pressure of 50 atm with the phenols from the liquid hydrogenation product, and at 475° and 100 atm with the tar phenols; the space rate was 1.2 liters per liter of catalyst per hour. As in the autoclave experiments, an increase in the temperature to 525° led to an increase in gas and coke formation, but did not increase the yield of lower phenols. As may be seen in Figure 1, a decrease in the pressure from 100 atm to 15-25 atm decreased the formation of neutral oils with practically constant yield of the desired phenols, but it was accompanied by an increase in coke formation (1.3 at 100 atm and 4.5% at 15 atm , based on the raw feed).

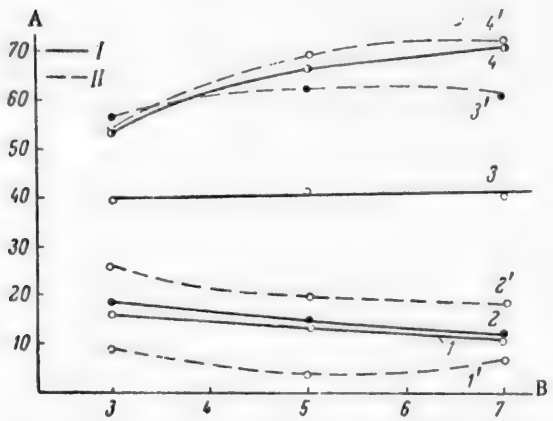

Fig. 2. Effect of duration of catalyst operation on the hydrogenation of higher phenols. Temperature, 475°; pressure, 50 atm (I) and 100 atm (II); space rate, 1.2 liters per liter of catalyst per hour; catalyst, Fe_2O_3/ Al_2O_3 (1% Fe); ratio of fresh to recycled phenols: feed I*, 4 : 6; feed II, 4.5 : 5.5. A) yield (in wt %), B) amount of feed passed over the catalyst (vol / vol catalyst). 1) Neutral oil, 2) lower phenols boiling up to 230°, 3) yield of lower phenols (in % of converted phenols), 4) unconverted phenols

* Feeds: 1) phenols from the liquid product of Cheremkhov tar hydrogenation, b.p. 117-135° at 10 mm Hg, II) Cheremkhov tar phenols, b.p. 117-138° at 10 mm Hg.

TABLE 3

Effect of Added Water or of Aqueous Ammonia on the Hydrogenation of Phenols Boiling at 117-135° at 10 mm Hg in the Hydrogenation Product of Cheremkhov Tar. (Phenol content of raw material, 97%; 2.5% boiled up to 230°; catalyst, 5% 10,927; initial pressure, 40 atm ; run time, 30 minutes)

Run temperature (in °C)	Added material	Yield of hydrogenation products (in % of higher phenols in raw material)							Yield of phenols boiling to 230° (in % of converted higher phenols)
		phenols with b.r. of (in °C)			unconverted phenols	neutral oils+ water	coke	gas + loss	
		to 185	185—205	205—230					
475	—	0.8	2.6	14.3	59.2	21.6	—	1.5	43.3
475	25ml H_2O	0.7	0.7	5.6	84.1	6.9	—	2.0	44.1
475	50ml H_2O	0.8	0.4	2.4	76.5	10.9	—	9.0	15.3
475	25ml 30% solution NH_3	0.6	1.3	5.3	73.8	18.7	—	0.3	27.5
475	50ml 30% solution NH_3	2.1	—	5.4	70.5	20.8	—	1.2	25.4
500	25ml 30% solution NH_3	1.0	2.6	8.6	70.6	15.7	—	1.5	41.5
525	25ml 30% solution NH_3	1.2	3.8	14.7	44.3	32.3	0.9	2.8	35.4

TABLE 4

Material Balance for the Conversion of Higher Phenols to Lower Phenols by Hydrogenation. (Temperature, 475°; catalyst, Fe_2O_3/ Al_2O_3; space rate, 1.2 liters per liter of catalyst per hour)

Cheremkhov tar phenols with a b. p. of 117-138° at 10 mm Hg	Phenols from Cheremkhov tar hydrogenation product with a b.p. of 117-135° at 10 mm Hg
100 atm. pressure	50 atm. pressure
Ratio of fresh to recycle higher phenols, 4.5 : 5.5; reactor walls lined with copper foil	Ratio of fresh to recycle higher phenols, 4 : 6; reactor not lined
Feed	
Raw material 100	Raw material 100
Hydrogen 2.2	Hydrogen 1.7
Total 102.2	Total 101.7
Products	
Phenol 5.7	Phenol 3.8
Cresols 17.6	Cresols 12.2
Xylenols 33.9	Xylenols 23.4
Total 57.2	Total 39.4
Neutral oils 20.2	Neutral oils 35.8
Water 11.7	Water 7.9
Gas and loss 12.4	Gas and loss 13.9
Coke 0.7	Coke 4.7
Total 102.2	Total 101.7

There was no substantial decrease in coke formation when the inner wall of the reactor was lined with copper foil to isolate the feed from the effect of steel with a high nickel content [31].*

The deposition of coke decreased the activity of the catalysts.

As may be seen in Figure 2, during the course of the process there was a continuous and rather rapid decrease in the depth of conversion of the feed, and catalyst regeneration was required. However, the yield of lower phenols calculated on the basis of the phenols converted remained constant.

18 catalyst regenerations were carried out over 56 hours of operation, and catalyst activity was always restored completely.

In commercial application of the process, it would obviously be expedient to use a moving-bed catalyst and continuous regeneration of a fraction of the catalyst in a special vessel.

It was shown experimentally that about the same results are obtained regardless of whether the feed consisted of fresh phenols or a mixture of them with recycle phenols, i.e., phenols which have already been through the process but which remained unconverted in the preceding cycle. It should be noted that the recycle phenols were not subjected to any additional operations (fractionation and removal of the neutral oils) before subsequent hydrogenation (4 cycles were carried out), since they had practically the same boiling range as the fresh feed and contained only slightly more neutral oils.

Table 4 presents material balances for hydrocracking of higher Cheremkhov tar phenols with a boiling range of 117-138° at 10 mm Hg and for hydrocracking of phenols with a boiling range of 117-135° at 10mm Hg obtained from Cheremkhov tar hydrogenation product. These were calculated on the basis of experiments carried out under process start-up conditions during the first 2.5 hours of catalyst operation (i.e., during processing of 3 volumes of feed per volume of catalyst; results from the hydrocracking of fresh phenols were practically unchanged from cycle to cycle).

The data of Table 4 show that as in the autoclave experiments, the higher phenols from the medium-temperature tar are better raw material for hydrocracking to lower-boiling phenols than the corresponding higher phenols obtained from the liquid hydrogenation product from this same tar. The ultimate yields of phenols boiling to 230° were 57.2 and 39.4%, respectively, for these two feeds.

SUMMARY

In an investigation of the conditions for the hydrocracking of higher phenols from a medium-temperaure Cheremkhov coal tar and phenols from the liquid product of the hydrogenation of this tar, the most suitable raw material for the production of lower phenols boiling up to 230° – phenol, cresols, xylenols – are the tar phenols with a boiling range of 230-255°, which are characterized by having the lowest content of bicyclic phenols. The yield of these phenols was 35% of the total higher phenols boiling from 230 to 320°. Other processing methods or means for their direct use must be found for the higher-boiling fraction (255-320°) of the higher phenols. Destructive hydrogenation of the indicated higher phenol fraction in a flow apparatus (Fe_2O_3/Al_2O_3 catalyst; temperature, 475°; pressure, 100 atm ; space rate, 1.2 liters per liter of catalyst per hour; ratio of fresh feed to recycle oil, 3 : 4) gave a 57% yield of lower phenols with 0.7% coke formation and a hydrogen consumption of 2.2%. In view of the decrease in catalyst activity, the processing of these phenols should be carried out as an alternating-cycle process.

LITERATURE CITED

[1] C. E. Senseman, Ind. Eng. Ch. 21, 81 (1930).

[2] V. I. Zabavin, Chem. Sol. Fuels, 593 (1932).

[3] B. W. Jones and M. B. Neuworth, Ind. Eng. Ch. 45, 12, 2704 (1953).

[4] A. P. Katkovskii, G. E. Fridman, and F. L. Dorskaya, Collected Works AN SSSR, 135 (1939).

* The cover of the reactor was not lined.

[5] M. I. Kuznetsov and K. I. Belov, Chem. of Solid Fuels, 592 (1933).

[6] I. B. Rappoport and M. S. Sudzilovskaya, Chem. of Solid Fuels, 9-10, 305 (1934).

[7] I. B. Rappoport and N. P. Masina, Chem. of Solid Fuels 7, 694 (1936).

[8] I. V. Kalechits and F. G. Salimgareeva, Coll. "Investigation of Cheremkhov Coals and the Products of Their Chemical Processing", 79 (1955).

[9] I. V. Kalechits and F.G. Salimgareeva, Coll. "Catalytic Hydrogenation". Izd. AN SSSR, 12 (1956).

[10] M. Orchin and H. H. Storch, J. Soc. Chem. Ind. 69, 121 (1950).

[11] O. Nadenik, Podklady Staza 24, 10 (1951).

[12] F. Perna and J. Pelčik, Paliva XXXIII, 6, 126 (1953).

[13] R. Kubička, Freiberger Forschungshefte, A, 36, 95 (1955).

[14] M. K. D'yakova and N. A. Davtyan, Trans. IGI [Institute of Mineral Fuels] AN SSSR IX (1959).

[15] V. P. Konov, Chem. of Solid Fuels 7, 711 (1936).

Received September 13, 1958

RESEARCH BY SOVIET EXPERTS

Translated by Western Scientists

BORATE GLASSES

by L. Ya. Mazelev

Boron as an element has been known for a long time, but the role of its oxide in glass has been studied little. This book is based mainly on the results of investigating silicate and borosilicate glasses. The purpose of the author's work was a systematic study of the technology of glass melting, the processes and reactions of glass formation, the crystallisation of glasses and the composition of the crystallisation products, the physicochemical properties and their relation to the composition and structure of glass and methods of calculating these properties. This book is important for all those interested in the problems of the structure of glass.

Cloth **176 pages** **$10.00**

SILICON AND ITS BINARY SYSTEMS

by A. S. Berezhnoi

Data accumulated on the physical chemistry of silicon and its binary systems are critically reviewed. The properties and descriptions of the crystal structures of silicon and all its binary compounds known at present are given in detail and the most important ways of using these substances in practical applications are indicated. Silicon carbide is treated in detail, as are silicon compounds of the transition metals. All sections have been provided with a historical outline and the basic literature is cited with each problem considered.

Cloth **265 pages** **$8.50**

CRYSTAL CHEMISTRY OF SIMPLE COMPOUNDS OF URANIUM, THORIUM, PLUTONIUM AND NEPTUNIUM

by E. S. Makarov

This book represents the first attempt to correlate crystal structure data on the simplest compounds of the most thoroughly studied actinide elements. No books dealing specifically with crystal chemistry of the actinides have been published hitherto either abroad or in the Soviet Union, although separate surveys by Zachariasen have appeared in various collective volumes.

The abundant factual data on crystal structures of actinide compounds are summarised in compact form. This work will enable research workers and engineers to make wider use of crystal structure data which, until now, have been scattered throughout numerous literature sources.

The author considers certain questions of general crystal chemistry, gives full details of the crystalline structures of the polymorphic modifications of the actinides and their simplest compounds, adopts Seaborg's cautious position regarding the parent of the "5f" family of elements, and advances an interesting theory concerning the dual chemical nature of the actinides.

Cloth **146 pages** **Illus.** **$5.25**

Payment may be made in sterling to Barclay's Bank in London, England.

Tables of contents upon request

CONSULTANTS BUREAU

227 W. 17th ST., NEW YORK 11, N. Y.

Research by Soviet Experts
Translated by Western Scientists

Soviet Research on the LANTHANIDE AND ACTINIDE ELEMENTS, 1949-1957

An important contribution to the literature of nuclear chemistry, this collection of papers is a comprehensive presentation of Soviet research on the chemistry of lanthanides and actinides. The 106 reports included in this collection appeared in the major Soviet chemical journals translated by Consultants Bureau, as well as in the Soviet Journal of Atomic Energy, 1949-1957.

The five sections, totalling 657 pages, provide broad representation of contemporary Soviet research in this important aspect of nuclear science. This collection should be accessible to all nuclear researchers, whether theoretical or applied.

Each part may be purchased as follows:

Basic Chemistry (25 papers) **$15.00**
Analytical and Separation Chemistry (30 papers) **$20.00**
Nuclear Chemistry (and Nuclear Properties) (32 papers) ... **$22.50**
Geology (10 papers) **$7.50**
Nuclear Fuel Technology (9 papers) **$7.50**
Complete collection **$65.00**

RADIATION CHEMISTRY, PROCEEDINGS OF THE FIRST ALL-UNION CONFERENCE MOSCOW, 1957

More than 700 of the Soviet Union's outstanding research scientists participated in this conference sponsored by the Academy of Sciences and the Ministry of the Chemical Industry. Each of the 56 reports read in the various sessions covers either the theoretical or practical aspects of radiation chemistry, and special attention is given to radiation sources used in radiation-chemical investigations. The general discussions which followed each report and reflected various points of view on the problem under analysis are also included.

Primary Acts in Radiation Chemical Processes
heavy paper covers 5 reports, plus discussion ..... illustrated **$25.00**
Radiation Chemistry of Aqueous Solutions (Inorganic and Organic Systems)
heavy paper covers 15 reports, plus discussion ..... illustrated **$50.00**
Radiation Electrochemical Processes
heavy paper covers 9 reports, plus discussion ..... illustrated **$15.00**
The Effect of Radiation on Materials Involved in Biochemical Processes
heavy paper covers 6 reports, plus discussion ..... illustrated **$12.00**
Radiation Chemistry of Simple Organic Systems
heavy paper covers 9 reports, plus discussion ..... illustrated **$30.00**
The Effect of Radiation on Polymers
heavy paper covers 9 reports, plus discussion ..... illustrated **$25.00**
Radiation Sources
heavy paper covers 3 reports ..... illustrated **$10.00**

Individual volumes may be purchased separately.

NOTE: Individual reports from each volume are available at $12.50 each. Tables of contents sent upon request.

special price for the 7-volume set **$125.00**

Payment in sterling may be made to Barclay's Bank in London, England.

CONSULTANTS BUREAU
227 West 17th Street · New York, N.Y., U.S.A.